Forschungszentrum Karlsruhe
in der Helmholtz-Gemeinschaft

Wissenschaftliche Berichte
FZKA 7259

Weiterentwicklung und Anwendung des prozessorientierten Modells PnET-N-DNDC zur Abschätzung der NO- und N_2O-Emissionen aus Waldböden Europas

M. Kesik

Institut für Meteorologie und Klimaforschung

November 2006

Forschungszentrum Karlsruhe
in der Helmholtz-Gemeinschaft

Wissenschaftliche Berichte
FZKA 7259

Weiterentwicklung und Anwendung des prozessorientierten Modells PnET-N-DNDC zur Abschätzung der NO- und N_2O-Emissionen aus Waldböden Europas

Magdalena Kesik

Institut für Meteorologie und Klimaforschung

von der Fakultät für Forst- und Umweltwissenschaften der Albert-Ludwigs-Universität Freiburg genehmigte Dissertation

Forschungszentrum Karlsruhe GmbH, Karlsruhe
2006

Forschungszentrum Karlsruhe GmbH
Postfach 3640, 76021 Karlsruhe

Mitglied der Hermann von Helmholtz-Gemeinschaft
Deutscher Forschungszentren (HGF)

ISSN 0947-8620

urn:nbn:de:0005-072592

Zusammenfassung

Die Vertragsstaaten, die das Kyoto-Protokoll unterzeichneten, haben das Ziel, ihre Emissionen bis zum Jahre 2012 um durchschnittlich 5,2% unter das Niveau von 1990 zu senken. Daher ist eine Abschätzung der Quellen- und Senkenstärke der einzelnen Treibhausgase notwendig. Waldböden sind signifikante Quellen für die Treibhausgase N_2O und NO. Ziel dieser Arbeit ist es, die N_2O- und NO-Emissionen aus Waldböden Europas zu quantifizieren und die N_2O- und NO-Emissionsquellen regional zu lokalisieren. Aufgrund der Heterogenität der Boden- und Vegetationseigenschaften sowie der meteorologischen Bedingungen weisen die N-Spurengasemissionen aus Böden eine hohe zeitliche und räumliche Variabilität auf.

Um diesen Herausforderungen zu begegnen, wurde das prozessorientierte Modell PnET-N-DNDC, das den N-Spurengasaustausch auf Basis der Prozesse, die an der Produktion, Konsumption und Emission von N-Spurengasen beteiligt sind, weiterentwickelt und angewandt, um zuverlässige N_2O- und NO-Emissionen aus den Waldböden Europas zu simulieren.

Im Rahmen der Weiterentwicklung des PnET-N-DNDC Modells wurde die Abhängigkeit der N_2O- und NO-Produktion durch die heterotrophen Nitrifizierer *Alcaligenes faecalis* subsp. *parafaecalis* und *Paracoccus pantotrophus* gegenüber pH, Temperatur und Substratqualität in Fermenterkulturen unter steady-state Bedingungen untersucht. Die N_2O-, NO- und CO_2-Produktion nahm mit steigender Temperatur zwischen 4 °C und 32 °C zu. Die höchsten N_2O- und CO_2-Produktionsraten wurden bei pH 7 beobachtet. Neben dem lokalen Optimum bei pH 7, nahm besonders die NO-Produktion, aber auch die N_2O-Produktion bei pH $\leq$ 4 signifikant zu. Die Zunahme der NO-Produktion unter sauren Bedingungen ist zum Teil auf die Chemodenitrifikation zurückzuführen, die bis zu 62% der Gesamt-NO-Produktion bei pH 3 ausmachte (0,8% der N_2O-Produktion). Die Substratqualität beeinflusste die N_2O-, NO- und CO_2-Produktion signifikant.

Die Ergebnisse dieser Fermenteruntersuchungen wurden teilweise in das PnET-N-DNDC implementiert, und das Modell wurde mit diesen Ergebnissen kalibriert, um eine verbesserte Beschreibung der pH- und Temperatur-Abhängigkeiten auf die N-Spurengasproduktion durch die Mikroorganismen und/oder durch die Chemodenitrifikation im PnET-N-DNDC Modell zu erzielen. Die Ergebnisse zeigen, dass heterotrophe Nitrifizierer geeignete Modellorganismen sind, um den Einfluss der Umweltfaktoren auf die mikrobielle N-Spurengasproduktion zu untersuchen.
Das PnET-N-DNDC Modell wurde anhand von Feldmessungen der N-Spurengasemissionen aus 19 Standorten validiert und sie zeigen, dass das Modell sowohl die gemessenen N_2O-Emissionen (r^2 = 0,68; Steigung = 0,76) als auch NO-Emissionen (r^2 = 0,78; Steigung = 0,73) gut simuliert.
Für die Berechnung eines europaweiten Emissionskatasters wurde das PnET-N-DNDC Modell an eine räumlich und zeitlich detailliert aufgelöste GIS-Datenbank gekoppelt. Diese Datenbank enthält Klimainformationen (in täglicher Auflösung), Informationen zu den Bodenparametern und zu den Waldflächen und Baumarten für die Jahre 1990, 1995 und 2000.
Die Berechnungen mit dem PnET-N-DNDC Modell zeigen, dass sich die N-Spurengasemissionen aus Waldböden von Jahr zu Jahr verändern und starke regionale Unterschiede auftreten. Die Schätzung der Gesamt-NO-Emissionen aus Waldböden Europas beträgt 98 kt N $Jahr^{-1}$, 85 kt N $Jahr^{-1}$ und 99 kt N $Jahr^{-1}$ für die Jahre 1990, 1995 bzw. 2000. Die Schätzung der Gesamt-N_2O-Emissionen beträgt 87 kt N $Jahr^{-1}$, 78 kt N $Jahr^{-1}$ bzw. 82 kt N $Jahr^{-1}$. Eine umfangreiche Unsicherheitsanalyse wurde durchgeführt; sie zeigt, dass die Emissionen in einem Bereich zwischen 44 bis 254 kt N $Jahr^{-1}$ für NO und 51 bis 97 kt N $Jahr^{-1}$ für N_2O im Jahr 2000 auftreten.
Auch wurden im Rahmen dieser Arbeit die möglichen Auswirkungen der vorhergesagten zukünftigen Klimaveränderung auf die NO- und N_2O-Emissionen aus Waldböden Europas untersucht. Hierfür wurden zwei Klimaszenarien verwendet. Das zehnjährige Szenario repräsentiert die Gegenwart (1991-2000) und das neunjährige Szenario repräsentiert die zukünftigen Klimabedingungen (2031-2039). Insgesamt sagt das PnET-N-DNDC Modell voraus, dass die N_2O-Emissionen aus den Waldböden Europas im Durchschnitt um 6% abnehmen. Diese Abnahme der N_2O-Emissionen ist vermutlich auf die Verschiebung des N_2O:N_2 Verhältnisses durch verstärkte Denitrifikation zurückzuführen. Die NO-Emissionen werden voraussichtlich um 9% zunehmen. Die Ursache für den Anstieg der NO-Emissionen liegt in der zukünftigen Temperaturzunahme.
Die Ergebnisse dieser Arbeit zeigen, dass prozessorientierte Modelle wie das PnET-N-DNDC, die an eine GIS-Datenbank gekoppelt sind, geeignete Hilfsmittel darstellen, regionale, nationale und globale Kataster der biogenen N-Spurengasemissionen aus Böden zu berechnen. Diese Arbeit repräsentiert den aktuellsten und umfangreichsten Versuch, N_2O- und NO-Emissionen aus europäischen Waldböden zu simulieren.

Further development and application of the process-oriented model PnET-N-DNDC for the estimation of the NO and N_2O emissions from European forest soils

Countries, that ratified the Kyoto protocol, commit to reduce their emissions until 2012 by 5.2% compared to the year 1990. Therefore, an estimation of the source- and sink-strength of the greenhouse gases is necessary. Forest soils are significant sources for the greenhouse gases N_2O and NO. The target of this work is to quantify the N_2O and NO emissions from European forest soils and to locate the regional source of the N_2O and NO emissions. Due to the heterogeneity of soil and vegetation properties or meteorological conditions N trace gas emissions show a high temporal and spatial variability.

To overcome these problems a process-oriented model, the PnET-N-DNDC model, which simulates the N trace gas exchange on the basis of the processes involved in production, consumption and emission of N trace gases, was further developed and applied in order to simulate reliable N_2O and NO emissions from European forest soils.

For this further development of the PnET-N-DNDC model the dependency of N_2O and NO on pH, temperature and substrate quality was studied in chemostat cultures under steady-state conditions using the heterotrophic nitrifiers *Alcaligenes faecalis* subsp. *parafaecalis* and *Paracoccus pantotrophus*. N_2O, NO and CO_2 production increased with temperature between 4°C and 32°C. Highest N_2O and CO_2 production rates were observed at pH 7. However, besides having an optimum at pH 7, especially NO production but also N_2O production increased significantly at pH $\leq$ 4. This increase in NO production under acidic conditions was partly due to chemo-denitrification, which contributed up to 62% of total NO production at pH 3 (0.8% for N_2O). Substrate quality significantly affected N_2O, NO and CO_2 production.

The results of the chemostat culture studies were partially implemented into the PnET-N-DNDC and the model was calibrated against the results in order to allow an improved description of the pH and temperature dependency of N trace

gas production by microbes and/or chemo-denitrification in the PnET-N-DNDC model. The results indicate that heterotrophic nitrifiers are suitable model organisms to study the influence of environmental factors on microbial N trace gas production.

The PnET-N-DNDC model was validated against field observations of N trace gas fluxes from 19 sites and shows to perform well for N_2O ($r^2 = 0.68$; slope = 0.76) and NO ($r^2 = 0.78$; slope = 0.73).

For the calculation of a European-wide emission inventory the PnET-N-DNDC model was linked to a detailed, regionally and temporally resolved GIS database, comprising climatic properties (daily resolution), soil parameters and information on forest areas and types for the years 1990, 1995 and 2000.

The PnET-N-DNDC calculations show that N trace gas fluxes from forest soils may vary substantial from year to year and that distinct regional patterns can be observed. The central estimate of NO emissions from forest soils in the EU amounts to 98, 85 and 99 kt N yr^{-1}, using meteorology from 1990, 1995 and year 2000, respectively. For N_2O emissions the central estimates were 87, 78 and 82 kt N yr^{-1}, respectively. An extensive sensitivity analysis was conducted which showed a range in emissions from 44 to 254 kt N yr^{-1} for NO and 51 to 97 kt N yr^{-1} for N_2O, for year 2000 meteorology.

Within this work also the possible feedbacks of predicted future climate change on forest soil NO and N_2O emissions in Europe were investigated. For this two climate scenarios were used, one representing a 10-year period of present day climate (1991-2000) and a nine-year period for future climate conditions (2031-2039). Overall, the PnET-N-DNDC model predicted that N_2O emissions from the European forest soils will in average decrease by 6%. This decrease was mainly due to the shift in N_2O:N_2 ratio driven by enhanced denitrification. NO emissions were found to increase by 9%. The increases in NO emissions were mainly due to increases in temperature.

The results of this work show that process-oriented models, as the PnET-N-DNDC, coupled to a GIS database are useful tools for the calculation of regional, national, or global inventories of biogenic N trace gas emissions from soils. This work represents the most comprehensive effort to date to simulate NO and N_2O emissions from European forest soils.

Inhaltsverzeichnis

Abbildungsverzeichnis

Tabellenverzeichnis

1 Einleitung

1.1 N_2O und NO als klimarelevante Treibhausgase

Die Konzentration der Treibhausgase in der Atmosphäre ist seit Beginn der Industrialisierung signifikant angestiegen und hat zu einer Klimaveränderung während der letzten hundert Jahre geführt. Diesen Zusammenhang hat das Klimagremium der Vereinten Nationen, das Intergovernmental Panel on Climate Change (IPCC) im ,,IPCC Third Assessment Report – Climate Change 2001“ erneut im Frühjahr 2001 bestätigt. Durch die Zunahme der Treibhausgaskonzentrationen kommt es zu einer Verstärkung des natürlichen Treibhauseffektes. Der natürliche Treibhauseffekt ist für das Klima der Erde von großer Bedeutung, denn durch die klimarelevanten Spurengase Wasserdampf (H_2O), Kohlendioxid (CO_2), Methan (CH_4) und Distickstoffoxid (N_2O) (Tabelle 1) wird die von der Sonne emittierte kurzwellige energiereiche Strahlung (300-800 nm) fast ungehindert auf die Erdoberfläche durchgelassen, wohingegen die von der Erdoberfläche emittierte langwellige Strahlung (4-100 μm) von den genannten Gasen stark absorbiert wird. Dies hat eine verringerte Wärmeabstrahlung der Erdoberfläche und der Troposphäre zur Folge, die zu einer troposphärischen Temperaturzunahme führt. Die in der Atmosphäre natürlich vorkommenden Treibhausgaskonzentrationen erhöhen die mittlere Temperatur an der Erdoberfläche von –18 °C auf etwa +15 °C, so dass ein Leben auf der Erde in seiner jetzigen Form überhaupt erst möglich wird (Enquete Kommission, 1992).

Anthropogene Aktivitäten, wie z.B. Verbrennung fossiler Brennstoffe oder Landnutzungsänderungen, haben jedoch zu einer signifikanten Änderung der atmosphärischen Spurengaskonzentrationen seit der vorindustriellen Zeit geführt. Die

am stärksten zum anthropogenen Treibhauseffekt beitragenden Gase sind Kohlendioxid, Methan und Distickstoffoxid (Tabelle 1).

Tabelle 1: Wichtigste anthropogen beeinflusste Treibhausgase (Houghton et al., 2001).

Spurengas	**CO_2**	**CH_4**	**N_2O**
Vorindustrielle Konzentration	280 ppm	700 ppb	270 ppb
Derzeitige Konzentration (1998)	365 ppm	1745 ppb	314 ppb
Derzeitige jährliche Zunahme [Jahr^{-1}]	1,5 ppm	7,0 ppb	0,8 ppb
Durchschnittliche Verweilzeit in der Atmosphäre [Jahre]	50-200	12	114
Jährliche Emission (2000)	3,3 Pg C	600 Tg C	16,4 Tg N
Treibhauspotential (100 Jahre)	1	23	296

Der dadurch ausgelöste, sogenannte zusätzliche anthropogene Treibhauseffekt hatte laut Intergovernmental Panel on Climate Change (Houghton et al., 2001) zur Folge, dass die Durchschnittstemperatur der Erdoberfläche (Durchschnittstemperatur der bodennahen Luftschicht über Land und den Meeresoberflächen) im 20. Jahrhundert um 0,6 ± 0,2 °C gestiegen ist (Abbildung 1).

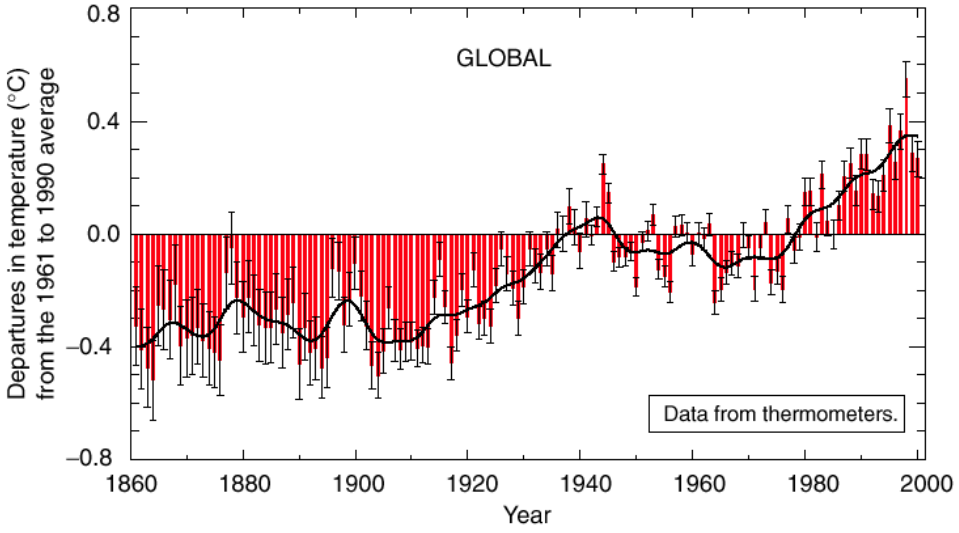

Abbildung 1: Darstellung der Abweichungen der jährlichen Oberflächentemperatur der Erde (Jahreswerte: rote Balken, 10 Jahresmittel: schwarze Linie) von der mittleren Erdtemperatur des 20. Jahrhunderts. Die Unsicherheiten der Jahresdaten (schwarze Streubalken) beruhen auf Datenlücken, Messfehler, Korrekturfaktoren (Houghton et al., 2001).

Dieser durch den Anstieg der atmosphärischen Konzentrationen klimarelevanter Spurengase hervorgerufene Temperaturanstieg wird auch in der Zukunft weiter voranschreiten. So wird für den Zeitraum zwischen 1990 und 2100 mit einer Temperaturerhöhung der Erdoberfläche von 1,4 - 5,8 °C gerechnet (Houghton et al., 2001). Um globale Aussagen über Klimaveränderungen treffen zu können, ist jedoch die Kenntnis über die Quellen und Senken atmosphärischer klimarelevanter Spurengase notwendig.
Im Gegensatz zu N_2O ist Stickstoffmonoxid (NO) kein direktes Treibhausgas, jedoch wirken laut Graedel und Crutzen (1994) hohe Konzentrationen von NO in der bodennahen Luftschicht als Katalysatoren für die Ozonproduktion. Ozon wird durch Methan- und/oder Kohlenmonoxid-Oxidationszyklen produziert. Dies führt bei atmosphärischen NO-Konzentrationen größer als 20 ppt zur Produktion von Hydroxyl-Radikalen (HO•) und daran anschließend zur Produktion von bodennahem Ozon (Crutzen, 1995). In den unteren Schichten der Atmosphäre besteht ein photostationäres Gleichgewicht zwischen ozonabbauenden und ozonbildenden chemischen Reaktionen.

Ozon-Abbau:	NO	+	O_3			$\rightarrow$	NO_2	+	O_2
Ozon-Bildung:	NO_2	+	$h\nu$ ($\lambda \leq 410$ nm)			$\rightarrow$	NO	+	O
	O	+	O_2	+	M	$\rightarrow$	O_3	+	M

Die Ozonbildung erfolgt, wenn katalytische Mengen von Stickoxiden intensiver Sonnenstrahlung ausgesetzt sind. Dabei dringt die solare Strahlung in die Troposphäre und bricht dort das NO_2 auf. Die Ozonbildung erfolgt dann durch die nachfolgende, rasche Rekombination von O mit molekularem Sauerstoff, wobei M sog. Stoßpartner (Stäube) sind. Ohne die solare Strahlung, d.h. z.B. in den Nachtstunden, verlaufen die Reaktionen in Richtung Ozon-Abbau (Graedel und Crutzen, 1994).

1.2 Waldökosysteme als Quellen für N_2O und NO

Nach Kohlendioxid und Methan ist N_2O das drittwichtigste Treibhausgas und trägt z.Z. mit ca. 6% zum zusätzlichen anthropogenen Treibhauseffekt bei (Houghton et al., 1990). Die Quellen für N_2O sind überwiegend biogenen Ursprungs (ca. 34-72%), jedoch werden die biogenen Quellstärken für atmosphärisches N_2O z.T. sehr stark durch anthropogene Aktivitäten beeinflusst (Tabelle 2).
Die stärksten biogenen Quellen sind landwirtschaftlich genutzte Böden und die Böden der tropischen Regenwälder. Bisher wurde jedoch der N_2O-Eintrag in

die Atmosphäre aus der Verbrennung fossiler Energieträger überschätzt und der Beitrag der Landwirtschaft und der Waldökosysteme unterschätzt. Der Beitrag der Wälder der Mittelbreiten zum globalen N_2O-Budget wird auf 1,0 Tg N Jahr^{-1} geschätzt (Houghton et al., 2001), dies entspricht einem Anteil von ca. 6% der Gesamtquellenstärke von N_2O, wobei die Unsicherheitsspanne 0,1-2,0 Tg N Jahr^{-1} beträgt. Dies ist vor allem darauf zurückzuführen, dass bodenbürtige N_2O-Emissionen durch eine hohe räumliche und zeitliche Variabilität (Papen und Butterbach-Bahl, 1999) gekennzeichnet sind, so dass die Berechnung globaler Budgets auf der Grundlage einzelner Messdaten sehr schwierig ist.

Tabelle 2: Geschätzte Quell- und Senkenstärke (in Tg N Jahr^{-1}) von N_2O (Houghton et al., 2001).

	MOSIER et al. (1998) KROEZE et al. (1999) Tg N Jahr^{-1}		**OLIVIER et al. (1998)** Tg N Jahr^{-1}	
Bezugsjahr	**Jahres-summe 1994**	**Unsicher-heitsspanne**	**Jahres-summe 1990**	**Unsicher-heitsspanne**
Natürliche Quellen				
Ozean	3,0	(1-5)	3,6	(2,8-5,7)
Atmosphäre (NH_3-Oxidation)	0,6	(0,3-1,2)	0,6	(0,3-1,2)
Tropische Böden				
- Feuchtwälder	3,0	(2,2-3,7)		
- Trockensavannen	1,0	(0,5-2,0)		
Böden der Mittelbreiten				
- Wälder	1,0	(0,1-2,0)		
- Grünland	1,0	(0,5-2,0)		
Alle Böden			6,6	(3,3-9,9)
Zwischensumme	*9,6*	*(4,6-15,9)*	*10,8*	*(6,4-16,8)*
Anthropogene Quellen				
Landwirtschaftliche Böden	4,2	(0,6-14,8)	1,9	(0,7-4,3)
Biomassenverbrennung	0,5	(0,2-1,0)	0,5	(0,2-0,8)
Industrie	1,3	(0,7-1,8)	0,7	(0,2-1,1)
Viehhaltung	2,1	(0,6-3,1)	1,0	(0,2-2,0)
Zwischensumme	*8,1*	*(2,1-20,7)*	*4,1*	*(1,3-7,7)*
Summe	**17,7**	**(6,7-36,6)**	**14,9**	**(7,7-24,5)**
Senken				
Aufnahme von Böden	?	?		
Photolyse in der Atmosphäre	12,3	(9-16)		
Atmosphärischer Anstieg	**3,9**	**(3,1-4,7)**		
Summe	**16,2**	**(12,1-20,7)**		

Böden sind mit einem Anteil von 16% am globalen Quell-Budget des sekundär klimarelevanten Spurengases NO beteiligt (Lee et al., 1997). Neuste Untersuchungen von Ganzeveld et al. (2002) schätzen die globale NO-Quellstärke aller Böden auf ca. 12 Tg N Jahr^{-1}. Wesentliche Quelle von atmosphärischem NO ist jedoch die Biomassenverbrennung, z.B. bei Brandrodung oder Savannenbränden, sowie die NO_x-Produktion bei der Verbrennung fossiler Brennstoffe. Eine weitere natürliche Quelle für atmosphärisches NO stellen Blitze dar (Tabelle 3).

Tabelle 3: Geschätzte Quellstärke (in Tg N Jahr^{-1}) von NO.

Quellen [Tg N Jahr $^{-1}$]	**LEE et al., 1997**	**DAVIDSON und KINGER-LEE, 1997**	**YAN et al., 2005**[a]
Tundrenböden	0,2	-	-
Grünlandböden der Mittelbreiten	0,7	1,1	1,32
Savannenböden	0,3	7,4	1,29
Böden der borealen Wälder	.	0,1	-
Waldböden der Mittelbreiten	0,4[b]	0,4	0,87
Subtropische Waldböden	0,2	4,7	0,79
Tropische Regenwaldböden	0,6	1,8	0,67
Landwirtschaftliche Böden	4,5	5,5	2,41
Wüsten	-	0,5	0,06
Summe Böden	**6,9**	**21,5**	**7,41**
Verbrennung fossiler Brennstoffe	22,0		
Biomassenverbrennung	7,9		
Blitze	5,0		
Flugzeuge	0,9		
NH_3-Oxidation	0,9		
Stratosphärischer Abbau von N_2O	0,6		
Summe	**44,3**		

[a] NO_x Quellstärkeangabe [Tg N Jahr^{-1}]
[b] beinhaltet NO-Quellstärke aus Böden der borealen Wälder

Neuere Untersuchungen zur Quellstärke von Böden mitteleuropäischer Wälder für N_2O und NO (Papen und Butterbach-Bahl, 1999; Gasche und Papen, 1999) haben jedoch gezeigt, dass der Beitrag der Wälder der Mittelbreiten zum globalen N_2O- und NO-Budget nicht zu vernachlässigen ist. So wurde z.B. in einer dreijährigen Dauermessung, die eine sehr hohe jahreszeitliche Variabilität der N_2O-Emissionen aufwies, festgestellt, dass während Frostperioden sehr hohe Emissionsraten auftraten. Demzufolge werden in der Literatur die jährlichen Emissionsraten temperater Wälder oft unterschätzt. Ebenso haben verschiedene Untersuchungen gezeigt, dass Böden von Wäldern Zentraleuropas aufgrund des chronischen N-Eintrages in den letzten Jahrzehnten nicht nur zu signifikanten Quellen für N_2O, sondern darüber hinaus auch zu starken Quellen für NO geworden sind (Aber et al., 1989; Bowden et al., 1991; Gasche und Papen, 1999; Pilegaard et al., 1999; Van Dijk und Duyzer, 1999).

NO- und N_2O-Emissionen aus Böden entstehen in Folge von mikrobiellen N-Umsetzungsprozessen in Böden. Die zentralen Prozesse der mikrobiellen N-Umsetzungen in Böden sind die Ammonifikation, Nitrifikation, Denitrifikation sowie die mikrobielle Immmobilisierung von anorganischen N-Verbindungen (Abbildung 2).
An der Produktion der N-Spurengase NO und N_2O sind jedoch vor allem die Prozesse Nitrifikation und Denitrifikation beteiligt. Wie alle biologischen Stoffwechselvorgänge sind auch die Prozesse Nitrifikation und Denitrifikation von einer Reihe von Umweltfaktoren abhängig.

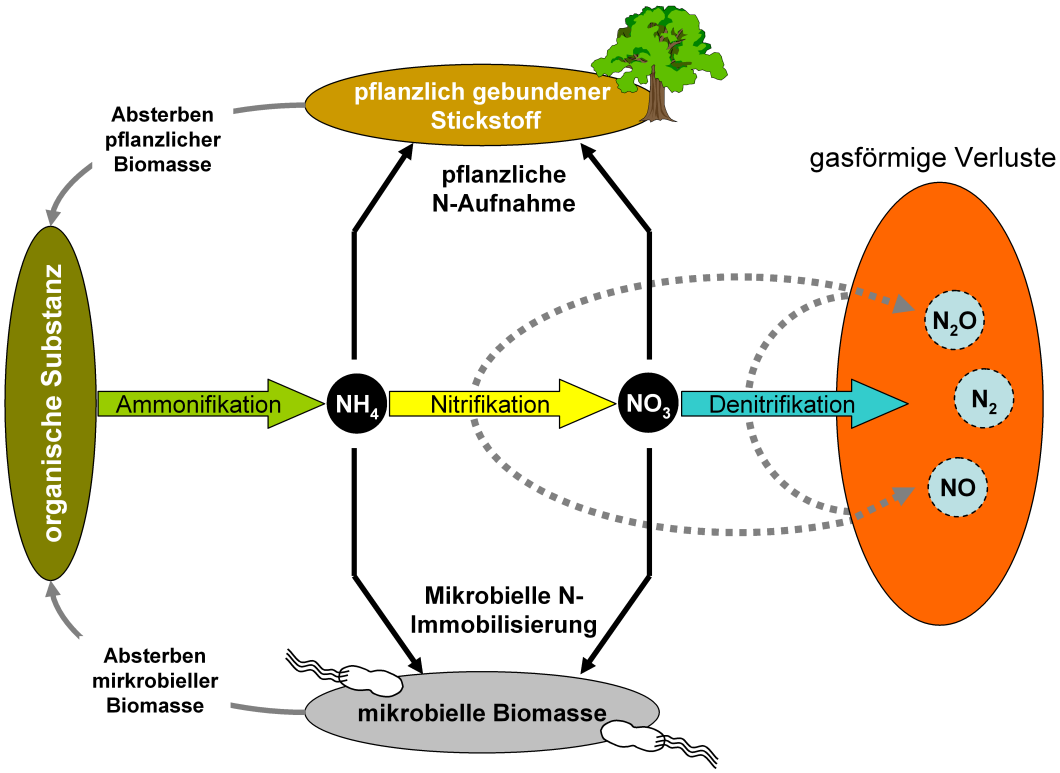

Abbildung 2: Kreislauf der primären N-Umsetzungsprozesse Ammonifikation, Nitrifikation, Denitrifikation und pflanzliche und mikrobielle N-Immobilisierung (Breuer, 2000)

Die Nitrifikation ist ein mikrobiologischer Prozess, bei dem Ammoniak (NH_3) bzw. Ammonium (NH_4^+) über Nitrit (NO_2^-) zu Nitrat (NO_3^-) oxidiert wird. Ammonium entsteht durch den mikrobiellen Abbau von organischen Stickstoffver-

bindungen im Prozess der Ammonifikation. Der Prozess der Nitrifikation erfolgt in zwei Schritten (Granli und Bøckman, 1994):

$$\begin{array}{lllllllll} NH_4^+ & + & 3/2\ O_2 & \rightarrow & NO_2^- & + & H_2O & + & 2H^+ \\ NO_2^- & + & 1/2\ O_2 & \rightarrow & NO_3^- & & & & \end{array}$$

Bei der autotrophen Nitrifikation wird laut Granli und Bøckman (1994) der erste Schritt von Ammoniak-Oxidierern (z.B. *Nitrosomonas* und *Nitrosospira*) durchgeführt. Für den zweiten Schritt sind die Nitrit-Oxidierer (z.B. *Nitrobacter*) verantwortlich. Diese Organismen benötigen CO_2, O_2 und NH_4^+ zum Wachstum und beziehen die notwendige Energie aus der Oxidation des Ammoniums (NH_4^+) bzw. des Nitrits (NO_2^-). Des Weiteren sind jedoch auch heterotroph lebende Mikroorganismen, die organischen Kohlenstoff als C- und Energiequelle nutzen, zur Nitrifikation fähig (Robertson und Kuenen, 1990; Wrage, 2001). Diese Organismen sind in der Lage, Ammonium direkt bis zum Nitrat zu oxidieren (Daum et al., 1998; Papen et al., 1993). Während der autotrophen und heterotrophen Nitrifikation wird N_2O und NO als fakultatives Zwischenprodukt gebildet und durch die Nitrifizierer an die Umwelt abgegeben.
Die NO- wie auch N_2O-Produktion erfolgt entweder über die Reduktion von NO_2^- oder durch die Oxidation von Hydroxylamin (NH_2OH) durch nitrifizierende Bakterien (Firestone und Davidson, 1989).
Die Denitrifikation ist ein anaerober Prozess, bei dem Nitrat über Nitrit zu NO, N_2O und N_2 reduziert wird. Die Reaktionskette erfolgt stufenweise:

$$\overset{(+5)}{NO_3^-} \rightarrow \overset{(+3)}{NO_2^-} \rightarrow \overset{(+2)}{NO} \rightarrow \overset{(+1)}{N_2O} \rightarrow \overset{(0)}{N_2}$$

Denitrifizierende Mikroorganismen sind fakultative Anaerobier, d.h. sie sind bei O_2-Mangel fähig, Nitrit- und Nitrat anstelle von elementarem Sauerstoff als Elektronenakzeptor zu verwerten. Typische Vertreter der denitrifizierenden Bakterien sind z.B. die Gattungen *Pseudomonas* und *Alcaligenes* (Paul und Clark, 1988).
N_2O wie auch NO sind obligatorische Zwischenprodukte innerhalb des Denitrifikationsprozesses. Die Menge des während der Denitrifikation produzierten NO bzw. N_2O hängt u.a. von der Verfügbarkeit von Nitrat im Boden ab. Wenn z.B. die Verfügbarkeit von Nitrat im Boden die Verfügbarkeit von organischem Kohlenstoff deutlich übersteigt, kann der Denitrifikationsprozess unvollständig ablaufen und bereits beim NO bzw. N_2O statt beim N_2 enden (Firestone und Davidson, 1989).

Die Produktion und Konsumption von N_2O und NO während der Nitrifikation und Denitrifikation sind im konzeptionellen ,,hole-in-the-pipe“ Modell von Firestone und Davidson (1989) veranschaulicht (Abbildung 3). Durch die vorhandenen ,,Löcher“ in den dargestellten ,,Röhren“ können sowohl Gase nach außen gelangen als auch aus der Umgebung in diese ,,Röhren“ eindringen.

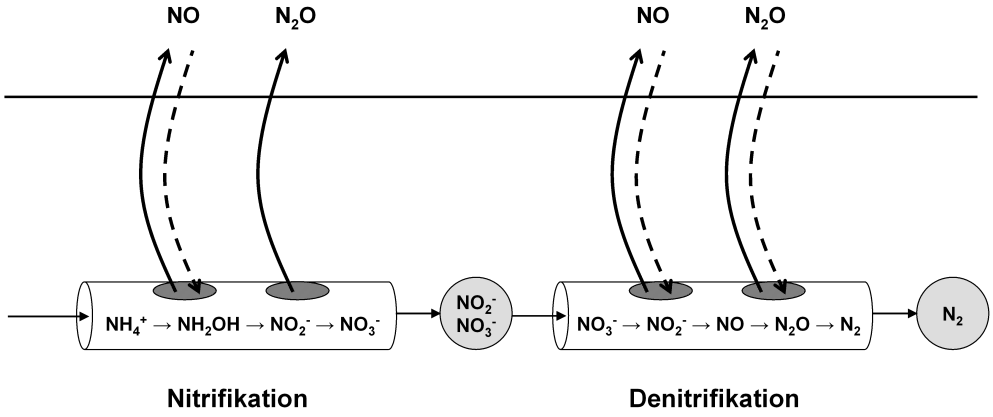

Abbildung 3: Darstellung des konzeptionellen ,,Hole-in-the-pipe“-Modells. Es reguliert auf zwei Ebenen die N-Spurengasproduktion über die Nitrifikation und Denitrifikation zum einen durch die Bewegung von N durch die ,,Röhren“ und zum anderen durch die ,,Löcher“, durch die N-Spurengase strömen können. (Firestone und Davidson, 1989)

Die Höhe der N-Spurengasfreisetzung ist einerseits von der Höhe der Umsetzungsraten des Nitrifikations- und Denitrifikationsprozesses (Durchfluss durch die Röhren), andererseits aber auch von der Höhe der dabei auftretenden Verlustraten während dieser Umsetzungsprozesse (Löcher in den Röhren) abhängig. Sowohl die Umsetzungs- als auch die Verlustraten werden von zahlreichen Umweltfaktoren beeinflusst.
So ist die Nitrifikation von Faktoren abhängig, die die mikrobielle Aktivität beeinflussen. Die wichtigsten Regulatoren sind die O_2-Konzentration und der Ammoniumgehalt (Li, 2000), da die Nitrifikationsraten als oxidativer Prozess im Allgemeinen bei geringer O_2-Verfügbarkeit abnehmen. Zusätzlich haben die Bodenfeuchte, die Bodentemperatur und der pH Wert Einfluss auf die Nitrifikation. Die Nitrifikation erreicht je nach Bodentextur ihr Optimum bei einer Bodenfeuchte von 30-60% wassergefülltem Porenraum des Bodens (Bouwman, 1998). Bei höheren Wassergehalten sinkt die Aktivität durch den zunehmenden Sauerstoffmangel, da der Boden zunehmend anaerobe Verhältnisse bei steigendem Bodenwassergehalt aufweist (Granli und Bøckman, 1994). Laut Bock et al. (1986) liegt das Tem-

peraturoptimum für die Nitrifikation zwischen 25 und 35 °C. Jedoch selbst bei Temperaturen um –1,5 °C findet Ammonifikation, Nitrifikation und Denitrifikation statt (Papen und Butterbach-Bahl, 1999). Die Verfügbarkeit von NH_4^+ für die nitrifizierenden Bakterien wird durch verschiedene Sekundärfaktoren bestimmt, wie die Mineralisations- und Immobilisationsraten, Pflanzenwachstum, Kationenaustausch und Diffusion. Die Zugabe von organischem Material in Böden steigert die mikrobielle Aktivität, verbraucht O_2, und anaerobe Bedingungen können sich entwickeln, so dass die Nitrifikation zunehmend eingeschränkt wird. Die Nitrifikationsrate nimmt von sauren (pH 3-5) über neutralen zu leicht basischen Bedingungen zu, die NO-Produktion hingegen ab. Jedoch sind die Auswirkungen des pH Wertes auf die nitrifikatorisch bedingten N_2O- und NO-Emissionen sehr komplex und nur unzureichend untersucht (Granli und Bøckman, 1994).

Da die Fähigkeit zur Denitrifikation unter Mikroorganismen sehr weit verbreitet ist, wird die Denitrifikation weniger durch die Präsenz der Mikroorganismen als vielmehr durch die ökologischen Bedingungen (z.B. Diffusion, O_2-Verfügbarkeit, NO_3^--Konzentration, Bodentemperatur) bestimmt. Robertson (1989) zeigt, dass das Vorhandensein von O_2 die Denitrifikation limitiert, da die Denitrifikation anaerobe Bedingungen benötigt. Die O_2-Verfügbarkeit im Bodenprofil wird durch den Bodenwassergehalt beeinflusst, der durch den Niederschlag und die Evapotranspiration kontrolliert wird, da mit zunehmender Bodenfeuchte sich der luftgefüllte Porenraum verringert. Die höchsten N_2O-Bildungsraten bei der Denitrifikation sind bei einem wassergefüllten Porenraum über 60% (abhängig von den Bodeneigenschaften) nachweisbar (Bouwman, 1998; Smith, 1997). Die Höhe der Denitrifikation ist von der NO_3^--Konzentration im Boden abhängig. Wenn in ungedüngten Böden anaerobe Bereiche vorkommen, kann die NO_3^-Verfügbarkeit die Denitrifikationsraten bestimmen (in N-gedüngten Böden limitiert zumeist die C-Verfügbarkeit die Denitrifikation). Die Denitrifikation ist darüber hinaus der einzig bekannte Prozess im Boden, bei dem N_2O verbraucht wird (Conrad, 1996). Unter sauren Boden-pH-Bedingungen kann auch der physikalisch-chemische Prozess der Chemodenitrifikation signifikant zur NO-Produktion im Boden beitragen. Bei der Chemodenitrifikation wird bei pH-Bedingungen < 4 disproportioniert HNO_2 letztendlich zu NO (Li et al., 2000; McKenney et al., 1990).

1.3 Zielsetzung der Arbeit

Im Rahmen des Kyoto-Protokolls sind die einzelnen Nationen dazu verpflichtet worden, Abschätzungen zur Quellen- und Senkenstärke der einzelnen Treibhausgase zu treffen. Ziel dieser Arbeit war es daher, die N_2O- und NO-Emissionen aus Waldböden Europas zu quantifizieren und regional die N_2O- und NO-Emissionsquellen zu lokalisieren.
Aufgrund der Heterogenität der Landschaftselemente (Boden, Vegetation) sowie der meteorologischen Bedingungen weisen die N-Spurengasemissionen aus Böden eine hohe zeitliche und räumliche Variabilität auf. Daher kann eine verbesserte Abschätzung des Beitrages von Böden zu nationalen/regionalen Budgets der N-Spurengasemissionen nicht über die Intensivierung von Feldmessungen allein erreicht werden. Als Lösungsweg bietet sich die prozessorientierte Modellierung an. Es wurden bereits mehrere biogeochemische Modelle, die den C- und N-Kreislauf im Boden sowie den Austausch von Spurengasen zwischen Boden und Atmosphäre simulieren in den letzten Jahren entwickelt. Hierzu zählen die Modelle CENTURY (Parton, 1996), CASA (Potter et al., 1996), DNDC (Li et al., 1992) und PnET-N-DNDC (Li et al., 2000). Das PnET-N-DNDC (**P**hotosy**n**thesis – **E**vapo**t**ranspiration – **N**itrification – **D**e**n**itrification – **D**e**c**omposition - Modell) ist ein prozessorientiertes Waldökosystemmodell, das die wesentlichen in die N- und C-Umsetzungen in forstlich genutzten Ökosystemen involvierten biotischen (z.B. Pflanzenwachstum, Mineralisierung, Nitrifikation, Denitrifikation) und abiotischen Prozesse (z.B. Diffusion von Gasen, wie z.B. O_2, N_2O, NO im Bodenprofil und O_2-Verfügbarkeit, N- und C-Verlagerung mit der Bodenwassersickerung, NH_4^+- Bindung an Tonminerale) simuliert. Letztendlich wird dann aus der komplexen Verflechtung von Produktions-, Konsumptions- und Diffusions-Prozessen von Spurengasen in verschiedenen Bodenschichten die N-Spurengasemission aus forstwirtschaftlich genutzten Böden berechnet.
Obwohl die Vorhersagegenauigkeit des prozessorientierten Modells PnET-N-DNDC inzwischen sehr weit fortgeschritten ist, sind dennoch Schwachpunkte in der Modellsimulation erkennbar. Besonders im Hinblick auf den Einfluss des pH Wertes, der Temperatur und der Substratverfügbarkeit auf die N_2O- und NO-Produktion, mussten die bereits im Modell bestehenden Algorithmen überprüft, gegebenenfalls verändert und kalibriert werden. Hierfür wurde die Abhängigkeit der N_2O- und NO-Produktion von der Temperatur, des pH Wertes und der Substratqualität mittels Reinkulturen von heterotrophen Nitrifizierern, die unter konstanten Bedingungen in einem Fermenter kultiviert wurden, untersucht. Die Ergebnisse der Laboruntersuchungen wurden parametrisiert und als Algorithmen in das PnET-N-DNDC implementiert. Das PnET-N-DNDC wurde mit Hilfe der in den Prozessstudien im Labor erhaltenen Ergebnisse kalibriert. Neben der Kalibrierung des PnET-N-DNDC ist eine Validierung des Modells von entscheidender Bedeutung für die Qualität der Simulationsergebnisse, denn nur

mittels einer umfassenden Validierung kann überprüft werden, ob die simulierten N_2O- und NO-Emissionen mit den tatsächlich gemessenen Raten übereinstimmen. Hierzu wurden die Datensätze zu N-Spurengasemissionen aus Waldböden an 18 europäischen Freilandstationen, die im Rahmen des EU-Projektes NOFRETETE (**N**itrogen **o**xides emissions **fr**om **E**uropean fores**t** **e**cosys**te**ms) erhoben wurden, sowie einem Standort in den USA für die Validierung des Modells PnET-N-DNDC verwendet. Die entsprechenden Standortdaten, wie die meteorologischen Bedingungen, die Bodeneigenschaften sowie die jeweiligen Waldinformationen wurden als Eingabedaten für das Modell aufbereitet und die Ergebnisse der Simulationsläufe mit den tatsächlich vor Ort gemessenen N_2O- und NO-Emissionswerten verglichen.
Für den Einsatz des PnET-N-DNDC Modells zur Berechnung eines Emissionskatasters der N-Spurengasemissionen aus Waldböden Europas wurde eine GIS (Geographisches Informations System)-Datenbank, die im Rahmen dieser Arbeit erstellt wurde, mit allen für die Modellsimulationen notwendigen Eingangsparametern und Modelltreibern benötigt. Diese Datenbank enthält Informationen zu Bodenparametern, Waldbestanddaten, Klimadaten und Rauminformationen, die in Bezug zu den drei genannten Komponenten stehen. Die GIS-Datenbank wurde an das Modell PnET-N-DNDC gekoppelt. Auf Basis eines 50km x 50km Rasters wurden für die Jahre 1990, 1995 und 2000 N_2O- und NO-Emissionen aus den Waldböden für Europa berechnet. Die Ergebnisse der Simulationsläufe des PnET-N-DNDC wurden aufbereitet und mit ArcGIS (ESRI) in Form eines europäischen N_2O- und NO-Emissionskatasters graphisch dargestellt.
Zusätzlich wurde mit Hilfe von globalen Klimaszenarien für Europa untersucht, inwieweit sich die Quellstärke der Wälder Europas für N_2O und NO in den nächsten 30 bis 40 Jahren aufgrund des prognostizierten Klimawandels verändern könnte.

Diese Arbeit kann in die folgenden vier chronologischen Abschnitte unterteilt werden, die schematisch in Abbildung 4 dargestellt sind:

1. Umfangreiche Prozessstudien im Labor: Untersuchung der Abhängigkeit der N_2O- und NO-Produktionsraten von pH, Temperatur und Substrateigenschaften, und zusätzliche Implementierug der Ergebnisse in das PnET-N-DNDC Modell.

2. Validierung des PnET-N-DNDC Modells mit 19 Datensätzen aus Feldmessungen zu N_2O- und NO-Emissionen aus Waldböden.

3. Erstellung einer umfassenden GIS-Datenbank für Waldböden Europas und Kopplung an das PnET-N-DNDC Modell.

4. Erstellung eines N_2O- und NO-Emissionskatasters für Waldböden Europas, und Berechnung der zukünftigen Veränderung der N_2O- und NO-Emissionen aus Waldböden.

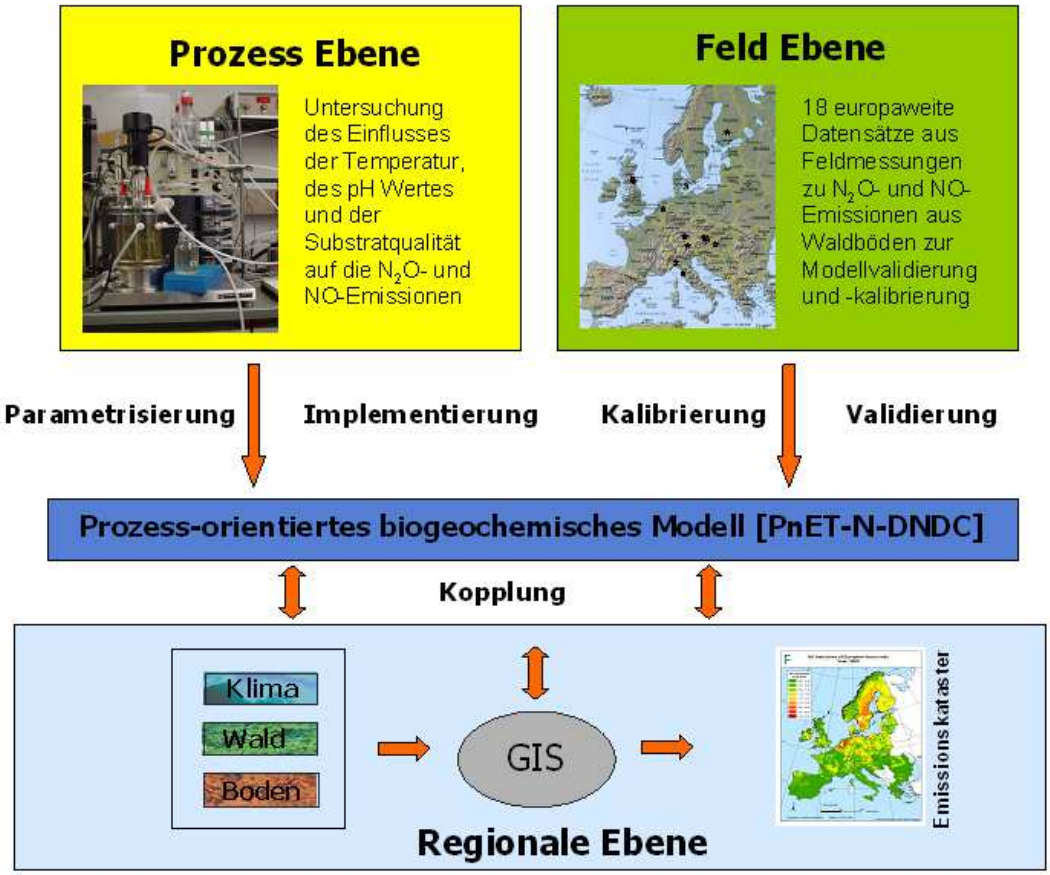

Abbildung 4: Schematische Darstellung der Gliederung dieser Arbeit. Sie beinhaltet auf Prozessebene die Prozessstudien im Labor, sowie die Parametrisierung und Implementierung der Laborergebnisse in das PnET-N-DNDC. Auf der Feldebene erfolgen die Validerung der Standorte, sowie die Kalibrierung des PnET-N-DNDC, auf regionaler Ebene die Erstellung der GIS-Datenbank mit den Klima-, Wald- und Bodeninformationen, sowie die Kopplung dieser Datenbank an das PnET-N-DNDC. Abschließend finden die Berechnung der N_2O- und NO-Emissionen, sowie deren Darstellung als Emissionskataster für europäische Waldböden auf regionaler Ebene statt.

2 Laborexperimente mit *Alcaligenes faecalis* subsp. *parafaecalis*

Wie bereits erwähnt wird N_2O und NO in Böden hauptsächlich durch die mikrobiellen Prozesse der Nitrifikation und der Denitrifikation produziert. Beide Prozesse werden durch eine Vielzahl an Umweltfaktoren beeinflusst bzw. reguliert, zu denen u.a. der Sauerstoffgehalt im Boden, die Temperatur, der pH Wert und die Bodenfeuchte zählen. Die Veränderung der mikrobiellen Produktion von N-Spurengasen durch Bodenorganismen unter unterschiedlichen pH Werten, Temperaturen oder Substrateigenschaften wurde unter kontrollierten Feldversuchen in zahlreichen Studien untersucht (Koskinen und Kenney, 1982; Goodroad und Keeney, 1984; Martikainen, 1985; Weier und Gilliam, 1986; Nägele und Conrad, 1990; Daum und Schenk, 1998; Ellis et al., 1998; Smith et al., 1998; Papen und Butterbach-Bahl, 1999; Gasche und Papen, 1999).
Aufgrund der räumlichen und zeitlichen Variabilität der Umweltfaktoren, die die N-Spurengase aus Böden beeinflussen, erhält man mittels Feldversuchen nur ein vergleichsweise eingeschränktes Bild über den Einfluss der Umweltfaktoren auf die im Boden ablaufenden Prozesse. Aus diesem Grund konnten einige Feldmessungen keinen klaren Zusammenhang zwischen pH Wert oder sogar Temperatur und N-Spurengasproduktion aufzeigen (Struwe und Kjøller, 1994; Yamulki et al., 1997; Simek et al., 2002).
Um unser Prozessverständnis gegenüber Umweltfaktoren, wie Temperatur, pH oder Substratqualität, die die N-Spurengasproduktion regulieren, zu verbessern, sind Laboruntersuchungen unter kontrollierten Bedingungen am besten geeignet (Yoshida und Alexander, 1970; Nägele und Conrad, 1990; Conrad, 2002). Insbesondere können Untersuchungen mit Reinkulturen von Mikroorganismen, die an der N-Spurengasproduktion in Böden beteiligt sind, in diesem Zusammenhang von fundamentaler Bedeutung sein. Im Vergleich zu Boden-Inkubationsversuchen ist es bei den Reinkulturuntersuchungen möglich, Umweltbedingungen konstant zu halten und solche Beeinträchtigungen zu vermeiden, die durch zeitliche Verände-

rungen in der mikrobiellen Gemeinschaft zwangsläufig entstehen. Diese Vorteile haben bereits vorangegangene Untersuchungen genutzt (Yoshida und Alexander, 1970; Robertson und Kuenen, 1988; Papen et al., 1989; Anderson et al., 1993; Thomsen et al., 1994; McKenney et al., 1994; Otte et al., 1996). Jedoch hatten diese Studien einige Nachteile. So wurde die NO- und N_2O-Produktion nicht parallel untersucht, bzw. diese Versuche fanden nur mittels Batch-Kulturen statt. Im Gegensatz zu kontinuierlichen Kulturen wachsen und sterben in Batch-Kulturen die Mikroorganismen im flüssigen Medium, bis das Substrat verbraucht ist. Die Mikroorganismen durchleben einen kompletten Wachstumszyklus; sie befinden sich zuerst in einer sog. Lag-Phase, in der die Produktivität der Mikroorganismen sehr gering ist, da sich die Mikroorganismen erst an die neuen Bedingungen adaptierten müssen, dann beginnt das exponentielle Wachstum der Mikroorganismen mit der höchsten Produktivität. Sobald das exponentielle Wachstum aufhört, erreichen die Mikroorganismen die stationäre Phase, in der die Zellzahl weder zunoch abnimmt. Schließlich, wenn das Substrat aufgebraucht ist, beginnt die Sterbephase mit abnehmender Produktivität. Da in solchen Versuchen der O_2-Gehalt stark variiert, können Batch-Versuche auch dazu genutzt werden, um u.a. herauszufinden, bei welchem Sauerstoffgehalt und in welcher Phase ihres exponentiellen Wachstums die Mikroorganismen die höchsten N_2O- und NO-Produktionsraten aufweisen. Mit Hilfe dieser Erkenntnisse können dann in kontinuierlichen Kulturen die Mikroorganismen bei entsprechendem Sauerstoffgehalt und zusätzlich konstanter Mediumzufuhr über mehrere Wochen in ihrer exponentiellen Wachstumsphase konstant gehalten werden. In dieser Phase ist zu beachten, dass bei der kontinuierlichen Kultur ein Gleichgewicht zwischen Wachstum und Mediumzufuhr herrscht. Die Mediumzufuhr und die entsprechende Entnahme von Flüssigkultur müssen so geregelt sein, dass die Mikroorganismen nicht ausgewaschen werden (bei zu hoher Mediumzufuhr).

Um zu einem besseren Verständnis über die Auswirkungen von Umweltfaktoren auf N-Spurengasproduktion beizutragen, wurden im Rahmen dieser Arbeit zahlreiche Fermenterversuche durchgeführt. Als Hauptorganismus wurde *Alcaligenes faecalis* subsp. *parafaecalis* gewählt, da *Alcaligenes faecalis* als heterotropher Nitrifizierer weltweit in Böden vorkommt (Gamble et al., 1977; Papen und von Berg, 1998) und auch zur Denitrifikation befähigt ist (Anderson et al., 1993). Des Weiteren ist gezeigt worden, dass *A. faecalis* sowohl in aeroben als auch in anaeroben Batch- und Fermenterkulturen N_2O und NO produziert (Kuenen und Robertson, 1987; Papen et al., 1989; Robertson et al., 1995; Otte et al., 1996). Um zu überprüfen, ob die gewonnenen Ergebnisse auch auf andere Mikroorganismen übertragbar sind - was z.T. in den vorangegangenen Studien ebenso vernachlässigt wurde -, wurden zusätzlich Untersuchungen mit *Paracoccus pantotrophus* (= *Thiosphaera pantotropha*) durchgeführt. *P. pantotrophus* ist ein Mikroorganismus im Boden, der hauptsächlich von Robertson et al. (1988) und Robertson und Kuenen (1988) untersucht wurde. Dieser Organismus kann

N_2O und NO über den Weg der heterotrophen Nitrifikation und/oder Denitrifikation produzieren. Die Laborarbeiten konzentrierten sich auf die Beantwortung folgender Fragen:

1. Welchen Einfluss haben Temperaturveränderungen über eine weite Skala (4 – 32 °C) auf die N_2O-, NO- und CO_2-Produktion?

2. Welche Auswirkungen hat der pH Wert (pH 3 bis pH 8; in einem Bereich, der in den meisten Böden weltweit auftritt) auf die N_2O-, NO- und CO_2-Produktion sowie auf das N_2O:NO Verhältnis?

3. Wie beeinflusst der Sauerstoffgehalt die N_2O- und NO-Produktion?

4. Wie beeinflusst die Substratqualität die N_2O- und NO-Produktion?

5. Verhalten sich beide Mikroorganismen im Hinblick auf Veränderungen in der N_2O- und NO-Produktion unter unterschiedlichen Umwelteinflüssen ähnlich?

Im Rahmen dieser Doktorarbeit wurden in den Laborexperimenten der Einfluss des pH Wertes, der Temperatur und der Substratabhängigkeit auf die N_2O-, NO- und CO_2-Produktion von *A. faecalis p.* untersucht und in dem Artikel von Kesik, M., Blagodatsky, S., Papen, H. und Butterbach-Bahl, K. (Kesik et al., 2005, **I**) beim Journal of Applied Microbiology eingereicht. Ebenso wurde im Rahmen dieser Doktorarbeit die N_2O- und NO-Produktion von *A. faecalis p.* unter verschiedenen Sauerstoffbedingungen untersucht und von Blagodatsky, S., Kesik, M., Papen, H., und Butterbach-Bahl, K. im Geomicrobiology Journal zur Veröffentlichung eingereicht.

2.1 Durchführung der Laboruntersuchungen

Insgesamt wurden 13 Experimente durchgeführt, die jeweils mindestens 20 Tage andauerten. Der schematische Versuchsaufbau ist in Abbildung 5 dargestellt. Bei allen Versuchen wurden die Mikroorganismen zuerst als Batch-Kultur im Fermenter (BioFloIII Fermentor, New Brunswick, Deutschland) kultiviert. Der pH Wert wurde auf pH 7 und die Temperatur auf 28 °C eingestellt. Während der exponentiellen Wachstumsphase von *A. faecalis p.* bzw. *P. pantotrophus* wiesen beide Mikroorganismen im Fermenter eine konstante Wachstumsrate von 0,1 h^{-1} auf dem reichen Substrat (Pepton-Fleischextrakt Medium) und von 0,05 h^{-1} auf dem limitierten Substrat (Ammonium-Citrat Medium) auf. Die Luftzufuhr wurde mittels einer Tylan Kontrolleinheit (Tylan Co., Deutschland) so kontrolliert, dass im Medium eine Sauerstoffsättigung zwischen 15-20% vorlag, da bei dieser Sauerstoffsättigung die höchsten N_2O- und NO-Produktionsraten in den vorangegangenen Batch-Versuchen gemessen wurden. Die Sauerstoffsättigung, sowie

der pH Wert, das Redox-Potential und die Temperatur wurden mittels Elektroden kontrolliert und die Ergebnisse auf den Mikroprozessor (MultiLoopController, New Brunswick, Deutschland) gespeichert. In der Abluft aus dem Fermenter wurden NO und CO_2 automatisch gemessen und aufgezeichnet. Für die Messung der N_2O-Produktionsrate wurde stündlich eine Gasprobe mittels einer gasdichten Spritze dem Fermenter entnommen und in einem Gaschromatographen analysiert (Abbildung 5).
Die Experimente wurden erst gestartet, wenn die Kultur den Zustand des steady-state (nach ca. 48h) erreicht hatte, d.h. die folgenden Parameter mussten für mindestens 15h konstant bleiben: mikrobielle Protein-Konzentration, Sauerstoffsättigung, N_2O-, NO- und CO_2-Produktion. Unter diesen Bedingungen konnte die Kultur für maximal drei Wochen im steady-state gehalten werden, bevor die Sterilität der Kultur nicht mehr gewährleistet werden konnte.
Die folgende Graphik zeigt den schematischen Versuchsaufbau der 13 durchgeführten Experimente. Für weitere Informationen zum Versuchsaufbau, der Versuchsdurchführung und der Bestimmung von NH_4^+, NO_2^-, NO_3^-, Protein-Gehalt sowie zur Messung der N_2O-, NO- und CO_2-Produktion, bzw. zu den beiden Bakterienkulturen und ihren Medien verweise ich auf den Material- und Methodenteil in der Arbeit von Kesik et al. (2005, **I**).

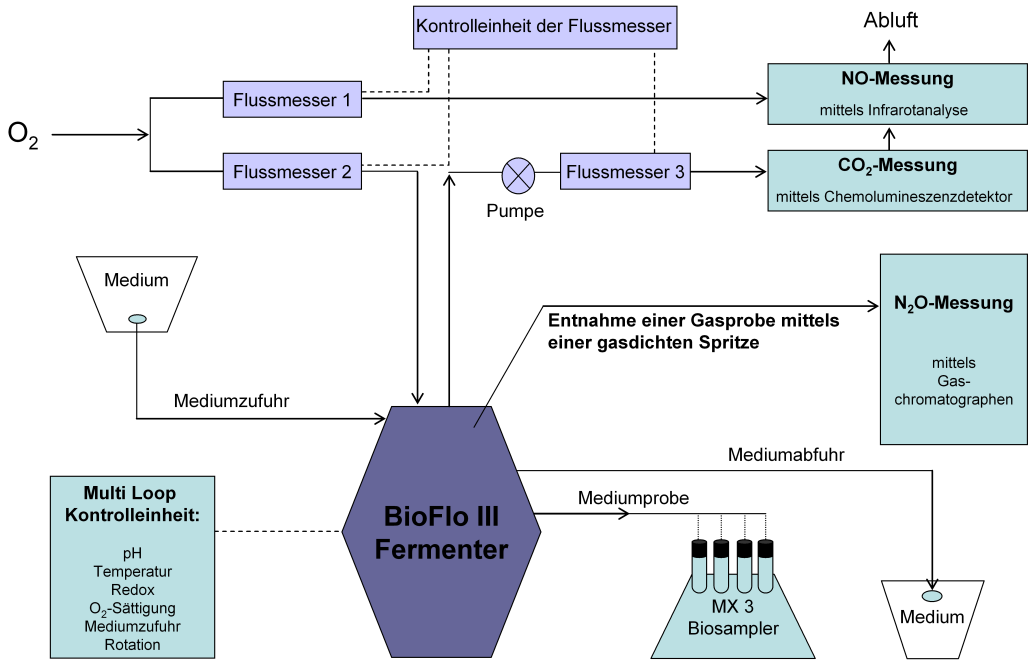

Abbildung 5: Schematische Darstellung des Versuchsaufbaus.

2.2 Abhängigkeit der N_2O- und NO-Emissionen von der Temperatur

Die Abhängigkeit der N_2O- und NO-Produktion von der Temperatur wurde im Temperaturbereich zwischen 4 °C und 32 °C untersucht. Der Einfluss der Temperatur auf die NH_4^+, NO_2^-, NO_3^- und Protein-Konzentrationen sind im Ergebnisteil und in Tabelle 2 in der Arbeit von Kesik et al. (2005, **I**) beschrieben.
Für den gesamten untersuchten Temperaturbereich korrelierten die NO-Produkionsraten positiv zur Temperatur. So verdoppelte sich die NO-Produktion von 0,007 μg NO-N mg Protein^{-1} h^{-1} auf 0,014 μg NO-N mg Protein^{-1} h^{-1} bei einer Temperaturerhöhung von 16 °C auf 24 °C. Die höchsten NO-Produktionsraten (0,042 ± 0,04 μg NO-N mg Protein^{-1} h^{-1}) wurden bei 32 °C beobachtet (Abbildung 6).

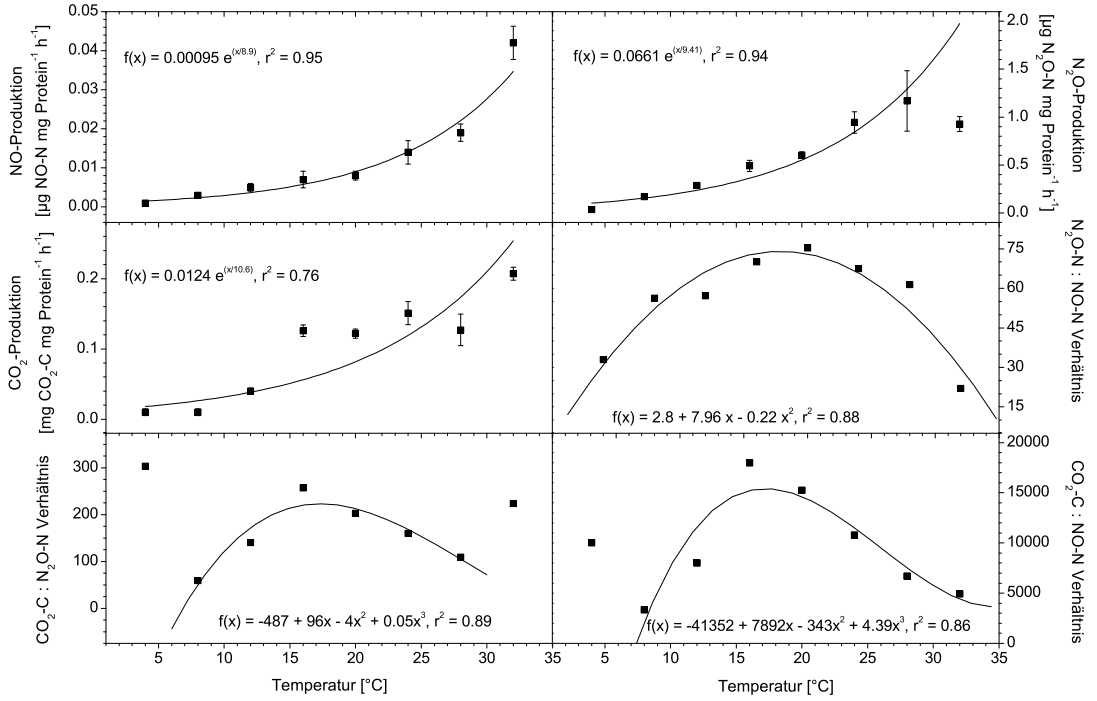

Abbildung 6: Einfluss der Temperatur auf die NO-, N_2O- und CO_2-Produktion von *A. faecalis p.* (für weitere Angaben siehe auch Kesik et al., **I**).

Der berechnete Q_{10} Wert für den Bereich von 4 °C und 32 °C, der die Temperaturabhängigkeit der NO-Produktion von *A. faecalis p.* widerspiegelt, beträgt 3,9. Für den Temperaturbereich zwischen 4 °C und 16 °C wurde ein Q_{10} Wert

von 3,1 berechnet. Dieser Wert ist nur geringfügig höher als der Q_{10} Wert, der von Gasche und Papen (1999) im Rahmen von Feldversuchen für den Temperaturbereich zwischen 5 °C und 15 °C berechnet wurde. Sie errechneten für die NO-Emissionen aus einem N-gesättigten Fichtenboden in Bayern einen Q_{10} Wert zwischen 2,6 und 2,9. Ebenso stimmen die Ergebnisse der vorliegenden Arbeit mit den Ergebnissen von Ormeci et al. (1999) überein, die die Temperaturabhängigkeit der mikrobiellen NO-Produktion in landwirtschaftlichen Böden untersucht haben. Die Arbeit von Ormeci et al. (1999) zeigt unter kontrollierten Laborbedingungen einen starken Anstieg der NO-Produktion von 0 bis fast auf 60 ng N m^{-2} s^{-1} für einen Temperaturbereich zwischen 1 °C und 48 °C. Entsprechend der Ergebnisse dieser Arbeit, konnten auch Ormeci et al. (1999) kein Temperaturoptimum der NO-Produktion aufzeigen.

Vergleichbare Ergebnisse zu der NO-Produktion von *A. faecalis p.* wurden für die Temperaturabhängigkeit der N_2O-Produktion erzielt (Abbildung 6). Der Q_{10} Wert der N_2O-Produktion für die Temperaturzunahme von 4 °C auf 32 °C beträgt 1,8. Im Gegensatz zur NO-Produktion erreichte die N_2O-Produktion bei 28 °C ihr Optimum mit 1,17 ± 0,32 μg N_2O-N mg Protein^{-1} h^{-1}, bei 32 °C nahm sie wieder ab (0,93 ± 0,8 μg N_2O-N mg Protein^{-1} h^{-1}). Die von *A. faecalis p.* produzierte N_2O-Rate war um ca. 20-70fach höher als die NO-Produktionsrate (Abbildung 6). Das Verhältnis der N_2O- zu NO-Produktion wurde signifikant durch die Temperatur beeinflusst; so betrug es >50 im Temperaturbereich zwischen 8 °C und 28 °C und <36 bei 4 °C und bei 32 °C. Diese Ergebnisse stimmen mit den Untersuchungen anderer Autoren, die den Temperatureffekt auf die N_2O-Produktion bzw. -Emission schätzten, überein. So berechneten Sitaula und Bakken (1993) für die meisten ihrer Standorte eines 63jährigen Fichtenwaldes Q_{10} Werte für die N_2O-Produktion von 1,5 bis 2,7 in einem Temperaturbereich zwischen 10 °C und 15 °C, und Q_{10} Werte von 0,3 bis 2,4 in einem Temperaturbereich von 3 °C bis 10 °C. Papen und Butterbach-Bahl (1999) fanden während einer 3jährigen Untersuchung, in der die N_2O-Produktion für eine Kontroll- und eine gekalkte Fichten- und Buchen-Fläche kontinuierlich aufgezeichnet wurde, heraus, dass die Bodentemperatur, dicht gefolgt von der Bodenfeuchte, den größten Einfluss auf die N_2O-Emission aufweist. Für einen Temperaturbereich von 5 °C bis 15 °C berechneten sie Q_{10} Werte für die N_2O-Emissionen zwischen 1,7 und 6,5. In diesem Q_{10} Wertebereich liegt der in dieser Arbeit berechnete Q_{10} Wert von 4,6 für die N_2O-Produktion durch *A. faecalis p.* für einem Temperaturbereich von 4 °C bis 16 °C.

Die Abhängigkeit der CO_2-Produktion durch *A. faecalis p.* von der Temperatur kann im Temperaturbereich zwischen 4 °C und 32 °C mit Hilfe einer Exponentialfunktion beschrieben werden (Abbildung 6). Der höchste Mittelwert der CO_2-Produktion wurde bei 32 °C gemessen (0,21 ± 0,009 mg CO_2-C mg Protein^{-1} h^{-1}). Der Q_{10} Wert für den Temperaturbereich zwischen 4 °C und 32 °C beträgt

1,9. Dieser Q_{10} Wert für die CO_2- Produktion befindet sich innerhalb von 1,3 und 2,7 für unterschiedliche Temperaturbereiche zwischen 7 °C und 17 °C, die von Brumme (1995) für die CO_2-Emissionen aus einem Buchenwald bei Solling berechnet wurden.
Das Verhältnis der CO_2- zu N_2O- und CO_2- zu NO-Produktion (Abbildung 6) in Abhängigkeit zur Temperatur kann mit einer Optimumkurve beschrieben werden. Das Optimum befindet sich bei 15 °C. Die Temperaturabhängigkeit der CO_2- zu N_2O- und CO_2- zu NO-Verhältnisse deuten darauf hin, dass sich bei Temperaturen oberhalb des Optimums der Anteil der Nitrifikation und Denitrifikation an der gesamten N-Spurengasproduktion durch *A. faecalis p.* verändert, d.h. die Denitrifikation als Quelle der N-Spurengasproduktion an Bedeutung gewinnt.

2.3 Abhängigkeit der N_2O- und NO-Emissionen vom pH Wert

Die Abhängigkeit der N_2O- und NO-Produktion vom pH Wert im Pepton-Fleischextrakt Medium wurde in dem pH Wertbereich zwischen pH 3 und pH 8 untersucht. Der Einfluss des pH Wertes auf die NH_4^+, NO_2^-, NO_3^- und Protein-Konzentrationen sind im Ergebnisteil und in Tabelle 2 in der Arbeit von Kesik et al. (2005, **I**) beschrieben.
Die höchste NO-Produktion wurde bei pH 3 ($0{,}45 \pm 0{,}12$ μg NO-N mg Protein^{-1} h^{-1}) und die niedrigste bei pH 5 ($4{,}21 \times 10^{-3} \pm 1{,}36 \times 10^{-4}$ μg NO-N mg Protein^{-1} h^{-1}) gemessen. Auch bei pH 7 nahm die NO-Produktion signifikant bis hin zu Produktionsraten von $0{,}18 \pm 0{,}02$ μg NO-N mg Protein^{-1} h^{-1} zu (Abbildung 7). Der Einfluss des pH Wertes auf die Produktion, Konsumption und Emission von NO in/aus Böden wurde von zahlreichen Publikationen bestätigt. So fanden Remde und Conrad (1991) heraus, dass im Vergleich zu einem sauren Waldboden (pH 4,7), niedrige Raten der aeroben und hohe Raten der anaeroben NO-Produktion im alkalischen landwirtschaftlichen Böden anzutreffen sind. Ebenso berichteten Baumgärtner und Conrad (1992) über höhere anaerobe NO-Produktionsraten aus alkalischen Graslandböden im Gegensatz zu sauren Waldböden (pH 4,4). Krämer und Conrad (1991) hingegen fanden höhere anaerobe und aeroben NO-Produktionsraten aus alkalischen Landwirtschaftsböden (pH 7,8), was wiederum mit den in dieser Arbeit vorgestellten Ergebnissen übereinstimmt, in der hohe NO-Produktionsraten bei pH 7 gemessen wurden.

Die N_2O-Produktion wurde ebenfalls signifikant durch den pH Wert im Medium beeinflusst. So wurde bei die N_2O-Produktion durch *A. faecalis p.* die höchsten Raten bei pH 7 ($2{,}57 \pm 0{,}17$ μg N_2O-N mg Protien^{-1} h^{-1}) beobachtet, wohingegen bei pH 3 und pH 4 die durchschnittlichen N_2O-Produktionsraten zwischen 1,61

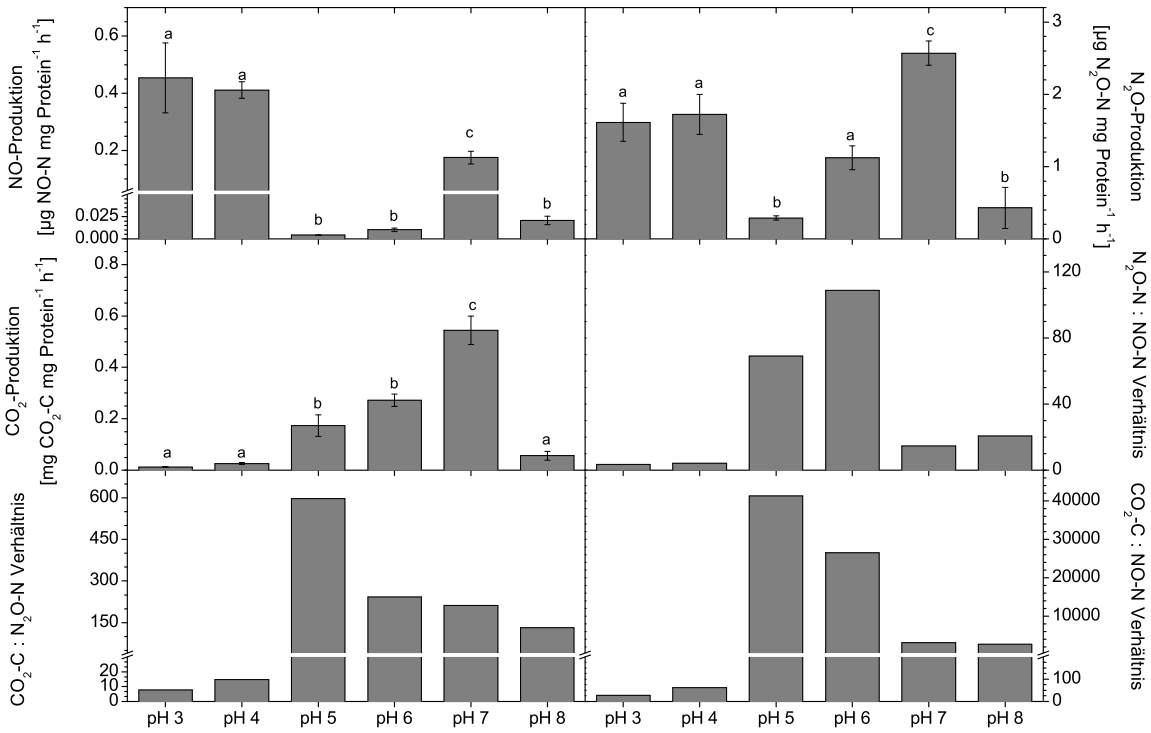

Abbildung 7: Einfluss des pH Wertes auf die NO-, N_2O- und CO_2-Produktion von *A. faecalis p.* Der Mittelwert der ± Standardfehler mit dem gleichen Buchstaben sind nicht signifikant unterschiedlich ($P < 0.05$) (für weitere Angaben siehe auch Kesik et al., **I**).

und 1,72 μg N_2O-N Protein^{-1} h^{-1} lagen. Die niedrigste N_2O-Produktion wurde bei pH 5 (0,29 ± 0,03 μg N_2O-N mg Protein^{-1} h^{-1}) gemessen (Abbildung 7). Die Ergebnisse der eigenen Laboruntersuchungen sind in Übereinstimmung mit den Experimenten von Yoshida und Alexander (1970). Bei der Untersuchung der N_2O-Produktion in den pH Bereichen zwischen pH 6,0 und pH 10,7 fanden die letztgenannten Autoren die höchsten N_2O-Raten, die vom autotrophen Nitrifizierer *Nitrosomonas europaea* produziert wurden, im Bereich zwischen pH 8,0 und pH 8,4. Bei zunehmenden bzw. abnehmenden pH Werten nahm die N_2O-Produktion ab. In den vorliegenden eigenen Untersuchungen nahm die N_2O-Produktion von *A. faecalis p.* bei pH ≤ 4 bis hin zu Raten von z.B. 1,72 μg N_2O-N mg Protein^{-1} h^{-1} erneut zu. Dieses Ergebnis stimmt mit den Untersuchungen von Yamulki et al. (1997) und Ellis et al. (1998) überein, die ebenso ein sekundäres Optimum der N_2O-Produktion bei niedrigen pH Werten beobachtet haben.

Der Einfluss des pH Wertes auf die CO_2-Produktion ist ähnlich dem auf die N_2O-Produktion, mit einer höchsten CO_2-Produktion bei pH 7 (0,54 ± 0,06 mg CO_2-C mg Protein^{-1} h^{-1}). Im Gegensatz zur N_2O- und NO-Produktion nahm die CO_2-Produktion bei pH Werten < 5 nicht zu, sondern stagnierte bis hin zu Produktionsraten von 0,01 ± 0,001 mg CO_2-C mg Protein^{-1} h^{-1} (Abbildung 7). Diese Tatsache und der Befund, dass sowohl die CO_2- zu N_2O-, als auch die CO_2- zu NO-Produktionsraten < 65 liegen, zeigen, dass die Verlustraten der N-Spurengasproduktion während der C- und N-Umsetzungsprozesse mit abnehmenden pH Werten im Medium signifikant zunehmen. In Übereinstimmung mit diesen Ergebnissen wurde von Sitaula et al. (1995) eine Abnahme der CO_2-Produktion mit abnehmendem pH Wert festgestellt. Der gleiche Effekt wurde von Ellis et al. (1998) im Rahmen vom Park Grass Experiment bestätigt.

Um den Einfluss unterschiedlicher Substrate auf die Produktion von N_2O und NO zu untersuchen, wurde die Produktion von N_2O und NO durch *A. faecalis p.* sowohl auf dem Pepton-Fleischextrakt Medium als auch auf einem Ammonium-Citrat Medium bei unterschiedlichen pH Werten im Fermenter betrachtet. Die N_2O- und besonders die NO-Produktion in Experimenten, in denen *A. faecalis p.* auf Ammonium-Citrat Medium wuchs, war signifikant niedriger als in den Experimenten mit *A. faecalis p.* auf Pepton-Fleischextrakt Medium. So produzierte *A. faecalis p.*, auf dem Ammonium-Citrat Medium wachsend, bei pH 7 0,013 ± 0,002 μg NO-N mg Protein^{-1} h^{-1} und 1,46 ± 0,13 μg N_2O-N mg Protein^{-1} h^{-1}, und auf dem Pepton-Fleischextrakt Medium wachsend 0,175 ± 0,022 μg NO-N mg Protein^{-1} h^{-1} und 2,57 ± 0,17 μg N_2O-N.
Die NO-Produktionsraten waren bei allen pH Werten < 0,020 μg NO-N mg Protein^{-1} h^{-1} (Durchschnitt: 0,012 ± 0,0012 μg NO-N mg Protein^{-1} h^{-1}). Daher konnte kein signifikanter Einfluss des pH Wertes auf die NO-Produktion auf dem Ammonium-Citrat Medium festgestellt werden.
Der pH Wert beeinflusste die N_2O-Produktion von *A. faecalis p.* auf dem Ammonium-Citrat Medium in ähnlicher Weise wie auf dem Pepton-Fleischextrakt Medium. Bei beiden Media war die N_2O-Produktion bei pH 7 am höchsten und nahm mit kleineren pH Werten ab. Jedoch konnte keine Zunahme der N_2O-Produktion bei pH Werten von pH < 4 beim Ammonium-Citrat Medium festgestellt werden, wie sie beim Pepton-Fleischextrakt Medium gemessen werden konnte. Ergebnisse für pH Werte < 4 konnten nicht erzielt werden, da *A. faecalis p.* auf dem Ammonium-Citrat Medium die Kriterien des steady-states bei solch niedrigen pH Werten nicht erfüllen konnte.
Die CO_2-Produktionsraten von *A. faecalis p.* auf dem Ammonium-Citrat Medium sind beinahe in der gleichen Größenordnung wie die von *A. faecalis p.* auf dem Pepton-Fleischextrakt Medium. So wurde wie auch schon beim Pepton-Fleischextrakt Medium die höchste CO_2-Produktion bei pH 7 gemessen (0,29 ± 0,03 mg CO_2-C mg Protein^{-1} h^{-1}).

Um herauszufinden, ob der Einfluss des pH Wertes auf die N-Spurengasproduktion, die bei *A. faecalis p.* beobachtet wurde, auf andere heterotroph nitrifizierende und denitrifizierende Mikroorganismen übertragbar ist, wurden Experimente mit *P. pantotrophus* auf dem Ammonium-Citrat Medium in einem pH Bereich zwischen pH 6 und pH 9 durchgeführt. Aufgrund des schlechten Wachstums von *P. pantotrophus* auf dem Ammonium-Citrat Medium war es nicht möglich, diesen Mikroorganismus unterhalb eines pH Wertes von pH 6 zu kultivieren. Bereits bei pH Werten von pH 6 und pH 9 war das Wachstum von *P. pantotrophus* auf dem Ammonium-Citrat Medium nicht konstant.
Innerhalb des untersuchten pH Wertbereiches konnte kein signifikanter Einfluss der unterschiedlichen pH Werte auf die NO-Produktion durch *P. pantotrophus* festgestellt werden.
Im Gegensatz hierzu konnte ein eindeutiger pH Einfluss auf die N_2O-Produktion durch *P. pantotrophus* aufgezeigt werden. Die höchste N_2O-Produktion (7,46 $\pm$ 0,36 μg N_2O-N mg Protein^{-1} h^{-1}) durch *P. pantotrophus* konnte bei pH 8 beobachtet werden. Die N_2O-Produktion nahm bei abnehmenden bzw. zunehmenden pH Werten evident ab. Zu betonen ist, dass die beobachtete maximale N_2O-Produktion durch *P. pantotrophus* um das 7fache höher war als die höchste N_2O-Produktionsrate von *A. faecalis p.* auf dem Ammonium-Citrat Medium (1,46 $\pm$ 0,13 μg N_2O-N mg Protein^{-1} h^{-1}). Das pH Optimum der N_2O-Produktion durch *P. pantotrophus* verglichen mit dem von *A. faecalis p.*, verschiebt sich von pH 7 zu pH 8.
Die CO_2-Produktion von *P. pantotrophus* auf dem Ammonium-Citrat Medium entspricht nahezu der von *A. faecalis p.* auf dem gleichen Medium. Beim pH Wert 7 beträgt die CO_2-Produktion von *A. faecalis p.* 0,2922 $\pm$ 0,0286 mg CO_2-C mg Protein^{-1} h^{-1} und die von *P. pantotrophus* 0,2965 $\pm$ 0,0314 mg CO_2-C mg Protein^{-1} h^{-1}. Sogar bei pH 6 konnten für beide Mikroorganismen fast gleiche CO_2-Produktionsraten beobachtet werden.

2.4 Chemodenitrifikation als Ursache für die erhöhte N_2O- und NO-Produktion unter sauren Bedingungen?

Um herauszufinden, ob die hohen N_2O- und NO-Produktionsraten bei pH < 4 allein abhängig von der mikrobiellen Aktivität sind, oder ob ein Teil des produzierten N_2O und NO durch die chemische Umwandlung von Nitrit über den Prozess der Chemodenitrifikation entsteht, wurde im Fermenter Nitrit in Konzentrationen, die in den vorangegangenen Experimenten gemessen wurden (0,01 - 0,2 mg NO_2^--N l^{-1}) zum sterilen Pepton-Fleischextrakt Medium zugegeben. Die Ergebnisse dieser Versuche für die pH Werte von pH 3, pH 3,5, pH 4, pH 4,5 und

pH 5 sind in Abbildung 8 (durchgezogene Linie) dargestellt. Sie werden mit den beobachteten N_2O- und NO-Produktionsraten von *A. faecalis p.* in den vorangegangenen Experimenten verglichen (gepunktete Line). Die Abbildung zeigt, dass die höchste NO:NO_2^- und N_2O:NO_2^- Produktion durch die Chemodenitrifikation bei pH 3 stattfindet. Bei diesem pH Wert betrug die N_2O-Produktion durch die Chemodenitrifikation für eine NO_2^--Konzentration im Medium von 0,40 ± 0,08 mg NO_2^--N l^{-1} 2,65 ± 0,6 μg N_2O-N l^{-1} h^{-1}. Das N_2O- zu NO_2^--Verhältnis beträgt somit 5,89 ± 0,98 × 10^{-3} h^{-1}.
Betrachtet man die NO-Produktion durch die Chemodenitrifikation, dann waren diese Werte mehr als 20mal höher als bei der N_2O-Produktion. Dies zeigt, dass bei niedrigen pH Werten vor allem NO und weniger N_2O ausgehend vom NO_2^- über die Chemodenitrifikation produziert wird. Die Höhe der NO- und N_2O-Produktion über den Weg des nicht-biologischen Prozesses der Chemodenitrifikation ist vom pH Wert des Mediums stark abhängig (Abbildung 8). Dieses Experiment zeigt, dass das mikrobiologisch produzierte Nitrit über die Chemodenitrifikation bei pH Werten <4 bis zu 62% zu NO und bis zu 0,8% zu N_2O umgewandelt wird. Im Gegensatz hierzu wird NO und N_2O bei pH Werten $\geq$ 4,5 ausschließlich über die Nitrifikation und Denitrifikation produziert.

Hohe NO-Produktionsraten bei niedrigen pH Werten wurden auch von zahlreichen Autoren beobachtet. So beschreibt Ormeci et al. (1999) einen starken Anstieg um zwei Größenordnungen der NO-Produktion, sobald der pH Wert der Bodenproben bei der Zugabe von 0,1 N HCl von pH 5,8 auf pH 4,5 reduziert wurde. Ebenso berichten andere Autoren über zunehmende NO-Produktion unter Bedingungen mit niedrigen pH Werten. Koskinen und Keeney (1982) beobachteten die höchste NO-Produktion während der Denitrifikation bei den landwirtschaftlichen Böden mit den sauersten Bedingungen. Yamulki et al. (1997) untersuchte die höchsten NO-Emissionsraten aus Grünlandböden bei pH Werten von pH 3,9.

Ohne Zweifel ist ein Teil der erhöhten NO-Emissionen bei niedrigen pH Werten auf die Chemodenitrifikation zurückzuführen, und hierbei spielt das Nitrit eine entscheidende Rolle (Van Cleemput und Baert, 1984). Daher sind die hohen NO- und z.T. auch N_2O-Produktionsraten bei niedrigen pH Werten auf die Kombination von mikrobiellen und chemischen Umwandlungsreaktionen zurückzuführen. Nur wenn Nitrit vorhanden ist und niedrige pH Werte vorherrschen, kann der Prozess der Chemodenitrifikation stattfinden.

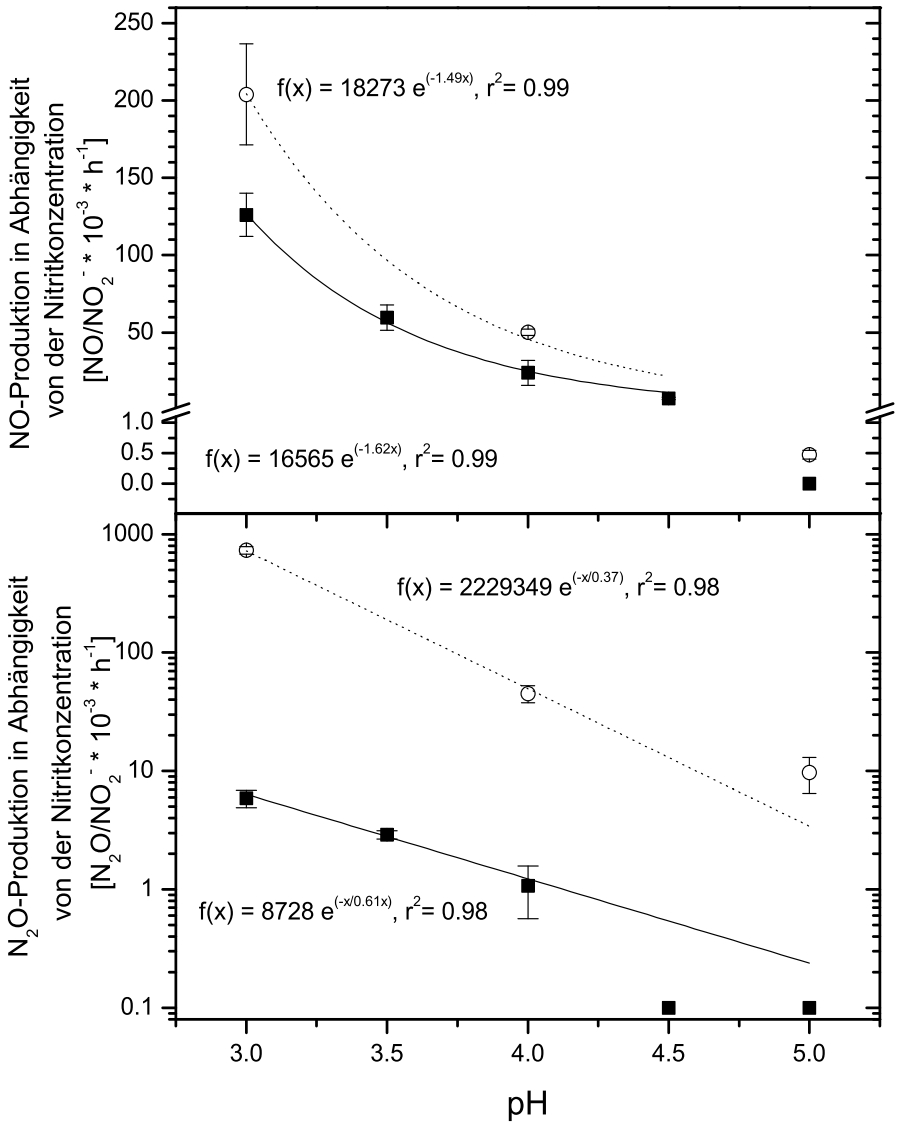

Abbildung 8: NO- und N_2O-Produktion durch den mikrobiologischen Prozess der Chemodenitrifikation in Abhängigkeit vom pH Wert des Mediums bei 28 °C. Für dieses Experiment wurde steriles Medium (durchgezogene Linie) mit einer Konzentration von 2 mM NO_2^--N angereichert bzw. Medium mit *A. faecalis p.* (gepunktete Linie) in einer sich im steady-state befindlichen Fermenterkultur untersucht. Es konnten beim pH Wert > 4,5 keine NO-Produktion und beim pH Wert > 4,0 keine N_2O-Produktion über die Chemodenitrifikation festgestellt werden.

2.5 Abhängigkeit der N_2O- und NO-Produktion vom O_2-Sättigungsgrad

Im Rahmen dieser Doktorarbeit sollte in diesem Experiment untersucht werden, wie sich die N_2O- und NO-Produktionsraten in Abhängigkeit von unterschiedlichen Sauerstoffkonzentrationen im Fermenter verändern. Am Anfang des Experimentes, bei einer O_2-Sättigung von 20-80%, befanden sich die N_2O- und NO-Produktionsraten auf niedrigem Niveau (siehe auch Blagodatsky, S., Kesik, M., Papen, H. und Butterbach-Bahl, K., 2005, **IV**). Daraus ist zu schließen, dass unter diesen aeroben Bedingungen die beiden Spurengase über die Nitrifikation gebildet werden. Sobald jedoch der Sauerstoffgehalt im Fermenter abnimmt, treten in diesem Übergangsbereich zwischen aeroben und anaeroben Bedingungen deutlich erhöhte NO- und N_2O-Produktionsraten auf (Abbildung 9). Ursache dafür ist, dass die denitrifikatorischen Enzyme Nitritreduktase und NO-Reduktase aufgrund der O_2-Empfindlichkeit angeregt werden, und somit zusätzlich N_2O und NO über den Weg der Denitrifikation produzieren können. Unter nahezu anaeroben Bedingungen wird die N_2O- und NO-Produktion wieder drastisch reduziert. Dies kann vermutlich darauf zurückgeführt werden, dass erst unter diesen starken anaeroben Bedingungen das Enzym N_2O-Reduktase, dass als Endprodukt der Denitrifikation N_2 bildet, angeregt wird und N_2O nahezu vollständig zu N_2 umwandelt. Bei erneuter O_2-Zufuhr der anaeroben Kultur kommt es bei noch sehr niedrigen O_2-Sättigungsgraden im Übergangsbereich sehr schnell zu einer Hemmung der extrem O_2-empfindlichen N_2O-Reduktase, so dass N_2O wieder mit steigenden Raten freigesetzt wird (vgl. Abbildung 9). Jedoch konnte eine simultane Stimulierung der NO-Freisetzung nicht beobachtet werden. Diese hohen NO- und N_2O-Produktionsraten im Übergangsbereich zwischen den aeroben und anaeroben Bedingungen und vice versa, die in diesem Experiment beobachtet werden konnten, wurden auch bei autotrophen (Remde und Conrad, 1990) und heterotrophen Nitrifizierern (Otte et al., 1996) und bei denitrifizierenden Mikroorganismen (McKenney et al., 1994) festgestellt.

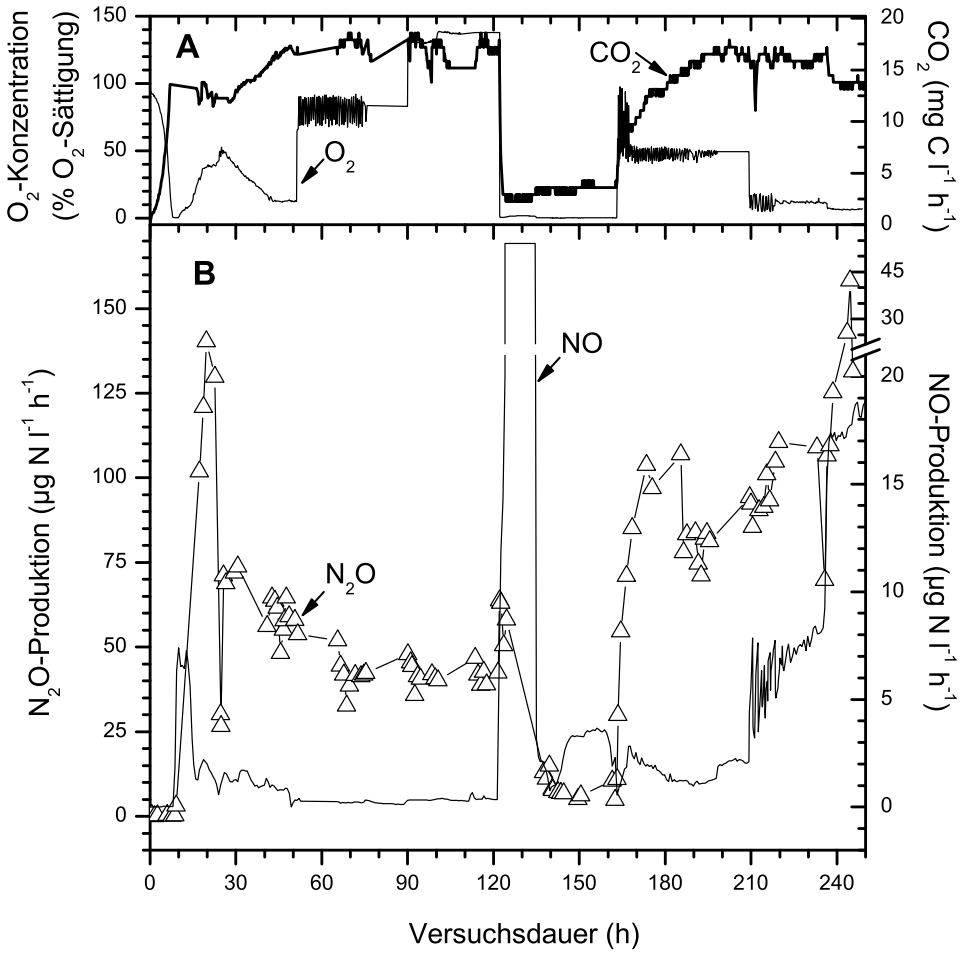

Abbildung 9: Einfluss der verschiedenen O_2-Konzentrationen auf die CO_2-Produktion (A) und die N_2O- und NO-Produktion (B) von *A. faecalis p.* in einer kontinuierlichen Kultur (verändert, aus Blagodatsky, S., Kesik, M., Papen, H., und Butterbach-Bahl, K., 2005, **IV**).

2.6 Parametrisierung der Laborexperimente

Um die Beschreibung der Prozesse im PnET-N-DNDC weiter zu entwickeln und zu verbessern, wurden die in den Laborversuchen mit *Alcaligenes faecalis p.* gefundenen Abhängigkeiten der NO- und N_2O-Produktion zum pH Wert in das Modell aufgenommen. Die Ergebnisse der Laboruntersuchungen wurden parametrisiert und als Algorithmen in das PnET-N-DNDC implementiert. Das PnET-N-DNDC wurde mit Hilfe der in den Prozessstudien im Labor erhaltenen Ergebnisse kalibriert.
Die Chemodenitrifikation ist bereits im PnET-N-DNDC als eigenständige chemische Reaktion, die zusätzlich mit einer Arrhenius-Funktion für die Temperaturabhängigkeit ($T[layer]$) ausgestattet ist, implementiert (Li et al., 2000; Stange, 2000). Im Rahmen dieser Arbeit wurde die Chemodenitrifikation ($Chem_{NO}$) in Abhängigkeit zu Boden pH Wert ($pH_{soil}[layer]$) zusätzlich an die Nitrit-Konzentration ($NO_2[layer]$) in den einzelnen Bodenhorizonten gekoppelt.

$$Chem_{NO}\,[kg\,N\,ha^{-1}\,day^{-1}] \;=\; 300 \cdot NO_2[layer] \cdot 16565 \cdot \exp^{(-1.62\,\cdot\,pH_{soil}[layer])} \cdot f1)$$

$$f1 \;=\; \exp^{\left(\frac{-31494}{(T[layer]+273.18)\,\cdot\,8.3144}\right)} \text{(Stange, 2000)}$$

2.7 Schlussbemerkung

Wie bereits erwähnt ist *A. faecalis p.* ein im Boden häufig vorkommender Mikroorganismus (Gamble et al., 1977). Aufgrund der guten Übereinstimmung zwischen den im Rahmen dieser Arbeit erhaltenen Ergebnisse der Fermenteruntersuchungen und anderer Feld- und Labormessungen zum Einfluss der Temperatur, der Sauerstoffsättigung, des Substrates und des pH Wertes auf die N_2O-, NO- und CO_2-Produktion, kann *A. faecalis p.* als Indikatororganismus für alle Mikroorganismen im Boden dienen. Daher ist *A. faecalis p.* ein idealer Modellorganismus für weitere Untersuchungen zur Kinetik der N-Spurengasproduktion durch die mikrobiellen Prozesse der Nitrifikation und Denitrifikation. Solche Prozessstudien werden besonders benötigt, um biogeochemische Modelle, wie z.B. das PnET-N-DNDC, weiterzuentwickeln und numerische Algorithmen zu testen, um schließlich die Vorhersagegenauigkeit solcher Modelle zu verbessern.

3 Modellierung der N_2O- und NO-Emissionen aus Waldböden Europas

Wie bereits in der Einleitung erwähnt, können verbesserte Abschätzungen des Beitrags von Böden zu nationalen bzw. regionalen Budgets der N-Spurengasemissionen nicht nur über die Intensivierung von Feldmessungen erreicht werden. Als Lösungsweg bietet sich allein die prozessorientierte Modellierung an. In dieser Arbeit wurde das biogeochemische Modell PnET-N-DNDC an ein GIS gekoppelt. Die Kopplung von GIS mit biogeochemischen Modellen wurde in jüngster Zeit bereits in einer Reihe von Studien zur Berechnung von regionalen bzw. globalen N_2O- und NO-Emissionskatastern aus Böden untersucht (z.B. Potter et al., 1996; Davidson et al., 1998; Butterbach-Bahl et al., 2001, 2004; Brown et al., 2002; Li et al., 2001, 2004). Diese Vorgehensweise hat Vorteile gegenüber reinen statistischen Ansätzen, in denen einzelne oder mehrere Feldmessungen an einem oder mehreren Standorten auf größere Regionen extrapoliert werden. Denn biogeochemische Modelle können unser jetziges Verständnis über die Umweltfaktoren, die die Höhe der Spurengasemissionen beeinflussen, wie die meteorologischen Bedingungen, die Bodeneigenschaften (pH, organischer Kohlenstoff im Boden, Bodentextur) oder – besonders im Zusammenhang mit landwirtschaftlichen Böden – die Bewirtschaftung der Böden, darstellen und zusammenfassen. Zahlreiche Untersuchungen haben gezeigt, dass diese Faktoren die Prozesse der Produktion, Konsumption und Emission von N-Spurengasen beeinflussen (z.B. Barnard et al., 2005; Conrad, 2002). Daher wird angenommen, dass die Komplexität dieser Prozesse, die die Ursache für die beobachtete große räumliche und zeitliche Variabilität der Emissionen ist, wenigstens zum Teil durch biogeochemische Modelle zur Berechnung von N-Spurengasemissionskatastern nachgeahmt werden kann (Li et al., 2000, 2001). In dieser Arbeit und in der Publikation von Kesik et al. (2005, **II**) wird gezeigt, dass das PnET-N-DNDC ein geeignetes Modell ist, um N-Spurengasemissionen aus Waldböden zu simulieren.

3.1 Beschreibung des biogeochemischen Modells PnET-N-DNDC

Das biogeochemische Modell PnET-N-DNDC wurde entwickelt, um die C- und N-Spurengase in temperaten Waldökosystemen vorherzusagen und die damit assoziierten NO- und N_2O-Emissionen aus Waldböden zu simulieren. Dieses Modell setzt sich aus drei bereits bestehenden Modellen zusammen: PnET- (= **P**hotosy**n**thesis-**E**vapo**t**ranspiration-Modell), DNDC- (= **D**e**ni**trification-**D**e**c**omposition-Modell) sowie das N-Modell (= **N**itrification-Modell). Das PnET ist ein waldphysiologisches Modell, das die Photosynthese, die Atmung, die organische Kohlenstoffproduktion und –verteilung sowie die Abfallproduktion des Waldes simuliert. Es wurde von Aber und Federer (1992) entwickelt. Das DNDC ist ein biogeochemisches Modell, das die organische Stoffzersetzung im Boden und den Stickstoffumsatz auf landwirtschaftlichen Flächen vorhersagt und von Li et al. (1992) entworfen wurde. Das N-Modell wurde von Stange (2000) entwickelt, um Nitrifikationsraten, das Wachstum der Nitifizierer und die durch die Nitrifikation bedingte NO- und N_2O-Produktion vorherzusagen. Zahlreiche Feld- und Labormessungen haben gezeigt, dass bodenbürtige N_2O- und NO-Emissionen direkt durch Umweltfaktoren, wie Temperatur, Feuchte, pH Wert und Substrateigenschaften (C-, N-Gehalte) beeinflusst werden. Diese Umweltfaktoren werden durch sog. ,,Ökologische Treiber“ (Abbildung 10), wie Klima, Bodeneigenschaften, Vegetation und anthropogene Eingriffe, gesteuert. Die Verbindung zwischen den beiden Komponenten (Umweltfaktoren und ,,Ökologischen Treiber“) und den N_2O- und NO-Emissionen bilden sechs Module. Das Bodenklima-Modul, das Waldwachstum-Modul (PnET), das Mineralisation-Modul (DC), das Nitrifikation-Modul (N), das Denitrifikation-Modul (DN) und das Methanoxidation-Modul (wird nicht näher erläutert) werden im Folgenden beschrieben.

3.1.1 Das Waldwachstum-Modul

Im Waldwachstum-Modul wird das durch Sonneneinstrahlung, Temperatur, Wasser- und Stickstoff-Belastung beeinflusste Waldwachstum simuliert. Es errechnet die Bruttophotosyntheseleistung eines Baumbestands anhand der einfallenden, photosynthetisch aktiven Strahlung (PAR), den pflanzenspezifischen Parametern und der Wasser- und Nährstoffversorgung der Pflanzen durch den Boden. Die tägliche Nettophotosyntheseleistung ergibt sich durch die Subtraktion der simulierten Respirationsraten (Blatt-, Stamm- und Wurzelrespiration). Die im Modul aufgebauten C-Verbindungen werden in einem pflanzeninternen Pool gespeichert und stehen im nächsten Simulationsjahr für den Aufbau von Wurzel-, Stamm- und Blattbiomasse zur Verfügung. Außerdem gibt das Modul die Abfallproduktion, Wasser und N-Anforderung zum Bodenklima- bzw. zum Mineralisation-Modul weiter (Aber und Federer, 1992; Stange, 2000).

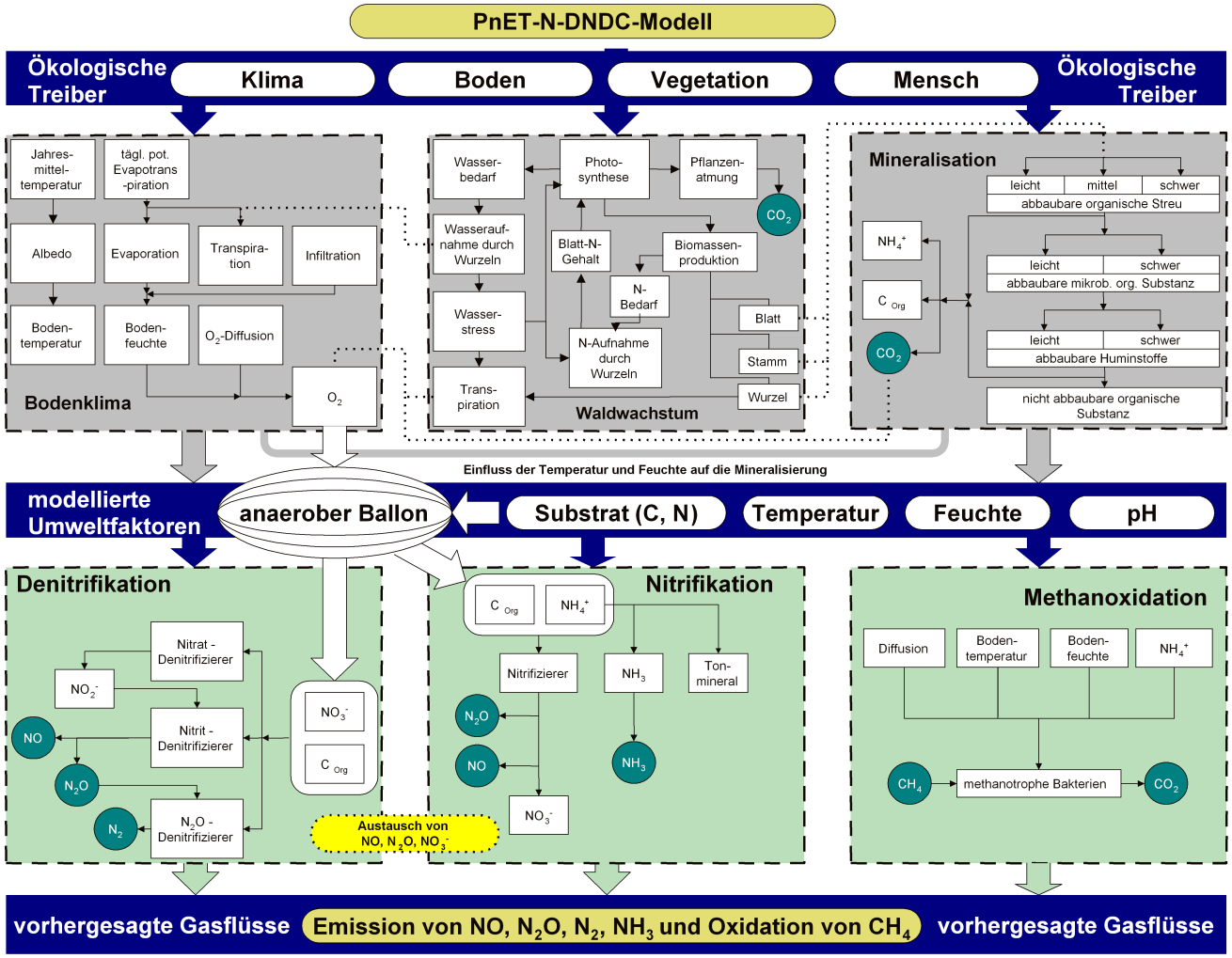

Abbildung 10: Schematische Darstellung des Modells PnET-N-DNDC, bestehend aus den sechs Einzelmodulen Bodenklima, Waldwachstum, Mineralisation, Nitrifikation, Denitrifikation und der Methanoxidation. Der Datenaustausch zwischen den Modulen wird durch die breiten Pfeile verdeutlicht (Li et al., 2000; modifiziert).

3.1.2 Das Bodenklima-Modul

Das Bodenklima-Modul wandelt Tagesklimadaten in Bodentemperatur und Bodenfeuchte um und berechnet die O_2-Konzentration der Bodenluft im Bodenprofil. Die berechnete O_2-Konzentration ist die Steuergröße des sogenannten ,,anaeroben Ballons“, d.h. des Bodenteils, in dem anaerobe Bedingungen herrschen und die Prozesse der Denitrifikation ablaufen (Stange, 2000). Aus dem Bodenwasserfluss, der Transpiration des Waldbestands sowie der Evaporation der Bodenoberfläche wird die Bodenfeuchte in den einzelnen Bodenschichten ermittelt. Die Bodentemperatur ist abhängig von der Lufttemperatur und der Temperatur in 1,5 m Bodentiefe (= mittlere Jahrestemperatur). Die Temperaturdifferenz im Boden wird durch ein Wärmetransportmodell beschrieben, in dem der stattfindende Wärmetransport durch die Temperaturdifferenz zwischen zwei Bodenschichten angetrieben wird. Ebenso wird der Einfluss des Schnees, der eine stark isolierende Wirkung aufweist, berücksichtigt. Wenn die Temperatur in einer Bodenschicht unter 0 °C sinkt, so gefriert im PnET-N-DNDC das vorhandene Wasser zu Eis (Abbildung 11). Mit Hilfe der Schmelzenthalpie für Wasser wird aus der Differenz zwischen Bodentemperatur und der benötigten Eistemperatur die Menge des zu gefrierenden Wassers berechnet (Stange, 2000).

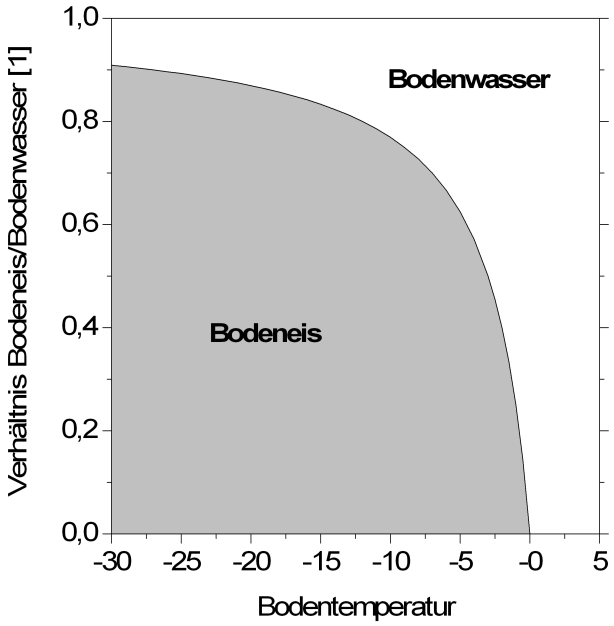

Abbildung 11: Verhältnis zwischen Bodenwasser und Bodeneis in Abhängigkeit von der Bodentemperatur (Stange, 2000).

3.1.3 Das Mineralisation-Modul

Das Mineralisation-Modul simuliert die Zersetzung von Waldbestandsabfall im Boden und setzt dabei Ammonium, Nitrat und gelösten organischen Kohlenstoff (C_{Org}) frei (Butterbach-Bahl et al., 2001). Die wichtigsten Steuergrößen für den Abbau von organischer Substanz in Böden sind die Bodenfeuchte und -temperatur. Im PnET-N-DNDC wird anhand der Weibull-Funktion berechnet, dass mit zunehmender Bodenfeuchte auch die Mineralisation zunimmt. Die Temperaturabhängigkeit wird anhand der O'Neill-Funktion, die im unteren Temperaturbereich exponentiell ansteigt und ein Optimum aufweist, errechnet. Die unterschiedliche Abbaubarkeit von organischen Verbindungen wird mit drei verschiedenen Komponenten, die unabhängig voneinander organische Stoffe zersetzen, den sog. Pools der organischen Streu (leicht abbaubar, mittel abbaubar und schwer abbaubar), simuliert. Das bei der Mineralisation freigesetzte Ammonium steht für weitere Prozesse, wie z.B. Nitrifikation, Pflanzenaufnahme oder mikrobielle Immobilisierung zur Verfügung (Li et al., 1992, 2000; Stange, 2000).

3.1.4 Das Nitrifikation-Modul

Das Nitrifikation-Modul trifft Vorhersagen über das Wachstum und das Sterben von Nitrifizierern und simuliert den N-Umsatz während der Nitrifikation und die an diese assoziierte Spurengasproduktion. Die Nitrifikationsrate und die NO- und N_2O-Produktion sind von der Bodentemperatur, der Feuchtigkeit, dem Ammonium- und dem C_{Org}-Gehalt abhängig. Die N-Umsetzungsgeschwindigkeiten werden von der Aktivität der Mikroorganismen und ihrer Enzyme bestimmt. Sowohl die N_2O- als auch die NO-Produktion durch die Nitrifikation basieren auf dem konzeptionellen „hole-in-the-pipe"-Modell von Firestone und Davidson (1989) (siehe Kapitel 1.2), das zusätzlich durch eine Temperatur- und Feuchtefunktion ergänzt wurde. Der Temperaturparameter wird ebenso wie beim Mineralisation-Modul durch die O'Neill-Funktion beschrieben, während der Feuchteparameter mittels der Weibull-Funktion bestimmt wird.
Die Chemodenitrifikation wurde im PnET-N-DNDC als eigenständige chemische Reaktion, die zusätzlich mit einer Arrhenius-Funktion für die Temperaturabhängigkeit ausgestattet ist, implementiert (Li et al., 2000; Stange, 2000). Im Rahmen dieser Arbeit wurde die Chemodenitrifikation zusätzlich an die Nitrit-Konzentration in den einzelnen Bodenhorizonten gekoppelt (siehe Kapitel 2.6).

3.1.5 Das Denitrifikation-Modul

Das Denitrifikation-Modul simuliert die Denitrifikation und den Wandel in der Populationsgröße von Denitrifizierern. Die Größe der Denitrifiziererpopulation berechnet sich aus den allgemeinen Umweltbedingungen für das Mikroorganismenwachstum (Bodentemperatur und Feuchtigkeit) und der Verfügbarkeit von Stoffwechselsubstraten ($C_{Org,}$ NO_3^-, NO_2^-, NO und N_2O). Die an die Denitrifikation gebundene NO- und N_2O-Produktion berechnet sich auf Grundlage des Belüftungszustandes des Bodens, der Substratverfügbarkeit und der Gasdiffusion (Butterbach-Bahl et al., 2001).
Da aerobe und anaerobe Kompartimente in derselben Bodenschicht vorkommen können, muss dieses auch im Modell simuliert werden. Hierfür wurde eine kinetische Methode entwickelt, der sog. ,,anaerobe Ballon“ (Abbildung 12). Die Größe des ,,anaeroben Ballons“ in einer Bodenschicht wird im PnET-N-DNDC mit Hilfe der O_2-Konzentration in dieser Bodenschicht berechnet. Wenn der ,,anaerobe Ballon“ anwächst, werden auch größere Anteile an Stoffmengen (C_{Org}, NH_4^+, NO_3^-, NO, N_2O) diesem anaeroben Bodenteil für die Denitrifikation zugeteilt und weniger Stoffmengen bleiben dann dem aeroben Teil für die Nitrifikation übrig. Zusätzlich wird der Weg für NO und N_2O, um den anaeroben Ballon zu verlassen, länger, so dass die Wahrscheinlichkeit, dass die N-Gase weiter durch die Denitrifikation reduziert werden, größer wird. Nimmt der ,,anaerobe Ballon“ ab, dann kehren sich die Prozesse entsprechend um (Li et al., 2000).

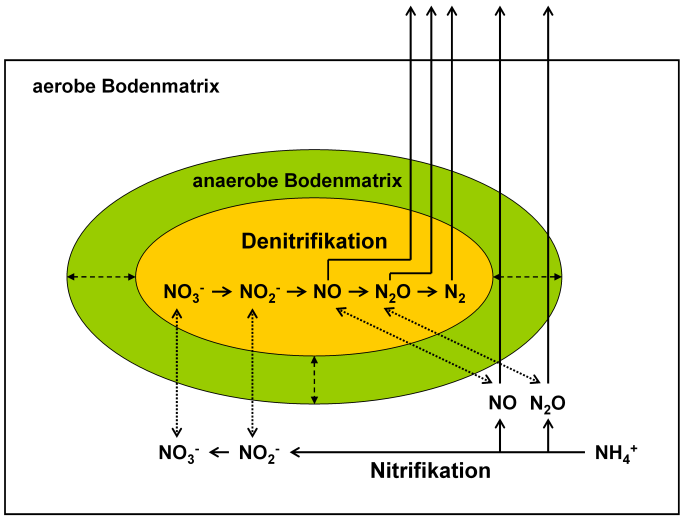

Abbildung 12: Schematische Darstellung des ,,anaeroben Ballons“, der das Verhältnis zwischen der aeroben und anaeroben Bodenmatrix beinhaltet. Nitrifikation findet in der aeroben Bodenmatrix (außerhalb des Ballons) und die Denitrifikation in der anaeroben Bodenmatrix (innerhalb des Ballons) statt (Li et al., 2000; modifiziert).

3.2 Validierung des Modells PnET-N-DNDC anhand von 19 Waldstandorten

Um zu überprüfen, ob das PnET-N-DNDC realistisch die Emission von N_2O und NO aus Waldböden simuliert, wurde das Modell mit Ergebnissen von Feldmessungen, die an 18 europäischen Messstandorten und einem Standort in den USA durchgeführt wurden, validiert (Tabelle 1 in Kesik et al. 2005, **II**). Das bedeutet, dass nach erfolgter Kalibrierung des Modells die vor Ort gemessenen N_2O- und NO-Emissionen mit den simulierten Emissionen für den jeweiligen Standort verglichen wurden. Die meisten dieser Waldstandorte sind Messstandorte innerhalb des EU-Projektes NOFRETETE. Die Standorte liegen über ganz Europa verteilt, mit einem borealen Waldstandort in Hyytiälä, Finnland; Waldstandorte mit maritim geprägtem Klima (z.B. Speulderbos, Niederlande; Sorø, Dänemark; und Glencorse, Schottland) und mit kontinental geprägtem Klima (Höglwald, Deutschland; Matrafüred, Ungarn) und Waldstandorte mit mediterranem Klimaeinfluss (San Rossore, Parco Ticino, Italien). Für alle Messstandorte wurden Informationen zu den Eingabegrößen des Modells PnET-N-DNDC und die N_2O- und NO-Emissionen in einer Datenbank für die Modellvalidierung aggregiert.

Der Vergleich der simulierten und gemessenen N_2O- und NO- Emissionen wird in Abbildung 13 exemplarisch für vier Standorte dargestellt. Die Abbildung zeigt in täglicher Auflösung die simulierten Ergebnisse gegenüber den gemessenen Ergebnisse der N_2O- und NO-Emissionen für die Messstandorte Höglwald (Fichte, Deutschland), Sorø (Buche, Dänemark), Hyytiälä (Kiefer, Finnland) und Glencorse (Sitka Fichte, Schottland).
Die simulierten N_2O-Emissionen auf dem Fichtenstandort im Höglwald waren durchschnittlich um 23% höher als die gemessenen Emissionen. Die Überschätzung der N_2O-Emissionen fand hauptsächlich in der ersten Hälfte des Jahres statt. Im Herbst dagegen wurden die N_2O-Emissionen um ca. 10-25% unterschätzt. Das PnET-N-DNDC konnte die beobachteten erhöhten Emissionen im Sommer gut darstellen, jedoch ist ein Zeitversatz von z.T. mehreren Tagen feststellbar. Dies bedeutet, dass in den Modellsimulationen erhöhte Emissionen früher als im Freiland beobachtet auftraten. Eine mögliche Ursache für diesen Zeitversatz ist, dass zum Zeitpunkt der simulierten erhöhten N_2O-Emissionen erhöhte Niederschläge auftraten, die sich im PnET-N-DNDC unmittelbar in diesem N_2O-Emissionspeak widerspiegeln. Da jedoch der Boden im Höglwald aufgrund der zahlreichen Sommerniederschläge bereits wassergesättigt war, reagierte er verzögert auf dieses starke Niederschlagsereignis.
Die simulierten NO-Emissionen für den Fichtenstandort im Höglwald stimmten mit den Feldmessungen im Hinblick auf die Saisonalität und die Höhe der Emissionsflüsse über das ganze Jahr hinweg gut überein. Mit Ausnahme von drei Zeiträumen von 1-2 Wochen im Juni, August und Oktober, variierten die si-

mulierten NO-Emissionen zu den gemessenen Emissionen nur um ca. 10-20%. Innerhalb dieser drei Zeiträume wurden die NO-Emissionen um den Faktor 2 überschätzt.
Die simulierte Saisonalität der NO- und N_2O-Emissionen am Höglwald Standort stimmte mit der beobachteten Saisonalität der Feldmessungen überein, d.h. hohe Emissionen im Sommer gegenüber niedrigen Emissionen im Winter (Abbildung 13). Auch der Unterschied in der N_2O- und NO-Emissionsstärke aufgrund unterschiedlicher Qualität der Humusauflage und des pH Wertes im Boden konnte gut vom Modell reproduziert werden.
Das PnET-N-DNDC konnte außerdem die Unterschiede in der Höhe der N-Spurengasemission für unterschiedliche Messstandorte in Europa realistisch vorhersagen, d.h. niedrige NO-Emissionen in Hyytiälä und Glencorse und leicht erhöhte N_2O-Emissionen in Sorø. Jedoch waren speziell für den Buchenstandort in Sorø die simulierten N_2O-Emissionen in den ersten Monaten 2002 etwas höher als in den Feldmessungen (Abbildung 13). Ursache hierfür war die Simulation von erhöhten N_2O-Emissionen während Frost-Tau Perioden durch das PnET-N-DNDC Modell, die nicht in den Feldmessungen nachgewiesen werden konnten. Jedoch zeigten in diesem Zeitraum die Feldmessungen eine erhöhte Variabilität der N_2O-Emissionen. Die N_2O- und die sporadischen NO-Emissionsmessungen am Standort Hyytiälä zeigten, dass die N-Spurengasemissionen um Null liegen. Ein vergleichbares Ergebnis wurde vom PnET-N-DNDC Modell geliefert. Für den Glencorse Standort konnte das Modell die zeitlichen Variationen der NO-Emissionen während der Sommermonate 2002 gut simulieren, versagte jedoch bei der Vorhersage der Zunahme der NO-Emissionen Ende Oktober. Für den Zeitraum, in dem NO-Feldmessungen stattfanden, unterschätzte das Modell die NO-Emissionen um ca. 30% (durchschnittliche Feldmessung: 4,9 g N ha^{-1} Tag^{-1}, Simulation: 3,4 g N ha^{-1} Tag^{-1}) (Abbildung 13).

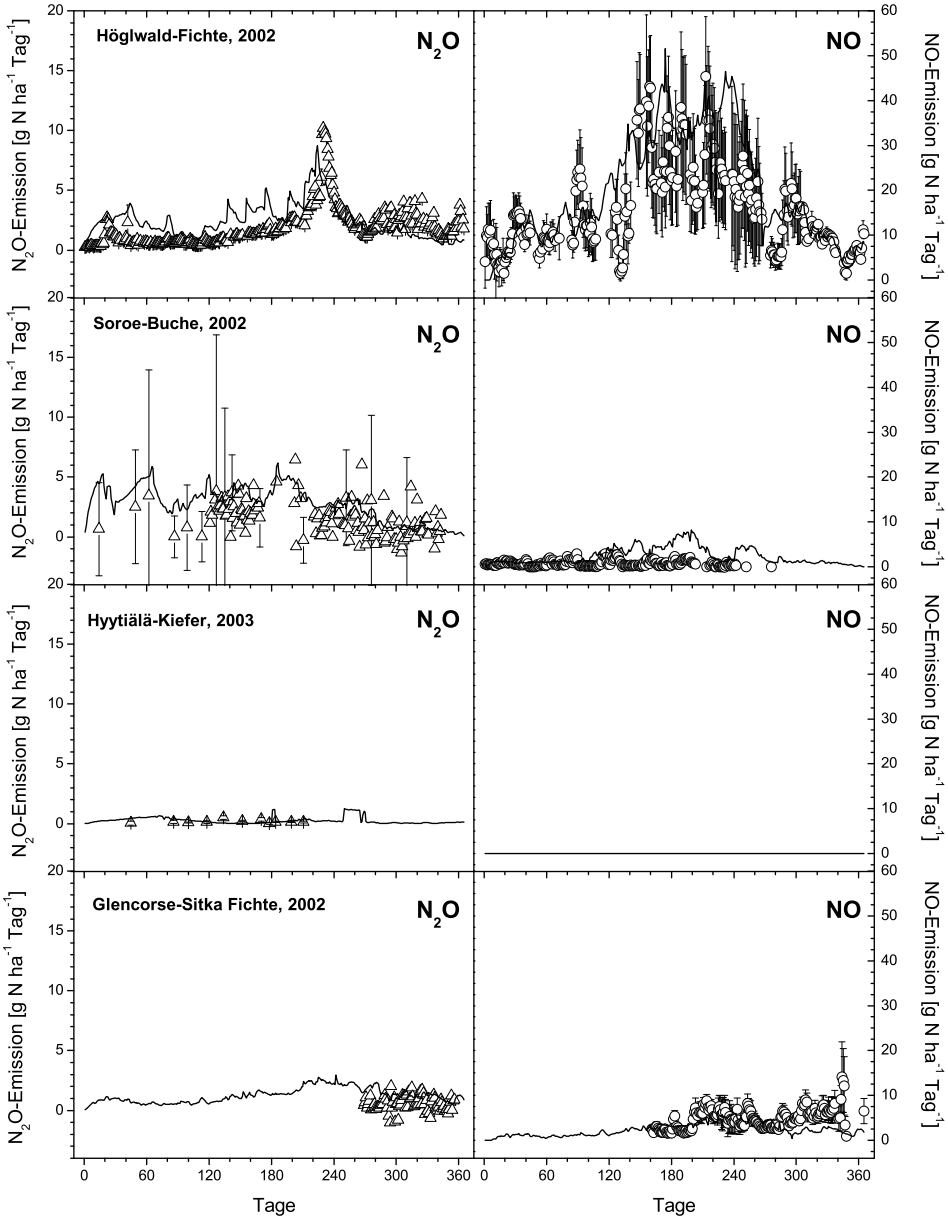

Abbildung 13: Vergleich der gemessenen (Dreiecke/Kreise) und der simulierten N_2O- und NO-Emissionen für die Waldstandorte Höglwald (Fichte, Deutschland), Sorø (Buche, Dänemark), Hyytiälä (Kiefer, Finnland) und Glencorse (Sitka Fichte, Schottland). Es sind keine NO-Flüsse für den Standort Hyytiälä dargestellt, da die Flüsse stets unterhalb der Nachweisgrenze lagen.

Zusammenfassende Darstellungen der Modellvalidierung der 19 Standorte, bei denen N-Spurengasemissionen gemessen wurden, sind in den Tabellen 2 und 3 und in den Abbildungen 7 und 8 in Kesik et al., 2005, **II** dargestellt. Die Abbildungen zeigen, dass das Model, basierend auf den Informationen der Boden- und Waldparameter sowie den lokalen meteorologischen Bedingungen, die gemessenen Unterschiede zwischen den Standorten mit niedrigen und hohen N-Emissionsraten gut vorhersagen kann. Die relative Variation zwischen den beobachteten und simulierten N_2O-Emissionen war für diejenigen Standorte höher, deren N- Spurengasemission < 3 g N ha^{-1} Tag^{-1} betrug, als für Standorte mit N-Spurengasemissionen > 5 g N ha^{-1} Tag^{-1}. Die lineare Regression aller simulierter und beobachteter durchschnittlicher N_2O-Emissionsraten beträgt $r^2 = 0{,}68$. Für alle Standorte unterschätze das Modell die N_2O-Emissionen um durchschnittlich 24% (f(x) = 0,76x). Bezug nehmend auf die NO-Emissionen beträgt der r^2 Wert 0,78. Genauso wie bei den N_2O-Emissionen unterschätzt das Modell die NO-Emissionen um durchschnittlich 27% (f(x)= 0,73x). Unter dem Gesichtspunkt der komplexen Prozesse, die die N-Spurengasemissionen beeinflussen, sind die Ergebnisse sehr ermutigend. Die Ergebnisse dieser Modellvalidierung für eine große Vielzahl von Waldökosystemen in Europa stellt eine solide Grundlage für die Anwendung des PnET-N-DNDC Modells auf regionaler Basis dar.

3.3 Erstellung einer GIS-Datenbank für Waldböden Europas

Nachdem das Modell umfangreich validiert wurde, musste eine umfassende und detaillierte Datenbank mit Informationen zu den Eingangsparametern (vgl. Kapitel 3.1) geschaffen werden. Diese Datenbank setzt sich aus vier Komponenten zusammen, den Bodenparametern, den Waldbestanddaten, den Klimadaten und den Rauminformationen, die in Bezug zu den drei genannten Komponenten stehen. Aufgrund unterschiedlicher Formate der Ursprungsdaten musste ein einheitlicher Raumbezug geschaffen werden. Hierfür wurde das 50km x 50km Raster des europäischen Überwachungsprogramms EMEP (European Monitoring and Evaluation Program) verwendet. Das EMEP wurde 1979 initialisiert, um den weiträumigen grenzüberschreitenden Transport von Luftverunreinigungen (Genfer Luftreinhaltekonvention) zu erfassen und in entsprechenden Protokollen zur Reduzierung der Emissionen umzusetzen. Die EMEP-Darstellung basiert auf einer polar-stereographischen Projektion. Jede einzelne Rasterzelle besitzt eine ID, die einen eindeutigen räumlichen Bezug aufweist und der auch alle Eingangsparameter zugewiesen sind.

3.3.1 Bodenphysiologische Daten

Die Bodendaten und ihr geographischer Bezug stammen aus der Soil Geographical Data Base für Europa (SGDBE), die mit ihrem Maßstab von 1: 1.000.000 Teil der European Soil Data Base ist (CEC-DGVI, 1985). Diese war aus einer Zusammenarbeit der Europäischen Union und einiger Nachbarstaaten hervorgegangen. Ziel war es, einen flächendeckenden Datensatz zur Diversität und räumlichen Verteilung verschiedener Bodentypen und Bodenparametern zur Verfügung zu stellen. Die SGDBE enthält eine Liste von typologischen Parametern, den sogenannten STU (Soil Typological Units), die neben den Bodentypen auch Attribute wie z.B. Tongehalt, Wasserregime oder Humustyp enthalten und so den Zustand und die Eigenschaft der jeweiligen Bodeneinheit spezifizieren. Um eine Darstellung der Einheiten auf den Maßstab von 1:1.000.000 zu vereinfachen und das Funktionieren des pedogenen Systems in einer Landschaft zu veranschaulichen, wurden die STU in eine größere Einheit zusammengefasst, den sogenannten Soil Mapping Units (SMU). Diese SMU besitzen ebenfalls Attributdaten, wie pH Wert und organischer Kohlenstoffgehalt (SOC) des Auflagehorizontes und des Mineralbodens. Diese SMU basierenden Parameter mussten auf die EMEP Bezugsbasis skaliert werden. Die Aggregierung dieser Daten erfolgte ebenso wie die STU Zusammenfassung mit dem so genannten UpScaling-Verfahren. So erhielt jede EMEP Rasterzelle einen Medianwert des jeweiligen Bodenparameters, gewichtet nach dem Anteil dieses Bodenparameters am EMEP, und zusätzlich den Maximum- und Minimumwert des Bodenparameters der jeweiligen Rasterzelle.

3.3.2 Daten zum Waldbestand

Informationen zu den Baumarten und ihrer Verteilung in Europa wurden aus den Daten des Netzwerks ICP Forest entnommen. Das Level I Programm, das 1984 durch die Europäische Kommission ins Leben gerufen wurde, um ein europaweites Messnetz zur Beobachtung des Waldzustands und der Waldentwicklung aufzubauen, lieferte die Daten für die Waldbestandkarten. Die räumliche Verteilung der Baumarten stammt für die meisten Gebiete Europas aus dem CORINE Landnutzungsdatensatz (CEC, 1994). Für die Gebiete, in denen keine CORINE Daten erhältlich waren, wurde die Information dem Pan-European Land Cover Mapping „PELCOM“ Projekt (Mücher, 2000) entnommen. Die Waldbestandkarten, die ebenso wie die Bodeninformationen vom JRC in Ispra im Rahmen des NOFRETETE Projektes stammen, lagen in einem 1km x 1km Rasterformat anteilig für 115 Baumarten für 30 europäische Länder vor. Die Rasterdaten wurden in dem 50km x 50km EMEP Raster zusammengefasst. Wichtig hierbei waren der Erhalt der exakten Flächeninformation und die Aufteilung aller Baumarten auf die neun im Modell PnET-N-DNDC zu simulierenden Baumarten. Das Modell ist derzeit noch für die folgenden neun Baumarten für temperate Wälder parametrisiert: Kiefer, Tanne, Fichte, Harthölzer, Lärche, sommergrüne Eiche, immergrüne Eiche, Birke und Buche. Die Baumarten Erle, Esche, Ulme, Pappel und Weide wurden den Harthölzer zugeordnet. Für Europa wurde eine Waldfläche von 1.410.477 km^2 simuliert. Da keine Informationen zur Baumalterzusammensetzung vorhanden waren, wurde für alle Baumarten ein Durchschnittsalter von 60 Jahren angenommen. Für die Länder Albanien, Serbien und Montenegro, Mazedonien und Bosnien-Herzegowina waren keine Walddaten vorhanden.

3.3.3 Klimatologische Daten

Klimadaten in täglicher Auflösung für die Jahre 1990, 1995 und 2000 wurden ebenso im Rahmen des NOFRETETE-Projektes vom Norwegischen Meteorologischen Institut (NMI) bereitgestellt. Diese Daten enthielten Informationen zu Tagesdurchschnittstemperaturen, zum täglichen Niederschlag und zur täglichen photosynthetisch aktiven Strahlung bezogen auf die EMEP-Rastergrundlage. Zusätzlich lieferte das NMI Daten zur jährlichen N-Feuchtedepositionsrate.

3.3.4 Verknüpfung der Datensätze

Letztendlich entstand eine umfangreiche Datenbank mit Boden-, Wald- und täglichen Klimadaten auf der EMEP-Bezugsbasis für 2527 EMEP Rasterzellen. Aus dieser Datenbank wurde mit Hilfe von ArcGIS von ESRI und python[2] eine Steuerdatei für das Modell PnET-N-DNDC erstellt. Für eine vollständige Simulation der N-Spurengasemissionen aus Waldböden Europas wurden 4527 Simulationsläufe benötigt. Da die Baumart innerhalb einer EMEP Rasterzelle variiert, wurde für jede Baumart ein Simulationslauf mit den identischen Informationen zu Klima und Boden zusätzlich durchgeführt. Bei der Berechnung der anschließenden Emissionen wurde jede Baumarten pro EMEP Rasterzelle berücksichtigt und der Emissionswert anteilig zu jeder Baumart im EMEP Raster berechnet.

3.4 N_2O- und NO-Emissionskataster für Waldböden Europas

3.4.1 N_2O-Emissionen

Im Folgenden werden die N_2O-Emissionen aus Waldböden Europas für die Jahre 1990, 1995 und 2000 aufgezeigt, die das Ergebnis der Modellsimulationen mit dem mit der GIS-Datenbank gekoppelten Modell PnET-N-DNDC darstellen. In den folgenden Abbildungen sind die Ergebnisse der Simulationsläufe des Jahres 2000 (Abbildung 14A) und der Vergleich zwischen den N_2O-Emissionsraten vom Jahr 1990 gegenüber dem Jahr 2000 (Abbildung 14B) dargestellt.

Im Jahr 2000 wurden für die europäischen Waldböden N_2O-Emissionen im Bereich von 0,01 bis 2,9 kg N ha^{-1} $Jahr^{-1}$ simuliert. N_2O-Emissionen $>$ 2,5 kg N ha^{-1} $Jahr^{-1}$ wurden für einige Regionen in den Niederlanden vorhergesagt. Ebenso wurden hohe Emissionen für Böden mit hohem Anteil an organischem Kohlenstoff in der Auflage im Südwesten Finnlands und in den nördlichen Gebieten Schwedens (1,0 bis 1,8 kg N ha^{-1} $Jahr^{-1}$) prognostiziert. Basierend auf Brumme et al. (2005) variieren die N_2O-Emissionen in borealen Wäldern zwischen 0,1 und 0,3 kg N ha^{-1} $Jahr^{-1}$. Für die meisten Waldflächen in Norwegen, Finnland und Schweden stimmen die im Rahmen dieser Arbeit erzielten Ergebnisse mit den Abschätzungen von Brumme et al. (2005) überein. Jedoch wurden für die Gebiete in Skandinavien und den Baltischen Staaten mit erhöhtem organischen Kohlenstoff in der Auflage deutlich höhere N_2O-Emissionen mit Raten $>$ 0,75 kg N ha^{-1} berechnet. Die Abschätzung von Brumme et al. (2005) basiert auf N_2O-Messungen in Mineralböden borealer Gebiete (z.B. Martikainen, 1996). Im Gegensatz hierzu berechneten andere Abschätzungen in kürzlich erschienenen Publikationen (von Arnold et al., 2005; Maljanen et al., 2001, 2003), in de-

nen N_2O-Emissionen aus borealen Waldböden mit hohem Humusanteil gemessen wurden, jährliche N_2O-Emissionsraten zwischen 1,0 und 10,0 kg N ha^{-1} $Jahr^{-1}$. Die höchsten N_2O-Emissionen in borealen Wäldern stammen aus Torfböden, die vor der Aufforstung als landwirtschaftliche Böden genutzt wurden (Maljanen et al., 2003). Im Gegensatz hierzu berichtete Regina et al. (1996), dass humusarme organische Waldböden vernachlässigbare N_2O-Emissionen emittieren. Der große Unterschied zwischen den beiden Abschätzungen ist deutlich und kann jedoch bis dato nicht hinreichend erklärt werden. Es kann nur angenommen werden, dass für ein verbessertes Waldwachstum in Skandinavien weitläufig drainierte Böden, die aufgrund ehemaliger Torfnutzung reich an organischem Kohlenstoff sind, eine größere N_2O-Emissionsquelle darstellen als Böden mit geringem organischem Kohlenstoffgehalt in diesen Regionen.

Mittlere N_2O-Emissionen von 0,75 bis 1,5 kg N ha^{-1} $Jahr^{-1}$ wurden für große Regionen Polens und der Baltischen Staaten simuliert. Im Vergleich zu den simulierten N_2O-Emissionsraten der temperaten Wälder in Europa variieren die gemessenen N_2O-Emissionsraten über einen weiten Bereich von 0 bis 20 kg N ha^{-1} $Jahr^{-1}$ (z.B. Papen und Butterbach-Bahl, 1999). Die durchschnittliche Emissionsstärke von 0,2 bis 2,0 kg N ha^{-1} $Jahr^{-1}$ entspricht jedoch der im Rahmen dieser Arbeit simulierten N_2O-Emissionsraten für ganz Europa von 0,01 bis 2,9 kg N ha^{-1} $Jahr^{-1}$.
Brumme et al. (1999), Butterbach-Bahl et al. (2002a), Jungkunst et al. (2004) und Zechmeister-Boltenstern et al. (2002) fanden heraus, dass die Unterschiede in der Emissionsstärke der gemessenen N_2O-Emissionen durch Bodeneigenschaften wie den organischen Kohlenstoffgehalt im Boden, pH Wert, N-Eintrag in die Waldböden und Baumarteneigenschaften beeinflusst werden. Zusätzlich wurde durch Papen und Butterbach-Bahl (1999) und durch Teepe und Ludwig (2004) gezeigt, dass die Tau- und Frostereignisse im Winter zu hohen N_2O-Emissionen führen.
Schulte-Bisping et al. (2003) schätzten durchschnittliche N_2O-Emissionen aus Waldböden Deutschlands von 0,32 kg N ha^{-1} $Jahr^{-1}$. Diese Schätzung stellt vermutlich die untere Grenze der N_2O-Emissionsabschätzungen für Deutschland dar, da sie weder den N-Eintrag aus der Atmosphäre in den Boden noch Frost-Tau Prozesse im Boden berücksichtigt. Beide Faktoren wurden jedoch in den Untersuchungen von Butterbach-Bahl et al. (2001, 2004) einbezogen, in denen eine ältere Version des PnET-N-DNDC Modells verwendet wurde, um die regionalen N_2O-Emissionsstärken aus Süddeutschland und Sachsen zu berechnen. Deren geschätzte durchschnittliche N_2O-Emission von ca. 2 kg N ha^{-1} $Jahr^{-1}$ ist signifikant höher als die von Schulte-Bisping et al. (2003) und ebenso höher als die Abschätzung für Deutschland, die im Rahmen dieser Arbeit mit der neuen Version des PnET-N-DNDC berechnet wurde (0,6 bis 0,8 kg N ha^{-1} $Jahr^{-1}$). Grund hierfür sind zum einen eine verbesserte Parametrisierung der biogeochemischen Prozesse, basierend auf den Laboruntersuchungen von Schindlbacher et

al. (2004) und Kesik et al.(2005, **I**), und zum anderen eine Aggregierung der Klima-, Wald- und Bodenparameter auf EMEP Rasterbasis (50km x 50km) und nicht wie in den vorangegangenen Untersuchungen eine Datenaggregierung auf Polygonbasis. Auch wurden unterschiedliche meteorologische Jahre für die jeweiligen Simulationen verwendet.

Bezogen auf die mediterranen Gebiete Europas gibt es nur sehr wenige Informationen über die Höhe der N_2O-Emissionen aus Böden (siehe Übersichtsartikel von Butterbach-Bahl und Kiese, 2005). Die wenigen vorhandenen Publikationen zeigen, dass mediterrane Waldböden sogar als N_2O-Senke fungieren können (Rosenkranz et al., 2005). Mit Ausnahme von wenigen Regionen im Osten Spaniens berechnete das PnET-N-DNDC geringe N_2O-Emissionsraten von $< 0{,}5$ kg N ha^{-1} $Jahr^{-1}$ für die meisten mediterranen und maritimen Länder, inkl. Frankreich, Großbritannien, Irland, Norwegen und für große Gebiete von Zentral- und Nord-Finnland (Abbildung 14A). Diese geringen Emissionsraten in den mediterranen Gebieten sind durch eine modellinterne Reduktion der mikrobiellen N-Umsetzungsprozesse bedingt, sobald die Pflanzen unter Wasserstress stehen.

Die durchschnittliche N_2O-Emissionsrate für alle Waldgebiete Europas beträgt für das Jahr 2000 0,58 kg N ha^{-1} $Jahr^{-1}$. Die durchschnittliche N_2O-Emission veränderte sich für die simulierten Jahre 1990 und 1995 nur gering. 1990 betrug die durchschnittliche Emissionsrate 0,62 kg N ha^{-1} $Jahr^{-1}$ und 1995 wurde eine durchschnittliche N_2O-Emissionsrate von 0,55 kg N ha^{-1} $Jahr^{-1}$ berechnet.

Regional betrachtet sind in Europa jedoch deutliche N_2O-Emissionsunterschiede zwischen den Jahren 1990 und 2000 zu erkennen (Abbildung 14B). So kann die regionale N_2O-Emissionsstärke in diesen Jahren signifikant variieren. Die Abbildung 14B zeigt, dass im Jahr 2000 die N_2O-Emissionen aus Waldböden Süd-Schwedens um $> 40\%$ höher waren als 1990, wohingegen in anderen Regionen wie den mediterranen Ländern die N_2O-Emissionen um ca. 10 bis 40% abnahmen. Die Gesamt-N_2O-Emissionen aus Waldböden Europas belaufen sich auf 78 bis 87 kt N $Jahr^{-1}$. Aufgrund der großen Waldflächen in Schweden und Finnland tragen diese beiden Länder am meisten zu den Gesamt-N_2O-Emissionen Europas bei (12 bzw. 10 kt N $Jahr^{-1}$). Betrachtet man jedoch die N_2O-Emissionsrate auf ha Basis, so sind die Wälder in den Niederlanden (1,26 kg N ha^{-1} $Jahr^{-1}$) und Rumänien (0,96 kg N ha^{-1} $Jahr^{-1}$) die größten Emittenten (siehe Tabelle 4 in Kesik et al., 2005, **II**).
Im Vergleich zu den N_2O-Emissionen aus landwirtschaftlichen Flächen, die von Boeckx und van Cleemput (2001) für Europa berechnet wurden, haben die simulierten Gesamt-N_2O-Emissionen aus Waldböden Europas einem Anteil von durchschnittlich 14,5% an der Gesamtemissionsstärke der landwirtschaftlichen Böden.

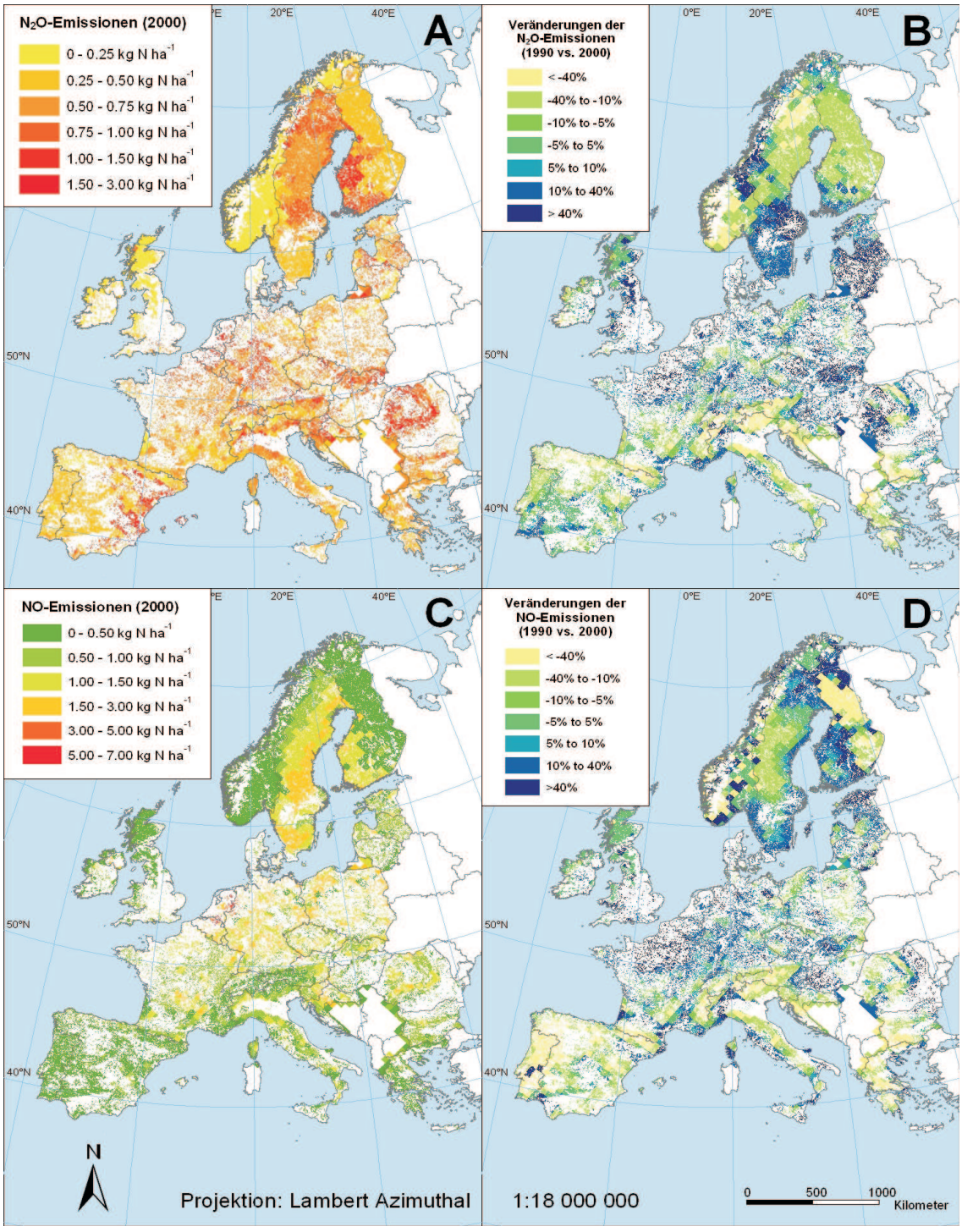

Abbildung 14: Regionale Verteilung der jährlichen N_2O- (A) und NO-Emissionen (C) aus Waldböden in Europa (in kg N ha^{-1} $Jahr^{-1}$). Abbildungen (B) und (D) stellen relative Veränderungen der N_2O- (B) bzw. NO-Emissionen (D) des Jahre 2000 im Vergleich zum Jahr 1990 dar.

3.4.2 NO-Emissionen

Im Folgenden werden die NO-Emissionen aus Waldböden Europas für die Jahre 1990, 1995 und 2000 aufgezeigt. In den folgenden Abbildungen sind die Ergebnisse der Simulationsläufe des Jahres 2000 (Abbildung 14C) und der Vergleich zwischen den NO-Emissionsraten vom Jahr 1990 gegenüber dem Jahr 2000 (Abbildung 14D) dargestellt.

Ebenso wie für N_2O wurden die höchsten NO-Emissionen für Waldböden in den Niederlanden und in den angrenzenden Gebieten Belgiens und Deutschlands berechnet. Die maximale NO-Emissionsrate eines Rasterzelle in dieser Region betrug 7,0 kg N ha^{-1} $Jahr^{-1}$. Ursache dieser hohen NO-Emissionen in dieser Region sind die hohen N-Einträge in die Waldböden, die zu einer verstärkten NO-Produktion führen. Diese hohen NO-Emissionsraten für die Beneluxstaaten und Norddeutschland stimmen mit den Untersuchungen von Van Dijk und Duyzer (1999) überein. Sie berichten von durchschnittlichen NO-Emissionsraten von > 6 kg N ha^{-1} $Jahr^{-1}$ für Buchen und Douglasietannen in Speulderbos, Niederlande, die einen N-Eintrag von ca. 40 kg N ha^{-1} $Jahr^{-1}$ aufweisen.

Für Waldböden in Deutschland, Belgien, Polen und dem Massiv Central in Frankreich wurden NO-Emissionen von 1,0 bis 3,0 kg N ha^{-1} $Jahr^{-1}$ simuliert.
Betrachtet man nun einen speziellen Standort, wie z.B. den Höglwald bei Augsburg, für den langjährige Feldmessungen der NO-Emissionen aus Buchen und Fichtenwälder existieren (Gasche und Papen, 1999; Butterbach-Bahl et al., 2002b), so sind die vom PnET-N-DNDC simulierten Ergebnisse im Einklang mit den Feldmessungen. Für die entsprechende Rasterzelle wurde eine durchschnittliche Emissionsrate zwischen 1,5 und 3,0 kg N ha^{-1} $Jahr^{-1}$ simuliert, die zwar niedriger als die NO-Emissionsrate für den Fichtenstandort im Höglwald (> 6 kg N ha^{-1} $Jahr^{-1}$) ist, jedoch mit der NO-Emissionsrate vom Buchenstandort (ca. 2,8 kg N ha^{-1} $Jahr^{-1}$) übereinstimmt (Butterbach-Bahl et al., 2002b). Die relativ kleinen Unterschiede zwischen den gemessenen und den für diese Rasterzelle simulierten NO-Emissionen sind auf die Generalisierung der GIS-Datenbank zurückzuführen, da für diese Rasterzelle sehr allgemeine Informationen (N-Eintrag, Bodeninformationen) vorliegen.

Erhöhte NO-Emissionen von bis zu 3,0 kg N ha^{-1} $Jahr^{-1}$ wurden für große Gebiete in Schweden berechnet, jedoch bis jetzt in keiner Veröffentlichung bestätigt. Johansson (1984), der Untersuchungen in Waldgebieten in der Nähe von Stockholm durchführte, fand heraus, dass die NO-Emissionen aus ungedüngten Waldböden niedriger als 0,1 kg N ha^{-1} $Jahr^{-1}$ betrugen. Aufgrund der großen Skalenunterschiede ist ein Vergleich zwischen den gemessenen und simulierten Emissionen schwierig. Bei der Ursachenermittlung der hohen NO-Emissionen für weite Teile Schwedens hat sich herausgestellt, dass die erhöhten NO-Emissionen

hauptsächlich auf die niedrigen pH Werte in den Waldböden dieser Gebiete zurückzuführen sind. Dadurch wird der Prozess der Chemodenitrifikation im PnET-N-DNDC Modell angetrieben und verursacht hohe NO-Produktionsraten. Diese Tatsache wurde von zahlreichen Labor- und Felduntersuchungen bestätigt (z.B. van Cleemput und Baert, 1984; Gasche und Papen, 1999; Kesik et al., 2005, **I**). Ein weiterer Grund für den Unterschied in den gemessenen und modellierten NO-Emissionsraten könnten auch die unterschiedlichen Bodeneigenschaften, die im Modell verwendet wurden, im Gegensatz zu denen sein, die am Messstandort vorlagen. So betrug der pH Wert am Messstandort, an dem Johansson (1984) Untersuchungen durchgeführt hat, pH 4,0 bzw. pH 4,5. Im Gegensatz hierzu betrug der pH Wert, der aus den Bodeninformationen der Soil Geographical Data Base of Europe stammt und für die Modellsimulationen verwendet wurde, für den Großteil Skandinaviens pH < 4; bei diesem pH Wert wird die Chemodenitrifikation im PnET-N-DNDC aktiviert und NO auf chemischem Reaktionsweg produziert (Li et al., 2000).
Niedrige NO-Emissionen ($<$ 0,5 kg N ha^{-1} $Jahr^{-1}$) wurden für Waldböden in Norwegen und großen Teilen Finnlands simuliert. Für die mediterranen Gebiete wurden NO-Emissionen $<$ 0,5 kg N ha^{-1} $Jahr^{-1}$ simuliert (Abbildung 14C).

Die durchschnittliche NO-Emissionsrate aus Waldböden Europas im Jahr 2000 war 0,7 kg N ha^{-1} $Jahr^{-1}$, und somit nur wenig höher als bei N_2O (0,6 kg N ha^{-1} $Jahr^{-1}$). Der Unterschied zwischen den NO-Emissionsraten von 2000 und den Jahren 1990 und 1995 ist gering (1990: 0,7 kg N ha^{-1} $Jahr^{-1}$, 1995: 0,6 kg N ha^{-1} $Jahr^{-1}$). Die durchschnittliche NO-Emissionsrate entspricht der Emissionsrate aus Waldböden im Südosten der USA (Davidson et al., 1998). Die Gesamt-NO-Emission für alle Waldböden Europas beträgt 99 kt N für das Jahr 2000. Dies entspricht nahezu den Gesamt-Emissionsraten in 1990 von 98 kt N und ist etwas niedriger als in 1995 (85 kt N). Die größten NO-Emittenten aus Waldböden Europas sind Schweden und Deutschland (Tabelle 4, Kesik et al., 2005, **II**). Der Unterschied der NO-Emissionen zwischen den Jahren 1990 und 2000 ist signifikant. So zeigt Abbildung 14D die relativen Veränderungen in der NO-Emissionsstärke der Waldböden in Europa. Hier wird deutlich, dass die NO-Emissionen im Jahr 2000 v.a. in Zentraleuropa und in Nordeuropa höher und in den mediterranen Gebieten niedriger sind als die NO-Emissionen im Jahr 1990.

Die im Rahmen dieser Arbeit gewonnenen Ergebnisse wurden von D. Simpson (Norwegian Meteorological Institut) verwendet, um den Einfluss der NO-Emissionen auf die N-Deposition von Wäldern auf den Ozon-Indikator AOT40 mit Hilfe des EMEP Eulerian Chemie-Transport Modells zu berechnen. Die im Rahmen dieser Arbeit berechneten Daten umfassen NO-Emissionen für alle Baumarten, die in jeder einzelnen EMEP-Rasterzelle vorkommen. Diese NO-Emissionen wurden in täglicher Auflösung für jede der 2527 EMEP-Rasterzellen mit dem PnET-N-DNDC Modell simuliert und standen somit Simpson sehr detailliert zur

weiteren Berechnung mit dem Eulerian Chemie-Transport Modell zur Verfügung. Simpson fand heraus, dass der Anteil der NO-Emissionen aus Waldböden zur Gesamt-N-Deposition zwar klein aber dennoch signifikant ist und dass er die N-Deposition in einigen Gebieten um bis zu 20% verändert (Simpson et al., 2005, **V**).

Betrachtet man die simulierten Gesamt-NO-Emissionen und vergleicht sie mit den NO_x-Emissionen aus Verbrennungsprozessen, die die Hauptquelle für atmosphärisches NO_x in Europa darstellen, so schätzte Vestreng et al. (2004), dass sich die Gesamt-NO_x-Emissionen für die hier simulierte Fläche Europas im Jahr 2000 auf ca. 10.000 kt N Jahr^{-1} beläuft. Die im Rahmen dieser Arbeit simulierten NO-Emissionen aus Waldböden (85-99 kt N Jahr^{-1}) haben somit einen Anteil von $< 1\%$ an den Gesamt-NO_x-Emissionen aus Verbrennungsprozessen.

3.5 Zukunftsszenarien des Klimas und der N_2O- und NO-Emissionen für Waldböden Europas

Mit Hilfe von Szenarien zur globalen Klimaveränderung für Europa sollte untersucht werden, inwieweit sich die zukünftigen N_2O- und NO-Emissionen aus Waldböden Europas aufgrund der Klimaveränderung in den kommenden 30-40 Jahren im Vergleich zu heute verändern und welche Auswirkungen diese Klimaveränderungen regional auf die beiden N-Spurengase haben. Hierzu wurde wie bereits bei den vorangegangenen N_2O- und NO-Abschätzungen für das europäische Emissionskataster aus Waldböden die meteorologischen Informationen für die Jahre 1991-2000 und 2031-2039 an das biogeochemische Modell PnET-N-DNDC gekoppelt.

3.5.1 GIS-Datengrundlage für die Zukunftsszenarien

Zur Regionalisierung der N-Spurengasemissionen musste eine detaillierte GIS-Datenbank für Europa geschaffen werden. Diese Datenbank bestand aus Informationen zum Klima, zu den Bodeneigenschaften und zum Waldbestand. Informationen zu den Bodeneigenschaften und zum Waldbestand wurden, entsprechend der bereits beschriebenen GIS-Datenbank (Kapitel 3.3), innerhalb des NOFRETETE Projektes von den jeweiligen Partnern zur Verfügung gestellt. Innerhalb der Modellläufe mit PnET-N-DNDC bleibt die N-Deposition auf dem Niveau vom Jahr 2000.
Die Klimainformationen für die Jahre 1991-2000 und 2031-2039 gehen auf Berechnungen des gekoppelten Klima-Chemie-Modells MCCM (Multiscale Climate and Chemistry Model, Grell et al., 2000) zurück, dass die Vorhersagen des globalen

Klimamodells ECHAM4 für das heutige und zukünftige Klima als Antriebsdaten verwendet. Das ECHAM4 Modell wird vom Max-Planck Institut für Meteorologie in Hamburg betrieben und berechnet das globale Klima basierend auf den atmosphärischen CO_2-Konzentrationen im Zeitraum von 1860-1990 und auf den IS92a Szenario des IPCC für den Zeitraum 1990-2100 (Houghton et al., 1992). Die Ergebnisse aus diesen Simulationen, die das Klima der Gegenwart (1991-2000) und der Zukunft (2031-2039) repräsentieren, wurden verwendet, um die regionalen Klimaszenarien für Europa mit dem MCCM Modell zu rechnen. Das MCCM Modell berechnet in hoher Auflösung die meteorologischen und gleichzeitig die chemischen Prozesse für eine bestimmte Region. Für die Klimasimulation für Europa (mit Ausnahme der Fläche Skandinaviens nördlich des 66 ° n. Br. und Islands) mit einer Auflösung von 60km x 60km wurde das MCCM Modell direkt in das globale ECHAM4 Modell ,,genestet". Bei diesem ,,nesting" Prozess wurde die Klimainformation des globalen ECHAM4 Modells mit einer Auflösung von nur 200-300km regionalisiert (Forkel und Knoche, 2005; Knoche et al., 2003).

Die Klimainformationen, die das Ergebnis der MCCM Simulationsläufe sind, wurden als Klimaeingangsparameter (Niederschlag, Minimum- und Maximumtemperatur, photosynthetisch aktive Strahlung in täglicher Auflösung) für das PnET-N-DNDC Modell verwendet. Somit entstand eine umfangreiche Datenbank mit Boden-, Wald- und täglichen Klimadaten auf der EMEP-Bezugsbasis für 2386 EMEP Rasterzellen. Aus dieser Datenbank wurde mit Hilfe von ArcGIS von ESRI und python[2] eine Steuerdatei für das Modell PnET-N-DNDC erstellt und die GIS-Datenbank and das PnET-N-DNDC gekoppelt (siehe auch Kesik et al., 2005, **III**).

3.5.2 Simulierte Klimaveränderung in Europa

Die regionalen Klimaszenarien berechneten, dass für den Zeitraum 2031-2039 die durchschnittliche Oberflächentemperatur für Europa um 1,8 °C höher sein wird als im gegenwärtigen Zeitraum (1990-1999). Das bedeutet, dass die durchschnittliche Jahrestemperatur Europas von 7,6 °C auf 9,4 °C ansteigen wird. Der höchste durchschnittliche Anstieg der Temperatur von 1,8 °C bzw. 2,2 °C wird für den Winter bzw. den Frühling vorhergesagt.
Die Modellsimulationen weisen ein differenziertes Muster der Temperaturveränderungen für Europa auf (Abbildung 15A). Die Abbildung 15A zeigt, dass die jährliche Durchschnittstemperaturzunahme in Skandinavien, den baltischen Staaten (mit Ausnahme Polens) und Teile der Ukraine und Russlands für den Zeitraum 2031-2039 größer als 2 °C sein wird. Für andere Regionen, wie die Westalpen und einige maritim beeinflusste Gebiete Portugals, Spaniens und Frankreichs wird sich der Temperaturanstieg zwischen 1,5-2,0 °C bewegen. Für alle anderen Gebiete Europas, v.a. für fast alle Mittelmeerländer, Mitteleuropa, sowie Großbritannien und Irland, wird der jährliche Temperaturanstieg weniger prägnant zwischen

0,75-1,5 °C ausfallen. Jedoch können in einigen Mittelmeergebieten die Sommertemperaturen um 2,5 °C ansteigen (Abbildung 15B). Auch im Süden Norwegens und Schwedens können die zukünftigen Sommertemperaturen um 2,5 °C ansteigen. Diese lokal eingeschränkten Temperaturerhöhungen im Süden Norwegens und Schwedens können auf eine Überschätzung der Temperaturzunahme in der Zukunft zurückzuführen sein, da diese lokalen Temperaturerhöhungen nicht in den Simulationen der Gegenwart zu sehen sind. Für das restliche Europa wird vermutlich die Temperatur um 1,5-2,0 °C ansteigen.

Der durchschnittliche Gesamtjahresniederschlag für Europa wird sich für den Zeitraum 2031-2039 im Vergleich zu 1990-1999 vermutlich nicht verändern. Das bedeutet jedoch nicht, dass saisonale Niederschlagsveränderungen nicht regional stattfinden können. Abbildung 15C zeigt, dass in einigen Mittelmeergebieten und in den maritim beeinflussten Regionen Frankreichs und Schottlands der durchschnittliche Jahresniederschlag um voraussichtlich 30% zunehmen wird. In allen anderen europäischen Regionen, mit Ausnahme von Teilen Norwegens und Finnlands, wird simuliert, dass die jährliche Niederschlagsmenge um 20% abnehmen wird.
Zusätzlich wird sich vermutlich die Saisonalität des Niederschlags verändern. Für die meisten Gebiete Europas sagt das MCCM Modell leichte Zunahmen des Winterniederschlags, jedoch geringere Frühjahrs- und Sommerniederschläge voraus. Besonders auffallend sind die saisonalen Niederschlagsveränderungen für einige mediterrane Gebiete, für die die Sommerniederschläge voraussichtlich um 80% abnehmen werden (Abbildung 15D). Ebenso werden für einige Regionen Mitteleuropas (mit Ausnahme Norddeutschland), Schwedens und Finnlands, sowie für Ost- und Südost-Europa Abnahmen der Sommerniederschläge für den Zeitraum 2031-2039 vorhergesagt. Entlang der Ostküste der Nordsee, hauptsächlich in Norwegen, Dänemark und Norddeutschland, in Teilen Schottlands und Irlands, sowie in Nordportugal werden die Niederschläge vermutlich um ca. 30% in den Sommermonaten zunehmen.

Die simulierten Veränderungen der Temperatur und des Niederschlags, sowie deren regionale Verteilung in Europa stimmen mit jüngsten Untersuchungen zu zukünftigen Klimaveränderungen in Europa überein (Maracchi et al., 2005; Benestad, 2005; Giorgi et al., 2004; Kjellstrom, 2004 und Räisänen et al., 2004).

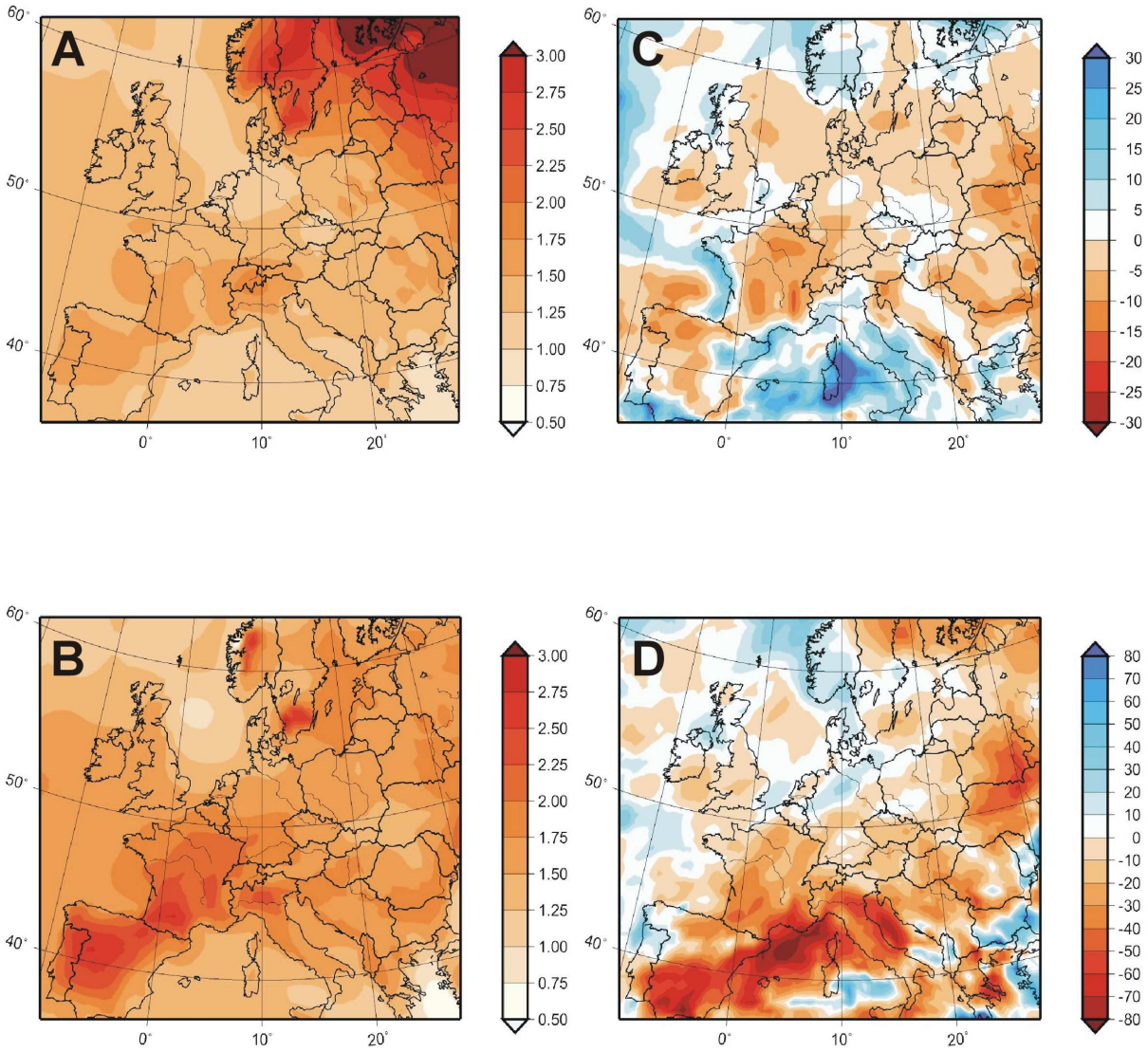

Abbildung 15: Veränderungen der durchschnittlichen jährlichen Temperatur (°C, A) und der Sommertemperatur (B) in der Zukunft (2031-2039) im Vergleich zur Gegenwart (1991-2000). Abbildungen C und D zeigen die relativen Veränderungen der jährlichen Niederschlagssumme und der Sommerniederschläge in der Zukunft (2031-2039) im Vergleich zur Gegenwart (1991-2000).

3.5.3 Zukünftige Veränderungen der N_2O-Emissionen

Um herauszufinden, wie sich die zukünftigen Klimaveränderungen auf die N-Spurengasemissionen aus europäischen Waldböden auswirken können, wurde das PnET-N-DNDC Modell für die Zeiträume 1990-1999 und 2031-2039 mit den bereits oben beschriebenen Klimaszenarien gekoppelt.
Mit Hilfe dieser PnET-N-DNDC Simulationen wurde berechnet, dass die durchschnittlichen Jahres-N_2O-Emissionen aus Waldböden in Europa leicht um 6% (4 kt N_2O-N) im Zeitraum 2031-2039 im Vergleich zum Zeitraum 1991-1999 abnehmen werden. Dies ist hauptsächlich auf die signifikante Abnahme der Emission während des Frühjahrs von 21 kt N_2O-N unter gegenwärtigen Klimabedingungen auf 17 kt N_2O-N unter zukünftigen Klimabedingungen zurückzuführen (Tabelle 1 in Kesik et al., 2005, **III**).
Jedoch zeigen die Berechnungen des PnET-N-DNDC Modells eine auffällige regionale Verteilung der zukünftigen Veränderungen in den N_2O-Emissionen aufgrund von Klimaveränderungen (Abbildung 16, siehe auch Tabelle 2 in Kesik et al., 2005, **III**). In Skandinavien und in einigen Regionen Polens, Estlands, Lettlands, Litauens, Rumäniens, der Slowakei und Bulgariens werden die zukünftigen N_2O-Emissionen voraussichtlich bis zu 33% abnehmen. Das Modell berechnete auch für die Alpen eine Abnahme der N_2O-Emissionen in der Zukunft um 30%. Jedoch wird für Zentraleuropa und die Mittelmeerländer eine Zunahme der N_2O-Emissionen aus Waldböden um ca. 15% vorhergesagt. In Norddeutschland, den Beneluxstaaten, Großbritannien und Irland könnten die N_2O-Emissionen sogar um 20% zunehmen.

Die Ergebnisse der Simulationen zeigen, dass sogar bei einer generellen Temperaturzunahme unter zukünftigen Klimabedingungen die N_2O-Emissionen leicht zurückgehen. Jedoch zeigen die meisten Labor- und Felduntersuchungen, dass die Temperatur einen positiven Einfluss auf die N_2O-Emissionen hat (z.B. Granli und Bøckman, 1994; Brumme, 1995; Papen und Butterbach-Bahl, 1999). Aus diesem Grund hätte man erwartet, dass unter einem veränderten Klima in der Zukunft die N_2O-Emissionen mit steigender Temperatur in Europa zunehmen. Jedoch liegt die Ursache für dieses gegensätzliche Verhalten der N_2O-Emissionen zur Temperatur, das vom PnET-N-DNDC Modell simuliert wurde, in der Komplexität der Prozesse, die an der Produktion und Konsumption von N_2O beteiligt sind. So zeigt Abbildung 17, dass die simulierten N_2O-Emissionen um mindestens 10% abnehmen, wenn unter den zukünftigen Klimabedingungen die durchschnittliche jährliche Bodenfeuchte und die durchschnittliche jährliche Bodentemperatur um mehr als 10% (relative Veränderung des wassergefüllten Porenraums [WFPS]) bzw. um mehr als 2 °C zunehmen. Nur wenn unter den zukünftigen Klimabedingungen die durchschnittliche jährliche Bodenfeuchte unverändert bleibt bzw. im Vergleich zur Gegenwart nur leicht abnimmt, werden die N_2O-Emissionen zunehmen. Die Ursache für die Abnahme der simulierten N_2O-Emissionen ist auf ei-

ne Verschiebung des N_2O:N_2 Verhältnisses unter zukünftigen Klimabedingungen zurückzuführen (Abbildung 18). In den Simulationen wird das N_2O:N_2 Verhältnis voraussichtlich abnehmen. Das bedeutet, dass unter den zukünftigen Klimabedingungen in Regionen mit einer höheren jährlichen Bodenfeuchte und höheren Temperaturen mehr N_2 auf Kosten des N_2O emittiert wird. Diese Vorhersagen stimmen mit Laboruntersuchungen überein, die gezeigt haben, dass das N_2O:N_2 Verhältnis mit zunehmender Temperatur abnimmt (Nommik, 1956; Keeney et al., 1979). So ist auch bekannt, dass wenn der wassergefüllte Porenraum eines Bodens auf ca. 70-80% (Davidson, 1991) anwächst, mehr N_2 als N_2O als Endprodukt der Denitrifikation produziert wird.

Diese direkten Modellzusammenhänge zwischen den Klimaveränderungen und den N_2O-Emissionen sind nur möglich, da im PnET-N-DNDC Modell die wichtigsten mikrobiellen und physikalisch-chemischen Prozesse, die an der Produktion, Konsumption und Emission von N-Spurengasen, wie die Prozesse der Nitrifikation, Denitrifikation, Immobilisierung und Chemodenitrifikation, implementiert sind (Li et al., 2000). Wenn der Boden zunehmend anaerobisch wird, z.B. aufgrund eines erhöhten wassergefüllten Porenraums, wird das Modell im Gegensatz zu Bedingungen, bei denen der Boden gut durchlüftet wird, simulieren, dass das entweder aus der Nitrifikation oder Denitrifikation stammende N_2O zu N_2 reduziert wird.

Diese Simulationsergebnisse der N_2O-Emissionen der Gegenwart (1991-2000) stimmen auch mit den Ergebnissen aus dem vorangegangenen Kapitel 3.4.1 sowie mit den Ergebnissen aus Kesik et al., 2005, **II** überein. Zwar sind die durchschnittlichen N_2O-Emissionen, die in Kesik et al., 2005, **II** bzw. in Kapitel 3.4.1. unter Verwendung der EMEP Klimadaten berechnet wurden, geringfügig höher (0,58 kg N_2O-N ha^{-1} $Jahr^{-1}$) als die mit MCCM Klimadaten berechneten N_2O-Emissionen (0,53 kg N_2O-N ha^{-1} $Jahr^{-1}$). Dies liegt jedoch an der unterschiedlichen Größe der Simulationsgebietes von Europa (Großteil Skandinaviens ist bei den MCCM Klimadaten nicht enthalten), der unterschiedlichen Simulationsdauer (10 Jahre gegenüber 3 Jahren) und an unterschiedlichen Klimadaten (MCCM gegenüber EMEP).

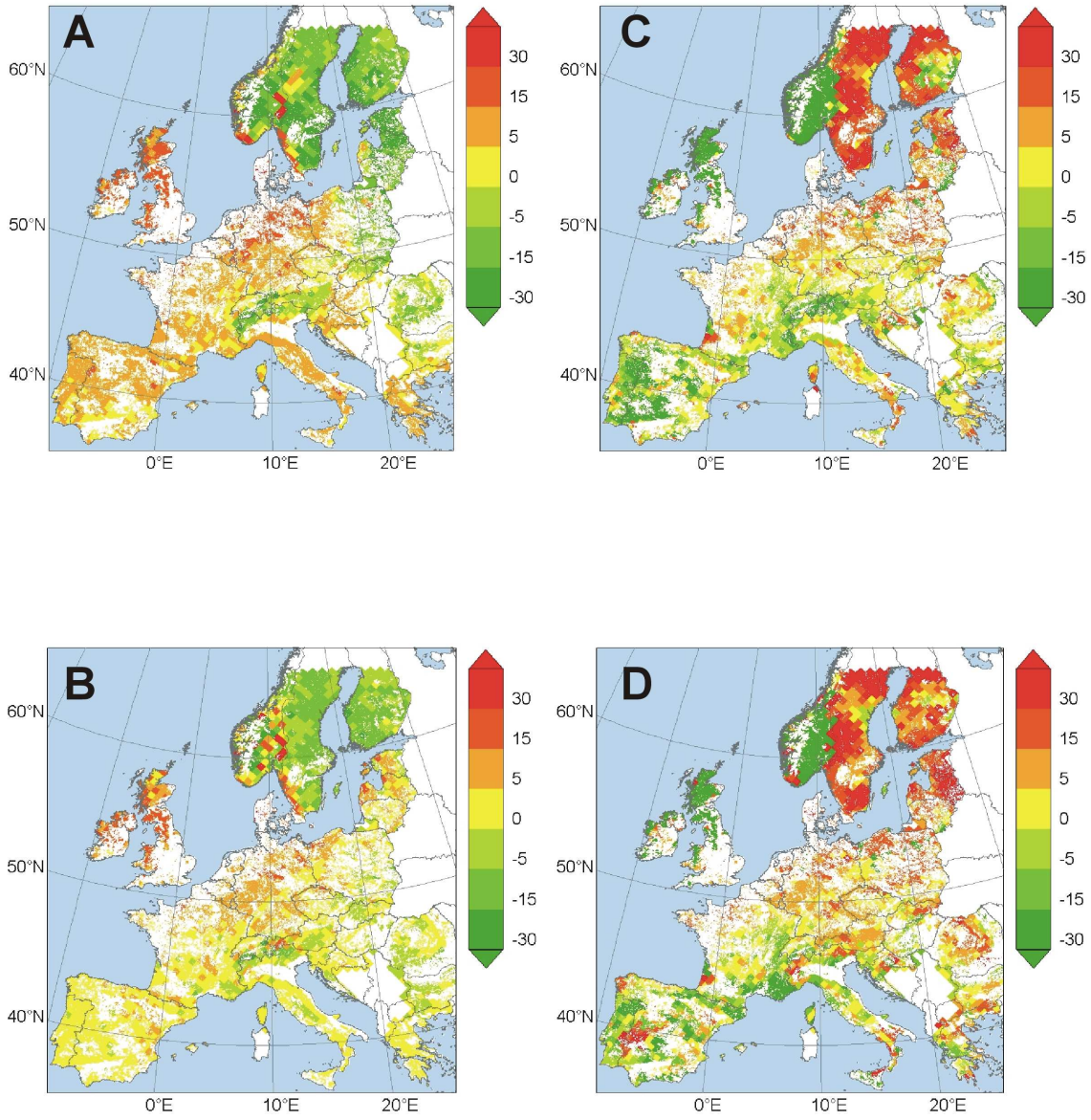

Abbildung 16: Relative Veränderungen der durchschnittlichen jährlichen N_2O-Emissionen (%, A) und der durchschnittlichen Sommer-N_2O-Emissionen (B) in der Zukunft (2031-2039) im Vergleich zur Gegenwart (1991-2000). Abbildungen C und D zeigen die relativen Veränderungen der jährlichen NO-Emissionen und der durchschnittlichen Sommer-NO-Emissionen in der Zukunft (2031-2039) im Vergleich zur Gegenwart (1991-2000).

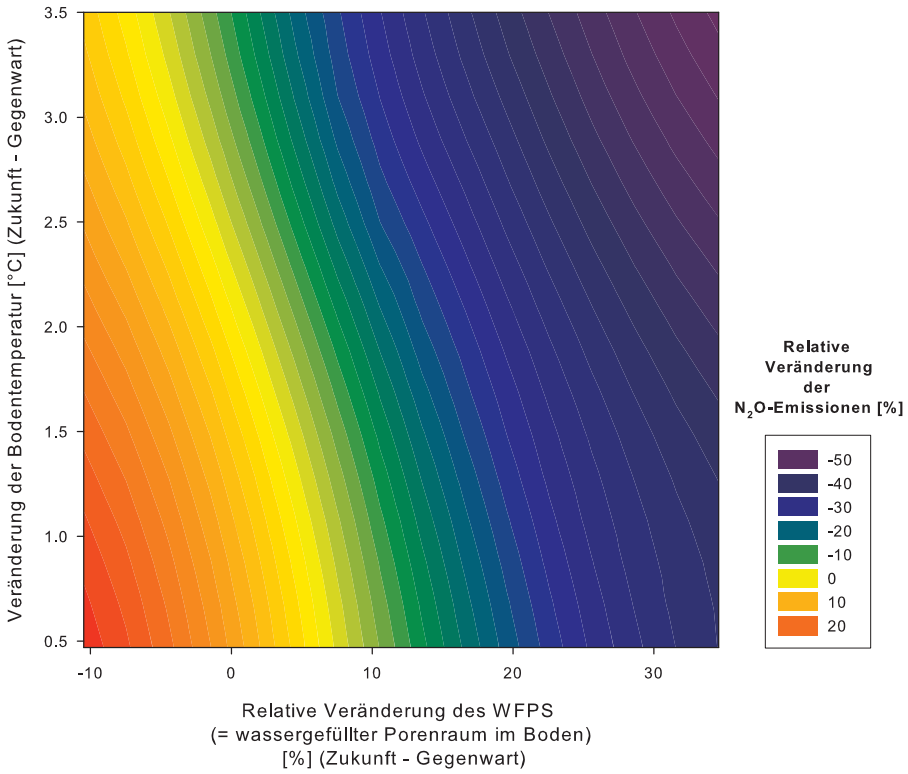

Abbildung 17: Höhenliniendiagramm, das den Einfluss der relativen Veränderung des wassergefüllten Porenraums (%) und der absoluten Bodentemperatur (°C) auf die relativen Veränderungen der N_2O-Emissionen darstellt. Für diese Analyse wurden alle Simulationsergebnisse für die gegenwärtigen und die zukünftigen Klimavorhersagen aller Rasterzellen Europas verwendet. Vor der Höhenlinienberechnung wurden die Daten mit SigmaPlot2000 (SPSS inc.) unter der Verwendung des Polynoms zweiten Grades geglättet.

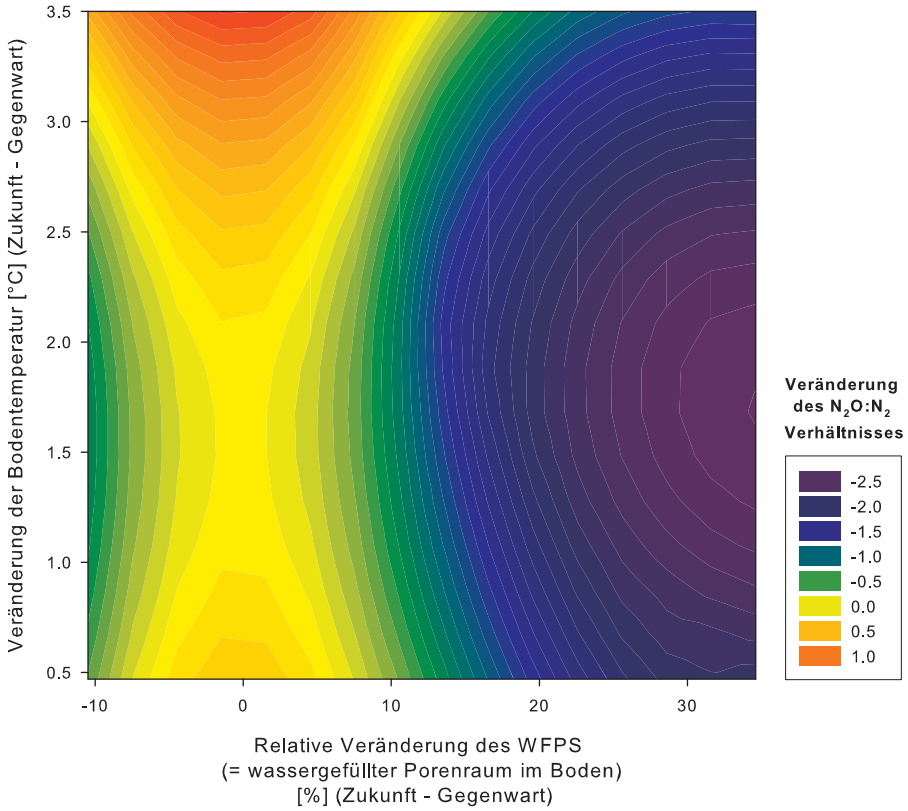

Abbildung 18: Höhenliniendiagramm, das die Unterschiede des N_2O:N_2 Verhältnisses zwischen den zukünftigen und gegenwärtigen Klimabedingungen darstellt. Diese Unterschiede werden von den relativen Veränderungen des wassergefüllten Porenraums (%) und der absoluten Bodentemperatur (°C) zwischen den zukünftigen und gegenwärtigen Klimabedingungen beeinflusst. Positive Werte des N_2O:N_2 Verhältnisses zeigen die Zunahme der N_2O-Emissionen und negative Werte zeigen die Zunahme der N_2-Emissionen. Für diese Analyse wurden alle Simulationsergebnisse für die gegenwärtigen und die zukünftigen Klimavorhersagen aller Rasterzellen Europas verwendet. Vor der Höhenlinienberechnung wurden die Daten mit SigmaPlot2000 (SPSS inc.) unter der Verwendung des Polynoms zweiten Grades geglättet.

3.5.4 Zukünftige Veränderungen der NO-Emissionen

Im Gegensatz zur durchschnittlichen Abnahme der N_2O-Emissionen aus Waldböden unter den vorhergesagten zukünftigen Klimaveränderungen, wird für die zukünftigen NO-Emissionen aus Waldböden Europas eine Zunahme um 9% (von 68 kt NO-N auf 74 kt NO-N) vorhergesagt (Tabelle 2 in Kesik et al., 2005, **III**). Die Zunahme der NO-Emissionen ist in den Sommermonaten am auffälligsten, für die die gegenwärtigen Emissionen von 29 kt NO-N auf 33 kt NO-N unter dem zukünftigen Klima ansteigen werden.
Auch bei den NO-Emissionen können regional deutliche Unterschiede festgestellt werden. Nur für einige wenige Gebiete, wie den Alpen, Großbritannien, Irland, Norwegen, Spanien, Portugal und für Teile Osteuropas (Bulgarien, Ungarn und Slowenien) wurde eine Abnahme der durchschnittlichen jährlichen NO-Emissionen (teilweise bis zu 62%) unter zukünftigen Klimabedingungen vorhergesagt. Für alle anderen Regionen hat das PnET-N-DNDC Modell eine Zunahme der NO-Emissionen für den Zeitraum 2031-2039 im Vergleich zum Zeitraum 1991-1999 vorhergesagt. Besonders in Regionen um die Ostsee können die NO-Emissionen um bis zu 29% zunehmen (Abbildung 16, siehe auch Tabelle 2 in Kesik et al., 2005, **III**). Die Veränderung der NO-Emissionen (Abbildung 16) im Sommer ist nicht signifikant unterschiedlich zu der Veränderung der NO-Jahresemissionen unter veränderten Klimabedingungen. Jedoch ist die Zunahme der NO-Emissionen aus Waldböden für die Sommermonate stärker als während des Jahres.

Die NO-Emissionen werden hauptsächlich durch die Aktivität der Nitrifizierer im Boden beeinflusst (z.B. Conrad, 1996, 2002). Die NO-Produktion in Böden sowie die NO-Emission zwischen Boden und Atmosphäre korreliert mit der Temperatur positiv (Valente und Thornton, 1993; Gasche und Papen, 1999; Ludwig et al., 2001). Dies ist hauptsächlich auf den positiven Einfluss der Temperatur auf die NO-Produktion über den Prozess der Nitrifikation zurückzuführen (Conrad, 2002).
Die optimale Bodenfeuchte für die Produktion von NO verschiebt sich im Vergleich zum N_2O zu niedrigeren Werten der Bodenfeuchte. Labor- und Felduntersuchungen haben gezeigt, dass bei einem wassergefüllten Porenraum von $> 60\%$ NO weiter zu N_2O und dann zu N_2 reduziert wird (z.B. Davidson, 1991; Bollmann und Conrad, 1998). Das bedeutet, dass das meiste NO bereits im Boden konsumiert wird, bevor es in die Atmosphäre entweichen kann. Vergleichbare Kinetiken sind im PNET-N-DNDC implementiert. Im PnET-N-DNDC ist das Konzept des ,,anaeroben Ballon“ enthalten (Kapitel 3.1.5) (Li et al., 2000). Wenn der Boden anaerober wird, z.B. aufgrund eines Sauerstoffdefizits durch Zunahme des wassergefüllten Porenraums, kann das durch die Nitrifikation (aber auch Denitrifikation) produzierte NO weiter durch die Denitrifizierer reduziert werden (bis jetzt ist die aerobe NO-Konsumption nicht im PnET-N-DNDC enthalten). Bei

dieser Simulation nehmen die durchschnittlichen Jahres-NO-Emissionen in den Rasterzellen zu, bei denen die durchschnittlichen Jahrestemperaturen zunahmen und die Zunahme des wassergefüllten Porenraum weniger als 18% betrug. (Abbildung 19). Sobald der wassergefüllte Porenraum unter zukünftigen Klimabedingungen weiter anstieg, reduzierten sich die NO-Emissionen deutlich, da das NO über den Prozess der Denitrifikation konsumiert wurde. Die Abnahme der NO-Emissionen für einige mediterrane Gebiete im Sommer ist im Wasserstress der mikrobiologischen Prozesse begründet. Diese Vorhersage ist in Übereinstimmung mit Ergebnissen aus Feld- und Laboruntersuchungen, die zeigen, dass bei länger anhaltenden Trockenperioden die NO-Emission stark zurückgeht (z.B. Davidson, 1991; Ludwig et al., 2001).

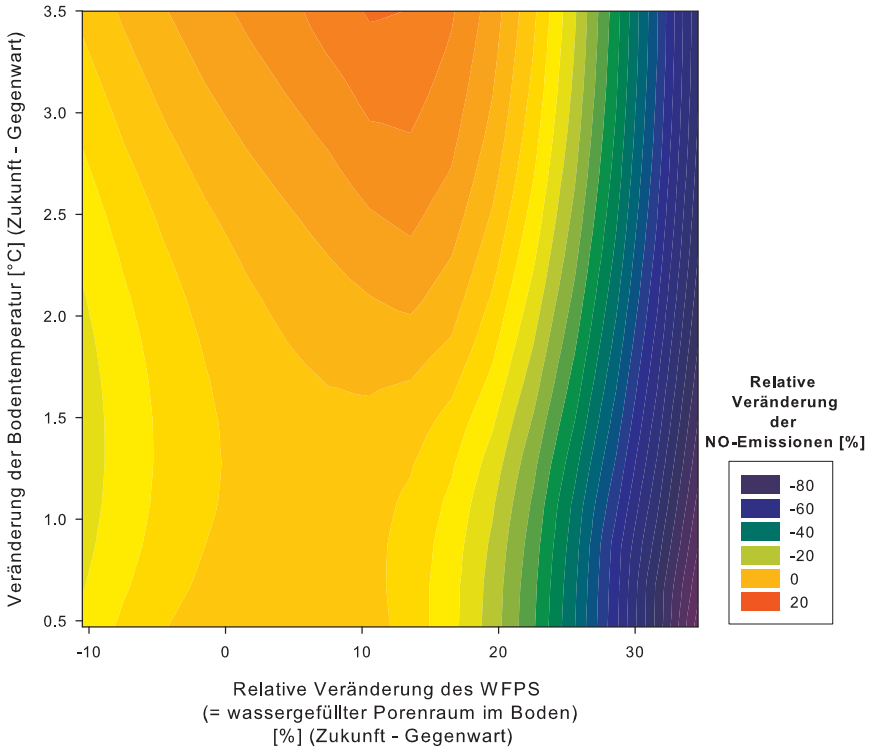

Abbildung 19: Höhenliniendiagramm, das den Einfluss der relativen Veränderung des wassergefüllten Porenraums (%) und der absoluten Bodentemperatur (°C) auf die relativen Veränderungen der NO-Emissionen darstellt. Für diese Analyse wurden alle Simulationsergebnisse für die gegenwärtigen und die zukünftigen Klimavorhersagen aller Rasterzellen Europas verwendet. Vor der Höhenlinienberechnung wurden die Daten mit SigmaPlot2000 (SPSS inc.) unter der Verwendung des Polynoms zweiten Grades geglättet.

3.6 Unsicherheitsanalysen für das Modell PnET-N-DNDC

Da das EMEP Raster mit einer Auflösung von 50km x 50km verwendet wurde, wurde angenommen, dass die Bedingungen (z.B. Bodenparameter) innerhalb jeder Rasterzelle gleich sind. Natürlich ist dies in der Realität nicht der Fall, da die Bodenparameter (z.B. pH Wert, organischer Kohlenstoffanteil) auf einer Fläche von 50km x 50km stark variieren. Diese Generalisierung der GIS-Datenbank im Hinblick z.B. auf Bodenparameter war notwendig, um die Computerrechenzeit zu minimieren und eine leichtere und übersichtliche Handhabung der GIS-Daten zu gewährleisten. Jedoch entstanden durch diese Generalisierung Unsicherheiten innerhalb der Ergebnisse der Modellsimulationen. Um diese Variabilität der Bodenparameter innerhalb der Zellen zu quantifizieren bzw. die Unsicherheitsspanne aufzuzeigen, innerhalb derer die N-Spurengase aus Waldböden einer Zelle vorkommen können, wurde sowohl die Most Sensitive Factor (MSF) Methode (Li et al., 2004) als auch die Monte Carlo Methode angewandt.

3.6.1 Most Sensitive Factor Methode (MSF)

Die sowohl vom PnET-N-DNDC als auch vom DNDC Modell simulierten N-Spurengasemissionen sind sehr sensitiv gegenüber Veränderungen in der Bodentextur, dem pH Wert und dem organischen Kohlenstoffgehalt des Bodens (Stange et al., 2000; Butterbach-Bahl et al., 2001; Li et al., 2004). Nach intensiven Sensitivitätsstudien der europäischen Bodendatenbank wurde im Rahmen dieser Arbeit festgestellt, dass es eine eindeutige Abhängigkeit zwischen den N_2O- und NO-Emissionen und den Bodenparametern (organischer Kohlenstoffgehalt, Tongehalt des Bodens und pH Wert) gibt. So nehmen die N_2O- und NO-Emissionen zu, sobald der organische Kohlenstoffgehalt und der Tongehalt ansteigen bzw. der pH Wert des Bodens abnimmt.
Diese Modellreaktionen stehen in Übereinstimmung mit einer Reihe von Labor- und Felduntersuchungen (Li et al., 2005). Die MSF Methode verwendet diesen Zusammenhang zwischen den einzelnen Bodenfaktoren zu der Höhe der N-Spurengasemissionen, indem eine Anzahl der Bodenparameter, für die die Minimum- und Maximumwerte des jeweiligen Parameters vorhanden sind, so gruppiert werden, dass sich die N-Spurengasemissionen entweder erhöhen oder verringern. Das bedeutet, das PnET-N-DNDC sucht automatisch den geringsten organischen Kohlenstoffgehalt der organischen Auflage und des Mineralbodens, den größten pH Wert der organischen Auflage und des Mineralbodens, sowie den höchsten Bodenskelettanteil und den geringsten Tongehalt einer Rasterzelle aus, um ein Szenario zu erschaffen, bei dem angenommen wird, dass es geringe N_2O- und NO-Emissionen für diese Rasterzelle produziert (Minimum-Szenario). Dann

sucht das Modell den größten organischen Kohlenstoffgehalt und kleinsten pH Wert der organischen Auflage und des Mineralbodens, sowie den geringsten Bodenskelettanteil und größten Tongehalt des Bodens einer Rasterzelle aus, um ein weiteres Szenario zu kreieren, das höchstwahrscheinlich die höchsten Werte der N_2O- und NO-Emissionen dieser Rasterzelle produziert (Maximum-Szenario). So wurden für diese beiden Szenarien für jede Rasterzelle in das PnET-N-DNDC zwei zusätzliche Läufe implementiert, die eine obere und untere Begrenzung für die erwarteten N_2O- und NO-Emissionen in dieser Rasterzelle darstellen. Es wird angenommen, dass diese berechnete Begrenzung für die N-Spurengasemissionen groß genug ist, um die tatsächliche N-Spurengasemission mit höchster Wahrscheinlichkeit zu beinhalten. Um diese MSF Methode zu überprüfen, wurde zusätzlich die Monte Carlo Methode in das PnET-N-DNDC implementiert. Dies erlaubt die direkte Quantifizierung der Unsicherheiten aufgrund der räumlichen Heterogenität der Bodenparameter für jede einzelne EMEP-Rasterzelle (siehe auch Li et al., 2004).

Für ganz Europa wurde mit Hilfe der MSF Methode eine kumulative Summe des Minimum-, Maximum- und eines sog. Durchschnittsszenarios für die N_2O- und NO-Emissionen für die Jahre 1990, 1995 und 2000 berechnet (Tabelle 4).
Für das Jahr 2000 wurde durchschnittlich eine Gesamt-N_2O-Emission aus Waldböden Europas von 82 kt N Jahr^{-1} berechnet. Die zugehörige Unsicherheitspanne für das Jahr 2000 erstreckt sich im Bereich zwischen 51 to 97 kt N Jahr^{-1}; dies entspricht einer Differenz zum Durchschnittsszenario von -40% (Minimumszenario) bzw. +16% (Maximumszenario).

Tabelle 4: Unsicherheitsbereich der berechneten Gesamt-N_2O- und NO-Emissionen aus Waldböden Europas. Die Unsicherheitsbereiche wurden mit der Most Sensitive Factor Methode (Li et al., 2004) berechnet.

Jahr	**Minimumszenario**	**Durchschnittsszenario**	**Maximumszenario**
		N_2O-Emission (kt N Jahr^{-1})	
1990	55	87	100
1995	50	78	96
2000	51	82	97
		NO-Emission (kt N Jahr^{-1})	
1990	45	98	248
1995	38	85	220
2000	44	99	254

Die Unsicherheit bei der Vorhersage der NO-Emissionen ist deutlich höher. So wurden für das Jahr 2000 im Durchschnittsszenario Gesamt-NO-Emissionen von 99 kt N Jahr^{-1} mit einem Unsicherheitsbereich zwischen 44 und 254 kt N Jahr^{-1} simuliert. Dies entspricht einer Differenz zum Durchschnittsszenario von -66% bzw. +156%. Der Unterschied zwischen den Unsicherheitsbereichen der N_2O- und NO-Emissionen ist auf die hohe Sensitivität des pH Wertes zur NO-Produktion über den Prozess der Chemodenitrifikation zurückzuführen.

3.6.2 Monte Carlo Methode

Bei der Monte Carlo Methode wurde der Bereich zwischen dem minimalen und maximalen Wert des jeweiligen Bodenparameters innerhalb einer Rasterzelle in acht Intervalle unterteilt. Wenn z.B. der pH Wert einer Rasterzelle zwischen pH 3,5 und pH 5,6 lag, so konnte die Monte Carlo Methode im PnET-N-DNDC aus dieser Rasterzelle die folgenden pH Wertintervalle wählen: pH 3,5, pH 3,8, pH 4,1, pH 4,4, pH 4,7, pH 5,0, pH 5,3, pH 5,6. Das PnET-N-DNDC wählt zufällig ein Intervall aus jedem der sechs Bodenparameter aus (Tongehalt, organischer Kohlenstoffgehalt der organischen Auflage und des Mineralbodens, pH Wert der organischen Auflage und des Mineralbodens, Bodenskelettanteil) und bildet hieraus ein Szenario. Dieser Vorgang wiederholt sich 5000 Mal, so dass 5000 N_2O- und 5000 NO-Emissionswerte für eine Rasterzelle berechnet werden. Die Ergebnisse werden dann mit den Ergebnissen der MSF Methode verglichen.
Für die Monte Carlo Methode wurden europaweit zufällig 50 Rasterzellen ausgewählt und die Ergebnisse der Häufigkeitsverteilung der N_2O- und NO-Emissionen mit den Ergebnissen der MSF Methode, d.h. mit dem Emissionswertebereich zwischen dem minimalen und maximalen Szenario für die jeweilige Rasterzelle verglichen. Der Vergleich der MSF Methode mit der Monte Carlo Methode für alle 50 Rasterzellen zeigt, dass die mit der Monte Carlo Methode berechneten NO-Emissionen zu 79% im NO-Emissionswertebereich der MSF Methode liegen. Die durch die MSF Methode berechneten maximalen N_2O-Emissionsraten waren um ca. 50% niedriger als die mit der Monte Carlo Methode berechneten N_2O-Emissionen. Die durch die MSF Methode berechneten minimalen N_2O-Emissionen waren um das zweifache höher als die durch die Monte Carlo berechneten Emissionen. Da jedoch die untere Grenze der N_2O-Emissionen zwischen 0,1 und 0,2 kg N ha^{-1} Jahr^{-1} lag, kann dieser Unterschied im Rahmen dieser Arbeit vernachlässigt werden.
Aufgrund dieser Unterschätzung der maximalen N-Spurengasemissionen sind die Unsicherheitsabschätzungen mittels der MSF Methode nicht gänzlich zufrieden stellend, aber sie repräsentieren die beste Unsicherheitsabschätzung, die mit vertretbarem Rechenaufwand im Rahmen dieser Arbeit geleistet werden konnte.

Für die Unsicherheitsabschätzung mittels der MSF Methode wird eine Rechenzeit für das Gesamtkataster von 30 h benötigt. Die Anwendung der Monte Carlo Methode auf alle Rasterzellen in Europa wäre die beste Methode, um die Unsicherheiten in den Vorhersagen am genausten abschätzen zu können. Hierzu ist jedoch eine Verbesserung des Modells im Hinblick auf eine Reduzierung der Rechenzeit notwendig, da das PnET-N-DNDC für eine Monte Carlo Simulation (5.000 Läufe) einer Rasterzelle 8h benötigt (Gesamtkataster = 36.216 h).

3.7 Schlussbemerkung und Ausblick

In dieser Arbeit und in den Publikationen von Kesik et al. (2005) **II**, **III** wird gezeigt, dass es sich beim PnET-N-DNDC um ein geeignetes Modell handelt, um N-Spurengasemissionen aus Waldböden zu simulieren. Die Anwendung des Modells über einen so großen Bereich an europaweiten Feldmessungen zeigt, dass das Modell die beobachteten Unterschiede in den N-Spurengasemissionen der einzelnen Messstandorte gut wiedergibt. So konnte das PnET-N-DNDC 68% der beobachteten N_2O-Emissionsmessungen und sogar 78% der beobachteten NO-Emissionen reproduzieren. Dennoch zeigt diese Validierung auch, dass das Modell weiter entwickelt werden muss, besonders der Zeitpunkt der höchsten Emissionen bzw. die Höhe der Saisonalität der N-Spurengasemissionen (Abbildung 13).

Eine weitere Verbesserung und Entwicklung des PnET-N-DNDC Modells bedarf eines besseren Verständnisses und einer besseren Parametrisierung der mikrobiellen N-Umsetzungsprozesse, v.a. im Hinblick auf die denitrifikatorische N_2-Produktion und damit auch in Bezug auf das N_2O- zu N_2-Verhältnis während der Denitrifikation.
Auch bleibt die mechanistische Beschreibung der N-Aufnahme der Pflanzen gegenüber der mikrobiellen N-Aufnahme weiterhin eine Herausforderung, da unser Verständnis vom Konkurrenzkampf um N zwischen Pflanze und mikrobieller Gemeinschaft immer noch eingeschränkt ist (Rennenberg et al., 1998).
Ebenso würde eine detaillierte Standortbeschreibung, wie z.B. die Veränderungen in den Bodenparametern in Abhängigkeit zur Bodentiefe und die hydrologischen Eigenschaften in Abhängigkeit zur Standortlage die Basis für die Simulationen verbessern. So ist ein weiterer Schritt zur Weiterentwicklung und Verbesserung des Modells die Anbindung eines hydrologischen Modells an das PnET-N-DNDC. Da das PnET-N-DNDC momentan den Bodenwasserhaushalt (Wasser- und Stofftransport) eindimensional simuliert, ist die Kopplung an ein dreidimensionales Niederschlags-Abflussmodell notwendig, um die hydrologischen Prozesse (Oberflächenabfluss, Inflow im Boden und Grundwasserbasisabfluss) im Boden realitätsnah wiedergeben zu können. Jedoch bedarf diese Veränderung des Modells eine Erweiterung der Initialisierungs- und Steuerungsparameter, was wiederum

die Anwendung eines solchen Modells aufgrund der eingeschränkten Verfügbarkeit dieser Parameter auf regionaler Ebene stark einschränkt.

Bei der Weiterentwicklung des Modells sollten zukünftig auch einige modellinterne Parameterunsicherheiten behoben werden. Im Rahmen dieser Arbeit konnte mit Hilfe der Laboruntersuchungen an *A. faecalis p.* der Prozess der Chemodenitrifikation im PnET-N-DNDC verbessert werden. Im Zusammenhang mit der pH Abhängigkeit der N_2O- und NO-Emissionen sollte in den zukünftigen Modellentwicklungen der Einfluss des pH Wertes auch auf kleinräumiger Skala, ähnlich dem Konzept des ,,anaeroben Ballons" (Kapitel 3.1) berücksichtigt werden. Denn besonders in sauren Böden kann der pH Wert kleinräumig stark (bis zu 3 pH-Werteinheiten) variieren (z.B. Häussling et al., 1985; Bruelheide und Udelhoven, 2005).

Im Rahmen dieser Arbeit erfolgte die Kalibrierung des Modells mittels einer einfachen Methode, bei der jeweils nur ein Parameter im Modell variiert wurde, während alle anderen konstant blieben. Wünschenswert ist eine multi-objektive Kalibrierung, d.h. ein Kalibrierungsverfahren für das PnET-N-DNDC, bei dem mehrere Eingangsvariablen gleichzeitig verändert werden können.

Weiterhin muss die Verfügbarkeit und die Qualität der GIS-Informationen für die Initialisierung und die Steuerung komplexer Modelle getestet und wenn möglich weiter verbessert werden. Aufgrund der räumlichen Unterschiede der Bodenparameter und der starken Sensitivität des PnET-N-DNDC gegenüber Veränderungen des organischen C-Gehaltes des Bodens oder des pH Wertes des Bodens (Stange et al., 2000) spiegelt sich die Unsicherheit über die regionale Verteilung dieser Parameter in einem signifikanten Anstieg des Vorhersagefehlers wider. Diese Unsicherheit wurde auf regionaler Ebene mit Hilfe der Most Sensitive Factor (MSF) Methode (Li et al., 2004) und der Monte Carlo Methode für zufällig ausgesuchte Rasterzellen in Europa versucht zu reduzieren. Somit konnte eine Unsicherheitsspanne kreiert werden, die mit höchster Wahrscheinlichkeit die mittlere N-Spurengasemission enthält.

Man mag vielleicht behaupten, dass biogeochemische Modelle wie das PnET-N-DNDC überparametrisiert seien und man mit einfacheren empirischen Ansätzen vergleichbare Ergebnisse erzielen könne. Dennoch wird aufgrund der immer noch eingeschränkten Zahl an Feldmessungen und der beobachteten Komplexität und Bedeutung der meteorologischen und der Boden-Parameter die Berechnung der Höhe der N-Spurengasemissionen aus Böden durch rein empirische Modelle nicht bzw. schwer möglich sein. Zudem können empirische Modelle nur für das Gebiet verwendet werden, für das sie auch validiert wurden, wohingegen biogeochemische Modelle – zumindest in der Theorie – zur Vorhersage von Emissionen aus Standorten mit signifikant unterschiedlichen Standorteigenschaften gegenüber denen,

für die sie getestet wurden, angewandt werden können.
Die Berechnung von N_2O- und NO-Emissionskatastern für Waldböden mit dem PnET-N-DNDC Modell für Süddeutschland, Sachsen (Butterbach-Bahl et al., 2001, 2004), aber auch für Queensland, Australien (Kiese et al., 2005) und im Rahmen dieser Arbeit sowie in Kesik et al. (2005, **II**) für die verschiedenen Waldböden Europas haben deutlich gezeigt, dass das Modell geeignet ist, die N-Spurengasemissionen aus verschiedenen Waldökosystemen weltweit zu simulieren. So ist eine Kopplung des PnET-N-DNDC Modells mit Klimamodellen wie z.B. dem gekoppelten Klima-Chemie-Modell MCCM (Multiscale Climate and Chemistry Model, Grell et al., 2000) oder dem globalen Klimamodell ECHAM4 zur Berechnung von Rückkopplungsmechanismen von N-Spurengasemissionen aus Wäldern auf die zukünftige Klimaveränderung wünschenswert. Die gewonnenen Ergebnisse aus den N-Spurengasemissionskatastern könnten dann mit Hilfe der inversen Modellierung überprüft werden. Aus diesen Gründen ist die Erstellung einer globalen GIS-Datenbank und die Berechnung eines N_2O- und NO-Emissionskatasters für weltweite Waldböden mit dem PnET-N-DNDC Modell zukünftig vorgesehen. Besonders im Hinblick auf das Kyoto-Protokoll, das zur Quantifizierung der einzelnen Treibhausgase verpflichtet, sind Kataster zur Abschätzung von globalen N-Emissionen aus Wäldern notwendig.

Literaturverzeichnis

Aber J. D. & Federer C. A. (1992): A generalized, lumped-parameter model of photosynthesis, evapotranspiration and net primary production in temperate and boreal forest ecosystems; *Oecologica*; Vol. 92(4): S. 463–474.

Aber J. D., Nadelhoffer K. J., Steudler P. & Melillo J. M. (1989): Nitrogen saturation in northern forest ecosystems; *Bioscience*; Vol. 39(6): S. 378–386.

Anderson I. C., Poth M., Homestead J. & Burdige D. (1993): A comparison of NO and N2O production by the autotrophic nitrifier Nitrosomonas europaea and the heterotrophic nitrifier Alcaligenes faecalis; *Appl.Environ.Microb.*; Vol. 59(11): S. 3525–3533.

Barnard R., Leadley P. W. & Hungate B. A. (2005): Global change, nitrification, and denitrification: A review; *GlobalBiogeochem.Cyc.*; Vol. 19(1): GB1007.

Baumgärtner M. & Conrad R. (1992): Role of nitrate and nitrite for production and consumption of nitric-oxide during denitrification in soil; *FEMS-Microbiol.Ecol.*; Vol. 101(1): S. 59–65.

Benestad R. E. (2005): Climate change scenarios for northern Europe from multi-model IPCC AR4 climate simulations; *Geophys.Res.Lett.*; Vol. 32(17): L17704.

Bock E., Koops H.-P. & Harms H. (1986): Cell biology of nitrifying bacteria; in: Prosser J. (Hg.): Nitrification; S. 17–38; IRL Press, Oxford, UK.

Boeckx P. & van Cleemput O. (2001): Estimates of N2O and CH4 fluxes from agricultural lands in various regions in Europe; *Nutr.Cycl.Agroecosys.*; Vol. 60(1-3): S. 35–47.

Bollmann A. & Conrad R. (1998): Influence of O2 availability on NO and N2O release by nitrification and denitrification in soils; *GlobalChange.Biol.*; Vol. 4(4): S. 387–396.

Bouwman A. (1998): Nitrogen oxides and tropical agriculture; *Nature*; Vol. 392: S. 886–887.

Bowden R. D., Melillo J. M., Steudler P. A. & Aber J. D. (1991): Effects of nitrogen additions on annual nitrous-oxide fluxes from temperate forest soils in the northeastern United States; *J.Geophys.Res.*; Vol. 96(D5): S. 9321–9328.

Breuer L. (2000): N2O-Freisetzung aus tropischen Waldböden Australiens – Anteil von Nitrifikation und Denitrifikation; in: Schriftenreihe des Fraunhofer-Instituts für Atmosphärische Umweltforschung; Vol. 64; Garmisch-Partenkirchen, Germany.

Brown L., Syed B., Jarvis S. C., Sneath R. W., Phillips V. R., Goulding K. W. T. & Li C. (2002): Development and application of a mechanistic model to estimate emission of nitrous oxide from UK agriculture; *Atmos.Environ.*; Vol. 36(25): S. 917–928.

Bruelheide H. & Udelhoven P. (2005): Correspondence of the fine-scale spatial variation in soil chemistry and the herb layer vegetation in beech forests; *ForestEcol.Manag.*; Vol. 210(1-3): S. 205–223.

Brumme R. (1995): Mechanisms of carbon and nutrient release and retention in beech forest gaps. 3. Environmental regulation of soil respiration and nitrous-oxide emissions along a microclimatic gradient; *PlantSoil*; Vol. 169: S. 593–600.

Brumme R., Borken W. & Finke S. (1999): Hierarchical control on nitrous oxide emission in forest ecosystems; *GlobalBiogeochem.Cyc.*; Vol. 13(4): S. 1137–1148.

Brumme R., Verchot L., Martikainen P. & C.S. P. (2005): Contribution of trace gases nitrous oxide (N2O) and methane (CH4) to the atmospheric warming balance of forest biomes; in: Griffiths H. & P.G. J. (Hg.): The Carbon Balance of Forest Biomes; S. 293–318; Taylor and Francis Group, Oxon, New York, USA.

Butterbach-Bahl K., Breuer L., Gasche R., Willibald G. & Papen H. (2002a): Exchange of trace gases between soils and the atmosphere in

Scots pine forest ecosystems of the northeastern German lowlands 1. Fluxes of N2O, NO/NO2 and CH4 at forest sites with different N-deposition; *ForestEcol.Manag.*; Vol. 167(1-3): S. 123–134.

Butterbach-Bahl K., Gasche R., Willibald G. & Papen H. (2002b): Exchange of N-gases at the Hoglwald Forest. A summary; *PlantSoil*; Vol. 240(1): S. 117–123.

Butterbach-Bahl K., Kesik M., Miehle P., Papen H. & Li C. (2004): Quantifying the regional source strength of N-trace gases across agricultural and forest ecosystems with process based models; *PlantSoil*; Vol. 260(1-2): S. 311–329.

Butterbach-Bahl K. & Kiese R. (2005): Significance of forests as sources for N2O and NO; in: Binkley D. & Menyailo O. (Hg.): Tree Species effects on soils: implications for global change; S. 173–191; Springer, Netherlands.

Butterbach-Bahl K., Stange F., Papen H. & Li C. S. (2001): Regional inventory of nitric oxide and nitrous oxide emissions for forest soils of southeast Germany using the biogeochemical model PnET-N-DNDC; *J.Geophys.Res.*; Vol. 106(D24): S. 34.155–34.166.

CEC (1994): Corine Landcover; Techn. Ber.; CEC; Luxembourg.

CEC-DGVI (1985): Soil map of European Communities at 1: 1,000,000; Techn. Ber.; CEC-DGVI; Brussels, Belgium.

Conrad R. (1996): Soil microorganisms as controllers of atmospheric trace gases (H2, CO, CH4, OCS, N2O, and NO); *Microbiol.Rev.*; Vol. 60(4): S. 609–640.

Conrad R. (2002): Microbiological and biochemical background of production and consumption of NO and N2O in soil; in: Gasche R., Papen H. & Rennenberg H. (Hg.): Trace gas exchange in forest ecosystems; S. 3–33; Kluwer Academic Publishers, Dordrecht, Boston, London, Netherlands, USA, UK.

Crutzen P. (1995): Ozone in the troposphere; in: Sing H. (Hg.): Composition, Chemistry, and Climate of the Atmosphere; S. 349–393; Van Nostrand-Reinold, New York, USA.

Daum D. & Schenk M. K. (1998): Influence of nutrient solution pH on N2O and N2 emissions from a soilless culture system; *PlantSoil*; Vol. 203(2): S. 279–287.

Davidson E. (1991): Fluxes of nitrous oxide and nitric oxide from terrestrial ecosystems; in: Rogers J. & Whitman W. (Hg.): Microbial Production and Consumption of Greenhouse Gases: Methane, Nitrogen Oxides and Halomethanes; S. 219–235; American Society for Microbiology, Washington D.C., USA.

Davidson E. A. & Kingerlee W. (1997): A global inventory of nitric oxide emissions from soils; *Nutr.Cycl.Agroecosys.*; Vol. 48(1-2): S. 37–50.

Davidson E. A., Potter C. S., Schlesinger P. & Klooster S. A. (1998): Model estimates of regional nitric oxide emissions from soils of the southeastern United States; *Ecol.Appl.*; Vol. 8(3): S. 748–759.

Ellis S., Howe M. T., Goulding K. W. T., Mugglestone M. A. & Dendooven L. (1998): Carbon and nitrogen dynamics in a grassland soil with varying pH: Effect of pH on the denitrification potential and dynamics of the reduction enzymes; *SoilBiol.Biochem.*; Vol. 30(3): S. 359–367.

Enquete-Kommission (1992): Klimaänderung gefährdet globale Entwicklung. Zukunft sichern – Jetzt handeln; Economica-Verlag, Bonn, Germany.

Firestone M. & Davidson E. (1989): Microbiological basis of NO and N2O production and consumption in soil; in: Andreae M. & Schimel D. (Hg.): Exchange of trace gases between terrestrial ecosystems and the atmosphere; S. 7–21; Wiley, Chichester, UK.

Forkel R. & Knoche R. (2005submitted): Regional climate change and its impacts on photooxidant concentrations in southern Germany: Simulations with a coupled regional climate-chemistry model; *J.Geophys.Res.*.

Gamble T., Betlach M. & Tiedje J. (1977): Numerically dominant denitrifying bacteria from world soils; *Appl.Environ.Microb.*; Vol. 33: S. 926–939.

Ganzeveld L. N., Lelieveld J., Dentener F. J., Krol M. C., Bouwman A. J. & Roelofs G.-J. (2002): Global soil-biogenic NOx emissions and the role of canopy processes; *J.Geophys.Res.*; Vol. 107(D16): S. 4298–4307.

Gasche R. & Papen H. (1999): A 3-year continuous record of nitrogen trace gas fluxes from untreated and limed soil of a N-saturated spruce and beech forest ecosystem in Germany: 2. NO and NO2 fluxes; *J.Geophys.Res.*; Vol. 104(D15): S. 18.505–18.520.

Giorgi F., Bi X. Q. & Pal J. (2004): Mean, interannual variability and trends in a regional climate change experiment over Europe. II: climate change scenarios (2071-2100); *Clim.Dynam.*; Vol. 23(7-8): S. 839–858.

Goodroad L. & Keeney D. (1984): Nitrous oxide production in aerobic soils under varying pH, temperature and water content; *SoilBiol.Biochem.*; Vol. 16: S. 39–43.

Graedel T. & Crutzen P. (1994): Chemie der Atmosphäre; Akademischer Verlag Spektrum, Heidelberg, Germany und Oxford, UK.

Granli T. & Bockmann O. (1994): Nitrous oxide from agriculture; in: Norwegian Journal od Agricultural Sciences; Vol. 12.

Grell G. A., Emeis S., Stockwell W. R., Schoenemeyer T., Forkel R., Michalakes J., Knoche R. & Seidl W. (2000): Application of a multiscale, coupled MM5/chemistry model to the complex terrain of the VOTALP valley campaign; *Atmos.Environ.*; Vol. 34(9): S. 1435–1453.

Houghton J., Callander B. & Varney S. (1992): IPCC 1992: The Supplementary Report to the IPCC Scientific Assessment; Cambridge University Press, Cambridge, UK.

Houghton J., Ding Y., Griggs D., Noguer M., van der Linden P., Dai X., Maskell K. & Johnson C. (2001): IPCC 2001: Climate Change 2001: The Scientific Basis. Contribution of Working Group I to the Third Assessment Report of the Intergovernmental Panel on Climate Change; Cambridge University Press, Cambridge, UK and New York, USA.

Houghton J., Jenkins G. & Ephraums J. (1990): IPCC 1990: Climate Change: The IPCC Scientific Assessment; Cambridge University Press, Cambridge, UK.

Häussling M., Leisen E., Marschner H. & Römheld V. (1985): An improved method for non-destructive measurements of the pH at the root-soil interface (rhizosphere); *J.PlantPhysiol.*; Vol. 117: S. 371–375.

Johansson C. (1984): Field measurements of emission of nitric oxide from fertilized and unfertilized forest soils in Sweden; *J.Atmos.Chem.*; Vol. 1: S. 429–442.

Jungkunst H., Fiedler S. & Stahr K. (2004): N2O emissions of mature Norway spruce (Picea abies) stand in the Black Forest (southwest Germany) as differentiated by soil pattern; *J.Geophys.Res*; Vol. 109: DOI: 10.1029/2003JD004344.

Keeney D., Fillery I. & Marx G. (1979): Effect of temperature on the gaseous nitrogen products of denitrification in a silt loam soil; *SoilSci.Soc.Am.J.*; Vol. 43: S. 1124–1128.

Kiese R., Li C. S., Hilbert D. W., Papen H. & Butterbach-Bahl K. (2005): Regional application of PnET-N-DNDC for estimating the N2O source strength of tropical rainforests in the Wet Tropics of Australia; *GlobalChangeBiol.*; Vol. 11(1): S. 128–144.

Kjellstrom E. (2004): Recent and future signatures of climate change in Europe; *Ambio*; Vol. 33(4-5): S. 193–198.

Knoche R., Forkel R. & Kunstmann H. (2003): Regionale Klimasimulationen für Süddeutschland und den Alpenraum; in: Forum für Hydrologie und Wasserbewirtschaftung; Vol. 4 (3); S. 11–18.

Koskinen W. & Kenney D. (1982): Effect of pH on the rate of gaseous products of denitrification in a silt loam soil; *SoilSci.Soc.Am.J.*; Vol. 46: S. 1165–1167.

Krämer M. & Conrad R. (1991): Influence of oxygen on production and consumption of nitric-oxide in soil; *Biol.Fert.Soils*; Vol. 11(1): S. 38–42.

Kroeze C., Mosier A. & Bouwman L. (1999): Closing the N2O Budget: A retrospective analysis; *GlobalBiogeochem.Cyc.*; Vol. 13: S. 1–8.

Kuenen J. & Robertson L. (1987): Ecology of nitrification and denitrification; in: Cole J. & Ferguson S. (Hg.): The nitrogen and sulphur cycles: Symposia of the Society for General Microbiology; Vol. 42; S. 161–218; Cambridge University Press, Cambridge, UK.

Lee D., Köhler I., Grobler E., Rohrer F., Sausen R., Gallardo-Klenner L., Olivier J., Dentener F. & Bouwman A. (1997): Estimation of global NOx emissions and their uncertainties; *Atmos.Environ.*; Vol. 31: S. 1735–1749.

Li C., Frolking S. & Butterbach-Bahl K. (2005): Carbon sequestration in arable soils is likely to increase nitrous oxide emissions, ofsetting reductions in climate radiative forcing; *ClimaticChange*; Vol. 72: S. 321–338.

Li C. S. (2000): Modeling trace gas emissions from agricultural ecosystems; *Nutr.Cycl.Agroecosys.*; Vol. 58(1-3): S. 259–276.

Li C. S., Aber J., Stange F., Butterbach-Bahl K. & Papen H. (2000): A process-oriented model of N2O and NO emissions from forest soils: 1. Model development; *J.Geophys.Res.*; Vol. 105(D4): S. 4369–4384.

Li C. S., Frolking S. & Frolking T. A. (1992): A model of nitrous-oxide evolution from soil driven by rainfall events: 1. Model structure and sensitivity; *J.Geophys.Res.*; Vol. 97(D9): S. 9759–9776.

Li C. S., Mosier A., Wassmann R., Cai Z. C., Zheng X. H., Huang Y., Tsuruta H., Boonjawat J. & Lantin R. (2004): Modeling greenhouse gas emissions from rice-based production systems: Sensitivity and upscaling; *GlobalBiogeochem.Cyc.*; Vol. 18(1): GB1043.

Li C. S., Zhuang Y. H., Cao M. Q., Crill P., Dai Z. H., Frolking S., Moore B., Salas W., Song W. Z. & Wang X. K. (2001): Comparing

a process-based agro-ecosystem model to the IPCC methodology for developing a national inventory of N2O emissions from arable lands in China; *Nutr.Cycl.Agroecosys.*; Vol. 60(1-3): S. 159–175.

Ludwig J., Meixner F. X., Vogel B. & Forstner J. (2001): Soil-air exchange of nitric oxide: An overview of processes, environmental factors, and modeling studies; *Biogeochemistry*; Vol. 52(3): S. 225–257.

Maljanen M., Hytonen J. & Martikainen P. J. (2001): Fluxes of N2O, CH4 and CO2 on afforested boreal agricultural soils; *PlantSoil*; Vol. 231(1): S. 113–121.

Maljanen M., Liikanen A., Silvola J. & Martikainen P. J. (2003): Nitrous oxide emissions from boreal organic soil under different land-use; *SoilBiol.Biochem.*; Vol. 35(5): S. 689–700.

Maracchi G., Sirotenko O. & Bindi M. (2005): Impacts of present and future climate variability on agriculture and forestry in the temperate regions: Europe; *ClimaticChange*; Vol. 70(1-2): S. 117–135.

Martikainen P. (1985): Nitrous oxide emission associated with autotrophic ammonium oxidation in acid coniferous forest soil; *Appl.Environ.Microb.*; Vol. 50: S. 1519–1525.

Martikainen P. (1996): Microbial processes in boreal forest soils as affected by forest management practices and atmospheric stress; in: Stotzky G. & Bollag J. (Hg.): Soil Biochemistry; S. 195–232; Dekker Ic., New York, USA.

Mücher C. (2000): Pan-European Land Cover Mapping (PELCOM) project. Development of a consistent methodology to derive landcover information on a European scale from remote sensing for environmental modelling.

McKenney D., Lazar C. & Findley W. (1990): Kinetics of the nitrite to nitric oxide reaction in peat; *SoilSci.Soc.Am.J.*; Vol. 54: S. 106–112.

McKenney D. J., Drury C. F., Findlay W. I., Mutus B., McDonnell T. & Gajda C. (1994): Kinetics of denitrification by Pseudomonas - Fluorescensoxygen effects; *SoilBiol.Biochem.*; Vol. 26(7): S. 901–908.

Mosier A., Kroeze C., Nevison C., Oenema O., Seitzinger S. & van Cleemput O. (1998): Closing the global N2O budget: nitrous oxide emissions through the agricultural nitrogen cycle. OECD/IPCC/IEA phase II development of IPCC guidelines for national greenhouse gas inventory methodology; *Nutr.Cycl.Agroecosys.*; Vol. 52(2-3): S. 225–248.

Nägele W. & Conrad R. (1990): Influence of pH on the release of NO and N2O from fertilzed and unfertilized soil; *Biol.Fert.Soils*; Vol. 10(2): S. 139–144.

Nommik H. (1956): Investigations on denitrification in soil; *ActaAgr.Scand.*; Vol. 6: S. 195–228.

Olivier J., Bouwman A., van der Hoek K. & Berdowski J. (1998): Global Air Emission Inventories for Anthropogenic Sources of NOx, NH3 and N2O in 1990; *Environ.Pollut.*; Vol. 102: S. 135–148.

Ormeci B., Sanin S. L. & Peirce J. J. (1999): Laboratory study of NO flux from agricultural soil: Effects of soil moisture, pH, and temperature; *J.Geophys.Res.*; Vol. 104(D1): S. 1621–1629.

Otte S., Grobben N. G., Robertson L. A., Jetten M. S. M. & Kuenen J. G. (1996): Nitrous oxide production by Alcaligenes faecalis under transient and dynamic aerobic and anaerobic conditions; *Appl.Environ.Microb.*; Vol. 62(7): S. 2421–2426.

Papen H. & von Berg R. (1998): A Most Probable Number method (MPN) for the estimation of cell numbers of heterotrophic nitrifying bacteria in soil; *PlantSoil*; Vol. 199(1): S. 123–130.

Papen H., von Berg R., Hinkel I., Thoene B. & Rennenberg H. (1989): Heterotrophic nitrification by Alcaligenes faecalis. NO2-, NO3-, N2O, and NO production in exponentially growing cultures; *Appl.Environ.Microb.*; Vol. 55(8): S. 2068–2072.

Papen H. & Butterbach-Bahl K. (1999): A 3-year continuous record of nitrogen trace gas fluxes from untreated and limed soil of a N-saturated spruce and beech forest ecosystem in Germany. 1. N2O emissions; *J.Geophys.Res.*; Vol. 104(D15): S. 18.487–18.503.

Papen H., Hellman B., Papke H. & Rennenberg H. (1993): Emission of N-oxides from acid irrigated and limed soils of a coniferous forest in Bavaria; in: Oremland R. (Hg.): Biogeochemistry of Global Change: Radiatively Active Trace Gases; S. 245–260; Chapman and Hall, New York, USA.

Parton W. (1996): The CENTURY model; in: Powlson D., Smith P. & Smith J. (Hg.): Evaluation of soil organic matter models using existing long-term datasets; NATO ASI Series I; Springer-Verlag, Berlin, Germany.

Paul E. & Clark F. (1988): Soil Microbiology and Biochemistry; Academic Press, San Diego, USA.

Pilegaard K., Hummelshoj P. & Jensen N. O. (1999): Nitric oxide emission from a Norway spruce forest floor; *J.Geophys.Res.*; Vol. 104(D3): S. 3433–3445.

Potter C. S., Matson P. A., Vitousek P. M. & Davidson E. A. (1996): Process modeling of controls on nitrogen trace gas emissions from soils worldwide; *J.Geophys.Res.*; Vol. 101(D1): S. 1361–1377.

Regina K., Nykanen H., Silvola J. & Martikainen P. J. (1996): Fluxes of nitrous oxide from boreal peatlands as affected by peatland type, water table level and nitrification capacity; *Biogeochemistry*; Vol. 35(3): S. 401–418.

Remde A. & Conrad R. (1990): Production of nitric oxide in Nitrosomonas europea by reduction of nitrite; *Arch.Mikrobiol.*; Vol. 154: S. 187–191.

Remde A. & Conrad R. (1991): Role of nitrification and denitrification for NO metabolism in soil; *Biogeochemistry*; Vol. 12(3): S. 189–205.

Rennenberg H., Kreutzer K., Papen H. & Weber P. (1998): Consequences of high loads of nitrogen for spruce (Picea abies) and beech (Fagus sylvatica) forests; *NewPhytol.*; Vol. 139(1): S. 71–86.

Räisänen J., Hansson U., Ullerstig A., Doscher R., Graham L. P., Jones C., Meier H. E. M., Samuelsson P. & Willen U. (2004): European climate in the late twenty-first century: regional simulations with two driving global models and two forcing scenarios; *Clim.Dynam*; Vol. 22(1): S. 13–31.

Robertson G. (1989): Nitrification and denitrification in humid tropical ecosystems: potential controls on nitrogen retention; in: Procter J. (Hg.): Mineral Nutrients in Tropical Forest and Savanna Ecosystems; Blackwell Scientific, Oxford, UK.

Robertson L. A., Dalsgaard T., Revsbech N. P. & Kuenen J. G. (1995): Confirmation of aerobic denitrification in batch cultures, using gas-chromatography and N-15 mass-spectrometry; *FEMSMicrobiol.Ecol.*; Vol. 18(2): S. 113–119.

Robertson L. A. & Kuenen J. G. (1988): Heterotrophic nitrification in Thiosphaera pantotropha: oxygen-uptake and enzyme studies; *J.Gen.Microbiol.*; Vol. 134: S. 857–863.

Robertson L. A. & Kuenen J. G. (1990): Combined heterotrophic nitrification and aerobic denitrification in Thiosphaera pantotropha and other bacteria; *Anton.Leeuw.Int.J.G.*; Vol. 57(3): S. 139–152.

Robertson L. A., van Niel E. W. J., Torremans R. A. M. & Kuenen J. G. (1988): Simultaneous nitrification and denitrification in aerobic chemostat cultures of Thiosphaera pantotropha; *Appl.Environ.Microb.*; Vol. 54(11): S. 2812–2818.

Rosenkranz P., Brüggemann N., Papen H., Xu Z., Seufert G. & Butterbach-Bahl K. (2006): N2O, NO and CH4 exchange, and microbial N turnover over a Mediterranean pine forest soil; *Biogeosciences*; Vol. 3: S. 121–133.

Schindlbacher A., Zechmeister-Boltenstern S. & Butterbach-Bahl K. (2004): Effects of soil moisture and temperature on NO, NO2, and N2O emissions from European forest soils; *J.Geophys.Res.*; Vol. 109(D17): D17302.

Schulte-Bisping H., Brumme R. & Priesack E. (2003): Nitrous oxide emission inventory of German forest soils; *J.Geophys.Res.*; Vol. 108(D4): D4132.

Simek M., Jisova L. & Hopkins D. W. (2002): What is the so-called optimum pH for denitrification in soil?; *SoilBiol.Biochem.*; Vol. 34(9): S. 1227–1234.

Sitaula B. K. & Bakken L. R. (1993): Nitrous-oxide release from spruce forest soil relationships with nitrification, methane uptake, temperature, moisture and fertilization; *SoilBiol.Biochem.*; Vol. 25(10): S. 1415–1421.

Sitaula B. K., Bakken L. R. & Abrahamsen G. (1995): N-fertilization and soil acidification effects on N2O and CO2 emissions from temperate pine forest soil; *SoilBiol.Biochem.*; Vol. 27(11): S. 1401–1408.

Smith K. A. (1997): The potential for feedback effects induced by global warming on emissions of nitrous oxide by soils; *GlobalChange.Biol.*; Vol. 3(4): S. 327–338.

Smith K. A., Thomson P. E., Clayton H., McTaggart I. P. & Conen F. (1998): Effects of temperature, water content and nitrogen fertilisation on emissions of nitrous oxide by soils; *Atmos.Environ.*; Vol. 32(19): S. 3301–3309.

Stange F.: (2000): Entwicklung und Anwendung eines prozeßorientierten Modells zur Beschreibung der N2O- und NO-Emissionen aus Böden temperater Wälder; Dissertation; University of Freiburg; Freiburg, Germany.

Stange F., Butterbach-Bahl K., Papen H., Zechmeister-Boltenstern S., Li C. S. & Aber J. (2000): A process-oriented model of N2O and NO emissions from forest soils: 2. Sensitivity analysis and validation; *J.Geophys.Res.*; Vol. 105(D4): S. 4385–4398.

Struwe S. & Kjoller A. (1994): Potential for N2O production from beech (fagus silvaticus) forest soils with varying pH; *SoilBiolBiochem.*; Vol. 26(8): S. 1003–1009.

Teepe R. & Ludwig B. (2004): Variability of CO2 and N2O emissions during freeze-thaw cycles: results of model experiments on undisturbed forest-soil cores; *J.PlantNutr.Soil.Sc.*; Vol. 167(2): S. 153–159.

Thomsen J. K., Geest T. & Cox R. P. (1994): Mass-spectronometric studies of the effect of pH on the accumulation of intermediates in denitrification by Paracoccus denitrificans; *Appl.Environ.Microb.*; Vol. 60(2): S. 536–541.

Valente R. J. & Thornton F. C. (1993): Emissions of NO from soil at a rural site in central Tennessee; *J.Geophys.Res.*; Vol. 98(D9): S. 16.745–16.753.

Van Cleemput O. & Baert L. (1984): Nitrite: A key compound in N loss processes under acid conditions?; *PlantSoil*; Vol. 76: S. 233–241.

Van Dijk S. M. & Duyzer J. H. (1999): Nitric oxide emissions from forest soils; *J.Geophys.Res.*; Vol. 104(D13): S. 15.955–15.961.

Vestreng V., Adams M. & Goodwin J. (2004): Inventory Review 2004: Emission Data reported to CLRTAP and under the NEC Directive, EMEP/EEA Joint Review Report, Tech. Report; in: EMEP-MSCW Report 1/2004; The Norwegian Meteorological Institute, Oslo, Norway.

Von Arnold K., Nilsson M., Hanell B., Weslien P. & Kledtsson L. (2005): Fluxes of CO2, CH4 and N2O from drained organic soils in deciduous forests; *SoilBiol.Biochem.*; Vol. 37: S. 1059–1071.

Weier K. L. & Gilliam J. W. (1986): Effect of acidity on nitrogen mineralization and nitrification in Atlantic coastal-plain soils; *SoilSci.Soc.Am.J.*; Vol. 50(5): S. 1210–1214.

Wrage N., Velthof G., van Beusichem M. & Oenema O. (2001): Role of nitrifier denitrification in the production of nirous oxide; *SoilBiol.Biochem.*; Vol. 33: S. 1723–1732.

Yamulki S., Harrison R. M., Goulding K. W. T. & Webster C. P. (1997): N2O, NO and NO2 fluxes from a grassland: Effect of soil pH; *SoilBiol.Biochem.*; Vol. 29(8): S. 1199–1208.

Yan X., Ohara T. & Akimoto H. (2005): Statistical modeling of global soil NOx emissions; *GlobalBiogeochem.Cyc.*; Vol. 19: GB 3019, 1-15.

Yoshida T. & Alexander M. (1970): Nitrous oxide formation by Nitrosomonas europaea and heterotrophic microorganisms; *SoilSci.Soc.Am.Proc.*; Vol. 34: S. 880–882.

Zechmeister-Boltenstern S., Hahn M., Meger S. & Jandl R. (2002): Nitrous oxide emissions and nitrate leaching in relation to microbial biomass dynamics in a beech forest soil; *SoilBiol.Biochem.*; Vol. 34(6): S. 823–832.

Publikationen

Publikation I

M. Kesik, S. Blagodatsky, H. Papen und K. Butterbach-Bahl

Effect of pH, temperature and substrate on N_2O, NO and CO_2 production by *Alcaligenes faecalis p.*
Journal of Applied Microbiology, 101, 655-667, 2006.

Diese Publikation untersucht den Einfluss von pH, Temperatur und Substrat auf die Höhe der N_2O- und NO-Produktion durch heterotrophe Nitrifizierer.

Publikation II

M. Kesik, P. Ambus, R. Baritz, N. Brüggemann, K. Butterbach-Bahl, M. Damm, J. Duyzer, L. Horváth, R. Kiese, B. Kitzler, A. Leip, C. Li, M. Pihlatie, K. Pilegaard, G. Seufert, D. Simpson, U. Skiba, G. Smiatek, T. Vesala und S. Zechmeister-Boltenstern

Inventories of N_2O and NO emissions from European forest soils
Biogeosciences, 2, 353-375, 2005

Diese Publikation beschreibt die Validierung und Weiterentwicklung des PnET-N-DNDC Modells und berechnet letztendlich ein N_2O- und NO-Emissionskataster für Europäische Waldböden.

Publikation III

M. Kesik, N. Brüggemann, R. Forkel, R. Kiese, R. Knoche, C. Li, G. Seufert, D. Simpson und K. Butterbach-Bahl

Future scenarios of N_2O and NO emissions from European forest soils
Journal of Geophysical Research, 111 (G02018), doi:10.1029/2005JG000115, 2006.

Diese Publikation zeigt die möglichen Auswirkungen von vorhergesagten zukünftigen Klimaveränderungen auf die N_2O- und NO-Emissionen aus Waldböden Europas.

Publikation IV

S.A. Blagodatsky, **M. Kesik**, H. Papen und K. Butterbach-Bahl

Production of NO and N_2O by the heterotrophic nitrifier *Alcaligenes faecalis parafaecalis* under varying conditions of oxygen saturation
Geomicrobiology Journal, 23, 165-176, 2006.

Diese Publikation untersucht den Einfluss von unterschiedlichen Sauerstoffbedingungen auf die Höhe der N_2O- und NO-Produktion durch heterotrophe Nitrifizierer.

Publikation V

D. Simpson, K. Butterbach-Bahl, H. Fagerli, **M. Kesik** und U. Skiba

Deposition and Emissions of Reactive Nitrogen over European Forests: A Modelling study
Atmospheric Environment, 40, 5712-5726, 2006.

Diese Publikation berechnet den Anteil der N-Spurengasemissionen aus Waldböden an der N-Deposition und N-Emission in Europa.

Mein Anteil an den Publikationen innerhalb dieser Doktorarbeit ist folgendermaßen:

Publikation	Konzeptioneller Anteil	Versuchsdurchführung bzw. Datenaufbereitung	Erstellung der Publikation
I	1	1	1
II	1	1	1
III	1	1	1
IV	1	1	2
V	2	2	3

1 = Hauptanteil
2 = Signifikanter Anteil, jedoch nicht Hauptanteil
3 = kleiner Anteil

Journal of Applied Microbiology ISSN 1364-5072

ORIGINAL ARTICLE

Effect of pH, temperature and substrate on N_2O, NO and CO_2 production by *Alcaligenes faecalis p.*

M. Kesik[1], S. Blagodatsky[1,2], H. Papen[1] and K. Butterbach-Bahl[1]

1 Karlsruhe Research Centre, Institute for Meteorology and Climate Research, Atmospheric Environmental Research (IMK-IFU), Garmisch-Partenkirchen, Germany

2 Institute of Physicochemical and Biological Problems in Soil Science, Russian Academy of Sciences, Moscow, Russia

Keywords
chemostat, heterotrophic nitrifiers, nitric oxide, nitrous oxide, pH, temperature.

Correspondence
Klaus Butterbach-Bahl, Institute for Meteorology and Climate Research, Atmospheric Environmental Research (IMK-IFU), Karlsruhe Research Centre, Kreuzeckbahnstr. 19, 82467 Garmisch-Partenkirchen, Germany.
E-mail: klaus.butterbach@imk.fzk.de

2005/0485: received 6 May 2005, revised 22 December 2005 and accepted 23 January 2006

doi:10.1111/j.1365-2672.2006.02927.x

Abstract

Aims: To study the effect of pH, temperature and substrate on the magnitude of N_2O and NO production by heterotrophic nitrifiers.

Methods and Results: The change in N_2O and NO production by the heterotrophic nitrifiers *Alcaligenes faecalis* subsp. *parafaecalis* and *Paracoccus pantotrophus* because of variations in pH, temperature and substrate was studied in chemostat cultures under steady-state conditions. N_2O, NO and CO_2 production increased with temperature between 4 and 32°C. For N_2O an optimum temperature of 28°C was observed. No optimum temperature was found for NO. Highest N_2O and CO_2 productions were observed at a pH of 7·0. However, besides having an optimum at pH 7·0, especially NO production but also N_2O production increased significantly at pH ≤ 4·0. This increase in NO production under acidic conditions was partly because of chemo-denitrification, which contributed up to 62% of total NO production at pH 3·0 (0·8% for N_2O). Furthermore, we could demonstrate that substrate quality significantly affects N_2O, NO and CO_2 production. N_2O and especially NO production by *A. faecalis p.* was significantly lower on an ammonium citrate medium when compared with rates obtained for a peptone-meat extract medium.

Conclusions: The results indicate that heterotrophic nitrifiers are suitable model organisms to study the influence of environmental factors on microbial N trace gas production.

Significance and Impact of the Study: The results allow an improved description, e.g. of the pH dependency of N trace gas production by microbes and/or chemo-denitrification in process-oriented models describing the exchange of N trace gases between soils and the atmosphere.

Introduction

On a global scale soils are important sources for the atmospheric trace gases nitrous and nitric oxides, both of which contribute either directly or indirectly to global warming (Houghton *et al.* 2001). Total emissions of the primarily active greenhouse gas, N_2O, from all soils are estimated to be in a range of $3{\cdot}3–9{\cdot}9 \times 10^9$ kg N year^{-1} and thus contribute approx. 22–66% of the total global atmospheric N_2O budget (Houghton *et al.* 2001). For the secondarily active greenhouse gas, NO, soils are with $4–21 \times 10^9$ kg NO_x-N year^{-1} (Holland *et al.* 1999), which is of similar importance for the global atmospheric NO budget as industrial sources ($20–24 \times 10^9$ kg NO_x-N year^{-1} from fossil fuel combustion; Holland *et al.* 1999). In soils, N_2O and NO are mainly produced by the microbial processes of nitrification and denitrification. Both processes are regulated by various environmental factors, among which the most prominent are: temperature, pH and soil moisture (which can be regarded as a proxy for the actual mean redox potential in soils). Several studies have been published in which changes in

microbial production of N trace gases by soil micro-organisms under different pH, temperature or substrate conditions have been investigated in the framework of controlled field experiments (Koskinen and Keeney 1982; Goodroad and Keeney 1984; Martikainen 1985; Weier and Gilliam 1986; Nägele and Conrad 1990; Daum and Schenk 1998; Ellis *et al.* 1998; Smith *et al.* 1998). Cates and Keeney (1987) found that an increase in soil temperature from 11 to 24°C in fertilized and manured maize fields resulted in a significant increase (approx. 60%) of N_2O emission. Based on results of field experiments, Papen and Butterbach-Bahl (1999) calculated average Q_{10} values (for the temperature increase from 5 to 15°C) for N_2O production of 1·74 and of 6·46 for spruce and beech forests, respectively. Similarly, Gasche and Papen (1999) calculated Q_{10} values of 2·89 and 2·83 respectively for NO. With regard to NO Koskinen and Keeney (1982) and Nägele and Conrad (1990) found in field and laboratory studies with soil samples, that NO production via denitrification increases with decreasing pH values. In addition, the production of NO from the nitrification intermediate nitrite via chemo-denitrification has been shown to strongly increase at pH values <4·0 (Van Cleemput and Baert 1984; Yamulki *et al.* 1997; Ormeci *et al.* 1999).

Due to the interaction and spatial and temporal variability of environmental factors affecting N trace gas emissions from soils, one will only gain a limited understanding of the critical processes from field studies. As a result, several field studies failed to demonstrate clear effects of pH or even temperature on N trace gas production (Struwe and Kjøller 1994; Yamulki *et al.* 1997; Simek *et al.* 2002). To improve our understanding of these processes and the environmental factors such as temperature, pH and substrate governing N trace gas production, laboratory studies under controlled conditions have been found to be most suitable (Nägele and Conrad 1990; Conrad 2002). Yoshida and Alexander (1970) used cell suspensions to demonstrate the pH sensitivity of N_2O production of *Nitrosomonas europaea*, though the investigated pH range was rather narrow (6–8). Studies of pure cultures of micro-organisms involved in N trace gas production in soils may, in this respect, be of fundamental importance. Compared with soil incubation studies, pure culture studies enable environmental conditions to be kept constant and effects coming from time-dependent changes in the microbial community structure to be excluded. The advantages of pure culture studies *vs* soil incubation studies have been used by several groups e.g.:

i N_2O and NO production by autotrophic and heterotrophic nitrifiers (e.g. Robertson and Kuenen 1988; Papen *et al.* 1989; Anderson *et al.* 1993),

ii The pH sensitivity of N_2O production by autotrophic nitrifiers and denitrifiers (Yoshida and Alexander 1970; Thomsen *et al.* 1994), or

iii The effect of O_2 partial pressure on N_2O production (McKenney *et al.* 1994; Otte *et al.* 1996).

Earlier studies have some drawbacks, as (i) either NO and N_2O were not studied simultaneously, (ii) experiments were only performed with batch cultures or (iii) the investigated ranges of environmental conditions were too limited. Therefore, the effect of pH on N trace gas production still remains uncertain (Simek and Cooper 2002).

To further contribute to the understanding of effects of environmental conditions on N trace gas production, we performed a series of chemostat experiments. The primary microbial model organism we chose was *Alcaligenes faecalis* subspecies *parafaecalis*. *Alcaligenes faecalis* is a heterotrophic nitrifier, globally found in high cell numbers in soil (Gamble *et al.* 1977; Anderson *et al.* 1993; Papen and von Berg 1998; H. Papen, unpublished data), which also can denitrify (Anderson *et al.* 1993). Furthermore, *A. faecalis* has been shown to produce N_2O as well as NO in aerobic as well as anaerobic batch and chemostat cultures (Kuenen and Robertson 1987; Papen *et al.* 1989; Robertson *et al.* 1995; Otte *et al.* 1996).

To prove the transferability of results for other micro-organisms, which was also partly neglected in earlier studies, we also performed experiments with *Paracoccus pantotrophus* (=*Thiosphaera pantotropha*). *Paracoccus pantotrophus* is a soil micro-organism which was mainly investigated by Robertson *et al.* (1988) and Robertson and Kuenen (1988). This organism can produce N_2O and NO either via heterotrophic nitrification and/or denitrification. By using the chemostat approach and the two model organisms *A. faecalis p.* and *P. pantotrophus*, we tried to clarify the following questions: (i) how do changes in temperature over a wide temperature range (4–32°C) affect the NO, N_2O and CO_2 production, (ii) what is the effect of substrate pH (for a range commonly observed for most soils worldwide, i.e. pH 3·0–8·0) on N_2O, NO and CO_2 production and on the NO : N_2O ratio, (iii) how does the substrate quality, i.e. the change from a nutrient-rich to a nutrient-poor media, affect N_2O and NO production, and (iv) do both soil micro-organisms in terms of N_2O and NO production react comparably to changes in the above-mentioned environmental parameters?

Material and methods

Bacterial strains and media

All 13 experiments were carried out with two strains of heterotrophic nitrifiers, i.e. *A. faecalis* subsp. *parafaecalis*

(DSM 13975) and *P. pantotrophus* (=*T. pantotropha*; DSM 11104). Cultures were obtained from the Deutsche Sammlung von Mikroorganismen und Zellkulturen GmbH, Braunschweig, Germany.

Alcaligenes faecalis p. and *P. pantotrophus* were grown either on a peptone-meat extract medium, containing 2·5 g peptone and 1·5 g meat extract in 1 l of bi-distilled water or on a medium containing sodium citrate and ammonium chloride (hereafter referred to this medium as ammonium citrate medium). Sterile peptone-meat extract medium already contained ammonium concentrations <2 mg NH_4^+-N l^{-1}. However, ammonium concentrations in sterile medium were at least one magnitude lower when compared with ammonium concentrations after establishment of the cultures. The ammonium citrate medium contained (g l^{-1}) KH_2PO_4 0·44, NH_4Cl 0·5, $MgSO_4{\cdot}7H_2O$ 0·1, $CaCl_2$ 0·2, $FeSO_4{\cdot}7H_2O$ 1·0, and 2 ml trace element solution. The trace element solution contained (g l^{-1}) $ZnSO_4{\cdot}7H_2O$ 3·92, $MnCl_2{\cdot}4H_2O$ 5·06, $(NH_4)_6Mo_7O_{24}{\cdot}4H_2O$ 1·1, $CuSO_4{\cdot}5H_2O$ 1·57, and $CoCl_2{\cdot}6H_2O$ 1·61. In addition 5 ml of a filter-sterilized $C_6H_5Na_3O_7{\cdot}2H_2O$ (279·4 g l^{-1}) solution was added after autoclaving. Before autoclaving 0·2 ml l^{-1} antifoam SE-15 (Sigma-Aldrich) was added to both media. The media used were adjusted to pH 6·8 with 2·4 N HCl or 1 N NaOH, respectively.

Chemostat cultures and N_2O, NO and CO_2 measurements

Both strains were maintained under aerobic conditions on peptone-meat extract agar plates. Chemostat cultures were derived by cultivating the strains for the first 10 h in test tubes containing liquid peptone-meat extract medium. Then the suspensions were centrifuged and the pellets added under sterile conditions in Erlenmeyer flasks containing fresh peptone-meat extract medium (150 ml). The cultures were then incubated over night at 28°C. The following day 150 ml of bacteria suspension was extracted from the Erlenmayer flasks and added to the autoclaved medium (2·48 l) into the chemostat with a volume of 3 l (BiofloIII Fermentor; New Brunswick, Nürtingen, Germany). Both strains were maintained in the chemostat at a constant growth rate of 0·1 h^{-1} on the peptone-meat extract medium. For the ammonium citrate medium a growth rate of 0·05 h^{-1} was established. Nutrient solution was added, unless otherwise noted, at a flow rate of 0·25 l h^{-1}. Air sparging of the chemostat culture was controlled by a Tylan Mass Flow Controller (Tylan Co., Eching, Germany) and varied in a range of 0·5–1·5 l min^{-1} in order to keep the dissolved O_2 level during the experiments in a range of 15–20%. Pre-experiments revealed that at this O_2 saturation level highest rates of N trace gas production can be observed (data not shown). Dissolved oxygen, pH, redox potential and temperature were controlled by respective electrodes and data were recorded continuously by a microprocessor (MultiLoop-Controller, New Brunswick). Calibration of electrodes for pH, redox and dissolved oxygen was carried out before the start of the experiments. The pH values in the media were adjusted by use of two peristaltic pumps which could either add 5% H_2SO_4 or 0·2 N NaOH. The activity of the pumps was controlled by the actual pH value of the media and by the limit given in the controlling software. In the exhaust air of the chemostat (0·5–1·5 l h^{-1}) NO and CO_2 were measured automatically either by a chemoluminescence detector (CLD 770 Al ppt; Eco Physics, Munich, Germany) or by an infrared gas analyser (Leybold-Heraeus, Hürth, Germany). N_2O in the exhaust air was measured by taking at least hourly gas samples with a gas-tight syringe and by analysing the N_2O concentration in the gas sample with a gas chromatograph equipped with an electron capture detector (for analytical details see Butterbach-Bahl *et al.* 1997). All gas analysers were calibrated hourly (N_2O) or at least bi-daily (NO and CO_2) by use of standard gases (Messer Griesheim, Griesheim, Germany). Concentrations of N_2O, NO and CO_2 in the exhaust air were converted to production rates by considering the air flow, the protein concentration and medium volume. The sterility of the culture was routinely controlled with a microscope.

Determination of NH_4^+, NO_2^-, NO_3^-, protein and C and N content

Parallel to the air sampling a defined sample of medium (approx. 5 ml) was automatically taken under sterile conditions via a MX3 Biosampler (New Brunswick). After centrifugation of the sample, ammonium, nitrate and nitrite were determined using the supernatant through photometric analysis. Protein concentration was also determined through photometric analysis (wavelength: 750 nm), after washing the pellet twice with a potassium-phosphate buffer. Protein concentration in the medium was determined by using a modified method of Lowry *et al.* (1951) by Holtzhauer (1997). Ammonium and nitrate were determined at the agricultural laboratory of Dr Janssen GmbH (Gillersheim, Germany) following the VD LUFA method A6141 (Hoffmann 1991). Nitrite concentrations were measured using the method as described by Griess-Ilosvay (1965).

Experimental design of the parameterization experiments

A total of 13 different experiments were carried out, each of them lasting at least 20 days. Details about the focus of

experiments, micro-organism and medium used, number of experiments and number of sampling points during steady-state conditions for individual parameters such as N_2O-concentration in exhaust air, NH_4^+-, NO_2^--, NO_3^-- and protein concentrations are provided in Table 1.

In all experiments the micro-organisms were first grown as a batch culture in the chemostat. At the exponential growth phase the fresh medium supply was switched on at a rate of 0·25 l h^{-1}. The experiments were started after approx. 48 h, when the culture reached steady-state, i.e. when no further significant temporal changes over a time period of at least 15 h in the following parameters were observed: microbial protein concentration, O_2 tension and N_2O, NO and CO_2 production. At maximum we were able to keep the culture in a steady-state for almost 3 weeks, before the sterility of the culture became a problem.

For the determination of the dependency of N_2O, NO and CO_2 production on temperature, chemostat cultures of *A. faecalis p.* were incubated at a temperature range from 4 to 32°C on the peptone-meat extract medium. On the ammonium citrate medium we could only conduct experiments with *A. faecalis p.* in the temperature range from 20 to 28°C. For the given dilution rate (0·05 h^{-1}) it was not possible to get the culture in a steady-state stage at temperatures below 20°C or above 28°C. When the incubation temperature was changed, e.g. from 28 to 24°C, the culture needed approx. 10 h to reach a new steady-state (see definition above). Only N_2O, NO and CO_2 measurements as well as medium samples for protein, ammonium, nitrate, and nitrite analysis taken during steady-state were used for examining effects of temperature. The number of sampling points for protein, ammonium, nitrate and nitrite during steady-state was between 6 and 10 over a time period of 20–30 h. N_2O production during steady-state was usually monitored hourly except during night hours, whereas NO and CO_2 production could even be calculated in 5-min resolution, as the concentration of these gases in the exhaust air was measured continuously throughout all experiments in 5-min intervals.

Experiments to determine the dependence of N_2O, NO and CO_2 production on medium pH were carried out with *A. faecalis p.* on the peptone-meat extract medium as well as on the ammonium citrate medium. As these experiments were carried out approx. 3 months after the start of the temperature experiments a new test culture was derived from microbial strain as delivered by the Deutsche Sammlung von Mikroorganismen und Zellkulturen GmbH. The investigated pH range was between 3 and 8 on the peptone-meat extract medium and between 4 and 7 on the ammonium citrate medium. In order to directly compare the magnitude of N_2O, NO and CO_2 production of *A. faecalis p.* with *P. pantotrophus*, experiments with *P. pantotrophus* on ammonium citrate medium were carried out. In these experiments the pH ranged between 6·0 and 9·0. As we changed the pH levels from 7·0 to 6·0 the culture needed at least 36 h to reach a new steady-state. As already outlined above we used only measuring points at steady-state conditions for evaluating effects of medium pH on N_2O, NO and CO_2 production. The sampling frequency and number of measuring points was comparable with those in the other experiments (see above).

Statistics

Differences between the pH, temperature and substrate dependency on N_2O, NO and CO_2 were analysed using analysis of variance (ANOVA, $\alpha = 0{\cdot}05$). The LSD test was used for multiple comparisons between mean values. All statistical analyses were performed with SPSS 8·0 (SPSS Inc., Chicago, IL, USA) and Microcal Origin 4·0 (Microcal Software, Northampton, MA, USA).

Results

Effect of temperature on nitrous, nitric oxide and carbon dioxide production

The effect of temperature on N_2O and NO production by *A. faecalis p.* was studied in the temperature range from 4

Table 1 Focus, micro-organism and medium used, number of experiments and number of sampling points during steady-state conditions for individual parameters such as N_2O concentration in exhaust air, NH_4^+, NO_2^-, NO_3^- and protein concentrations. At each sampling time three individual probes were taken for analysing the above parameters. Note that NO and CO_2 concentrations in the exhaust air was measured continuously in 5-min intervals during the entire experiments (duration of each individual experiment: >20 days)

		Temperature effect		pH effect	
Micro-organism	Medium	No. of experiments	No. of sampling points	No. of experiments	No. of sampling points
Alcaligenes faecalis p.	Peptone-meat extract	3	116	5	37
	Ammonium citrate	1	26	1	30
Paracoccus pantotrophus	Ammonium citrate	–	–	2	36
Chemo-denitrification	Peptone-meat extract	–	–	1	17

to 32°C with a constant medium pH of 7·0 (Fig. 1). Ammonium concentrations in the medium tended to increase with temperature, thus indicating that ammonification activity by *A. faecalis p.* was positively correlated with temperature. Ammonium concentrations were approximately one magnitude higher than nitrite and nitrate concentrations (Table 2). Protein concentrations were very stable at pH 7·0 in the temperature range from 16 to 32°C (Table 2). As temperature decreased, the protein concentration also decreased. For the entire temperature range investigated, NO production was positively correlated with temperature. NO production doubled by increasing the medium temperature from 16 to 24°C. Highest NO production rates were observed at 32°C (Fig. 1a). The respective Q_{10} value for the temperature dependency of NO production by *A. faecalis p.* for the temperature ranges from 4 to 32°C is 3·93.

Comparable results were also obtained for the temperature dependency of N_2O production by *A. faecalis p.* (Fig. 1b). The Q_{10} value of the N_2O production for the temperature increase from 4 to 32°C is 1·81. However, in contrast to NO production, N_2O production showed a defined optimum at 28°C, where N_2O production peaked with $1{\cdot}17 \pm 0{\cdot}32$ μg N_2O-N mg^{-1} protein h^{-1}. At 32°C the N_2O production slowed down. The rate of N_2O production by *A. faecalis p.* was approx. 20–70 times higher than NO production (Fig. 1d). However, the ratio of N_2O : NO production was significantly affected by temperature, and was >50 for the temperature range 8–28°C but <36 for 4–32°C.

The dependency of CO_2 production by *A. faecalis p.* on temperature could be described best with an S-shaped curve for the temperature range from 4 to 32°C (Fig. 1c). The highest mean value of CO_2 production was measured at 32°C. The Q_{10} value for the temperature range from 4 to 32°C is 1·86.

The temperature dependency of the ratio of CO_2 : N_2O production (Fig. 1e) or CO_2 : NO production (Fig. 1f) could be best described by a curve with an optimum at 15°C. The temperature dependencies of the CO_2 : N_2O and CO_2 : NO ratios (optimum values at 15°C) indicate that above this temperature, changes in the contribution of nitrification and denitrification to total N trace gas production by *A. faecalis p.* occurs. As during denitrification metabolism more N trace gases can be produced than during oxidative N trace gas production via nitrifica-

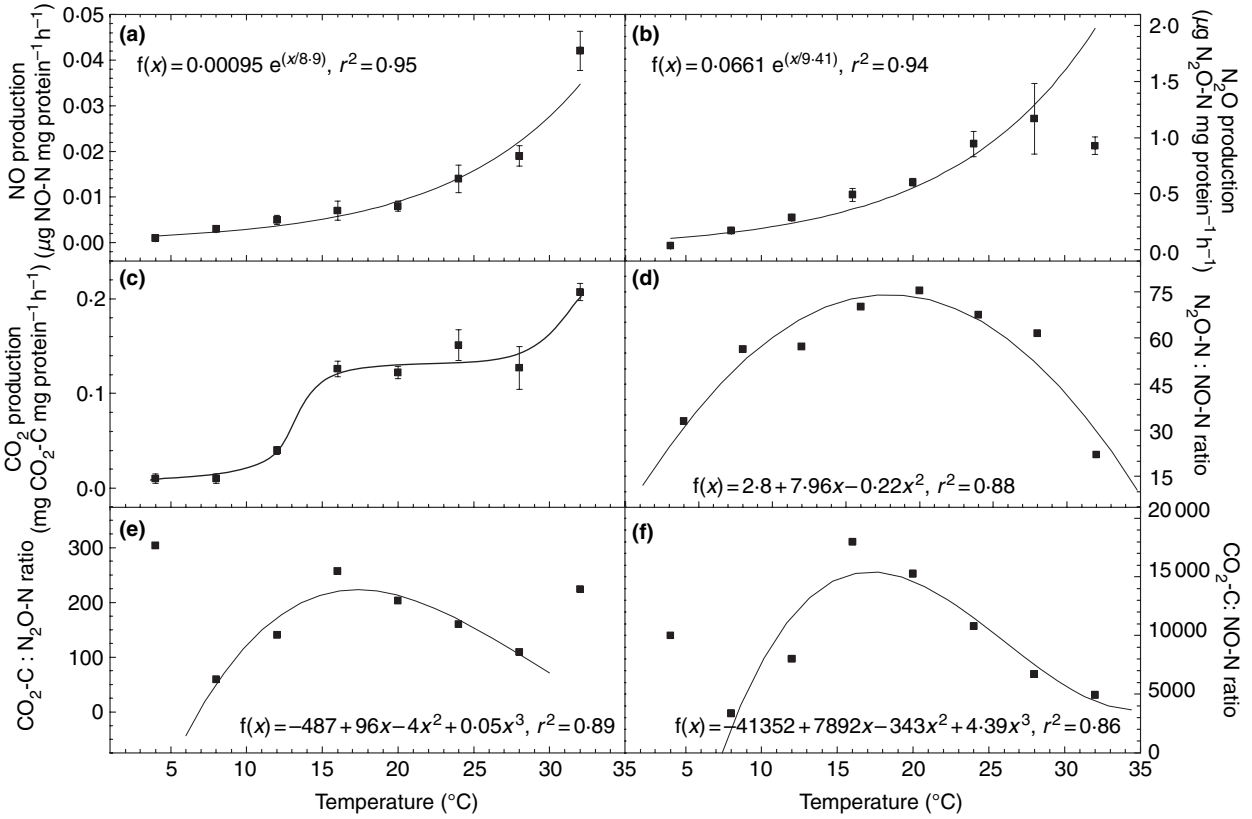

Figure 1 Dependency of NO, N_2O and CO_2 production rates by *Alcaligenes faecalis p.* from temperature. Provided are mean values of all sampling points at steady-state conditions as obtained within three independent sets of temperature experiments.

Table 2 Concentrations of NH_4^+, NO_2^- and NO_3^- and protein in *Alcaligenes faecalis p.* chemostat cultures growing on peptone-meat extract media under different experimental conditions

Conditions		NH_4^+ concentration (mg NH_4^+-N l^{-1})	NO_2^- concentration (mg NO_2^--N l^{-1})	NO_3^- concentration (mg NO_3^--N l^{-1})	Protein concentration (mg protein l^{-1})
pH 3·0	28°C	55·2 ± 11·6^{a}	0·1 ± 0·1^{bc}	0·7 ± 0·8^{df}	26·5 ± 1·9^{ab}
pH 4·0	28°C	27·9 ± 0·2^{b}	1·4 ± 0·1^{d}	0·9 ± 0·1^{df}	38·7 ± 3·1^{ac}
pH 5·0	28°C	32·9 ± 0·7^{b}	1·3 ± 0·1^{d}	1·2 ± 0·2^{cef}	27·3 ± 1·7^{ab}
pH 6·0	28°C	29·9 ± 0·5^{a}	0·7 ± 0·1^{bd}	0·5 ± 0·1^{ef}	31·9 ± 1·9^{abd}
pH 7·0	4°C	8·1 ± 0·4^{c}	0·8 ± 0·1^{cd}	0·7 ± 0·1^{df}	47·9 ± 4·4^{cd}
	8°C	10·9 ± 1·0^{cd}	0·9 ± 0·1de	0·8 ± 0·1^{df}	35·2 ± 3·4^{ad}
	12°C	15·7 ± 0·6de	1·3 ± 0·1^{d}	1·5 ± 0·1^{cd}	52·9 ± 5·0^{ce}
	16°C	25·8 ± 1·1^{bf}	2·5 ± 0·2^{a}	2·4 ± 0·2^{ab}	74·7 ± 4·7^{fg}
	20°C	28·4 ± 1·5^{b}	2·8 ± 0·3^{a}	2·9 ± 0·3^{a}	77·3 ± 2·6^{f}
	24°C	20·1 ± 3·0^{e}	1·1 ± 0·2^{d}	2·1 ± 0·3^{bc}	64·9 ± 5·19^{g}
	28°C	20·2 ± 1·0^{ef}	0·3 ± 0·1^{bc}	1·3 ± 0·2de	71·9 ± 5·4^{fg}
	32°C	31·9 ± 0·9^{b}	0·1 ± 0·1^{b}	0·3 ± 0·1^{f}	64·5 ± 2·6^{efg}
pH 8·0	28°C	60·2 ± 8·7^{a}	0·4 ± 0·1^{bce}	0·3 ± 0·4^{f}	19·4 ± 4·8^{b}

Mean ± standard errors followed by the same letter are not significantly different ($P < 0·05$).

tion (Conrad 1996), we conclude that above 15°C denitrification gains further importance as a source for N trace gas production.

Effect of pH on nitrous, nitric oxide and carbon dioxide production

In order to determine the effect of medium pH on the production of nitrous and nitric oxide by *A. faecalis p.*, the pH of the peptone-meat extract medium was varied between 3·0 and 8·0 at a constant temperature of 28°C (Fig. 2). In these experiments ammonium concentrations varied in a range of 2·0–6·0 mg NH_4^+ l^{-1}, whereas nitrite and nitrate concentrations in the media were at least one magnitude lower (Table 2). Protein concentrations were in the range of 19·4–77·3 mg protein l^{-1}. NO production by *A. faecalis p.* was significantly affected by the medium pH. NO production was highest at pH 3·0 and lowest at pH 5·0. At pH 7·0, NO production increased again significantly to values of up to 0·18 ± 0·02 μg NO-N mg^{-1} protein h^{-1}. A comparable pattern was also observed for N_2O production by *A. faecalis p.*. The highest N_2O production was observed at pH 7·0, whereas at pH 3·0 and 4·0 the mean N_2O production was in a range of 1·61–1·72 μg N_2O-N mg^{-1} protein h^{-1}. As with NO production, the lowest N_2O production was observed at pH 5·0. The effect of pH on the CO_2 production was similar to that of the N_2O production rates, with an optimum CO_2 production at pH 7·0. However, in contrast to N_2O and NO production, CO_2 production did not increased at pH values <5·0, but further decreased to a value of 0·01 ± 0·001 mg CO_2-C mg^{-1} protein h^{-1}. This, combined with the increase of NO and N_2O production contributes to the decline of CO_2 : N_2O and CO_2 : NO production ratios at low pH to values <15 (N_2O) or <61 (NO) (see Fig. 2), and indicates that loss rates of N trace gases during microbial C and N turnover processes significantly increase with declining medium pH values.

To clarify whether the high N_2O and NO production at pH levels <4·0 was only due to microbial activity or if part of the N_2O and NO was produced by chemical decomposition of nitrite via chemo-denitrification, nitrite was added to sterile peptone-meat extract medium in concentrations usually found in our chemostat experiments (0·01–0·2 mg NO_2-N l^{-1}). Experiments in sterile medium without *A. faecalis p.* were carried out for pH levels of 3·0, 3·5, 4·0, 4·5 and 5·0, and the results are shown in Fig. 3 (solid lines). These results are compared with observed values of N_2O and NO production by *A. faecalis p.* for the respective pH values (dotted lines). Figure 3 shows that chemo-denitrification represents up to 62% of the total NO production. On the contrary, N_2O production by chemo-denitrification is insignificant. Low pH favours NO production by chemo-denitrification. The magnitude of N_2O and NO production via the nonbiological process of chemo-denitrification was strongly dependent on the pH of the medium (Fig. 3). The experiment showed that at pH values <4·0 up to 62% of NO and up to 0·8% of N_2O production was due to the chemo-denitrification of microbiologically produced nitrite, whereas at pH values ≥4·5 NO and N_2O was solely produced by nitrification or denitrification.

To study the combined effect of substrate quality and pH on nitrous and nitric oxide production, *A. faecalis p.* was also grown on ammonium citrate medium at different pH levels (Fig. 4). Figure 4 shows that N_2O and especially NO production by *A. faecalis p.* growing on ammonium citrate medium was significantly lower than

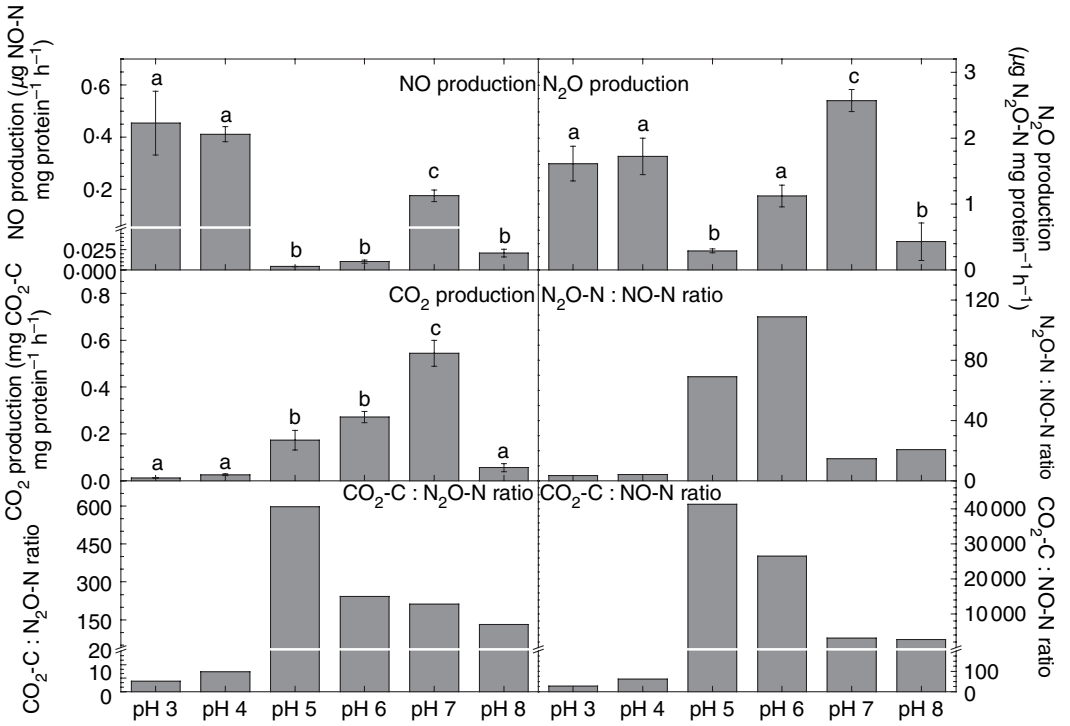

Figure 2 Dependency of NO, N_2O and CO_2 production rates by *Alcaligenes faecalis p.* from the pH of the medium. Provided are mean values of all sampling points at steady-state conditions as obtained within five independent sets of pH experiments. Mean ± standard errors followed by the same letter are not significantly different ($P < 0{\cdot}05$).

when growing on peptone-meat extract medium. NO production rates on the ammonium citrate medium at all pH levels were <0·020 μg NO-N mg^{-1} protein h^{-1} (mean: 0·012 ± 0·0012), and no significant pH effect on NO production could be detected on the ammonium citrate medium. We observed for *A. faecalis p.* either growing on ammonium citrate or peptone-meat extract medium comparable effects of different pH values on N_2O production. This means, that for both media N_2O production was highest at pH 7·0 and decreased with decreasing pH levels. The increase of N_2O production for a medium pH of 4·0, as observed for the peptone-meat extract medium (Fig. 4) could not be detected. The results for pH values <4·0 could not be obtained, as on ammonium citrate medium *A. faecalis p.* could not maintain steady-state criteria for such low pH values. CO_2 production rates of *A. faecalis p.* on the ammonium citrate medium were almost at the same magnitude as on the peptone-meat extract medium (Table 3). As was already observed for the peptone-meat extract medium, the highest production rate of CO_2 was observed at pH 7·0.

In order to prove whether the pH effect on N trace gas production as observed for *A. faecalis p.* is also transferable to other soil micro-organisms, capable of performing heterotrophic nitrification and denitrification reactions, experiments with *P. pantotrophus* on ammonium citrate medium in a pH range of 6·0–9·0 were carried out. Due to the limited growth of *P. pantotrophus* on ammonium citrate medium, it was not possible to cultivate the organism below a medium pH of 6·0. But already at pH 6·0 and 9·0 the growth of *P. pantotrophus* on ammonium citrate medium was erratic, which explains the high standard error associated especially with N_2O production (see Table 4). NO production of *P. pantotrophus* at pH 6·0 was 0·0076 ± 0·001 μg NO-N mg^{-1} protein h^{-1}, which is comparable with the rate observed for *A. faecalis p.* on the same medium type (0·0068 ± 0·0003 μg NO-N mg^{-1} protein h^{-1}). In the investigated pH range, changes of the medium pH exerted no significant effect on the NO production by *P. pantotrophus*. In contrast to NO a pronounced pH effect was observed for N_2O production by *P. pantotrophus*. Maximum N_2O production by *P. pantotrophus* occurred at pH 8·0, whereas N_2O production sharply decreased if the pH medium was changed to higher or lower pH values (Table 4). It must be noted that the observed maximum N_2O production by *P. pantotrophus* was five times higher than the highest N_2O production rate of *A. faecalis p.*, when growing on ammonium citrate medium (1·46 ± 0·13 μg N_2O-N mg^{-1} protein h^{-1}). The pH optimum of N_2O produc-

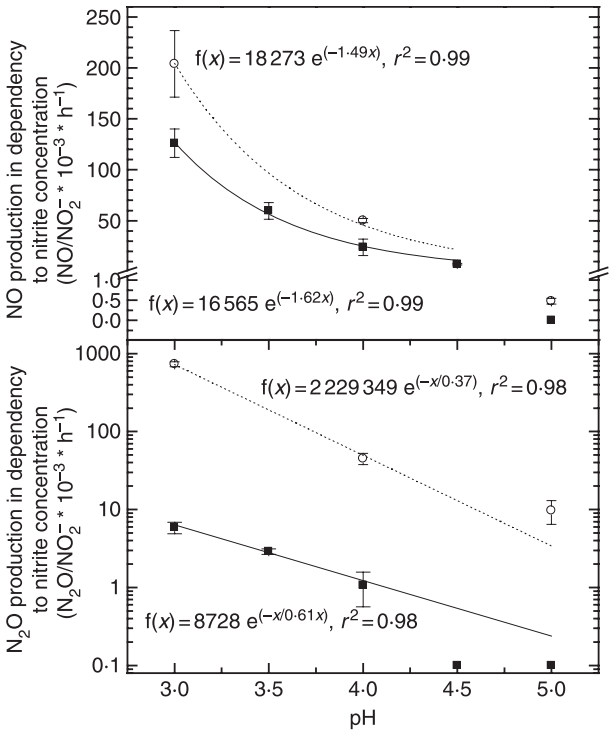

Figure 3 Production of NO and N_2O by microbiological processes and chemo-denitrification in dependency of medium pH at 28°C. For this experiment sterilized medium (solid line) with a concentration of 2 mmol l^{-1} NO_2^--N or medium with *Alcaligenes faecalis p.* (dashed line) growing in steady-state culture (chemostat) was used. Note that at pH values >4·5 no NO and at pH values >4·0 no N_2O production via chemo-denitrification could be detected.

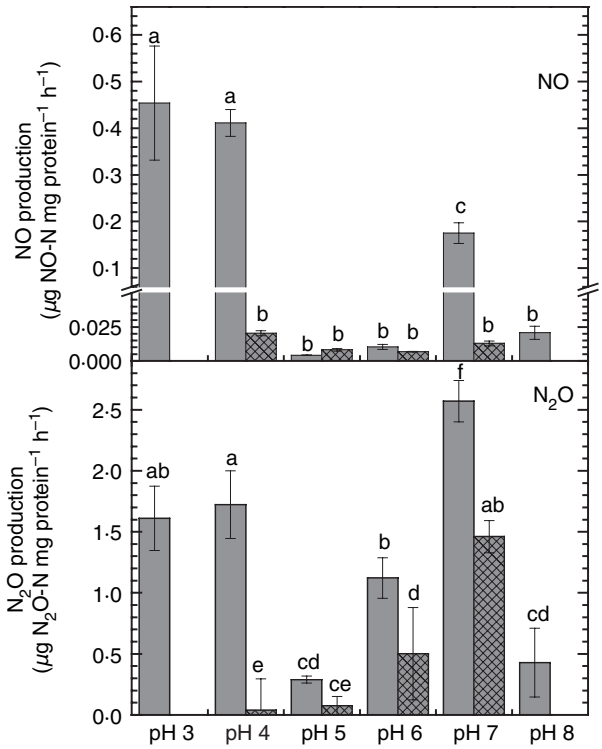

Figure 4 Effect of peptone-meat extract medium (▩) or ammonium citrate medium (▨) on NO and N_2O production rates by *Alcaligenes faecalis p.* for different pH levels. Mean ± standard errors followed by the same letter are not significantly different ($P < 0·05$).

tion by *P. pantotrophus* shifted from 7·0 to 8·0 if compared with *A. faecalis p.* With regard to CO_2 production *P. pantotrophus* showed a comparable activity as *A. faecalis p.* at the same medium type (see Tables 3 and 4). At pH 7·0 *A. faecalis p.* showed an average CO_2 production of 0·2922 ± 0·0286 mg CO_2-C mg^{-1} protein h^{-1}, whereas this value for *P. pantotrophus* was 0·2965 ± 0·0314 mg CO_2-C mg^{-1} protein h^{-1}. Even at pH 6·0 for *A. faecalis p.* and for *P. pantotrophus* nearly equal CO_2 production rates were observed.

Discussion

Effect of temperature on nitrous, nitric oxide and carbon dioxide production

The chemostat experiments on the temperature dependency of N_2O and NO production by *A. faecalis p.* showed a significant positive correlation of N trace gas production with temperature. For the investigated temperature range between 4 and 32°C we observed for N_2O production an optimum temperature of approx. 30°C, whereas such an optimum did not exist for NO. The overall Q_{10} values for this temperature range were 1·8 for N_2O production and 3·9 for NO production. The latter results are consistent with reported results on temperature stimulation of bacterial NO production in agricultural soils (Ormeci *et al.* 1999). Ormeci *et al.* (1999) showed a strong increase of NO production from 0 to nearly 60 ng N m^{-2} s^{-1} for a temperature range of 1–48°C under controlled laboratory conditions. Even for this temperature range they did not observe a temperature optimum. The estimated Q_{10} value for the experiment by Ormeci *et al.* (1999) was 2·3 and thus, somewhat lower than the Q_{10} value of 3·9, as observed in our experiments. This may be due to the fact, that NO production may be substrate limited in soil incubation experiments. Based on field measurements for temperature-stratified data in a range of 5–15°C, Gasche and Papen (1999) calculated Q_{10} values for NO emissions from the soil of a N-saturated spruce stand in Bavaria. These Q_{10} values ranged between 2·6 and 2·9. The Q_{10} value for NO production, observed in a temperature range of 4–16°C in our experiment resulted in a value of 3·1, which compares well with the values given by Gasche and Papen (1999).

Table 3 Effect of peptone-meat extract medium or ammonium citrate medium on CO_2 production rates by *Alcaligenes faecalis p.* for different pH levels

	CO_2 production (mg CO_2-C mg^{-1} protein h^{-1})	
pH	Peptone-meat extract medium	Ammonium citrate medium
3·0	0·012 ± 0·0009[a]	–
4·0	0·026 ± 0·004[a]	0·049 ± 0·009[a]
5·0	0·173 ± 0·042[bc]	0·089 ± 0·008[ab]
6·0	0·273 ± 0·024[d]	0·239 ± 0·037[cd]
7·0	0·544 ± 0·055[e]	0·292 ± 0·029[d]
8·0	0·056 ± 0·017[a]	–

Mean ± standard errors followed by the same letter are not significantly different ($P < 0·05$).

Table 4 Dependency of NO, N_2O and CO_2 production rates by *Paracoccus pantotrophus* from the pH of the ammonium citrate medium

pH	NO production (μg NO-N mg^{-1} protein h^{-1})	N_2O production (μg N_2O-N mg^{-1} protein h^{-1})	CO_2 production (mg CO_2-C mg^{-1} protein h^{-1})
6·0	0·0076 ± 0·0011[a]	0·73 ± 0·84[a]	0·252 ± 0·10[ab]
7·0	0·0004 ± 0·0001[b]	1·16 ± 0·36[a]	0·297 ± 0·03[b]
8·0	0·0073 ± 0·0010[a]	7·46 ± 0·36[b]	0·081 ± 0·01[c]
9·0	0·0025 ± 0·0009[b]	0·21 ± 0·37[a]	0·159 ± 0·06[ac]

Mean ± standard errors followed by the same letter are not significantly different ($P < 0·05$).

With regard to N_2O our results are in accordance with reported temperature effects on N_2O production and emission by other authors. Sitaula and Bakken (1993) estimated for the majority of sampling sites of a 63-year-old spruce forest Q_{10} values between 1·5 and 2·7 for the temperature range 10–15°C, and from 0·3 to 2·4 for the temperature range 3–10°C. Goodroad and Keeney (1984) showed that rates of nitrification and N_2O production in Plano silt loam soils with a water content of 0·1 and 0·2 m^3 m^{-3} increased by 27%, when the temperature was increased from 10 to 30°C. Their calculated Q_{10} value for N_2O production is 1·9, which is in agreement to our Q_{10} value of 1·8 for the temperature range 4–32°C. Papen and Butterbach-Bahl (1999) found during a 3-year continuous record of N_2O from untreated and limed soil of an N-saturated spruce and beech forest site, that soil temperature was the most important factor modulating N_2O emissions closely followed by WFPS (=water filled pore space in soil). For a temperature range of 5–15°C they calculated Q_{10} values for N_2O emissions in a range of 1·74–6·46. This range is in agreement with our calculated Q_{10} value of 4·63 for N_2O production by *A. faecalis p.* in a temperature range of 4–16°C. Also in pure culture studies (e.g. for the autotrophic nitrifier *N. europaea*) comparable effects of temperature on N_2O production were observed (Yoshida and Alexander 1970). Yoshida and Alexander (1970) found highest N_2O production with 14–15 μg N ml^{-1} cell suspension h^{-1} at a temperature from 35 to 45°C. However, a temperature optimum for N_2O production, as observed in our experiments, was not found.

In a laboratory experiment Fang and Moncrieff (2001) measured the effect of temperature on CO_2 production in soil cores, which were collected from a farmland and a Sitka spruce site near Edinburgh. Using an Arrhenius type model they calculated Q_{10} values for CO_2 production at 10°C of 2·4 and of 3·4 for soils, either derived from farmland or forests. In this experiment Q_{10} values for CO_2 production were slightly lower at 30°C (farmland soils: 2·2; forest soils: 2·9). In our experiment with *A. faecalis p.* the overall Q_{10} value for the temperature range of 4–32°C was 1·86, significantly lower than in the work of Fang and Moncrieff (2001). However, it was within the range calculated by Brumme (1995) for CO_2 emissions from a beech forest in the Solling area, Germany (1·3–2·7 for different temperature classes ranging from 7 to 17°C). The specific curve shape of the temperature dependency of specific CO_2 production by *A. faecalis p.* (Fig. 1c) in our experiments supports further interpretations. The figure shows that the CO_2 production per unit microbial protein approaches an optimum, which is close to 0·1 mg CO_2-C mg^{-1} protein h^{-1}. This optimum metabolic rate is rather stable and independent from temperature within a range of 17–30°C. Only when temperature increases above 30°C a further increase in specific CO_2 production is observed. This final increase may be due to the increased use of nitrogen oxides (i.e. nitrite and nitrate) as additional electron acceptors by the bacteria even under aerobic conditions (Robertson and Kuenen 1990; Arts *et al.* 1995). In agreement with Robertson and Kuenen (1990) one can hypothesize that heterotrophic nitrifiers like *A. faecalis p.* may have an advantage in growth rate (not in efficiency) by using nitrate as an additional electron acceptor. This may be especially true if substrate with low C : N ratio (C : N ratio of 3 on peptone-meat extract medium) is in excess relative to the availability of the preferential electron acceptor oxygen in the microbial cells.

Our experiments showed that Q_{10} values observed for N_2O and NO production are higher than for CO_2 production. This indicates that N trace gas production via nitrification and denitrification is not tightly coupled to the metabolic activity of *A. faecalis p.*

The higher Q_{10} value for NO production when compared with N_2O production by *A. faecalis p.* may indicate that at temperatures >30°C chemical decomposition of microbial produced nitrite may be involved in NO production. This hypothesis is in agreement with previous

observations by Van Cleemput and Baert (1984) or Ormeci *et al.* (1999). However, more specific studies using stable isotope techniques are required to determine nitrification- and denitrification-specific temperature responses for N trace gas production.

Effect of pH on nitrous, nitric oxide and carbon dioxide production

It is widely acknowledged that soil pH has a significant effect on the production and emission of N trace gases from soils, as it influences the three most important processes that generate nitrous oxide and nitrogen: nitrification, denitrification and dissimilatory NO_3^- reduction to NH_4^+ (Stevens *et al.* 1998). Yamulki *et al.* (1997) and Ellis *et al.* (1998) investigated soil plots with four different pH levels (3·3, 3·9, 4·9 and 6·1) at the Park Grass Experiment, Rothamsted. They found that on the silty clay loam soil the emission of N_2O decreased with decreasing pH. However, if pH of soil cores (3·9) taken from the plot was increased from 3·9 to 6·5 a reduction in N_2O emissions was observed. In our experiments highest N_2O production was observed at pH 7·0 (2·57 μg N_2O-N mg^{-1} protein h^{-1}). N_2O production decreased with either increasing or decreasing pH. This observation is in agreement with previous experiments by Yoshida and Alexander (1970). By investigating a pH range of 6·0–10·7 these authors found highest N_2O production by the autotrophic nitrifier *N. europaea* at pH 8·0–8·4, whereas N_2O production sharply decreased or ceased at lower or higher medium pH values. However, in our experiments N_2O production by *A. faecalis p.* increased again at pH values ≤4·0 to values of 1·72 μg N_2O-N mg^{-1} protein h^{-1} at pH 4·0. The latter finding, i.e. a secondary optimum of N_2O production at lower pH values is in very good agreement with the study of Yamulki *et al.* (1997) and Ellis *et al.* (1998). The increase in N_2O production at low pH values can be explained by the pH sensitivity of the N_2O reductase for low pH values, rather than by N_2O production via chemo-denitrification. As it has been shown in our experiments that N_2O production via chemo-denitrification does not significantly contribute to N_2O production even at pH values <4·0 (maximum contribution 0·8% at pH 3·0). On the one hand, the N_2O : N_2 ratio of denitrification increases at low pH values due to the pH sensitivity of N_2O reductase (e.g. Ottow *et al.* 1985; Thomsen *et al.* 1994). On the other hand, acidic conditions may also favour N_2O production by autotrophic and heterotrophic nitrifiers, as was pointed out by Martikainen and De Boer (1993). In summary it can be concluded that field studies on effects of soil pH on N_2O production gave contradictory results. In these experiments the pH was either adjusted for longer periods by acid additions or soils were chosen which naturally differed in pH. Therefore, one can assume that the nitrifier and denitrifier populations involved in N_2O production were already adapted to the predominant pH conditions. In agreement with earlier statements on the same topic (Struwe and Kjøller 1994; Yamulki *et al.* 1997; Simek *et al.* 2002) it can be concluded that the obtained results in such studies do not reflect the direct effect of pH on loss rates of NO and N_2O during nitrification and denitrification.

For NO, significant effects of pH on production, consumption and emission in/from soils have been reported. Remde and Conrad (1991) found lower rates of aerobic and higher rates of anaerobic NO production in an alkaline (pH 7·8) agricultural soil when compared with an acidic (pH 4·7) forest soil. Baumgärtner and Conrad (1992) similarly reported higher rates of anaerobic NO production from an alkaline (pH 7·3) meadow soil when compared with an acidic (pH 4·4) forest soil. In contrast to these findings, Krämer and Conrad (1991) noted higher rates of aerobic as well as anaerobic NO production from an alkaline (pH 7·8) agricultural soil, which is in agreement with our results, as we also found high NO production at pH 7·0. Krämer and Conrad (1991) did not find high values of NO production at low pH levels. Ormeci *et al.* (1999) described a sharp increase in NO production by approximately two magnitudes if the pH of soil samples was reduced from 5·8 to 4·5 by additions of 0·1 N HCl. Other authors reported increased NO emissions under low pH conditions as well. Koskinen and Keeney (1982) reported that the highest amount of NO produced during denitrification events was observed under the most acidic conditions in pH-adapted agricultural soil. Yamulki *et al.* (1997) found the highest rates of NO emission from a grassland soil plot at pH 3·9. Without any doubt, part of the increased NO emissions at low pH values is due to chemo-denitrification, and here nitrite plays a key role (Van Cleemput and Baert 1984). The importance of chemo-denitrification could also be demonstrated in our experiments, where chemo-denitrification contributed up to 62% to total NO production at pH 3·0. However, at a pH value of 4·0 the importance of chemo-denitrification for total NO production was almost negligible and was even 0 at pH values >4·5. Chemo-denitrification, i.e. the chemical decomposition of NO_2^-, has no temperature optimum, which is not surprising (Van Cleemput and Baert 1984; Saad and Conrad 1993) and will further increase with increasing temperature. However, we have to emphasize that nitrite, which is essential for the process of chemo-denitrification, is derived from the nitrification process, which has a temperature optimum at around 30–35°C (e.g. Grunditz and Dalhammar 2001). We conclude that the high production rates of NO and partly also of N_2O at low pH values are a result of the combination of microbial and chemical decomposition reactions.

Only if nitrite is available and low pH values occur, can chemo-denitrification take place.

Ellis *et al.* (1998) observed that CO_2 production under anaerobic conditions decreased with decreasing pH. In accordance to our experiments, Sitaula *et al.* (1995) also measured a decrease in soil CO_2 concentration with lower pH. The same effect was also observed by Ellis *et al.* (1998) within the Park Grass Experiment. At pH 8·0, total CO_2 production is most likely underestimated as CO_2 dissolution in the media was not measured. However, this underestimation should be rather limited in view of the medium exchange rate (0·1 h^{-1}), so that measurements of CO_2 emissions from the medium should still be a reliable proxy for total CO_2 production. The observed strong decrease in CO_2 production at pH 8·0 is in accordance with strongly declining protein concentrations (see Table 2) which were also lowest at a pH of 8·0.

As outlined earlier, *A. faecalis* is a widespread organism which can be found in soils worldwide (e.g. Gamble *et al.* 1977). Based on the good agreement between our chemostat results and field and laboratory results on effects of temperature and pH on N_2O, NO and CO_2, we hypothesize that *A. faecalis p.* is an indicator organism for all groups of microorganisms normally found in soils. Therefore, *A. faecalis p.* may have the potential to serve as a model organism in process studies on N and C trace gas production.

Conclusions

Our experiments with pure chemostat cultures of the heterotrophic nitrifiers *A. faecalis p.* and *P. pantotrophus* yielded results for the temperature and pH dependencies of N_2O, NO and CO_2 production comparable with those observed in field flux measurements and laboratory soil incubation experiments. This shows that heterotrophic nitrifiers, which can be found widely and in high cell numbers in any soil, and which are thought to be of central importance for observed nitrification and denitrification activities in predominant acidic forest soils (Kreitinger *et al.* 1985; Martikainen and De Boer 1993; Papen and von Berg 1998), are ideal model organisms to further study the kinetics of N trace gas production by the microbial processes of nitrification and denitrification. Such process studies are needed to further improve and test numerical algorithms in biogeochemical models such as the PnET-N-DNDC model (Li *et al.* 2000) and ultimately improve the ability of such models to simulate the biosphere-atmosphere exchange of N trace gases.

Acknowledgements

We thank Dr Ralf Kiese, Dr Markus Teuber and Dr Rainer Gasche for scientific advice and Elisabeth Zumbusch and Georg Willibald for expert technical assistance. We also thank an anonymous reviewer for his very constructive comments on the manuscript. The work was funded by the European Commission in the NOFRETETE project (EVK2-CT2001-00106) of the fifth framework program.

References

Anderson, I.C., Poth, M., Homstead, J. and Burdige, D. (1993) A comparison of NO and N_2O production by the autotrophic nitrifier *Nitrosomonas europaea* and the heterotrophic nitrifier *Alcaligenes faecalis*. *Appl Environ Microbiol* **59**, 3525–3533.

Arts, P.A.M., Robertson, L.A. and Kuenen, J.G. (1995) Nitrification and denitrification by *Thiosphaera pantotropha* in aerobic chemostat cultures. *FEMS Microbiol Ecol* **18**, 305–315.

Baumgärtner, M. and Conrad, R. (1992) Role of nitrate and nitrite for production and consumption of nitric oxide during denitrification in soil. *FEMS Microbiol Ecol* **101**, 59–65.

Brumme, R. (1995) Mechanisms of carbon and nutrient release and retention in beech forest gaps. *Plant Soil* **168–169**, 593–600.

Butterbach-Bahl, K., Gasche, R., Breuer, L. and Papen, H. (1997) Fluxes of NO and N_2O from temperate forest soils: impact of forest type, N deposition and of liming on the NO and N_2O emissions. *Nutr Cycl Agroecosys* **48**, 79–90.

Cates, R.L. and Keeney, D.R. (1987) Nitrous oxide production throughout the year from fertilized and manured maize fields. *J Environ Qual* **16**, 443–447.

Conrad, R. (1996) Soil microorganisms as controllers of atmospheric trace gases (H_2, CO, CH_4, OCS, N_2O, and NO). *Microbiol Rev* **60**, 609–640.

Conrad, R. (2002) Microbiological and biochemical background of production and consumption of NO and N_2O in soil. In *Trace Gas Exchange in Forest Ecosystems* ed. Gasche, R., Papen, H. and Rennenberg, H. pp. 3–33. Dordrecht: Kluwer Academic Publishers.

Daum, D. and Schenk, M.K. (1998) Influence of nutrient solution pH on N_2O and N_2 emissions from a soilless culture system. *Plant Soil* **203**, 279–287.

Ellis, S., Howe, M.T., Goulding, W.T., Mugglestone, M.A. and Dendooven, L. (1998) Carbon and nitrogen dynamics in a grassland soil with varying pH: effect of pH on the denitrification potential and dynamics of the reduction enzymes. *Soil Biol Biochem* **30**, 359–367.

Fang, C. and Moncrieff, J.B. (2001) The dependence of soil CO_2 efflux on temperature. *Soil Biol Biochem* **33**, 155–165.

Gamble, T.N., Betlach, M.R. and Tiedje, J.M. (1977) Numerically dominant denitrifying bacteria from world soils. *Appl Environ Microbiol* **33**, 926–939.

Gasche, R. and Papen, H. (1999) A 3-year continuous record of nitrogen trace gas fluxes from untreated and limed soil of a N-saturated spruce and beech forest ecosystem in Germany. 2. NO and NO_2 fluxes. *J Geophys Res* **104**, 18505–18520.

Goodroad, L.L. and Keeney, D.R. (1984) Nitrous oxide production in aerobic soils under varying pH, temperature and water content. *Soil Biol Biochem* **16**, 39–43.

Griess-Ilosvay, M. (1965) Colorimetric nitrite method. In *Modern Methods of Plant Analysis* ed. Linskens, H., Sanwal, B. and Tracey, M. pp. A1–A6. Berlin: Springer-Verlag.

Grunditz, C. and Dalhammar, G. (2001) Development of nitrification inhibition assays using pure cultures of *Nitrosomonas* and *Nitrobacter*. *Water Res* **35**, 433–440.

Hoffmann, G. (1991) VD LUFA, A6141. In *Methodenbuch, Band 1, Die Untersuchung von Böden, 4. Auflage*, pp. 1–14. Darmstadt: VDLUFA-Verlag.

Holland, E.A., Dentener, F.J., Braswell, B.H. and Sulzman, J.M. (1999) Contemporary and pre-industrial global reactive nitrogen budgets. *Biogeochemistry* **46**, 7–43.

Holtzhauer, M. (1997) *Biochemische Labormethoden*. Berlin: Springer-Verlag.

Houghton, J.T., Ding, Y., Griggs, D.J., Noguer, M., van der Linden, P.J., Dai, X., Maskell, K. and Johnson, C.A. (2001) *IPCC 2001: Climate Change 2001: The Scientific Basis. Contribution of Working Group I to the Third Assessment Report of the Intergovernmental Panel on Climate Change*. Cambridge, UK, and New York: Cambridge University Press.

Koskinen, W.C. and Keeney, D.R. (1982) Effect of pH on the rate of gaseous products of denitrification in a silt loam soil. *Soil Sci Soc Am J* **46**, 1165–1167.

Krämer, M. and Conrad, R. (1991) Influence of oxygen on production and consumption of nitric oxide in soil. *Boil Fertil Soils* **11**, 38–42.

Kreitinger, J.P., Klein, T.M., Novick, N.J. and Alexander, M. (1985) Nitrification and characteristics of nitrifying microorganisms in an acid forest soil. *Soil Sci Soc Am J* **49**, 1407–1410.

Kuenen, J.G. and Robertson, L.A. (1987) Ecology of nitrification and denitrification. In *The Nitrogen and Sulphur Cycles: Symposia of the Society for General Microbiology 42* ed. Cole, J.A. and Ferguson, S.J. pp. 161–218. Cambridge: Cambridge University Press.

Li, C., Aber, J., Stange, F., Butterbach-Bahl, K. and Papen, H. (2000) A process oriented model of N_2O and NO emissions from forest soils: 1. Model development. *J Geophys Res* **105**, 4369–4384.

Lowry, O.H., Rosebrough, N.J., Farr, A.L. and Randall, R.J. (1951) Protein measurement with the folin phenol reagent. *J Biol Chem* **193**, 265–275.

Martikainen, P.J. (1985) Nitrous oxide emission associated with autotrophic ammonium oxidation in acid coniferous forest soil. *Appl Environ Microbiol* **50**, 1519–1525.

Martikainen, P.J. and De Boer, W. (1993) Nitrous oxide production and nitrification in acidic soil from a Dutch coniferous forest. *Soil Biol Biochem* **25**, 343–347.

McKenney, D.J., Drury, C.F., Findlay, W.I., Mutus, B., McDonnell, T. and Gajda, C. (1994) Kinetics of denitrification by *Pseudomonas fluorescens*: oxygen effects. *Soil Biol Biochem* **26**, 901–908.

Nägele, W. and Conrad, R. (1990) Influence of pH on the release of NO and N_2O from fertilized and unfertilized soil. *Biol Fertil Soils* **10**, 139–144.

Ormeci, B., Sanin, S.L. and Peirce, J.J. (1999) Laboratory studies of NO flux from agricultural soil: effects of soil moisture, pH, and temperature. *J Geophys Res* **104**, 1621–1629.

Otte, S., Grobben, N.G., Robertson, L.A., Jetten, M.S.M. and Kuenen, J.G. (1996) Nitrous oxide production by *Alcaligenes faecalis* under transient and dynamic aerobic and anaerobic conditions. *Appl Environ Microbiol* **62**, 2421–2426.

Ottow, J.G.G., Burth-Gebauer, I. and El Demerdash, M.E. (1985) Influence of pH and partial oxygen pressure on the N_2O-N to N_2 ratio of denitrification. In *Denitrification in the Nitrogen Cycle* ed. Goltermann, H.L. pp. 101–120. New York: Plenum Press.

Papen, H. and von Berg, R. (1998) A Most Probable Number method (MPN) for the estimation of cell numbers of heterotrophic nitrifying bacteria in soil. *Plant Soil* **199**, 123–130.

Papen, H. and Butterbach-Bahl, K. (1999) A 3-year continuous record of nitrogen trace gas fluxes from untreated and limed soil of a N-saturated spruce and beech forest ecosystem in Germany. 1. N_2O emissions. *J Geophys Res* **104**, 18487–18503.

Papen, H., von Berg, R., Hinkel, I., Thoene, B. and Rennenberg, H. (1989) Heterotrophic nitrification by *Alcaligenes faecalis*: NO_2^-, NO_3^-, N_2O and NO production in exponentially growing cultures. *Appl Environ Microbiol* **55**, 2068–2072.

Remde, A. and Conrad, R. (1991) Role of nitrification and denitrification for NO metabolism in soil. *Biogeochemistry* **12**, 189–205.

Robertson, L.A. and Kuenen, J.G. (1988) Heterotrophic nitrification in *Thiosphaera pantotropha*: oxygen uptake and enzyme studies. *J Gen Microbiol* **134**, 857–863.

Robertson, L.A. and Kuenen, J.G. (1990) Combined heterotrophic nitrification and aerobic denitrification in *Thiosphera panthotropha* and other bacteria. *Antonie van Leeuwenhoek* **57**, 139–152.

Robertson, L.A., van Niel, E.W.J., Torremans, R.A.M. and Kuenen, J.G. (1988) Simultaneous nitrification and denitrification in aerobic chemostat cultures of *Thiosphaera pantotropha*. *Appl Environ Microbiol* **54**, 2812–2818.

Robertson, L.A., Dalsgaard, T., Revsbeck, N.P. and Kuenen, J.G. (1995) Confirmation of 'aerobic denitrification' in batch cultures, using gas chromatography and ^{15}N mass spectrometry. *FEMS Microbiol Ecology* **18**, 113–120.

Saad, O. and Conrad, R. (1993) Temperature-dependence of nitrification, denitrification, and turnover of nitric-oxide in different soils. *Biol Fert Soil* **15**, 21–27.

Simek, M. and Cooper, J.E. (2002) The influence of soil pH and denitrification: progress towards the understanding of

this interaction over the last 50 years. *Eur J Soil Sci* **53**, 345–354.

Simek, M., Jisova, L. and Hopkins, D.W. (2002) What is the so-called optimum pH for denitrification in soil? *Soil Biol Biochem* **34**, 1227–1234.

Sitaula, B.K. and Bakken, L.R. (1993) Nitrous oxide release from spruce forest soil: relationships with nitrification, methane uptake, temperature, moisture and fertilization. *Soil Biol Biochem* **25**, 1415–1421.

Sitaula, B.K., Bakken, L.R. and Abrahamsen, G. (1995) N-fertilization and soil acidification effects on N_2O and CO_2 emission from temperate pine forest soil. *Soil Biol Biochem* **27**, 1401–1408.

Smith, K.A., Thomson, P.E., Clayton, H., McTaggart, I.P. and Conen, F. (1998) Effects of temperature, water content and nitrogen fertilization on emissions of nitrous oxide by soils. *Atmos Environ* **33**, 3301–3309.

Stevens, R.J., Laughlin, R.J. and Malone, J.P. (1998) Soil pH affects the process reducing nitrate to nitrous oxide and di-nitrogen. *Soil Biol Biochem* **26**, 1003–1009.

Struwe, S. and Kjøller, A. (1994) Potential for N_2O production from beech (*Fagus sylvaticus*) forest soils with varying pH. *Soil Biol Biochem* **30**, 1119–1126.

Thomsen, J.K., Geest, T. and Cox, R.P. (1994) Mass spectrometric studies of the effect of pH on the accumulation of intermediates in denitrification by *Paracoccus denitrificans*. *Appl Environ Microbiol* **60**, 536–541.

Van Cleemput, O. and Baert, L. (1984) Nitrite: a key compound in N loss processes and acid conditions? *Plant Soil* **76**, 233–241.

Weier, K.L. and Gilliam, J.W. (1986) Effect of acidity on denitrification and nitrous oxide evolution from Atlantic coastal-plain soils. *Soil Sci Soc Am J* **50**, 1202–1205.

Yamulki, S., Harrison, R.M., Goulding, K.W.T. and Webster, C.P. (1997) N_2O, NO and NO_2 fluxes from a grassland: effect of soil pH. *Soil Biol Biochem* **29**, 1199–1208.

Yoshida, T. and Alexander, M. (1970) Nitrous oxide formation by *Nitrosomonas europaea* and heterotrophic microorganisms. *Soil Sci Soc Am Proc* **34**, 880–882.

Biogeosciences, 2, 353–375, 2005
www.biogeosciences.net/bg/2/353/
SRef-ID: 1726-4189/bg/2005-2-353
European Geosciences Union

Biogeosciences

Inventories of N_2O and NO emissions from European forest soils

M. Kesik[1], P. Ambus[2], R. Baritz[3], N. Brüggemann[1], K. Butterbach-Bahl[1], M. Damm[1], J. Duyzer[4], L. Horváth[5], R. Kiese[1], B. Kitzler[6], A. Leip[7], C. Li[8], M. Pihlatie[9], K. Pilegaard[2], G. Seufert[7], D. Simpson[10], U. Skiba[11], G. Smiatek[1], T. Vesala[9], and S. Zechmeister-Boltenstern[6]

[1]Karlsruhe Research Centre, Institute for Meteorology and Climate Research, Atmospheric Environmental Research (IMK-IFU), Kreuzeckbahnstr. 19, 82 467 Garmisch-Partenkirchen, Germany
[2]Risoe National Laboratory, Department for Plant Biology and Biogeochemistry, Risø, Denmark
[3]Federal Institute for Geosciences and Natural Resources (BGR), Hannover, Germany
[4]The Netherlands Organization for Applied Scientific Research, Apeldoorn, Netherlands
[5]Hungarian Meteorological Service, Department for Analysis of Atmospheric Environment, Budapest, Hungary
[6]Federal Forest Research Centre, Institute for Forest Ecology and Soil, Soil Biology, Vienna, Austria
[7]Commission of the European Communities, Environmental Institute, JRC Ispra, Italy
[8]Institute for the Study of Earth, Oceans and Space, Univ. of New Hampshire, Durham, USA
[9]University of Helsinki, Department of Physical Sciences, Helsinki, Finland
[10]Norwegian Meteorology Institute, Oslo, Norway
[11]Natural Environment Research Council, Centre for Ecology and Hydrology, Edinburgh, UK

Received: 9 June 2005 – Published in Biogeosciences Discussions: 15 July 2005
Revised: 21 September 2005 – Accepted: 18 November 2005 – Published: 5 December 2005

Abstract. Forest soils are a significant source for the primary and secondary greenhouse gases N_2O and NO. However, current estimates are still uncertain due to the still limited number of field measurements and the herein observed pronounced variability of N trace gas fluxes in space and time, which are due to the variation of environmental factors such as soil and vegetation properties or meteorological conditions. To overcome these problems we further developed a process-oriented model, the PnET-N-DNDC model, which simulates the N trace gas exchange on the basis of the processes involved in production, consumption and emission of N trace gases. This model was validated against field observations of N trace gas fluxes from 19 sites obtained within the EU project NOFRETETE, and shown to perform well for N_2O (r^2=0.68, slope=0.76) and NO (r^2=0.78, slope=0.73). For the calculation of a European-wide emission inventory we linked the model to a detailed, regionally and temporally resolved database, comprising climatic properties (daily resolution), and soil parameters, and information on forest areas and types for the years 1990, 1995 and 2000. Our calculations show that N trace gas fluxes from forest soils may vary substantial from year to year and that distinct regional patterns can be observed. Our central estimate of NO emissions from forest soils in the EU amounts to 98.4, 84.9 and 99.2 kt N yr^{-1}, using meteorology from 1990, 1995 and year 2000, respectively. This is <1.0% of pyrogenic NO_x emissions. For N_2O emissions the central estimates were 86.8, 77.6 and 81.6 kt N yr^{-1}, respectively, which is approx. 14.5% of the source strength coming from agricultural soils. An extensive sensitivity analysis was conducted which showed a range in emissions from 44.4 to 254.0 kt N yr^{-1} for NO and 50.7 to 96.9 kt N yr^{-1} for N_2O, for year 2000 meteorology.

The results show that process-oriented models coupled to a GIS are useful tools for the calculation of regional, national, or global inventories of biogenic N trace gas emissions from soils. This work represents the most comprehensive effort to date to simulate NO and N_2O emissions from European forest soils.

Correspondence to: K. Butterbach-Bahl
(klaus.butterbach@imk.fzk.de)

1 Introduction

The atmospheric concentration of nitrous oxide (N_2O) has been increasing in recent decades with a rate of approx. 0.25% yr^{-1} (IPCC, 2001). Among other sources, forest soils have been acknowledged to represent significant sources of this potent greenhouse gas (e.g. Schmidt et al., 1988; Skiba et al., 1994). Emissions of N_2O from forest soils have most likely increased in recent decades and will probably increase in the future due to the anthropogenic perturbation of the global N cycle (Galloway et al., 2004) and hence high rates of atmospheric N deposition to many forest ecosystems in Europe, North America and Asia (Aber et al., 1989; Bowden et al., 1991). In a series of recent

publications evidence has been provided that N deposition to forest ecosystems are positively correlated with N_2O emissions (Brumme and Beese, 1992; Butterbach-Bahl et al., 1998; Zechmeister-Boltenstern et al., 2002).

On a global scale soils have been identified as sources of atmospheric NO_x of a comparable magnitude like combustion processes (Davidson and Kingerlee, 1997). This especially applies to acidic forest soils, which have been shown to act primarily as sources of NO, a reactive trace gas involved in the production of tropospheric ozone (Williams et al., 1992; Butterbach-Bahl et al., 2002a). However, due to its reactivity only a part of the NO emitted from forest soils will reach the atmosphere, whereas some of the NO will react with ozone to NO_2, associated with a partial re-deposition of NO_2 to plant and soil surfaces or an uptake by plant tissues (Duyzer and Fowler, 1994; Meixner, 1994; Gessler et al., 2001; Dorsey et al., 2004). As for N_2O, atmospheric N deposition to forest ecosystems has been shown to be closely related to the source strength of forest soils for NO (Gasche and Papen, 1999; Pilegaard et al., 1999; Van Dijk and Duyzer, 1999).

The emission of NO and N_2O from forest soils is mainly the result of simultaneously occurring production and consumption processes, most of which are directly linked to the microbial N turnover processes of nitrification and denitrification (Conrad, 1996, 2002). With regard to NO also the abiotic process of chemo-denitrification, during which biologically produced nitrite is chemically decomposed to NO, has been shown to be an important production process in soils at pH values lower than 4.0 (Van Cleemput and Baert, 1984). Like most other biological processes, microbial turnover processes vary largely on spatial and temporal scales, since they are significantly influenced by a number of environmental factors such as climate and meteorological conditions, soil and vegetation properties or human management of the land surface. Due to this also the emission of N trace gases from forest soils have been observed to vary over several orders of magnitudes between seasons, years or measuring sites (Papen and Butterbach-Bahl, 1999; Brumme et al., 1999; Butterbach-Bahl et al., 2002b). This variability is the reason for the still high uncertainty of current regional and global estimates of N trace gas emissions from soils. In recent years it has been proposed that linking process-oriented models, which are able to simulate the processes involved in N trace gas emissions from soils, to detailed GIS databases, holding explicit spatial information on major drivers of microbial processes, can serve as tools to improve current estimates of the magnitude of terrestrial sources and sinks of atmospheric trace gases (Brown et al., 2002).

This approach, i.e. the use of process-oriented biogeochemical models for calculating inventories of N trace gas emissions from soils, was also followed within the EU funded project NOFRETETE (**N**itrogen **O**xides Emissions **fr**om **E**uropean Fores**t** **E**cosys**te**ms). This manuscript provides details of model modifications, model testing and the establishment of a GIS database which was finally used to initialize and drive the PnET-N-DNDC model for the calculation of inventories of N trace gas emissions of forest soils of Europe. It represents the most comprehensive effort to date to simulate NO and N_2O emissions from European forest soils.

2 Materials and methods

2.1 The PnET-N-DNDC model

For the calculation of N_2O and NO emission inventories of European forest soils the biogeochemical model PnET-N-DNDC was used. The model has been already applied for regional emission inventories for temperate forest ecosystems (Butterbach-Bahl et al., 2001, 2004), and recently, after some adaptation, also for the calculation of a N_2O emission inventory for tropical rainforests in Australia (Kiese et al., 2005). The PnET-N-DNDC model was developed to predict soil carbon and nitrogen biogeochemistry in temperate forest ecosystems and to simulate the emissions of N_2O and NO from forest soils (Li et al., 2000; Stange et al., 2000). The model is mainly based on the PnET model (= **P**hotosy**n**thesis-**E**vapo**t**ranspiration-Model), the DNDC model (=**D**e**n**itrification-**Dec**omposition-Model) and a nitrification module. The PnET model is a forest physiology model used for predicting forest photosynthesis, respiration, organic carbon production and allocation, and litter production. It was originally developed by Aber and Federer (1992). This model has already been used in regional studies in order to predict the sensitivity of forest production to climate variability and site quality (e.g. Goodale et al., 1998). DNDC is a soil biogeochemistry model used for predicting soil organic matter decomposition, nitrogen turnover and N_2O production in agricultural soils (Li et al., 1992). This model has also been used to predict regional N_2O emissions from agriculture in US, China and UK (Li et al., 1996, 2001, 2004; Brown et al., 2002). The nitrification module was developed by Stange (2000) in order to simulate nitrification rates, the growth of nitrifier populations and the nitrification induced N_2O and NO emissions associated with nitrification.

In the PnET-N-DNDC model N_2O and NO emissions from soils are directly influenced by environmental factors, such as soil temperature and moisture, pH and substrate availability (C- and N-content). These environmental factors are driven by different ecological drivers, namely climate, soil properties, vegetation and anthropogenic activities. Five modules for predicting forest growth, soil climate, decomposition, nitrification and denitrification are linked to translate the environmental factors and ecological drivers into predicted N_2O and NO emissions. The functions of the different modules are as follows: a) the soil climate module is used to convert daily climate data into soil temperature and moisture profiles and to calculate soil oxygen availability in the forest soil

profile; b) the forest growth module simulates forest growth as a function of solar radiation, temperature, water and N availability. The forest growth module is linked to the soil climate and decomposition modules via litter production and water and N demand; c) the decomposition module simulates the turnover of litter and other organic matter and, hence, the production of ammonium, nitrate and dissolved organic carbon (DOC) in the soil driven by temperature, moisture and O_2 availability in the soil profile; d) the nitrification module predicts growth and death of nitrifiers, the nitrification rate as well as N_2O and NO production during nitrification depending on soil temperature, moisture, ammonium and DOC concentrations; e) depending on the population size of denitrifiers, soil temperature, moisture and substrate concentrations (DOC, NO_3^-, NO_2^-, NO and N_2O), the denitrification module simulates the individual steps of the sequential reduction of nitrate or other oxidized N compounds (NO_2^-, NO, N_2O) to the final product N_2.

The nitrification and denitrification induced N_2O and NO fluxes are calculated based on the dynamics of soil aeration status, substrate supply and gas diffusion. Chemo-denitrification, i.e. chemical decomposition of NO_2^- to NO, is considered as another source of NO production in soils. This chemical reaction is controlled by the concentration of nitrite in the soil, soil pH and temperature. To handle the problem of simultaneously occurring aerobic and anaerobic processes in adjacent microsites, the PnET-N-DNDC model uses the concept of a so-called "anaerobic balloon". Based on the O_2 diffusion from the atmosphere into the soil and the O_2 consumption during heterotrophic and autotrophic respiration the O_2 concentration is calculated for a given soil layer. The O_2 concentration is assumed to be reciprocally proportional to the anaerobic fraction within this soil layer (Li et al., 2000). For further details on the PnET-N-DNDC model we refer to Li et al. (1992, 1996, 2000), Li (2000), Stange et al. (2000), Butterbach-Bahl et al. (2001, 2004) and Kiese et al. (2005).

To simulate N trace gas emissions for a specific site the PnET-N-DNDC requires the following input parameters: daily climate data (precipitation, minimum and maximum air temperature, optional: solar radiation), soil properties (texture, clay content, pH, soil organic carbon content, stone content, humus type), and forest data (forest type and age, above-ground and below-ground biomass, plant physiology parameters). The PnET-N-DNDC is currently parameterized for 12 tree species/genera, i.e. pine, spruce, hemlock, fir, hardwoods, oak, birch, beech, slash pine, larch, cypress and evergreen oak. Whenever there are no site-specific forest data available except for the forest type and age, the model calculates with default values for each forest type taken from an internal database of literature data (Li et al., 2000).

Since several authors have discussed the importance of the forest floor humus type for N trace gas emissions (e.g. Brumme et al., 1999; Butterbach-Bahl et al., 2002a), we shortly want to discuss how the PnET-N-DNC model deals with the effect of humus type on processes involved in N trace gas emissions. In the model the effect of the humus on N trace gas production is indirect: the humus type influences the partitioning of SOC into different fractions (humus, humads, litter) with their specific decay constants (Li et al., 2000). For a forest floor with mull as humus type the SOC fractions with short turnover times are highest, medium in moder and smallest if the humus type is rawhumus. This does affect the C as well as N availability and, thus, the C and N turnover rates and finally also the processes involved in N trace gas emissions. Furthermore, the humus type is also influencing the density and the porosity of the organic layer, which also results in differences in soil climatic conditions such as water and temperature distribution in the soil layers.

Furthermore, the model needs information about inorganic N concentrations in rainfall which are used to calculate throughfall values for N. Throughfall is a surrogate of wet and dry deposition and is depending on forest type and N concentration. The equations used in PnET-N-DNDC to calculate throughfall values are described by Li et al. (2000).

No structural changes were applied to the PnET-N-DNDC model for its use within the NOFRETETE project. However, based on results from laboratory studies by Kesik et al. (2005)[1] the parameterisation of NO production by chemo-denitrification (Chem_NO) in dependency on the soil pH (soil_pH[layer]) and the nitrite concentration (NO_2[layer]) in the respective soil layers was changed as follows:

$$\text{Chem\_NO}\,[\text{kg N ha}^{-1}\,\text{day}^{-1}] = 300 \times \text{NO}_2[\text{layer}] \times 16\,565 \times \exp^{(-1.62\times \text{soil\_pH[layer]})} \times f1)$$

f1 is an Arrhenius type function describing the temperature dependency (temp[layer]) of chemo-denitrification:

$$f1 = \exp^{\left(\frac{-31494}{(\text{temp[layer]}+273.18)\times 8.3144}\right)} \quad \text{(Stange, 2000)}$$

It should be noted that these algorithms do not consider the pH microsite variability in soils, which have been found to be significant in some soils (Häussling et al., 1985; Strong et al., 1997; Bruelheide and Udelhoven, 2005). This means that we assume a uniform bulk soil pH. However, future model developments may be necessary to address the microsite variability of soil pH and to assess consequences of this variability on NO production via chemo-denitrification.

Furthermore, the parameters for the moisture dependency of gross nitrification and N_2O and NO production and consumption during nitrification and denitrification (see Li et al., 2000) were optimised according to the results from laboratory studies (see Schindelbacher et al., 2004; Kesik et al., 2005[1]).

[1]Kesik, M., Blagodatsky, S., Papen, H., and Butterbach-Bahl, K.: Effect of pH, temperature and substrate on N_2O, NO and CO_2 production by Alcaligenes faecalis p. J. Applied Microb., submitted, 2005.

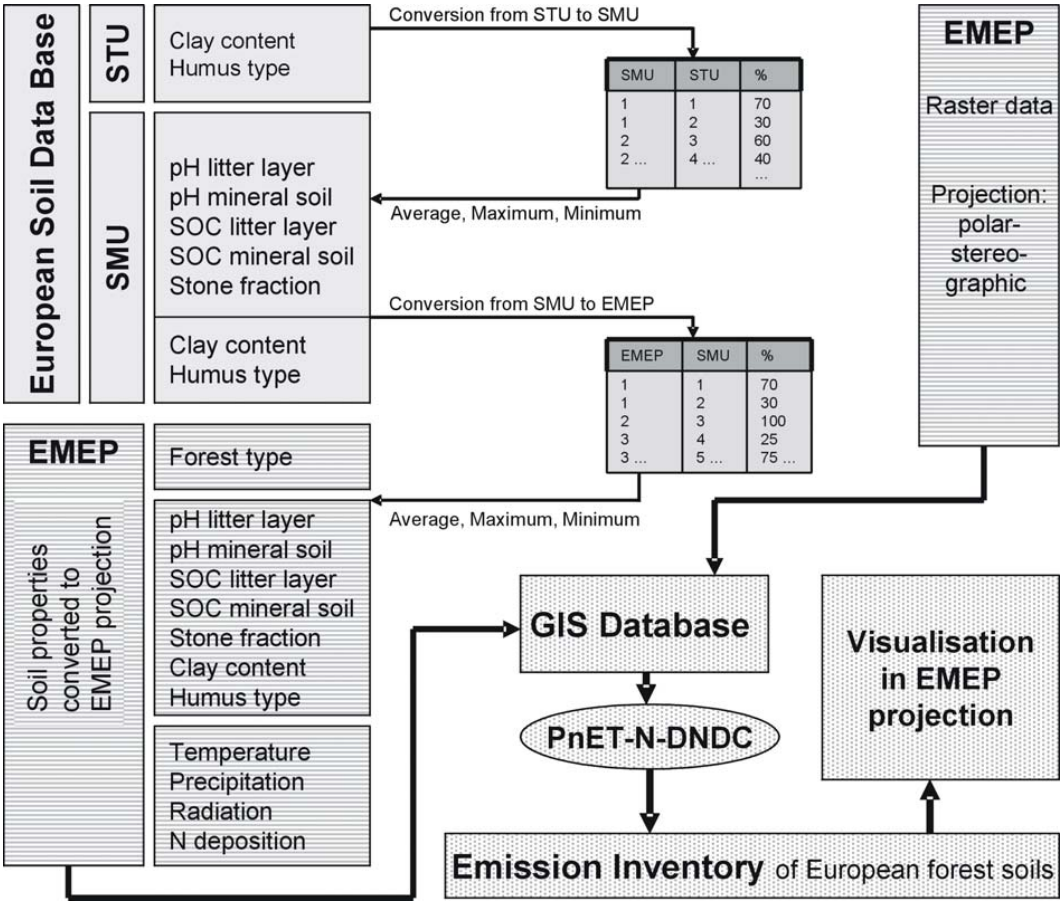

Fig. 1. Scheme for data aggregation and visualisation used for the calculation of a regional inventory of N trace gas emissions from forest soils.

2.2 Evaluation sites

The capability of the PnET-N-DNDC model to simulate N trace gas emissions from forest soils was tested by comparing model results with results from field measurements at 19 different field sites across Europe and US (Table 1). Most of these sites were measuring sites within the NOFRETETE project. The testing sites were well distributed across Europe, with a boreal forest site at Hyytiälä, Finland, forest sites in temperate maritime climate (e.g. Speulderbos, Netherlands, Sorø, Denmark, and Glencorse, UK) and temperate continental climate (Matrafüred, Hungary) and forest sites exposed to Mediterranean climate (San Rossore, Parco Ticino, Italy) (Table 1). For all sites information on model input parameters (see Sect. 2.1) as well as on N trace gas fluxes were aggregated in a database for model testing.

2.3 GIS database

A detailed GIS database covering all EU states plus Romania, Bulgaria, Switzerland and Norway with all relevant initialization and driving parameters and variables was created for the regionalization of N trace gas emissions by use of the PnET-N-DNDC. Spatially resolved information included soil, forest and climate properties. Within the NOFRETETE project information on meteorological data and on atmospheric N deposition was provided by the Norwegian Meteorological Institute (MET.NO), from the inputs of the EMEP MSC-W photo-oxidant model (Sandnes-Lenschow et al., 2000; Simpson et al., 2003), on soil properties and on forest information by the Joint Research Centre (JRC) at Ispra, Italy. Since data were delivered in different formats and projections, transformations into the ArcGIS format and the Lambert Azimuthal projection on the basis of the EMEP (European Monitoring and Evaluation Program) raster were necessary. The used EMEP raster is a polar stereographic projected grid with a resolution of 50 km×50 km at 60° North (Simpson et al., 2003; http://www.emep.int).

2.3.1 Soil information

The soil data were retrieved from the Soil Geographical Data Base of Europe (SGDBE) at a scale of 1:1 000 000. This data base is part of the European Soil Data Base (http://eusoils.

Table 1. Site characteristics of the temperate forest sites used for model testing.

Site, Country	Coordinate	Forest Type	Forest Age [yr]	Humus Type	Soil Texture	Clay [%]	pH Forest floor	pH Mineral soil	SOC [kg C kg^{-1}]	Years	N Input [kg N yr^{-1}]	Annual temperature [°C]	Annual precipitation [mm]
Achenkirch, Austria[a]	47° N 11° E	Spruce	125	Mull	Loam	19	5.7	7.0	0.077	1998–99	2.7–7.7	6.8–6.9	1691–1976
										2002–03	6.8–5.0	7.5–7.0	1747–1275
Copenhagen, Denmark[b]	55° N 12° E	Spruce	30	Moder	Loamy sand	6	3.7	3.7	0.061	1992	11.3	8.6	756
Glencorse, UK	55° N 3° W	Birch	21	Moder	Silty loam	18	4.8	4.8	0.070	2002–03	12.9–9.2	9.1–7.9	1183–840
Glencorse, UK	55° N 3° W	Sitka spruce	19	Moder	Silty loam	18	4.2	4.2	0.070	2002–03	12.9–9.2	9.1–7.9	1183–840
Harvard Forest, USA[c]	42° N 72° W	Hard-woods	79	Moder	Sandy loam	9	3.3	3.8	0.076	1989	2.2	7.4	1120
Höglwald, Germany[de]	48° N 11° E	Beech	87	Mull	Loam	19	4.0	3.7	0.051	1994–97	18.3–26.0	6.1–10.1	731–1041
Höglwald, Germany	48° N 11° E	Beech	110	Mull	Sandy loam	9	4.5	4.0	0.051	2002–03	26.3–14.3	9.1–8.9	1054–571
Höglwald, Germany[de]	48° N 11° E	Spruce	96	Moder	Loam	19	3.2	3.5	0.029	1994–97	18.3–26.0	6.1–10.1	731–1041
										2002–03	26.3–14.3	9.1–8.9	1054–571
Hyytiälä, Finland	61° N 24° E	Pine	41	Moder	Sandy loam	9	3.2	3.7	0.029	2002–03	0.09–0.1	4.2–4.1	535–644
Klausenleopoldsdorf, Austria[a]	48° N 16° E	Beech	55	Moder	Sandy clay loam	27	5.2	4.5	0.051	1996–97	9.5–12.9	8.6–8.9	763–1035
										2002–03	12.0–6.4	9.0–8.3	959–515
Matrafüred, Hungary	48° N 20° E	Spruce	35	Moder	Sandy loam	9	4.5	3.9	0.019	2002–03	13.3–7.3	9.0–8.1	809–678
Matrafüred, Hungary	48° N 20° E	Oak	63	Mull	Sandy loam	9	5.7	4.3	0.036	2002–03	8.7–6.5	9.0–8.1	809–678
Parco Ticino, Italy	45° N 9° E	Hard-woods	150	Mull	Loamy sand	6	4.1	4.2	0.067	2002–03	10.7–6.0	14.3–14.5	1066–602
Parco Ticino, Italy	45° N 9° E	Poplar	13	Moder	Sandy loam	9	5.8	5.9	0.010	2002–03	10.7–6.0	14.3–14.5	1066–602
San Rossore, Italy	43° N 10° E	Pine	38	Raw humus	Sand	3	5.0	5.8	0.007	2002–03	5.5–3.7	14.4–14.7	1101–742
Schottenwald, Austria[f]	48° N 16° E	Beech	135	Moder	Silty loam	18	5.0	4.2	0.068	1996–97	25.1–34.1	9.4–9.7	718–973
										2002–03	33.6–16.3	10.3–10.0	959–467
Sorø, Denmark	55° N 12° E	Beech	80	Moder	Loamy sand	9	4.3	4.5	0.040	2002–03	45.6–23.9	8.8–8.6	1013–532
Speulderbos, Netherlands	52° N 5° E	Douglas fir	43	Moder	Sand	3	3.7	3.7	0.090	2002–03	56.7–37.6	10.6–10.2	924–613
Wildbahn, Germany[g]	53° N	Pine	65	Moder	Loamy sand	6	3.3	3.6	0.035	1997	12.3	8.3	616

[a] Data of Forstliche Bundesversuchsanstalt, Vienna, [b] Ambus and Christensen (1995), [c] Bowden et al. (1991), [d] Göttlein and Kreutzer (1991), [e] Papen and Butterbach-Bahl (1999), [f] Jandl et al. (1997), [g] Böß (2000).

jrc.it/). The SGDBE is the resulting product of a collaborative project involving the European Union and neighbouring countries. It is a simplified representation of the diversity and spatial variability of the soil coverage (CEC, 1985). The SGDBE provides typological information according to so-called Soil Typological Units (STU; N: 5306). The STU are grouped into Soil Mapping Units (SMU; N: 1650) to form soil associations (for details see CEC, 1985). The STU attribute data contain information about specific soil properties, such as textural class, humus type, water regime, etc. Additionally data for soil carbon and pH for the organic layer and the mineral soil, stone content on SMU level were needed. Therefore preliminary results from the ongoing research project (CarboInvent) were used (aggregated soil C data for organic layer and mineral soil). Regarding these data it has to be noted that the SOC content may not yet represent the final level of quality. For example, data for the continental Eastern part of Europe (e.g. Poland) appear to be too high, and in the case of the mountainous areas such as the Alps, no stratification was found although local data clearly indicate elevated SOC content (R. Baritz, personal information). To aggregate the STU- and SMU-based attributes on the scale of the EMEP raster an up-scaling strategy was applied (Fig. 1). At first the soil properties as derived from the STU were scaled to the SMU level, thereby considering the relative area covered. Secondly, a weighted average value was calculated for the individual soil parameters for each EMEP grid cell, i.e. for clay content, humus type, forest floor and mineral soil pH, stone content and organic carbon mass in the forest floor and mineral soil. Additionally the maximum and minimum value of each soil parameter was recorded for each EMEP grid cell to retrieve the range for a sensitivity analysis with a maximum and a minimum scenario (see Sect. 2.5) (Fig. 1). Even though forest information for Belarus and Moldavia was available, these countries were excluded from the calculations since details about soil properties were not available.

Figure 2 shows the distribution of forest areas (Fig. 2a) and of selected soil properties (0–0.2 m soil depth: SOC, clay content, soil pH) in Europe as derived from CORINE/PELCOM land cover data sets and the SGDBE dataset on soil properties. The maps show that soils rich in organic carbon (SOC) in the mineral soil (>75 t C ha^{-1}) predominate in Northern Europe including the UK and Ireland (Fig. 2b), whereas heavily textured soils (clay content >20%) are often found in the Mediterranean and the Balkan region (Fig. 2c). Predominantly acidic soils with a low base saturation are reported for large parts of Sweden and Finland, but also for the Northern parts of the UK (Fig. 2d).

2.3.2 Forest distribution and forest stand information

Information about the distribution of forest types across Europe has recently been published by Köble and Seufert (2001). They adopted the spatial distribution of forest area for most parts of Europe from the CORINE land cover data set (CEC, 1994) or from the Pan-European Land Cover Mapping project "PELCOM" (Mücher, 2000). In addition Köble and Seufert (2001) used tree species information from the measurement network of the transnational survey (ICP Forest

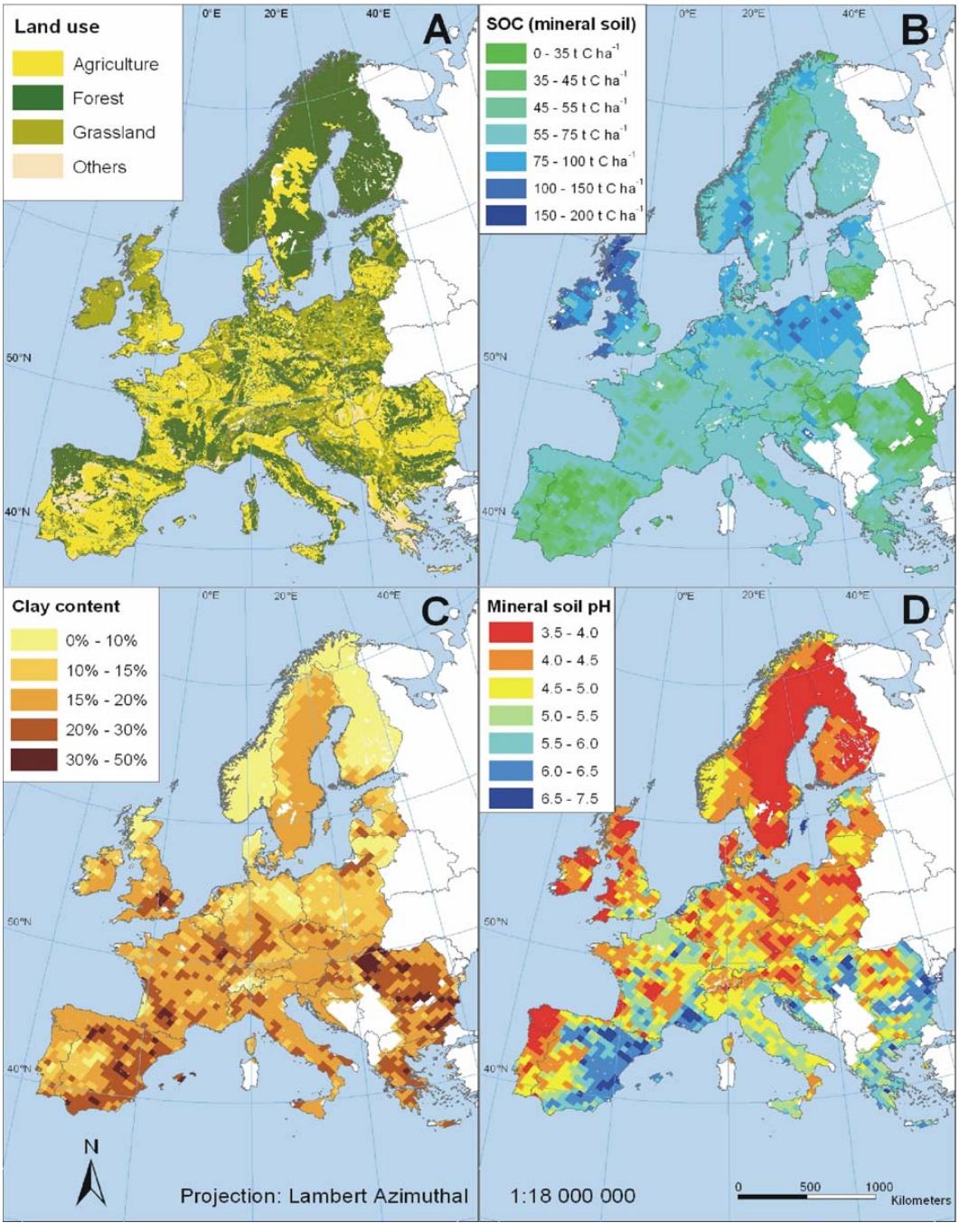

Fig. 2. Distribution of land cover types and selected soil properties across Europe. Data were derived either from CORINE or PELCOM land cover data sets or from the Soil Geographical Data Base of Europe. Note that soil property information is only valid for forest soils.

Level I) of forest condition in Europe (UN-ECE, 1998) to retrieve maps of forest type and tree species distribution on a 1 km×1 km raster format for 30 European countries. Since the PnET-N-DNDC model is currently only parameterized for the simulation of 12 forest types (see Sect. 2.1), we grouped some forest types together in order to simulate most of the forested areas in Europe. This means, that e.g. the forest types alder, ash, elm, poplar and willow were simulated with the parameterization for hardwoods. However, some forest types such as *Juniperus spec.* dominated forests were excluded from our simulations a) since such forests cover only small areas in Europe (approx. 3.5%) and b) to reduce the parameterization and computation complexity. The forest area considered in our simulations was 1 410 477 km^2,

which is in accordance with official national reports (Köble and Seufert, 2001). As there was no information about forest age available we assumed an average age of 60 years for all forest types. Forest areas in the countries of Albania, Serbia and Montenegro, Macedonia and Bosnia-Herzegovina were excluded from the simulations since no detailed forest information was available.

2.3.3 Climate and N deposition

Simulation runs were performed meteorology for the three years 1990, 1995 and 2000. Meteorological data in daily resolution was provided from the inputs of the EMEP MSC-W oxidant model (Sandnes-Lenschow et al., 2000; Simpson et al., 2003) including information about average temperature, and sum precipitation as well as photosynthetically active radiation (PAR). Figure 3 shows a map of the regional distribution of mean annual temperature and sum of annual precipitation across Europe for the year 2000 and relative differences of these parameters in 1990 as compared to the year 2000. The maps show a typical South-North gradient in temperature and reveal that e.g. in the year 2000 mean annual temperature was >10% higher in Central Europe and approx. 5% lower in Spain and Central Europe as compared to the year 1990. The variation in precipitation between the years 1990 and 2000 was pronounced and in many regions in Europe such as Central Finland, Southern UK or Portugal received >25% precipitation in 1990 than in the year 2000 (Fig. 3).

Additionally, the EMEP MSC-W model was used to calculate annual data on atmospheric N deposition (dry and wet) for each EMEP grid cell. Emissions of all pollutants were set to those of the year 2000 (Vestreng et al., 2004), whereas meteorology scenarios were taken from the years 1990, 1995 and 2000 in order to asses meteorological variability. This EMEP model's simulations of concentrations and deposition have been extensively evaluated elsewhere (e.g. Fagerli et al., 2003) and for forests in particular by Westling et al. (2005). Since the PnET-N-DNDC model does not allow consideration of dry deposition of N to forests, we only used the wet deposition values (Fig. 4). The map shows that wet deposition of N with values $>13\,kg\,N\,ha^{-1}\,yr^{-1}$ are especially observed for the Benelux countries and neighbouring North Germany and for parts of South Germany and Northern Italy.

2.4 Coupling of the GIS database to the PnET-N-DNDC model

The forest, soil, and climate information was aggregated and linked to the EMEP raster. An individual identification number was assigned to each of the 2527 grid cells of the simulated area. By calling the ID numbers the PnET-N-DNDC model automatically received the individual initialisation and driving parameters of each grid cell. The number of model runs per grid cell depended on the number of forest types found within this cell. For example, three different forest types in one grid cell resulted in three model runs. The results of the individual model runs for one grid cell were weighted depending on the total area of each forest type in the respective grid cell.

2.5 Uncertainty analysis (Monte Carlo, MSF)

The focus of the uncertainty analysis was the assessment of the uncertainty of simulation results caused by the necessary generalisations within the GIS database on e.g. soil and vegetation properties. By using the EMEP grid with cells of $50\,km \times 50\,km$ across Europe it was assumed that soil properties within a grid cell were uniform. However, this is of course not the case, since soil properties (e.g. pH, soil organic carbon (SOC) content) are highly variable in space. To assess the effect of sub grid cell variability in soil properties on simulated N trace gas emissions from forest soils the Most Sensitive Factor (MSF) method (Li et al., 2004) as well as a Monte Carlo approach was used with the same set of parameters. N trace gas fluxes simulated with the PnET-N-DNDC and also with the DNDC have been shown to be very sensitive to changes in soil texture, pH and SOC (Stange et al., 2000; Butterbach-Bahl et al., 2001; Li et al., 2004). After extensive sensitivity studies of the soil database of Europe we found out that there were general trends regarding the relationship between N_2O and NO emissions and the soil factors. For example, the modelled N_2O and NO emissions usually increase along with an increase in SOC content and clay fraction as well as a decrease in pH. These model reactions are in accordance with a series of results from field and laboratory observations (Li et al., 2005). The MSF method uses the generalized relationships between individual soil factors and the magnitude of N trace gas emissions by grouping a series of soil factors for which minimum and maximum values are available in such a way that N trace gas emissions are either maximized or minimized. This means that PnET-N-DNDC automatically selected the minimum organic matter mass in the forest floor and mineral soil, maximum pH in the forest floor and mineral soil, maximum stone content and minimum clay content to form a scenario which was assumed to produce a low value of N_2O and NO flux for this grid cell and the model then selected the maximum organic matter mass and minimum pH in the forest floor and mineral soil, minimum stone content and maximum clay content to form another scenario, which was assumed to produce a high value of N_2O and NO flux for the grid cell. Thus PnET-N-DNDC ran twice with the two scenarios for each grid cell to produce an upper and a lower boundary of expected N_2O and NO emission rates (three times if the average scenario is included). The calculated N trace gas emission range was assumed to be wide enough to cover the real flux with a high probability. To verify the MSF method, we also implemented a Monte Carlo routine into the PnET-N-DNDC. This allowed us to directly quantify the uncertainties derived by soil heterogeneity

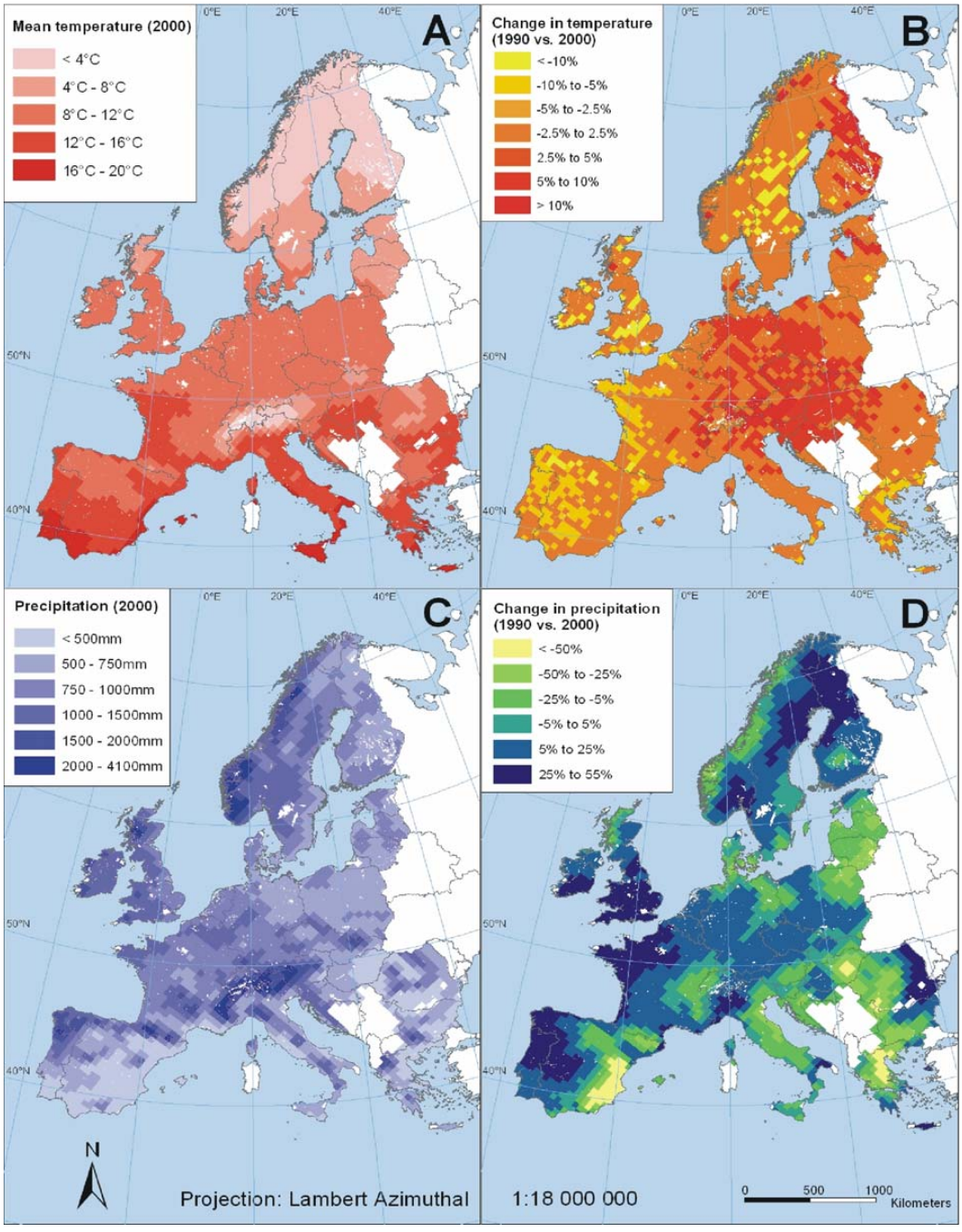

Fig. 3. Regional distribution of mean annual air temperature **(A)** and sum of annual precipitation **(C)** in the year 2000 across Europe. Panels **(B)** and **(D)** show the relative change in temperature or precipitation between the years 2000 and 1990. Meteorological data were provided by the Norwegian Meteorological Institute.

of individual EMEP grid cells (for details see Li et al., 2004). When PnET-N-DNDC ran in the Monte Carlo mode, the observed range for each soil factor in a grid cell was divided into eight intervals. For example, if the pH in a grid cell ranged from 3.5 to 5.6 the Monte Carlo approach would run with the pH values 3.5, 3.8, 4.1, 4.4 . . . , 5.6. PnET-N-DNDC selected randomly an interval of each of the six soil properties (clay content, organic mass in mineral soil and forest floor, forest floor and mineral soil pH, and stone content) to form a scenario. The process was repeated 5000 times so that 5000 N_2O and NO emission estimates were calculated for one grid cell. The results were then compared with the results

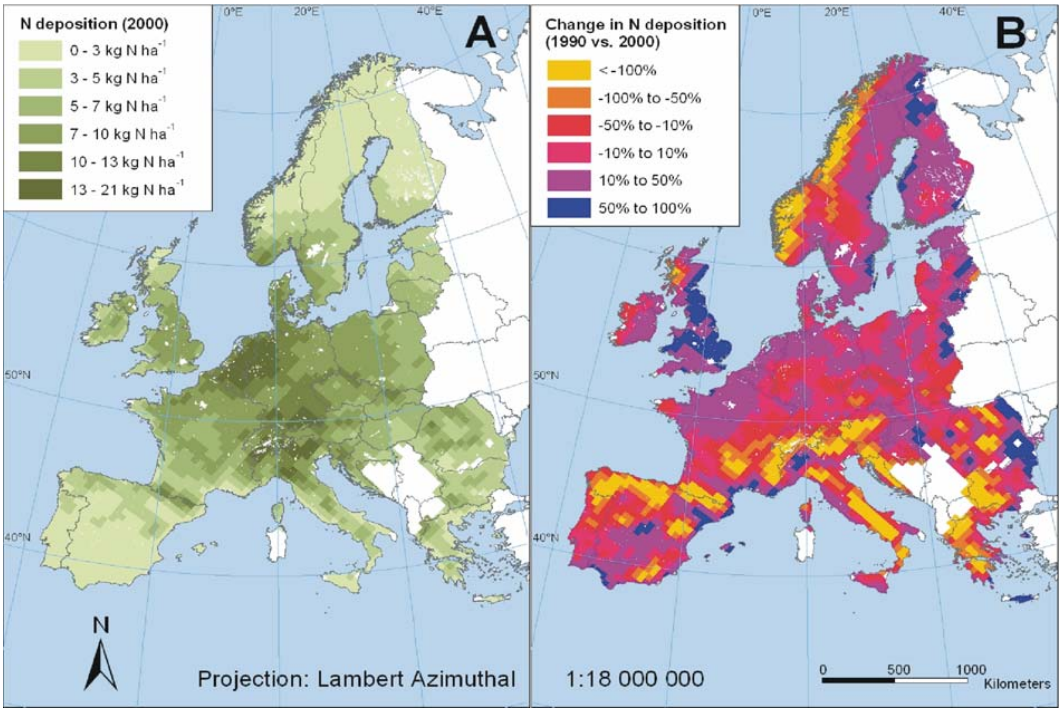

Fig. 4. Annual values of wet deposition of N in Europe in the year 2000 **(A)** and changes in wet deposition of N using 1990 meteorology versus 2000 meteorology (year 2000 emissions) **(B)**. Calculations with EMEP MSC-W Photo-oxidant model.

of the MSF method. For the Monte Carlo approach we selected randomly 50 EMEP grid cells across Europe and compared the results of the frequency distribution of N_2O and NO emissions with the ranges of N_2O and NO emissions as derived from the MSF method. The comparison of the MSF method with the Monte Carlo approach showed that the range of NO emissions calculated with the MSF method covered in average more than 79% of the variability in N trace gas emissions calculated with the Monte Carlo approach. However, this value was remarkably lower with regard to N_2O. The maximum N_2O emissions calculated with the MSF method were in average approx. 50% lower compared to the emissions using the Monte Carlo approach. The minimum N_2O emissions calculated with the MSF method were in average two fold higher than the N_2O emissions calculated with the Monte Carlo method. However, since the lower boundary of N_2O emissions ranged between 0.1 to 0.2 kg N ha^{-1} yr^{-1} this difference can be neglected for the purpose of this study. Due to the underestimation of maximum N trace gas emissions the uncertainty estimates with the MSF method are not fully satisfactory, but represent at present the best uncertainty estimate we can achieve. The full application of the Monte Carlo method (or of comparable methods) to all grid cells would be the favourable method to estimate prediction uncertainties. But for this a further optimisation of the model code with regard to the reduction of computation time is required.

Due to the lack of an uncertainty range for regional N deposition, the effect of this on N trace gas fluxes was not included in the uncertainty analysis. However, Fig. 5 shows on a site scale that variations in N deposition will significantly feedback on soil NO and N_2O fluxes even in one year simulation runs. I.e. increases in N deposition by e.g. 50% would increase simulated N_2O and NO fluxes at our 19 test sites by approx. 38% or 21% (Fig. 5).

3 Results

3.1 Model testing

The model was applied to the different field sites with identical and fixed internal parameter settings for microbial C and N turnover processes. Figure 6 shows daily simulation results for NO and N_2O emissions for the sites Höglwald (spruce, Germany), Sorø (beech, Denmark), Hyytiälä (Pine, Finland) and Glencorse (Sitka spruce, Scotland) as compared to observed N trace gas emissions. For the Höglwald spruce site simulated N_2O emissions were in average 23% higher than the observed emissions. Overestimation of N_2O emissions mainly occurred during the first of half of the year, whereas in autumn N_2O emissions tended to be underestimated in average by approx. 10–15%. The model captured the period with peak emissions in summer, but predicted the peak emission a few days earlier than observed in the field

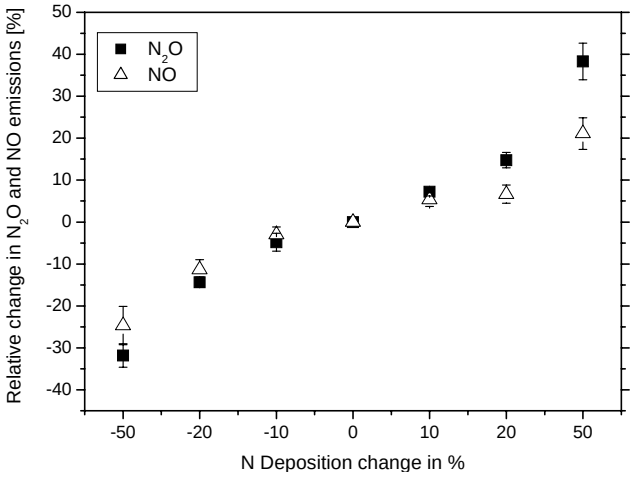

Fig. 5. Effect of changes in N deposition (−50%–+50%) on simulated N_2O and NO emissions at the 19 test sites. Given are mean values ±SE.

(Fig. 6). Simulated NO emissions for the Höglwald spruce site were in good agreement with field observations throughout the year with respect to seasonality and magnitude of fluxes. For most periods, except for three 1–2 week long periods in June, August and October, simulated results deviated only within 10–20% from observed NO emissions. However, in the short periods mentioned emissions were overestimated by a factor of two. The simulated seasonality of NO and N_2O emissions at the Höglwald site matched the seasonality as observed in the field, e.g. high NO emissions during summer versus comparably low emissions in the winter period (Fig. 6). Also the differences in magnitude of NO and N_2O emissions between both sites, which are mainly due to differences in litter quality and soil pH, were well reproduced by the model. The model also realistically predicted differences in the magnitude of N trace gas emissions for different field sites across Europe, i.e. low N_2O emissions in Hyytiälä and Glencorse, and slightly elevated N_2O emissions at Sorø. However, especially for the beech site at Sorø simulated emissions for the first few months of 2002 tended to be higher than field observations. This was mainly due to a simulation of elevated N_2O emissions during freezing-thawing events by the PnET-N-DNDC model, which were not confirmed during field measurements. However, for this period field measurements also revealed a pronounced spatial variability of N_2O emissions (Fig. 6). N_2O and sporadically performed NO emission measurements at the Hyytiälä site showed that N trace gas emissions are close to zero. A comparable result was also delivered by the PnET-N-DNDC model. For the Glencorse site the model captured the temporal variation in NO emissions during the summer period of 2002, but failed to predict the increase in NO emissions from the end of October onwards (Fig. 6). For the period during which NO field measurements had been performed the model underestimated NO emissions by approx. 30% (field mean: 4.9 g N ha^{-1} day^{-1}; simulation: 3.4 g N ha^{-1} day^{-1}).

Figures 7 and 8 and Tables 2 and 3 summarize results of model testing for all 19 field sites for which data from N trace gas emission measurements were available. The graph shows that the model was capable of capturing observed differences between high and low emitting sites, based on general information on soil and vegetation properties and by considering the local meteorological conditions. The relative variation between observed and simulated N_2O emissions was higher for sites with N trace gas emissions <3 g N ha^{-1} day^{-1} as compared to sites with N trace gas emissions >5 g N ha^{-1} day^{-1}. The linear regression of all simulated and observed mean N_2O emission rates resulted in r^2=0.68 (Fig. 7). On average over all test sites the model underestimated emissions by 24% (f(x)=0.76x). For NO the r^2 value was 0.78 (Fig. 8). Like in the case of N_2O the model also tended to underestimate NO emissions at the test sites by on average 27% (f(x)=0.73x). Given the wide range of complex processes involved in mediating soil N emissions, these results are very encouraging. These results of model testing for a wide variety of forest ecosystems across Europe (see also details in Tables 2 and 3) provided solid basis for the application of the PnET-N-DNDC model on a regional scale.

3.2 N_2O emissions from European forest soils

Figure 9a shows modelled N_2O emissions from forest soils across Europe resulting from the regional application of the GIS-coupled PnET-N-DNDC model. For the year 2000 simulated N_2O emissions from European forest soils ranged between 0.01 to 2.9 kg N ha^{-1} yr^{-1}. N_2O emissions >2.5 kg N ha^{-1} yr^{-1} were predicted for some forest ecosystems in the Netherlands. Simulated annual N_2O emissions for wide areas of Central Europe, West Spain, Slovakia and Romania were also found to be >1.0 kg N ha^{-1} yr^{-1}. Furthermore, high N_2O emissions were also predicted for soils with high amounts of organic carbon content in the forest floor in Southwest Finland and in the Northern parts of Sweden (1.0 to 1.8 kg N ha^{-1} yr^{-1}). Intermediate emissions in the range of 0.75 to 1.5 kg N ha^{-1} yr^{-1} were simulated for large parts of Poland and the Baltic states, whereas N_2O emissions <0.5 kg N ha^{-1} yr^{-1} were calculated for most Mediterranean and maritime regions including France and the UK, Ireland and Norway as well as large parts of central and northern Finland (Fig. 9a). The average N_2O emission of all forest sites across Europe calculated for the year 2000 was 0.58 kg N ha^{-1} yr^{-1} (Table 4). This average N_2O emission value changed only slightly when the model was initialized with the meteorological drivers for the years 1990 and 1995. For 1990 an average value of 0.62 kg N ha^{-1} yr^{-1} was calculated, whereas for 1995 the mean N_2O emission was 0.55 kg N ha^{-1} yr^{-1} (Table 4). However, on a regional scale the magnitude of N_2O emissions between individual years can change significantly, as shown in Fig. 9b. The

Table 2. Compilation of results for N_2O emissions from the different field sites as derived from model runs with PnET-N-DNDC and from field measurements.

Site-No.	Site-name	Year	Measuring days	Mean N_2O emission Measured	Simulated	Model performance R^2	RMSE
				$g\,N\,ha^{-1}\,day^{-1}$			$g\,N\,ha^{-1}\,day^{-1}$
1	Achenkirch	1998	18	4.0±0.6	2.3±0.4	0.48	2.55
2	Achenkirch	1999	19	2.4±0.5	2.3±0.4	0.37	1.74
3	Achenkirch	2002	122	1.1±0.1	2.9±0.1	0.00	2.43
4	Achenkirch	2003	194	0.8±0.1	3.0±0.1	0.11	2.88
5	Copenhagen	1992	17	2.3±0.5	0.5±0.1	0.02	2.88
8	Glencorse Sitka	2002	87	0.5±0.1	1.3±0.0	0.00	1.06
9	Glencorse Sitka	2003	122	0.2±0.0	0.6±0.2	0.00	0.70
10	Höglwald Beech	1994	105	2.7±0.1	7.6±0.5	0.47	6.39
11	Höglwald Beech	1995	341	10.0±0.5	11.3±0.4	0.11	9.19
12	Höglwald Beech	1996	307	18.2±1.0	15.7±0.8	0.42	13.63
13	Höglwald Beech	1997	348	5.5±0.3	9.6±0.3	0.09	7.91
14	Höglwald Beech	2002	103	2.3±0.2	1.6±0.2	0.20	2.87
15	Höglwald Beech	2003	158	3.9±0.3	7.6±0.4	0.22	5.74
16	Höglwald Spruce	1994	345	1.1±0.0	2.4±0.1	0.14	1.74
17	Höglwald Spruce	1995	359	2.1±0.1	2.8±0.9	0.01	1.92
18	Höglwald Spruce	1996	343	8.5±0.8	4.6±0.2	0.48	13.83
19	Höglwald Spruce	1997	346	1.8±0.2	2.3±0.1	0.44	2.38
20	Höglwald Spruce	2002	343	1.9±0.1	2.4±0.1	0.25	1.62
21	Höglwald Spruce	2003	340	1.0±0.1	2.0±0.5	0.27	1.41
22	Hyytiälä	2002	17	0.1±0.1	0.5±0.1	0.15	0.74
23	Hyytiälä	2003	11	0.2±0.0	0.2±0.1	0.26	0.27
24	Klausenleopoldsdorf	1996	16	6.6±1.0	3.8±0.4	0.41	4.20
25	Klausenleopoldsdorf	1997	21	5.2±1.1	3.1±0.5	0.69	4.08
26	Klausenleopoldsdorf	2002	119	1.9±0.2	3.1±0.2	0.00	2.68
27	Klausenleopoldsdorf	2003	178	1.5±0.1	3.8±0.1	0.04	3.11
28	Matrafüred Oak	2002	10	4.0±1.4	1.4±0.2	0.60	4.64
29	Matrafüred Oak	2003	27	6.6±0.8	5.3±0.5	0.00	4.91
30	Matrafüred Spruce	2002	11	4.8±1.5	0.4±0.2	0.28	6.71
31	Matrafüred Spruce	2003	28	4.8±0.7	1.3±0.1	0.29	4.97
32	P. Ticino BoscoNegri	2002	57	1.4±0.3	1.6±0.2	0.14	2.15
33	P. Ticino BoscoNegri	2003	177	0.5±0.0	1.2±0.1	0.10	1.02
34	P. Ticino Poplar	2002	48	0.5±0.2	1.0±0.1	0.04	1.38
35	P. Ticino Poplar	2003	17	0.7±0.2	0.6±0.1	0.11	0.92
36	San Rossore	2002	65	0.9±0.1	4.1±0.1	0.00	3.52
37	San Rossore	2003	183	0.2±0.0	2.1±0.1	0.14	2.21
38	Schottenwald	1996	16	15.9±2.8	9.0±1.2	0.19	11.85
39	Schottenwald	1997	21	13.4±3.3	8.3±1.1	0.66	12.43
40	Schottenwald	2002	162	11.4±0.9	8.0±0.3	0.05	11.98
41	Schottenwald	2003	252	9.8±0.5	6.4±0.2	0.00	9.29
42	Sorø	2002	19	2.4±0.5	1.7±0.2	0.04	2.18
43	Sorø	2003	156	1.5±0.1	2.5±0.1	0.21	1.70
44	Speulderbos	2002	107	0.8±0.1	1.8±0.1	0.28	1.19
45	Speulderbos	2003	216	0.4±0.0	2.7±0.1	0.32	2.51
46	Harvard Forest	1989	10	0.1±0.2	0.2±0.1	0.06	0.60
47	Wildbahn	1997	10	1.7±0.2	1.2±0.2	0.63	0.70
	Total		5971	4.2±0.1	4.7±0.1	0.51	6.50

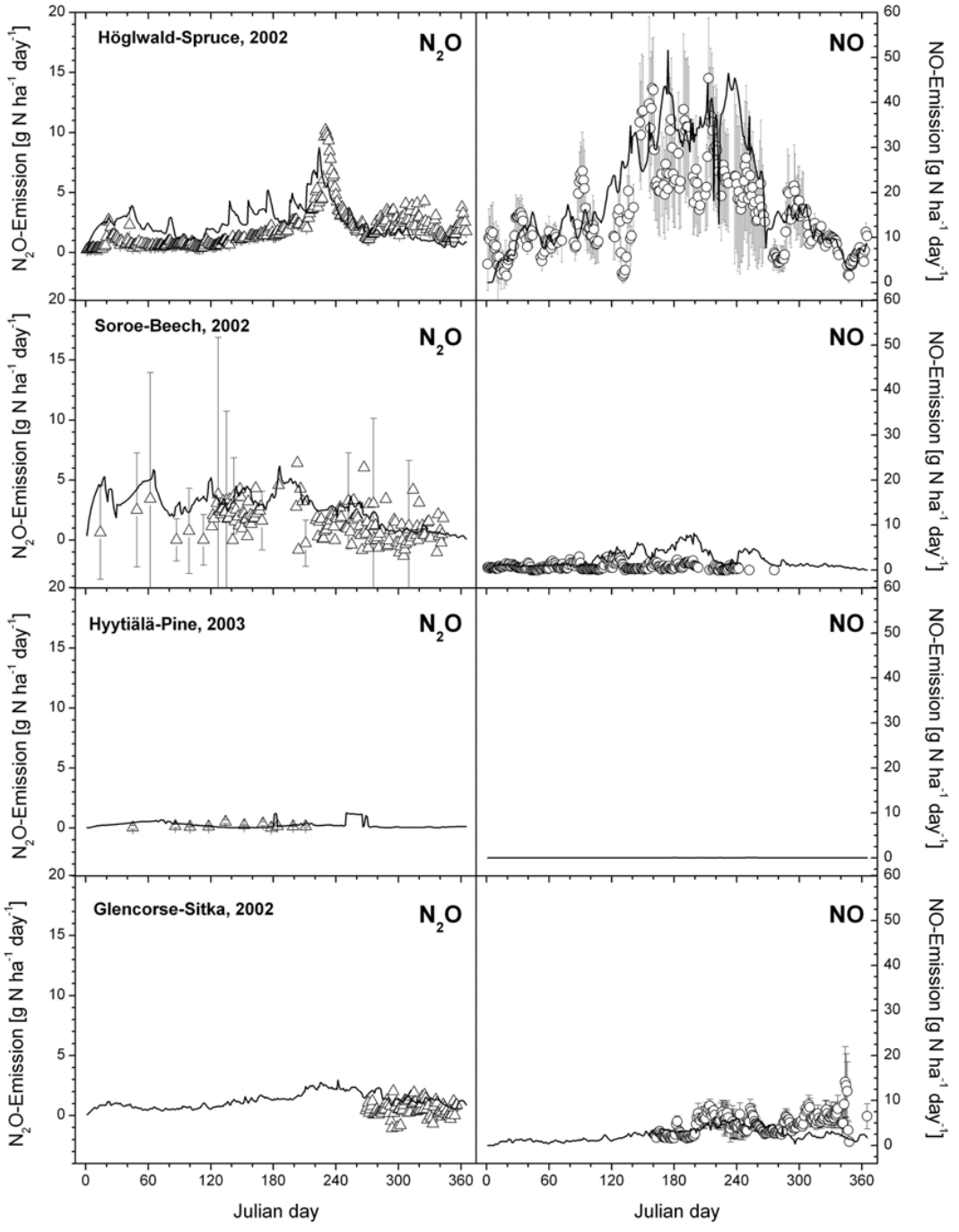

Fig. 6. Comparison of measured (triangles/circles) and simulated (solid line) N_2O and NO emissions for the forest sites Höglwald (spruce, Germany), Sorø (beech, Denmark), Hyytiälä (Pine, Finland) and Glencorse (Sitka spruce, Scotland). No measuring points are shown for NO fluxes at Hyytiälä since fluxes were always below the detection limit.

map shows that e.g. in the year 2000 the N_2O emissions from forest soils in Southern Sweden were >40% higher than in the year 1990, whereas in other areas such as the Mediterranean region N_2O emissions were 10 to >40% lower. Total N_2O emissions from forest soils across Europe for the years 1990, 1995 and 2000 were in a range of 77.6 to 86.8 kt N year^{-1} (Table 4). Due to their large forested areas Sweden and Finland contributed most to the total N_2O emissions (11.9 and 10.3 kt N yr^{-1}). However, on a per hectare basis forests in the Netherlands (1.26 kg N ha^{-1} yr^{-1}) and Romania (0.96 kg N ha^{-1} yr^{-1}) were found to be the strongest emitters (Table 4).

Table 3. Compilation of results for NO emissions from the different field sites as derived from model runs with PnET-N-DNDC and from field measurements.

Site-No.	Site-name	Year	Measuring days	Mean NO emission Measured	Simulated	Model performance R^2	RMSE
				g N ha^{-1} day^{-1}			g N ha^{-1} day^{-1}
3	Achenkirch	2002	93	0.2±0.0	3.1±0.1	0.00	3.26
4	Achenkirch	2003	153	0.1±0.0	3.6±0.2	0.01	4.33
6	Glencorse Birch	2002	197	−0.1±0.1	1.6±0.1	0.00	2.03
7	Glencorse Birch	2003	176	1.0±0.1	0.7±0.1	0.23	0.99
8	Glencorse Sitka	2002	182	4.9±0.2	3.4±0.1	0.00	3.01
9	Glencorse Sitka	2003	176	7.6±0.4	1.4±0.1	0.11	7.70
10	Höglwald Beech	1994	104	2.1±0.1	3.9±0.2	0.05	2.84
11	Höglwald Beech	1995	334	6.2±0.2	5.5±0.3	0.23	4.73
12	Höglwald Beech	1996	327	7.5±0.4	4.3±0.2	0.12	7.37
13	Höglwald Beech	1997	337	9.8±0.4	6.1±0.2	0.24	7.51
14	Höglwald Beech	2002	134	2.7±0.1	2.3±0.2	0.08	2.28
15	Höglwald Beech	2003	176	6.9±0.6	3.3±0.2	0.22	8.52
16	Höglwald Spruce	1994	357	17.5±0.5	20.7±0.7	0.57	9.02
17	Höglwald Spruce	1995	332	23.6±0.7	19.3±0.7	0.45	11.51
18	Höglwald Spruce	1996	349	24.9±1.0	16.1±0.7	0.41	16.32
19	Höglwald Spruce	1997	359	19.4±0.6	17.7±0.6	0.38	10.25
20	Höglwald Spruce	2002	277	15.4±0.6	19.4±0.8	0.53	9.47
21	Höglwald Spruce	2003	209	32.2±1.9	18.9±0.8	0.54	24.29
27	Klausenleopoldsdorf	2003	63	0.2±0.0	2.4±0.2	0.22	2.63
30	Matrafüred Spruce	2002	6	0.2±0.1	0.1±0.1	0.14	0.25
31	Matrafüred Spruce	2003	13	0.5±0.2	1.6±0.3	0.15	1.47
40	Schottenwald	2002	125	3.5±0.1	7.0±0.4	0.09	5.25
41	Schottenwald	2003	132	5.6±0.3	4.4±0.3	0.02	0.02
43	Sorø	2003	231	0.8±0.0	2.7±0.1	0.03	12.26
44	Speulderbos	2002	112	15.4±1.2	9.1±0.4	0.30	15.62
45	Speulderbos	2003	229	20.4±1.0	9.7±0.4	0.51	0.38
47	Wildbahn	1997	5	2.7±0.1	2.6±0.2	0.03	2.63
	Total		5191	11.7±0.2	9.5±0.2	0.70	9.90

3.3 NO emissions from European forest soils

Figure 9c shows the modelled NO emissions from forest soils across Europe for the year 2000. As for N_2O, the highest NO emissions were simulated for forest soils in the Netherlands and neighbouring areas in Belgium and Germany. The maximum NO emission for a grid cell in this area was 7.0 kg N ha^{-1} yr^{-1}. For forest soils in most parts of Germany, Belgium, Poland and the Massif Central in France, simulated NO emissions were in a range of 1.0 to 3.0 kg N ha^{-1} yr^{-1}. Furthermore, elevated NO emissions of up to 3.0 kg N ha^{-1} yr^{-1} were found for large areas of Sweden. This finding was mainly related to the low soil pH values usually found for forest soils in this region, causing a high NO production via chemo-denitrification in the model. Mostly low emissions of NO (<0.5 kg N ha^{-1} yr^{-1}) were simulated for forest soils in Norway, most of Finland and the Mediterranean region (Fig. 9c). The average NO emission from forest soils across Europe in the year 2000 was calculated to be 0.7 kg N ha^{-1} yr^{-1} and, thus, slightly higher than for N_2O (0.58 kg N ha^{-1} yr^{-1}). However, the average NO emission from forest soils varied only slightly between individual simulation years (1990: 0.7 kg N ha^{-1} yr^{-1}, 1995: 0.6 kg N ha^{-1} yr^{-1}) (Table 4). Total NO emission for all forests within the simulation area was 99.2 kt N in the year 2000 which was almost the same as in the year 1990 (98.3 kt N) and slightly lower than in the year 1995 with 84.9 kt N. The major contributors to total NO emissions from forest soils in Europe were Sweden and Germany (Table 4). The interannual variability in NO emissions due to changes in meteorological conditions was pronounced. Figure 9d shows relative changes in the NO emission strength of forest soils across Europe. The map shows that NO emissions were mostly higher in Central Europe and Northern Europe but lower in the Mediterranean Region for meteorology from the year 2000 as compared to using meteorology from the

Table 4. Average and total simulated N_2O and NO emissions from forest soils for individual European countries using meteorology for the years 1990, 1995 and 2000.

Country	Forested Area	1990				1995				2000			
		N_2O		NO		N_2O		NO		N_2O		NO	
	km^2	kg N $ha^{-1}\,yr^{-1}$	kt N yr^{-1}	kg N $ha^{-1}\,yr^{-1}$	kt N yr^{-1}	kg N $ha^{-1}\,yr^{-1}$	kt N yr^{-1}	kg N $ha^{-1}\,yr^{-1}$	kt N yr^{-1}	kg N $ha^{-1}\,yr^{-1}$	kt N yr^{-1}	kg N $ha^{-1}\,yr^{-1}$	kt N yr^{-1}
Andorra	232	0.70	1.6×10^{-2}	1.04	0.02	0.20	5.0×10^{-3}	0.28	6.6×10^{-3}	0.23	5.3×10^{-3}	0.36	8.4×10^{-3}
Austria	24 032	0.86	2.08	0.72	1.73	0.60	1.44	0.48	1.14	0.64	1.53	0.62	1.50
Belgium	7699	0.76	0.58	1.56	1.20	0.61	0.47	1.26	0.97	0.94	0.72	1.96	1.51
Bulgaria	28 494	0.95	2.71	0.80	2.27	0.58	1.64	0.64	1.82	0.70	1.99	0.56	1.61
Croatia	12 574	0.86	1.08	0.93	1.16	0.58	0.73	0.72	0.91	0.60	0.76	0.69	0.87
Czech. Republic	20 406	0.60	1.23	1.05	2.13	0.52	1.07	0.80	1.63	0.68	1.38	1.09	2.23
Denmark	18 608	0.58	1.08	0.85	1.58	0.48	0.90	0.68	1.26	0.70	1.30	0.94	1.75
Estonia	18 341	0.51	0.93	0.49	0.90	0.70	1.28	0.60	1.11	0.57	1.05	0.72	1.32
Finland	159 676	0.77	12.35	0.56	8.88	0.74	11.79	0.64	10.25	0.65	10.30	0.58	9.32
France	132 395	0.57	7.60	0.67	8.84	0.46	6.07	0.53	7.07	0.55	7.26	0.72	9.58
Germany	117 848	0.72	8.48	1.16	13.70	0.58	6.84	0.93	10.93	0.77	9.09	1.30	15.28
Gibraltar	0.43	0.55	2.4×10^{-5}	0.07	3.0×10^{-6}	0.54	2.3×10^{-5}	0.03	1.3×10^{-6}	0.55	2.4×10^{-6}	0.05	2.2×10^{-6}
Greece	30 676	0.68	2.09	0.45	1.38	0.53	1.64	0.36	1.11	0.55	1.68	0.35	1.07
Hungary	21 181	0.57	1.21	0.49	1.03	0.57	1.22	0.49	1.03	0.75	1.59	0.49	1.04
Irish Republic	5523	0.17	0.09	0.34	0.19	0.14	0.08	0.25	0.14	0.18	0.10	0.37	0.20
Italy	59 834	0.91	5.43	0.78	4.68	0.60	3.57	0.64	3.84	0.59	3.56	0.63	3.78
Latvia	28 229	0.42	1.19	0.72	2.04	0.74	2.08	0.74	2.08	0.73	2.07	0.79	2.24
Liechtenstein	89	0.87	7.7×10^{-3}	0.39	3.4×10^{-3}	0.97	8.6×10^{-3}	0.23	2.1×10^{-3}	0.77	6.8×10^{-3}	0.27	2.4×10^{-3}
Lithuania	18 843	0.63	0.55	0.43	0.82	0.43	0.81	0.42	0.79	0.53	1.01	0.52	0.98
Luxembourg	1032	0.29	0.07	0.98	0.10	0.53	0.05	0.84	0.09	0.64	0.07	1.09	0.11
Monaco	0.21	0.21	4.3×10^{-6}	0.12	2.5×10^{-6}	0.26	5.4×10^{-6}	0.22	4.7×10^{-6}	0.26	5.5×10^{-6}	0.16	3.3×10^{-6}
Netherlands	8271	0.99	0.82	2.39	1.98	0.77	0.64	1.84	1.52	1.26	1.04	3.01	2.49
Norway	159 482	0.19	2.99	0.05	0.86	0.23	3.62	0.04	0.63	0.17	2.69	0.05	0.72
Poland	76 358	0.52	4.00	1.10	8.37	0.50	3.79	0.87	6.65	0.59	4.53	1.06	8.06
Portugal	32 713	0.39	1.26	0.20	0.66	0.38	1.26	0.13	0.42	0.36	1.18	0.10	0.33
Romania	41 284	0.85	3.50	0.76	3.13	0.60	2.49	0.68	2.80	0.96	3.95	0.70	2.88
San Marino	0.35	0.27	9.4×10^{-6}	0.31	1.1×10^{-5}	0.28	9.8×10^{-6}	0.31	1.1×10^{-5}	0.30	1.0×10^{-5}	0.26	9.1×10^{-6}
Slovakia	9162	0.70	0.64	0.83	0.76	0.74	0.67	0.67	0.61	0.94	0.86	0.87	0.80
Slovenia	7881	1.14	0.90	1.30	1.02	0.67	0.52	0.87	0.69	0.82	0.65	1.10	0.87
Spain	138 484	0.65	8.97	0.37	5.19	0.60	8.36	0.29	3.98	0.57	7.94	0.27	3.80
Sweden	196 236	0.68	13.43	1.14	22.33	0.68	13.34	1.03	20.20	0.61	11.94	1.19	23.27
Switzerland	12 407	0.81	1.01	0.54	0.67	0.54	0.67	0.33	0.41	0.60	0.75	0.47	0.58
United Kingdom	22 481	0.22	0.49	0.33	0.75	0.24	0.53	0.35	0.80	0.27	0.60	0.44	0.99
Sum	1 410 477		86.78		98.37		77.59		84.89		81.59		99.20
Average		0.62		0.70		0.55		0.60		0.58		0.70	

year 1990.

Figure 10 shows the calculated NO: N_2O emission ratio for EU forests. The figure shows that for Central Europe and most of Sweden simulated NO emissions are dominating over N_2O emissions, whereas in other parts of Scandinavia, UK and South/ South East Europe N_2O emissions dominate over NO emissions. In our model simulation the NO: N_2O ratio was significantly correlated with the soil parameters SOC (r=0.129), mineral soil pH (r=−0.360) and atmospheric N deposition (r=0.356). However, all these correlations are rather weak.

3.4 Uncertainty estimates

Using the Most Sensitive Factor (MSF) method, which was re-evaluated prior to its use with a Monte Carlo approach (see Sect. 2.5), we calculated for each grid cell a minimum and a maximum scenario for the emission strength of N_2O and NO from forest soils. The cumulative sum for the minimum and the maximum scenarios as well as the results from the "average" scenario for the years 1990, 1995 and 2000 are given in Table 5. The table shows that e.g. in the year 2000 model initialisation with mean values for all grid cells resulted in a total N_2O emission from forest soils of 81.6 kt N yr^{-1}. The range of uncertainty for this respective year was 50.7 to 96.9 kt N yr^{-1}, which is equivalent to a relative range of −40 to +16% as compared to the average scenario. The uncertainty for the prediction of NO emissions was significantly higher as compared to N_2O. Here, we calculated a total NO emission of 99.2 kt N yr^{-1} (year 2000) for the average scenario with a range of uncertainty of 44.3 to 254.0 kt N yr^{-1}. The relative range as compared to the mean value thus equals to −66 to +156%. These remarkable differences in the uncertainty ranges between modelled N_2O and NO emissions were found to be mainly due to the pH sensitivity of NO production via chemo-denitrification.

Table 5. Range of uncertainty for calculated total N_2O and NO emissions from forest soils across Europe. The uncertainty ranges were calculated by use of the Most Sensitive Factor method (Li et al., 2004).

Meteorology Year	N_2O emission (kt N yr^{-1}) Minimum Scenario	Average Scenario	Maximum Scenario
1990	55.1	86.8	100.3
1995	50.0	77.6	96.2
2000	50.7	81.6	96.9
Meteorology Year	**NO emission (kt N yr^{-1}) Minimum Scenario**	**Average Scenario**	**Maximum Scenario**
1990	44.6	98.4	247.8
1995	38.3	84.9	220.2
2000	44.4	99.2	254.0

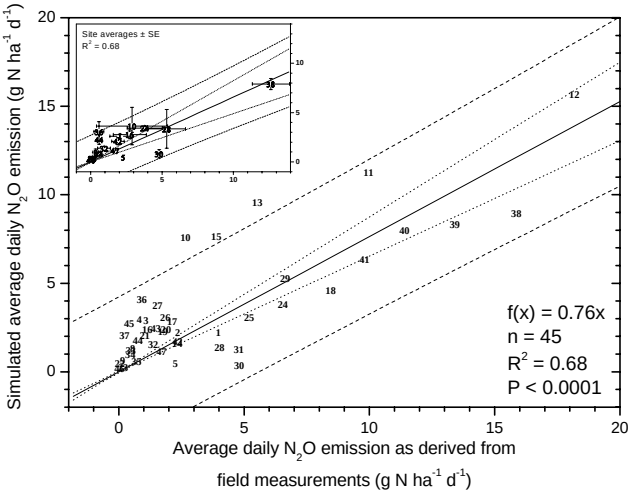

Fig. 7. Comparison of measured and simulated average daily N_2O emissions for different forest sites across Europe. The numbers refer to the individual sites and observation years as listed in Table 2. Regression line (solid line), 95% confidence limits for the slope (short dashes), and 95% prediction limits (long dashes) are provided.

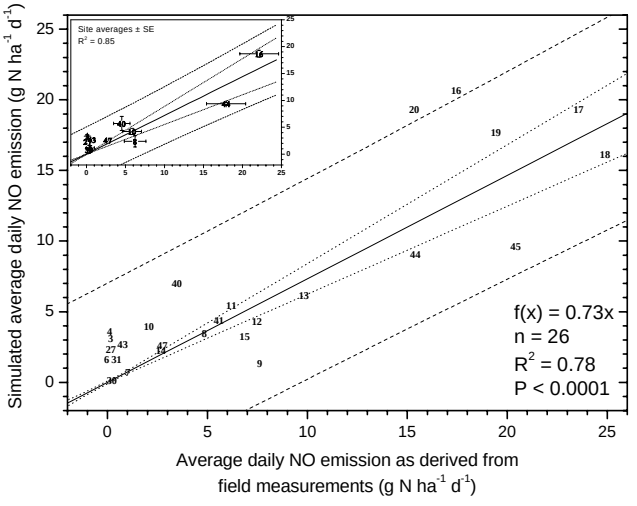

Fig. 8. Comparison of measured and simulated average daily NO emissions for different forest sites across Europe. The numbers refer to the individual sites and observation years as listed in Table 3. Regression line (solid line), 95% confidence limits for the slope (short dashes), and 95% prediction limits (long dashes) are provided.

4 Discussion

GIS coupled biogeochemical models have recently been used in a number of studies for the calculation of regional or global inventories of N_2O and NO emissions from soils (e.g. Potter et al., 1996; Davidson et al., 1998; Butterbach-Bahl et al., 2001, 2004; Brown et al., 2002; Li et al., 2001, 2004). This approach has several advantages as compared to a pure statistical approach where single or a series of field measurements at one or several site(s) are extrapolated to larger regions. Advanced biogeochemical models summarize our current understanding of environmental factors which are affecting the magnitude of trace gas emissions from soils such as meteorological conditions, soil properties (pH, SOC, texture) or – if turning especially to agricultural soils – management practices. In a series of studies all these factors have been shown to largely influence the production, consumption and emission of N trace gases (e.g. Barnard and Leadley, 2005; Conrad, 2002). By using biogeochemical models in inventory studies one assumes that the complexity of processes involved in N trace gas emissions and interacting factors, which is the main reason for the widely observed spatial and temporal variability in emissions, will at least partly be mimicked by the models (Li et al., 2000, 2001). In this paper we provided evidence that the PnET-N-DNDC model is indeed a powerful and reliable tool to simulate N trace gas

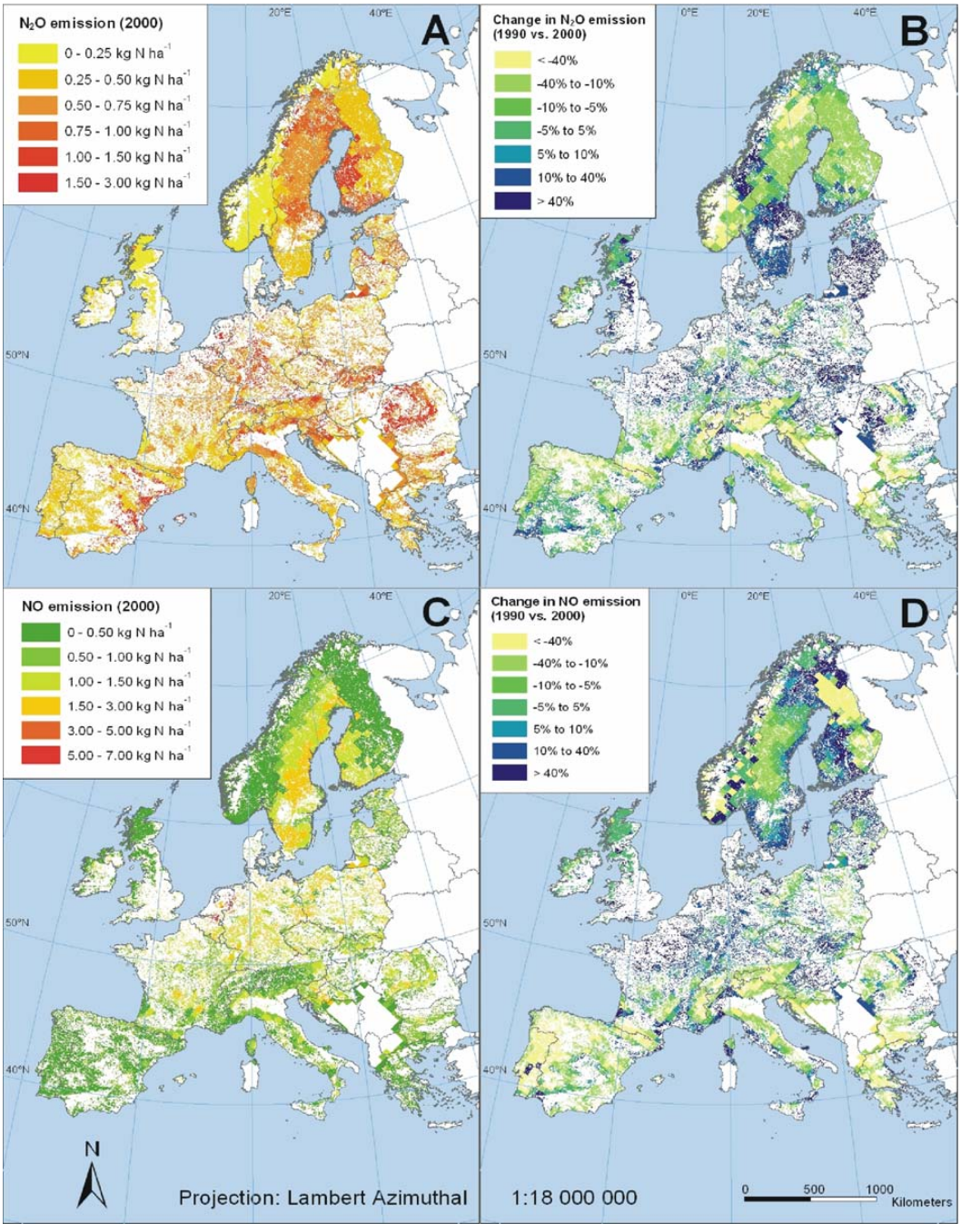

Fig. 9. Regional distribution of annual N_2O **(A)** and NO emissions **(C)** from forest soils in Europe (in kg N ha^{-1} yr^{-1}). Panels **(B)** and **(D)** show relative changes in the N_2O (B) or NO (D) emission strength if meteorological data for the year 2000 were exchanged with those of the year 1990.

emissions from forest soils. The application of the model to a range of field sites showed that the model can reproduce observed differences in N trace gas fluxes. The model was able to explain 68% of the site variability for N_2O and even 78% of the site variability for NO. However, the detailed site evaluation also showed that the model is still far from perfect, e.g. with regard to the timing of peak emissions or the magnitude of the seasonality of N trace gas emissions (see e.g. Fig. 6 and Tables 2 and 3). Further improvement requires a better understanding and parameterisation of the microbial N turnover processes, especially with regard to denitrification with an emphasis on the ratio of N_2 to N_2O

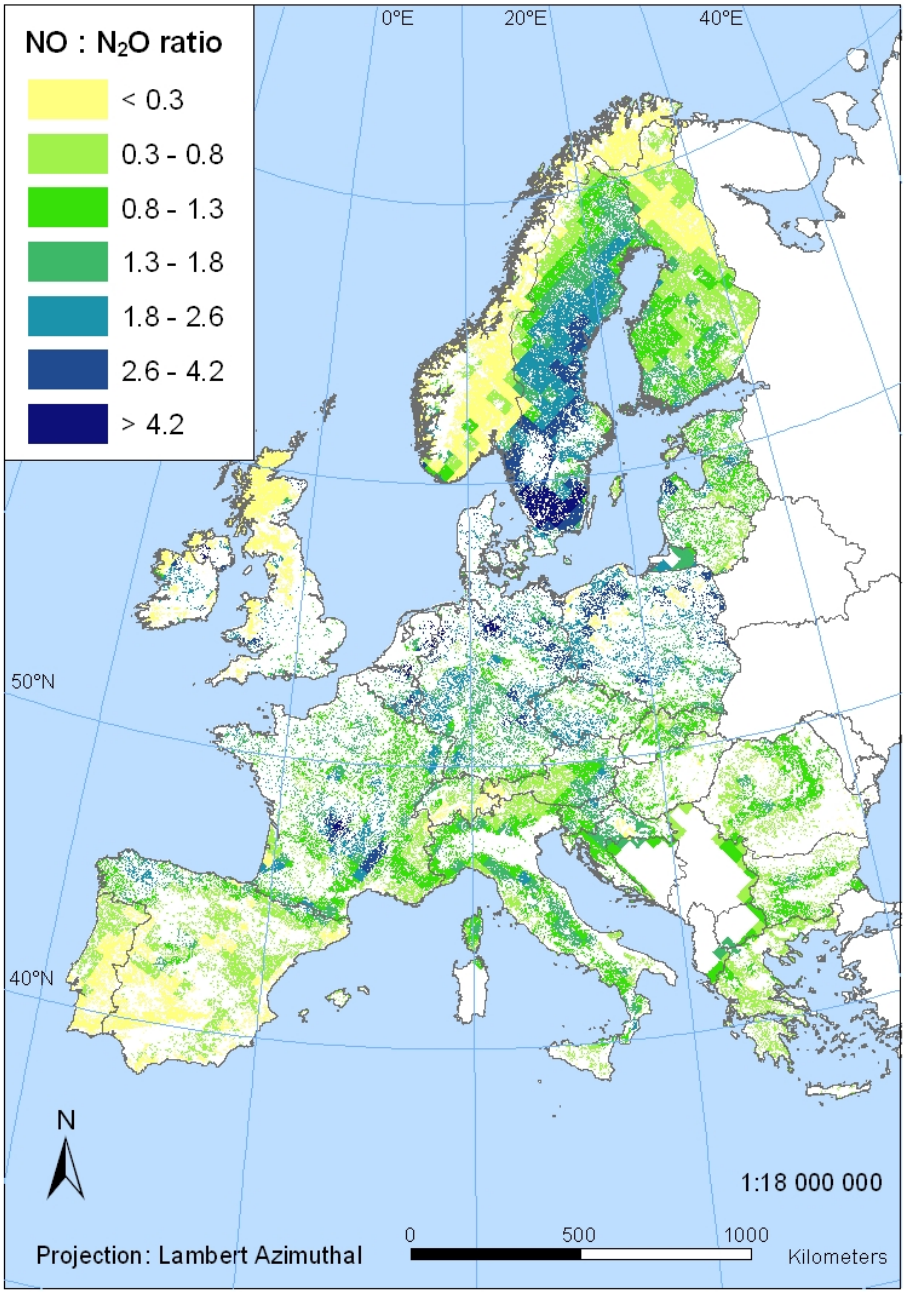

Fig. 10. Regional distribution of a NO to N_2O emission ratio from forest soils in Europe for the year 2000.

production. Furthermore, also the mechanistic description of the dynamics of plant N uptake versus microbial N uptake remains a challenge, since our understanding of the competition between the plant and microbial communities for N is still limited (Rennenberg et al., 1998). Also, more detailed site specifications such as the changes in soil properties with soil depth or the hydrological condition of a site in relation to its landscape position (e.g. with regard to the distance to the groundwater or occurrence of interflow) would further improve the basis for the simulation results. On the other hand this would require a further extension of the list of initializing and driving parameters and thus would strongly reduce the applicability of such a model on a regional basis due to the restricted availability of such data on a regional scale.

One can still find arguments that biogeochemical models such as the PnET-N-DNDC model are over-parameterised and that one may produce comparable results with more simple empirical approaches. However, due to the still limited number of field measurements and the observed importance of meteorological conditions and soil properties for the

magnitude of N trace gas emissions from soils a pure empirical approach is unlikely to work. Furthermore, empirical models can only be used for the range for which they have been validated, whereas in theory biogeochemical models can also be used as predicting tools e.g. for sites with significant different site properties as the one for which the model was tested.

There still remains an argument with regard to the availability and quality of GIS information for initializing and driving complex models. In view of e.g. the spatial inhomogeneity of soil properties and the sensitivity of the PnET-N-DNDC model to changes in e.g. SOC or soil pH (Stange et al., 2000) the uncertainty about the regional distribution of these parameters results in a significant increase of the prediction error. In this study we addressed this problem on a regional scale with the Most Sensitive Factor (MSF) method (Li et al., 2004) and with a Monte Carlo approach for selected grid cells across Europe. By this we were able to produce an uncertainty range, which most probably covers the mean N trace gas emission of a given grid cell.

4.1 N_2O emissions

In our study we estimated that total average N_2O emissions from forest soils across Europe in the years 1990, 1995 and 2000 were in the range of 77.6 to 81.6 kt N yr^{-1}. The respective uncertainty range – as calculated with the MSF method by Li et al. (2004) – is 50 to 100 kt N yr^{-1}. Furthermore, we calculated that the average N_2O emission per ha forest soil and year was 0.55 to 0.62 kg N ha^{-1} yr^{-1}, with elevated emissions in Central Europe and Western Spain but also in parts of Scandinavia where soils with high organic C content in the forest floor are found. Lower emissions were calculated for the UK and some boreal forest areas. Based on a literature review by Brumme et al. (2005) N_2O emissions from boreal forests ranged between 0.1 and 0.3 kg N ha^{-1} yr^{-1}. For most forested areas in Norway, Finland and Sweden our simulation results are in line with this estimate. However, especially for those areas in Scandinavia and the Baltic States for which elevated C stocks in the forest floor are reported, considerably higher N_2O emissions with values >0.75 kg N ha^{-1} were calculated. The estimate by Brumme et al. (2005) was mainly based on N_2O emission measurements from mineral soils in the boreal region (e.g. Martikainen, 1996), whereas estimates in other recent publications, in which N_2O emissions in the boreal zone from forest soils rich in humus were reported (von Arnold et al., 2005; Maljanen et al. 2001, 2003), resulted in annual N_2O emission rates in the range of 1.0 to 10.0 kg N ha^{-1} yr^{-1}. The highest N_2O emissions from boreal forest soils have been reported from peat soils, which have been used for agriculture prior to forestation (Maljanen et al., 2003). In the contrary, nutrient poor organic forest soils have been reported to emit negligible amounts of N_2O to the atmosphere (Regina et al., 1996). The huge discrepancy between both estimates is obvious and cannot be further clarified at present. We only can assume that C-rich soils from former peatlands, which have widely been drained in Fennoscandia for improving forest growth (Paavilainen and Päivänen, 1995) are indeed a stronger source for atmospheric N_2O than other soils poorer in C content in this area. In agreement with field studies, also other modelling studies dealing with effects of management practices such as no-till on N_2O emissions from agricultural soils, show that the magnitude of N_2O emissions is most likely positively correlated with SOC (Six et al., 2004; Li et al., 2005). However, further field studies on soils, differing in SOC but also in the ratio of C:N, are needed to further evaluate this interrelation and to proof the model algorithms and predictions.

N_2O emission measurements from temperate forest soils in Europe have been reported to vary substantially over a wide range from 0 to 20 kg N ha^{-1} yr^{-1} (see e.g. data compilation by Papen and Butterbach-Bahl, 1999) with a mean range of 0.2 to 2.0 kg N ha^{-1} yr^{-1}. The variability in the emission strength was found to be influenced by soil properties such SOC, pH, N deposition and forest stand properties (e.g. Papen and Butterbach-Bahl, 1999; Brumme et al., 1999; Zechmeister-Boltenstern et al., 2002; Jungkunst et al., 2004). Furthermore, the occurrence of high winter N_2O emissions during freezing and thawing events was acknowledged as a major factor determining the magnitude of annual N_2O emissions (Butterbach-Bahl et al., 2002b; Teepe and Ludwig, 2004). To reduce the uncertainty in estimates of N_2O emissions from temperate forest ecosystems different approaches from empirical based stratifications (Brumme et al., 1999) towards the use of process-oriented models (Butterbach-Bahl et al., 2001, 2004) have been followed. Using a stratification approach in combination with functions for N_2O production in dependency from soil water content and temperature, Schulte-Bisping and Brumme (2003) estimated that the average N_2O emission from forest soils in Germany is 0.32 kg N_2O N ha^{-1} yr^{-1}. This estimate may represent the lower boundary of emissions since neither N deposition effects nor freezing-thawing events were considered in this approach (Schulte-Bisping and Brumme, 2003). Both of these factors were considered in the studies by Butterbach-Bahl et al. (2001, 2004) who used an older version of the PnET-N-DNDC model for estimating the regional emission strength of forest soils in South Germany and Saxony. Their estimate of a mean annual N_2O emission of approx. 2 kg N ha^{-1} yr^{-1} is significantly higher than the one of Schulte-Bisping and Brumme (2003). It is also higher than estimates calculated with the recent version of PnET-N-DNDC for Germany as presented in this paper (0.6 to 0.8 kg N ha^{-1} yr^{-1}, see Table 4), which is partly due to a) an improved parameterisation of processes in the new model which was based on laboratory studies (Schindlbacher et al., 2004; Kesik et al., 2005[1]), b) the aggregation of site information on the EMEP grid (50 km by 50 km) raster instead of defined polygons as in the earlier studies, and c) different simulation years.

With regard to the Mediterranean region only limited information about the magnitude of N_2O emissions from soils is available (see review by Butterbach-Bahl and Kiese, 2005). The few publications available show that forest soils in this area can even function as sinks for atmospheric N_2O (Rosenkranz et al., 2005). Except for parts of Eastern Spain also our model calculated low estimates of N_2O emissions in the Mediterranean region (<0.5 kg N m^{-2} yr^{-1}), which was largely due to a model-intrinsic limitation of microbial N turnover processes by water stress.

4.2 NO emissions

NO emissions from forest soils across Europe in the years 1990, 1995 and 2000 were calculated to be in the range of 84.9 to 98.4 kt N yr^{-1} and, thus, approx. 10% higher than for N_2O. The range of uncertainty as calculated with the MSF method is 38.3 to 254.0 kt N yr^{-1}. Using either a methodology based on Skiba et al. (1997) or Davidson and Kingerlee (1997), Simpson et al. (1999) estimated NO emissions from soils covered with natural or semi-natural vegetation in Europe. By applying the Skiba et al. (1997) methodology excluding Russia, Ukraine and the former Yugoslavia the authors came up with an estimated NO emission of approx. 20 kt N yr^{-1} from forest soils across Europe. The respective range for the Davidson and Kingerlee methodology was 10 to 300 kt N yr^{-1} (Simpson et al., 1999). The differences in the magnitude of estimated NO emissions from forest soils in Europe between the Skiba et al. (1997) methodology as applied in Simpson et al. (1999) and our approach is mainly due to the intended simplicity of the Skiba et al. (1997) methodology which mainly considers temperature and N input to natural systems as parameters for estimating soil bound NO emissions but neglects effects of texture, SOC or pH.

The simulated average NO emission per ha forest soil was 0.6 to 0.7 kg N ha^{-1} yr^{-1}, which is in agreement with estimated average NO emissions from forest soils in the Southeastern United States (Davidson et al., 1998). In our study the highest emissions of NO from forest soils (>3 kg N ha^{-1} yr^{-1}) were simulated for highly N-affected forest areas in the Benelux states and Northern Germany, which is in accordance with field observations by Van Dijk and Duyzer (1999), who reported average NO emissions >6 kg N ha^{-1} yr^{-1} for beech and Douglas fir forests exposed to an atmospheric N deposition of approx. 40 kg N ha^{-1} yr^{-1} at Speulderbos, Netherlands. The latter results were also confirmed by measurements within the NOFRETETE project. Also for the Höglwald region in Southern Germany, for which long-term measurements of NO emissions from beech and spruce forests are available (Gasche and Papen, 1999; Butterbach-Bahl et al., 2002b) simulated emissions are in accordance with field observations. For the respective grid cell we simulated an average emission of 1.5 to 3.0 kg N ha^{-1} yr^{-1}, which is lower than the observed NO emissions from the spruce site of the Höglwald Forest (>6 kg N ha^{-1} yr^{-1}), but in agreement with observed average NO emissions from the beech site (approx. 2.8 kg N ha^{-1} yr^{-1}) (Butterbach-Bahl et al., 2002b). The relatively minor discrepancies are only due to differences in scale, since in our approach generalized information for the 50 km by 50 km grid cell was used, e.g. with regard to soil properties or atmospheric N deposition. However, for large forest areas in Sweden also NO emissions in a range of 1.5 to 3.0 kg N were calculated (Fig. 9c), that are not confirmed by any measurements at present. Johansson (1984) who carried out measurements in forests close to Stockholm found that NO emissions from unfertilized forest soils were lower than 0.1 kg N ha^{-1} yr^{-1}. One still can argue that the differences in scales make it difficult to compare the results, but by studying the reasons why simulated NO emissions in large parts of Sweden were elevated we found that this was mainly due to increased NO production via chemo-denitrification. Since the mechanisms in the PnET-N-DNDC model which are dealing with NO production via chemo-denitrification are in accordance with results from laboratory and field studies (e.g. van Cleemput and Baert, 1984; Gasche and Papen, 1999; Kesik et al., 2005[1]), the main reason for such a discrepancy may be due to an underestimation of NO consumption in the model. At present the model only considers that NO can be consumed by denitrification, but in soil incubation studies it was shown that also oxidative NO consumption may significantly contribute to NO consumptions especially in soils rich in SOC (Dunfields and Knowles, 1997). However, since the mechanistic basis of oxidative NO consumption is not well described at present this process is still not included in the model. A further reason for the discrepancy between observed and simulated NO emissions for parts of Scandinavia may be due to differences in soil properties which were used in our model simulations as compared to those found in the individual studies. The soil pH at the sites where Johansson (1984) carried out his measurements was 4.0 or 4.5, respectively. But the soil information derived from the Soil Geographical Data Base of Europe and used in the present work revealed that the soil pH in most parts of Scandinavia is <4.0 (see Fig. 2d), i.e. at a level where chemo-denitrification in the PnET-N-DNDC model is active (Li et al., 2000). Furthermore, in our model approach we do not consider the microsite variability of soil pH. It has been shown in several studies that e.g. in acid forest soils the soil pH can vary on a microsite scale for up to 3 pH units (e.g. Häussling et al., 1985; Strong et al., 1997; Bruelheide and Udelhoven, 2005). If nitrite production by e.g. nitrification would mainly be associated with the higher pH microsites and if one would disregard transport and other consumption except chemo-denitrification, the model would certainly overestimate NO production by chemo-denitrification. For the given reasons, there is a need to develop algorithms which are addressing microsite variability of soil pH in future model versions.

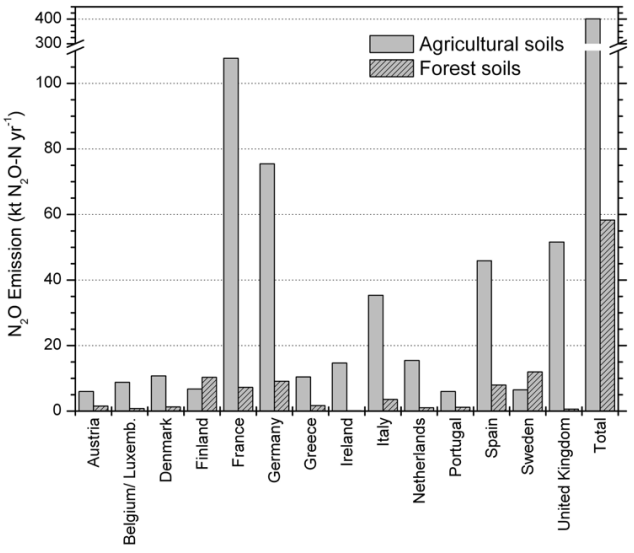

Fig. 11. Comparison of total direct N_2O emissions from agricultural soils (data for the year 1996 by Boeckx and van Cleemput, 2001) and of N_2O emissions from forest soils (data for the year 2000, this paper) for the EU15 countries.

4.3 Relevance of N trace gas emissions from forests soils in Europe as compared to other sources

Fertilized agricultural soils are assumed to be the predominant source for atmospheric N_2O. Boeckx and Van Cleemput (2001) evaluated the emission of N_2O from agricultural soils in Europe using the IPCC methodology (Mosier et al., 1998). They estimated that the average direct N_2O emission from agricultural soils across Europe is 5.6 kg N $ha^{-1}\,yr^{-1}$. Somewhat lower numbers where calculated by Freibauer and Kaltschmitt (2003) who considered besides the amount of N fertilization also climatic, soil and management factors for the calculation of their estimate. For agricultural, minerotrophic soils for the temperate and sub-boreal climate regions in Europe they came up with an average emission of 2.0 kg N $ha^{-1}\,yr^{-1}$. This means that agricultural soils are approx. a four to ten-fold stronger source for N_2O as compared to forest soils, where the average emission was calculated to be in a range of 0.55 to 0.62 kg N $ha^{-1}\,yr^{-1}$. However, if the total N_2O emissions for each land use type for different countries are calculated, the importance of forest soils as sources for atmospheric N_2O becomes evident. Using our approach and the estimates by Boeckx and Van Cleemput (2001) the emission strength of forest soils for N_2O is on average 14.5% of the emission strength of agricultural soils in Europe (Fig. 11).

Pyrogenic emissions are the dominating source for atmospheric NO_x in Europe. Using estimates of Vestreng et al. (2004), total pyrogenic emissions for our simulation area in the year 2000 would amount to approx. 10 000 kt N yr^{-1}. Our calculations for NO emissions from forest soils using meteorology for the years 1990, 1995 and 2000 was in the range of 85 to 99 kt N yr^{-1}, which is <1% of the pyrogenic NO_x emissions. Using a temperature function developed by Williams et al. (1992), Stohl et al. (1996) estimated that emissions of NO from all soils including forest, grassland and arable soils, to be only 1.6% of total pyrogenic emissions. Simpson et al. (1999) presented calculations of soil-NO emissions with a range of methods (a modified version of Skiba et al., 1997; BEIS-2 – from Novak and Pierce, 1993; Yienger and Levy, 1995; Davidson and Kingerly, 1997) accounting in some of these for N inputs from atmospheric N deposition or fertilizer. The range of estimates was very large. Using the Davidson and Kingerly methodology to derive an upper and lower boundary, with the extreme assumptions of no N affected forest, or 100% N-affected forest, yielded a range of 13 to 350 kt N yr^{-1} for forests. Compared to the approaches documented in Simpson et al. (1999), the PnET-N-DNDC approach as presented here is by far more complicate but with sounder physical basis, since it considers besides temperature and N availability also the effect of e.g. soil pH, moisture or texture on NO emissions from forest soils.

It needs to be noted that the NO once emitted from the soil underlies rapid oxidation to NO_2 in the presence of O_3. E.g. Rummel et al. (2002) showed, that during daytime up to 90% of the NO emitted from the soil may get converted to NO_2 within the trunk space and canopy of forests by the reaction of NO with O_3, which is transported from above the canopy by turbulence. NO_2 can be re-deposited to plant or soil surfaces or metabolised by plant tissues (Meixner, 1994; Ludwig et al., 2001; Sparks et al., 2001), so that the amount of NO and NO_2 (summarized as NO_x, i.e. NO+NO_2) finally emitted to the atmosphere at the canopy level may get strongly reduced. For tall vegetation covers such as forests, the so called canopy reduction factor for NO_x emissions is correspondingly estimated to be in the order of 50% (Jacob and Bakwin, 1991; Yienger and Levy, 1992; Ganzefeld et al., 2002).

5 Conclusions

The GIS-coupled process-oriented model PnET-N-DNDC, which was tested prior to its regional use on a large field data set, was used for the calculation of inventories of N_2O and NO emissions from forests soils in Europe. The results demonstrate that forest soils are a significant source of N_2O in Europe. With regard to NO forest soils only contribute <1.0% to total NO_x emissions in Europe. This number may even be lower if deposition processes of NO_x in the canopy are considered (canopy reduction). However, due to the seasonality of NO emissions the relative contribution of NO emissions from forest soils to total NO_x emissions can be larger during the vegetation period and can be of importance especially in rural areas. After a thorough validation of the

model against field observations and an extensive sensitivity analysis of the model performance, we conclude that the PnET-N-DNDC performs very well simulating NO and N_2O emissions from European forest soils. This work demonstrates that GIS-coupled process-oriented models are valuable tools to realistically estimate biogenic N trace gas emissions from soils. From our point of view this is the most comprehensive effort to date to simulate NO and N_2O emissions from European forest soils.

Acknowledgements. The work was funded by the European Commission in the NOFRETETE project (EVK2-CT2001-00106) of the fifth framework program.

Edited by: F. X. Meixner

References

Aber, J. D., Nadelhoffer, K. J., Steudler, P., and Melillo, J. M.: Nitrogen saturation in northern forest ecosystems, BioScience, 39, 378–386, 1989.

Aber, J. D. and Federer, C. A.: A generalized, lumped-parameter model of photosynthesis, evaporation and net primary production in temperate and boreal forest ecosystems, Oecologia, 92, 463–474, 1992.

Ambus, P. and Christensen, S.: Spatial and seasonal nitrous oxide and methane fluxes in Danish forest-, grassland-, and agroecosystems, J. Environ. Qual., 24(5), 993–1001, 1995.

Barnard, R., Leadley, P. W., and Hungate, B. A.: Global change, nitrification and denitrification: a review, Global Biogeochem. Cycl., 19, B1007, doi:10.1029/2004GB002282, 2005.

Boeckx, P. and Van Cleemput, O.: Estimates of N_2O and CH_4 fluxes from agricultural lands in various regions in Europe, Nutr. Cycl. Agroecosys., 60, 35–47, 2001.

Böß, A.: Quantifizierung der gasförmigen Stickstoffverluste (N_2, N_2O) aus Böden unterschiedlich stickstoffbelasteter Kiefernwald-Ökosystemen im Norddeutschen Tiefland, Diploma thesis at the University Trier, Institute of Geography, 2000.

Bowden, R. D., Melillo, J. M., Steudler, P. A., and Aber, J. D.: Effects of nitrogen additions on annual nitrous oxide fluxes from temperate forest soils in the Northeastern United States, J. Geophys. Res., 96, 9321–9328, 1991.

Brown, L., Syed, B., Jarvis, S. C., Sneath, R. W., Phillips, V. R., Goulding, K. W. T., and Li, C.: Development and application of a mechanistic model to estimate emission of nitrous oxide from UK agriculture, Atmos. Environ., 36, 917–928, 2002.

Bruelheide, H., and Udelhoven, P.: Correspondence of the fine-scale spatial variation in soil chemistry and the herb layer vegetation in beech forests, Forest Ecol. Managem., 210, 205–223, 2005.

Brumme, R. and Beese, F.: Effects of liming and nitrogen fertilization on emissions of CO_2 and N_2O from a temperate forest, J. Geophys. Res., 97, 12 851–12 858, 1992.

Brumme, R., Borken, W., and Finke, S.: Hierarchical control on nitrous oxide emission in forest ecosystems, Global Biogeochem. Cycl., 13, 1137–1148, 1999.

Brumme, R., Verchot, L. V., Martikainen, P. J., and Potter, C. S.: Contribution of trace gases nitrous oxide (N_2O) and methane (CH_4) to the atmospheric warming balance of forest biomes, in: The Carbon Balance of Forest Biomes, edited by: Griffiths, H. and Jarvis, P.G., Taylor & Francis Group, Oxon, New York, p. 293–318, 2005.

Butterbach-Bahl, K., Gasche, R., Huber, C., Kreutzer, K., and Papen, H.: Impact of N-input by wet deposition on N-trace gas fluxes and CH_4-oxidation in spruce forest ecosystems of the temperate zone in Europe, Atmos. Environ., 32, 559–564, 1998.

Butterbach-Bahl, K., Stange, F., Papen, H., and Li, C.: Regional inventory of nitric oxide and nitrous oxide emissions for forest soils of Southeast Germany using the biogeochemical model PnET-N-DNDC, J. Geophys. Res., 106, 34 155–34 166, 2001.

Butterbach-Bahl, K., Breuer, L., Gasche, R., Willibald, G., and Papen, H.: Exchange of trace gases between soils and the atmosphere in Scots pine forest ecosystems of the North Eastern German Lowlands, 1. Fluxes of N_2O, NO/NO_2 and CH_4 at forest sites with different N-deposition, Forest Ecol. Manag., 167, 123–134, 2002a.

Butterbach-Bahl, K., Willibald, G., Papen, H., and Gasche, R.: Exchange of N-gases at the spruce and beech sites at the Höglwald Forest – A summary, Plant Soil, 240, 117–123, 2002b.

Butterbach-Bahl, K., Kesik, M., Miehle, P., Papen, H., and Li, C.: Quantifying the regional source strength of N-trace gases across agricultural and forest ecosystems with process based models, Plant Soil, 260, 311–329, 2004.

Butterbach-Bahl, K. and Kiese, R.: Significance of forests as sources for N_2O and NO, in: Tree species effects on soils: implications for global change edited by: Binkley, D. and Menyailo, O., Springer, Netherlands, p. 173–191, 2005.

CEC: Soil map of European Communities at 1:1 000 000. CEC-DGVI, Brussels, Belgium, 124 pp., 1985.

CEC: Corine Landcover, Technical Guide, Luxembourg, 1994.

Conrad, R.: Soil microorganisms as controllers of atmospheric trace gases (H_2, CO, CH_4, OCS, N_2O and NO), Microbiol. Rev., 60, 609–640, 1996.

Conrad, R.: Microbiological and biochemical background of production and consumption of NO and N_2O in soil, in: Trace Gas Exchange in Forest Ecosystems, edited by: Gasche, R., Papen, H. and Rennenberg, H., p. 3–33, Kluwer Academic Publishers, Dordrecht, Boston, London, 2002.

Davidson, E. A. and Kingerlee, W.: A global inventory of nitric oxide emissions from soils, Nutr. Cycl. Agroecosys., 48, 37–50, 1997.

Davidson, E. A., Potter, C. S., Schlesinger, P., and Klooster, S. A.: Model estimates of regional nitric oxide emissions from soils of the southeastern United States, Ecol. Appl., 8(3), 748–759, 1998.

Dorsey, J. R., Duyzer, J. H., Gallagher, M. W., Coe, H., Pilegaard, K., Westrate, J. H., Jensen, N. O. and Walton, S.: Oxidized nitrogen and ozone interaction with forests. I: Experimental observations and analysis of exchange with Douglas fir, Q. J. R. Meteorol. Sci., 130, 1941–1955, 2004.

Dunfield, P. F., and Knowles, R.: Biological oxidation of nitric oxide in a humisol., Biol. Fertil. Soils, 24, 294-300, 1997.

Duyzer, J. H. and Fowler, D.: Modeling land atmosphere exchange of gaseous oxides of nitrogen in Europe, Tellus, 46B, 353–372, 1994.

Fagerli, H., Simpson, D., and Aas, W.: Model performance for sulphur and nitrogen compounds for the period 1980 to 2000, in: Transboundary acidification, eutrophication and ground level

ozone in Europe, EMEP Status Report 1/2003, Part II: Unified EMEP model Performance, edited by: Tarrason, L., The Norwegian Meteorological Institute, Oslo, Norway, 1–66, 2003.

Freibauer, A. and Kaltschmitt, M.: Controls and models for estimating direct nitrous oxide emissions from temperate and sub-boreal agricultural mineral soils in Europe, Biogeochem., 63, 93–115, 2003.

Galloway, J. N., Dentener, F. J., Capone, D. G., Boyer, E. W., Howarth, R. W., Seitzinger, S. P., Asner, G. P., Cleveland, C. C., Green, P. A., Holland, E. A., Karl, D. M., Michaels, A. F., Porter, J. H., Townsend, A. R., and Vörösmarty, C. J.: Nitrogen cycles: past, present and future, Biogeochemistry, 70, 153–226, 2004.

Ganzeveld, L. N., Lelieveld, J., Dentener, F. J., Krol, M. C., Bouwman, A. J., and Roelofs, G. J.: Global soil-biogenic NO_x emissions and the role of canopy processes, J. Geophys. Res., 107, 1, doi:10.1029/2001JD001289, 2002.

Gasche, R. and Papen, H.: A 3-year continuous record of nitrogen trace gas fluxes from untreated and limed soil of a N-saturated spruce and beech forest ecosystem in Germany: 2. NO and NO_2 fluxes, J. Geophys. Res., 104, 18 505–18 520, 1999.

Gessler, A., Rienks, M., and Rennenberg, H.: Stomatal uptake and cuticular adsorption contribute to dry deposition of NH_3 and NO_2 to needles of adult spruce (*Picea abies*) trees, New Phytol., 156, 179–194, 2001.

Göttlein, A. and Kreutzer, K.: The Höglwald experimental site as compared to other ecological field studies, Forstwiss. Forsch., 39, 22–29, 1991.

Goodale C. L., Aber, J. D., and Farrell, E. P.: Predicting the relative sensitivity of forest production in Ireland to site quality and climate change, Climate Res., 10(1), 51–67, 1998.

Häussling, M., Leisen, E., Marschner, H., and Römheld, V.: An improved method for non-destructive measurements of the pH at the root-soil interface (rhizosphere), J. Plant. Physiol. 117, 371–375, 1985.

IPCC, Intergovernmental Panel on Climate Change, Climate Change 2001: The Scientific Basis. Contribution of Working Group I to the Third Assessment Report of the Intergovernmental Panel on Climate Change, edited by: Houghton, J. T., Ding, Y., Griggs, D. J., Noguer, M., van der Linden, P. J., Dai, X., Maskell, K., and Johnson, C. A., 881 pp., Cambridge University Press, Cambridge, United Kingdom and New York, USA, 2001.

Jacob, D. J. and Bakwin, P. S.: Cycling of NO_x in tropical forest canopies and its implications for the global source of biogenic NO_x to the atmosphere, in: Microbial Production and Consumption of Greenhouse Gases, edited by: Rogers, J. E. and Whitman, W. B., American Soc. Microbiol., Washington, D.C., p. 237–253, 1991.

Jandl, R., Kopezki, H., and Glatzel, G.: Effect of a dense *Allium ursinum* (L.) ground cover on nutrient dynamics and mesofauna of *Fagus sylvatica* (L.) woodland, Plant Soil, 189, 245–255, 1997.

Johansson, C.: Field measurements of emission of nitric oxide from fertilized and unfertilized forest soils in Sweden. J. Atmos. Chem., 1, 429–442, 1984.

Jungkunst, H., Fiedler, S., and Stahr, K.: N_2O emissions of a mature Norway spruce (Picea abies) stand in the Black Forest (southwest Germany) as differentiated by the soil pattern, J. Geophys. Res,. 109, doi:10.1029/2003JD004344, 2004.

Kiese, R., Li, C., Hilbert, D. W., Papen, H., and Butterbach-Bahl, K.: Regional application of PnET-N-DNDC for estimating the N_2O source strength of tropical rainforests in the Wet Tropics of Australia, Global Change Biol., 11(1), 128–144, 2005.

Köble R. and Seufert G.: Novel maps for forest tree species in Europe, Proceedings of the 8th European Symposium on the Physico-Chemical Behaviour of Air Pollutants: "A Changing Atmosphere!", Torino (It), 17–20 September 2001.

Li, C., Frolking, S., and Frolking, T. A.: A model of nitrous oxide evolution from soil driven by rainfall events: 1. Model structure and sensitivity, J. Geophys. Res., 97, 9759–9776,1992.

Li, C., Narayanan, V., and Harris, R.: Model estimates of nitrous oxide emissions from agricultural lands in the United States, Global Biogeochem. Cycl., 10, 297–306, 1996.

Li, C.: Modeling trace gas emissions from agricultural ecosystems, Nutr. Cycl. Agroecos., 58, 259–276, 2000.

Li, C., Aber, J., Stange, F., Butterbach-Bahl, K., and Papen, H.: A process oriented model of N_2O and NO emissions from forest soils: 1. Model development, J. Geophys. Res., 105, 4369–4384, 2000.

Li, C., Zhuang, Y., Cao, M., Crill, P., Dai, Z., Frolking, S., Moore, B., Salas, W., Song, W., and Wang, X.: Comparing a process-based agro-ecosystem model to the IPCC methodology for developing a national inventory of N_2O emissions from arable lands in China, Nutr. Cycl. Agroecosys., 60, 159–175, 2001.

Li, C., Mosier, A., Wassmann, R., Cai, Z., Zheng, X., Huang, Y., Tsuruta, H., Boonjawat, J., and Lantin, R.: Modeling greenhouse gas emissions from rice-based production systems: Sensitivity and upscaling, Global Biogeochem. Cycl., 18, 1, doi:10.1019/2003GB002045, 2004.

Li, C., Frolking, S., and Butterbach-Bahl, K.: Carbon Sequestration can increase nitrous oxide emissions, Climatic Change, 72, 321–338, 2005.

Ludwig, A., Meixner, F. X., Vogel, B, and Förstner, J.: Soil-air exchange of nitric oxide: An overview of processes, environmental factors, and modelling studies, Biogeochemistry, 52, 225–257, 2001.

Maljanen, M., Hytönen, J., and Martikainen P. J.: Fluxes of N_2O, CH_4 and CO_2 on afforested boreal agricultural soils, Plant Soil, 231, 113–121, 2001.

Maljanen, M., Liikanen, A., Silvola, J., and Martikainen, P. J.: Nitrous oxide emissions from boreal organic soil under different land-use, Soil Biol. Biochem., 35, 1–12, 2003.

Martikainen, P. J.: Microbial processes in boreal forest soils as affected by forest management practices and atmospheric stress, in: Soil Biochemistry, edited by: Stotzky, G. and Bollag, J. M., Dekker Ic., NY, p. 195–232, 1996.

Meixner, F. X.: Surface exchange of odd nitrogen oxides, Nova Acta Leopold., NF70, 299–348, 1994.

Mosier, A. R., Kroeze, C., Nevison, C., Oenema, O., Seitzinger, S., and Van Cleemput, O.: Closing the global N_2O budget: nitrous oxide emission through the agricultural nitrogen cycle, Nutr. Cycl. Agroecosys., 52, 225–248, 1998.

Mücher, C. A.: Pan-European Land Cover Mapping (PELCOM) project. Development of a consistent methodology to derive land-cover information on a European scale from remote sensing for environmental modelling, 299 p., 2000.

Novak, J. H. and Pierce, T. E.: Natural emissions of oxidant precursors, Water, air, and soil pollution, 67, 57–77, 1993.

Paavilainen, E. and Päivänen, J.: Peatland forestry –ecology and

principles, Ecological Studies, 111, 248 p., Springer, Berlin, 1995.

Papen, H. and Butterbach-Bahl, K.: A 3-year continuous record of nitrogen trace gas fluxes from untreated and limed soil of a N-saturated spruce and beech forest ecosystem in Germany. 1. N_2O emissions, J. Geophys. Res., 104, 18 487–18 503, 1999.

Pilegaard, K., Hummelshøj, P., and Jensen, N. O.: Nitric oxide emission from a Norway spruce forest floor, J. Geophys. Res., 104, 3433–3445, 1999.

Potter, C. S., Matson, P. A., Vitousek, P. M., and Davidson, E. A.: Process modeling of controls on nitrogen trace gas emissions from soils worldwide, J. Geophys. Res., 101, 1361–1377, 1996.

Regina, K., Nykänen, H., Silvola, J., and Martikainen, P.: Fluxes of nitrous oxide from boreal peatlands as affected by peatland type, water table level and nitrification capacity, Biogeochem., 35, 401–418, 1996.

Rennenberg, H., Kreutzer, K., Papen, H., and Weber, P.: Consequences of high loads of nitrogen for spruce (*Picea abies*) and beech (*Fagus sylvatica*) Forests, New Phytol., 139, 71–86, 1998.

Rosenkranz, P., Brüggemann, N., Papen, H., Xu, Z., Seufert, G., and Butterbach-Bahl, K.: Microbial N turnover and N_2O, NO and CH_4 exchange in a Mediterranean pine forest, Biogeosciences Discuss., 2, 673–702, 2005,
SRef-ID: 1810-6285/bgd/2005-2-673.

Rummel, U., Ammann, C., Gut, A., Meixner, F. X., and Andreae, M. O.: Eddy covariance measurements of nitric oxide flux within an Amazonian rain forest, J. Geophys. Res., 107, 8057, doi:10.1029/2001JD000520, 2002.

Sandnes-Lenschow, H. and Tsyro, S.: Meteorological input data for EMEP/MSC-W air pollution models, EMEP MSC-W Note 2/2000, The Norwegian Meteorological Institute, Oslo, Norway, 2000.

Schindlbacher, A., Zechmeister-Boltenstern, S., and Butterbach-Bahl, K.: Effects of soil moisture and temperature on NO, NO_2 and N_2O emissions from forest soils, J. Geophys. Res., 109, D17302, 17 302–17 309, 2004.

Schmidt, J., Seiler, W., and Conrad, R.: Emission of nitrous oxide from temperate forest soils into the atmosphere, J. Atmos. Chem., 6, 95–115, 1988.

Schulte-Bisping, H. and Brumme, R.: Nitrous oxide inventory of German forest soils, J. Geophys. Res., 108, D4132, 148–227, 2003.

Simpson, D., Fagerli, H., Jonson, J. E., Tsyro, S., Wind, P., and Tuovinen, J.-P.: The EMEP Unifed Eulerian Model. Model Description. EMEP MSC-W Report 1/2003, The Norwegian Meteorological Institute, Oslo, Norway, 2003.

Simpson, D., Winiwarter, W., Börjesson, G., Cinderby, S., Ferreiro, A., Guenther, A., Hewitt, C. N., Janson, R., Khalil, M. A. K., Owen, S., Pierce, T. E., Puxbaum, H., Shearer, M., Skiba, U., Steinbrecher, R., Tarrason, L., and Öquist, M. G.: Inventorying emissions from nature in Europe, J. Geophys. Res., 104, 8113–8152, 1999.

Six, J., Ogle, S. M., Breidt, F. J., Conant, R. T., Mosier, A. R., and Paustian, K.: The potential to mitigate global warming with no-tillage management is only realized when practiced in the long term, Global Change Biol., 10, 155–160, 2004.

Skiba, U., Fowler, D., and Smith, K. A.: Emissions of NO and N_2O from soils, Environ. Mon. Assess., 31, 153–158, 1994.

Skiba, U., Fowler, D., and Smith, K. A.: Nitric oxide emissions from agricultural soils in temperate and tropical climates: source, controls and mitigation options, Nutr. Cycl. Agroecosys., 48, 139–153, 1997.

Sparks, J. P., Monson, R. K., Sparks, K. L., and Lerdau, M.: Leaf uptake of nitrogen dioxide (NO_2) in a tropical wet forest: implications for tropospheric chemistry, Oecologia, 127, 214–221, 2001.

Stange, F.: Entwicklung und Anwendung eines prozeßorientierten Modells zur Beschreibung der N_2O und NO-Emissionen aus Böden temperater Wälder. Dissertation at the Albert-Ludwigs-Universität Freiburg, Freiburg, Germany, 2000.

Stange, F., Butterbach-Bahl, K., and Papen, H.: A process-oriented model of N_2O and NO emissions from forest soils, 2. Sensitivity analysis and validation, J. Geophys. Res., 105, 4385–4398, 2000.

Stohl, A., Williams, E., Wotawa, G., and Kromp-Kolb, H.: A European inventory of soil nitric oxide emissions and the effect of theses emissions on the photochemical formation of ozone, Atmos. Environ., 30(22), 3741–3755, 1996.

Strong, D. T., Sale, P. W. G., and Helyar, K. R.: Initial soil pH affects the pH at which nitrification ceases due to self-induced acidification of microbial microsites, Austral. J. Soil Res., 35(3), 565–570, 1997.

Teepe, R. and Ludwig, B.: Variability of CO_2 and N_2O emissions during freeze-thaw cycles: results of model experiments on undisturbed forest-soil cores, J. Plant Nutr. Soil Sci., 167, 153–159, 2004.

UN-ECE: International Co-operative Programme on Assessment and Monitoring of Air Pollution Effects on Forests. Manual on methods and criteria for harmonized sampling, assessment, monitoring and analysis of the effects of air pollution on forests (http://www.icp-forests.org), 1998.

Van Cleemput, O. and Baert, L.: Nitrite: A key compound in N loss processes under acid conditions?, Plant Soil, 76, 233–241, 1984.

Van Dijk, S. M. and Duyzer, J. H.: Nitric oxide emissions from forest soils, J. Geophys. Res., 104, 15 955–15 961, 1999.

Vestreng, V., Adams, M, and Goodwin, J.: Inventory Review 2004. Emission Data reported to CLRTAP and under the NEC Directive, EMEP/EEA Joint Review Report, Tech. Report, EMEP-MSCW Report 1/2004, The Norwegian Meteorological Institute, Oslo, Norway, 2004.

Von Arnold, K., Nilsson, M., Hånell, B., Weslien, P., and Kledtsson, L.: Fluxes of CO_2, CH_4 and N_2O from drained organic soils in deciduous forests, Soil Biol. Biochem., 37, 1059–1071, 2005.

Westling, O., Fagerli, H., Hellsten, S., Knulst, J. C., and Simpson, D.: Comparison of modelled and monitored deposition fluxes of sulphur and nitrogen to ICP-forest sites in Europe, Biogeosciences Discuss., 2, 933–975, 2005,
SRef-ID: 1810-6285/bgd/2005-2-933.

Williams, E. J., Hutchinson, G. L., and Fehsenfeld, F. C.: NO_x and N_2O emissions from soil, Global Biogeochem. Cycl., 6, 351–388, 1992.

Yienger, J. J. and Levy, H.: Empirical model of global soil-biogenic NO_x emissions, J. Geophys. Res., 100, 11 447–11 464, 1995.

Zechmeister-Boltenstern, S., Hahn, M., Meger, S., and Jandl, R.: Nitrous oxide emissions and nitrate leaching in relation to microbial biomass dynamics in a beech forest soil, Soil Biol. Biochem., 34, 823–832, 2002.

JOURNAL OF GEOPHYSICAL RESEARCH, VOL. 111, G02018, doi:10.1029/2005JG000115, 2006

Future scenarios of N_2O and NO emissions from European forest soils

Magda Kesik,[1] Nicolas Brüggemann,[1] Renate Forkel,[1] Ralf Kiese,[1] Richard Knoche,[1] Changsheng Li,[2] Guenther Seufert,[3] David Simpson,[4] and Klaus Butterbach-Bahl[1]

Received 26 October 2005; revised 10 February 2006; accepted 2 March 2006; published 15 June 2006.

[1] In this study we investigated possible feedbacks of predicted future climate change on forest soil NO and N_2O emissions in Europe. For this we used two climate scenarios, one representing a 10-year period of present-day climate (1991–2000) and a 9-year period for future climate conditions (2031–2039). The climate scenarios were used to drive the GIS-coupled biogeochemical model Photosynthesis-Evapotranspiration-Model–Denitrification-Decomposition-Model (PnET-N-DNDC), which has currently been tested for its predicting capability for soil N trace gas emissions for various sites across Europe. The model results show a complex, spatially differentiated pattern of changes in future N_2O and NO emissions from the forest soils across Europe, which were driven by the combined effect of changes in precipitation and temperature. Overall, the model predicted that N_2O emissions from the European forest soils will on average decrease by 6%. This decrease was mainly due to the shift in N_2O:N_2 ratio driven by enhanced denitrification. NO emissions were found to increase by 9%. The increases in NO emissions were mainly due to increases in temperature. Only for the regions where soil moisture was predicted to markedly increase or suffer from water stress during the vegetation period, a reduction of NO emissions was simulated. The simulations show the possibility and feasibility for assessing climate change feedbacks on biogenic N trace gas emissions from soils at a regional scale.

Citation: Kesik, M., N. Brüggemann, R. Forkel, R. Kiese, R. Knoche, C. Li, G. Seufert, D. W. Simpson, and K. Butterbach-Bahl (2006), Future scenarios of N_2O and NO emissions from European forest soils, *J. Geophys. Res.*, *111*, G02018, doi:10.1029/2005JG000115.

1. Introduction

[2] Nitrous oxide (N_2O) and nitric oxide (NO) are atmospheric trace gases, which are of importance for atmospheric chemistry and global warming [e.g., *Cicerone*, 1987]. The main sink for N_2O is its stratospheric destruction by photolysis to NO. For that reason N_2O is also involved in stratospheric ozone chemistry [*Crutzen*, 1976, 1995]. N_2O is also an important greenhouse gas, and its globally averaged surface abundance was 314 ppb in 1998 [*Intergovernmental Panel on Climate Change* (*IPCC*), 2001]. In view of its atmospheric increase of about 0.3% per year and of its atmospheric life time of about 150 years [*Khalil and Rasmussen*, 1992] it can be expected that the contribution of N_2O to global warming will further increase in the future. Approximately two thirds of the sources of atmospheric N_2O and approximately one third of tropospheric NO are linked to the biogenic processes of nitrification and denitrification [*IPCC*, 2001; *Davidson and Kingerlee*, 1997], two key processes of global nitrogen turnover driven by microbes. Here soils play a dominant role as habitats for these microbes. Besides agricultural soils, the source strength of which is estimated to be approximately 3.3 Tg N yr^{-1} or 20% of total atmospheric N_2O sources [*IPCC*, 2001], forest soils have been identified as significant sources for atmospheric N_2O and NO [*Potter et al.*, 1996; *IPCC*, 2001], and NO [e.g., *Potter et al.*, 1996; *Pilegaard et al.*, 1999]. *Kesik et al.* [2005] estimated that forest soils in Europe emit approximately 82 kilotonnes (kt) N_2O per year (94 kt NO yr^{-1}), which is approximately 15% of the N_2O source strength of agricultural soils in Europe [*Boeckx and Van Cleemput*, 2001]. This relatively high contribution of forest soils, which cover approximately 22% of the simulated land area of Europe, to total N_2O emissions is at least partly a result of chronically high rates of atmospheric N deposition to formerly N limited forest ecosystems in Europe [e.g., *Brumme and Beese*, 1992; *Butterbach-Bahl et al.*, 2002]. Recent research has shown that the increased availability of N in temperate forest ecosystems has stimulated soil N_2O and NO emissions [e.g., *Butterbach-Bahl et al.*, 1997; *Van*

[1]Institute for Meteorology and Climate Research, Atmospheric Environmental Research (IMK-IFU), Karlsruhe Research Center, Garmisch-Partenkirchen, Germany.
[2]Complex Systems Research Center, Institute for the Study of Earth, Oceans and Space, University of New Hampshire, Durham, New Hampshire, USA.
[3]Institute for Environment and Sustainability, Joint Research Centre, Ispra, Italy.
[4]Norwegian Meteorology Institute, Oslo, Norway.

0148-0227/06/2005JG000115$09.00

Dijk and Duyzer, 1999; *Zechmeister-Boltenstern et al.*, 2002].

[3] Like all biogenic processes, the microbial processes of nitrification and denitrification vary highly in magnitude with variations of environmental conditions. Soil temperature and soil moisture have been identified as major drivers on hourly to interannual timescales for observed temporal changes of N_2O and NO emissions from forest soils [e.g., *Firestone and Davidson*, 1989; *Gasche and Papen*, 1999; *Butterbach-Bahl et al.*, 2004a]. The effect of temperature for soil NO and N_2O emissions is mostly direct. With increase in temperature, enzyme kinetics and thus metabolic turnover rates of nitrifiers and denitrifiers will increase up to an optimum at approximately 30°–35°C [*Granli and Bøckmann*, 1994]. In contrast to temperature the effect of soil moisture is mostly indirect. Soil moisture largely effects the rate of O_2 diffusion into the soil profile and thus also determines if a soil is predominantly aerobic or anaerobic [*Smith*, 1980]. The oxygen status of the soil determines whether the aerobic process of nitrification or the anaerobic process of denitrification predominates. Although both processes can produce NO as well as N_2O, production of N_2O by denitrification can be more pronounced, since loss rates of N_2O during the denitrification process are higher than during the nitrification process. Nitrification was identified as the dominating microbial production process for NO production [*Conrad*, 2002]. For the given reasons the optimum soil moisture for NO emissions is lower (approximately 50% water filled pore space) than for N_2O emissions (approximately 60–65% WFPS). At soil moisture values >70–80%, N_2O emissions will be strongly reduced, since N_2O in the soil profile will be further reduced to N_2 [*Davidson et al.*, 2000]. However, under certain environmental conditions (e.g., high soil nitrate concentration), N_2O instead of N_2 can be the end product of denitrification [e.g., *Firestone and Davidson*, 1989; *Conrad*, 1996, 2002].

[4] Owing to the sensitivity of microbial N_2O and NO production and consumption processes to changes in environmental conditions, one can assume that future changes in climate will strongly affect the magnitude of N_2O and NO exchange between forest soils and the atmosphere. Owing to the complexity of these feedback processes, they cannot be adequately addressed in field studies from a limited number of sites. However, recently, a process-oriented biogeochemical model capable of simulating C and N cycling and the associated soil-atmosphere N trace gas exchange processes has been recently developed [*Li et al.*, 2000; *Butterbach-Bahl et al.*, 2001]. This model, the so-called PnET-N-DNDC model, has been successfully validated for its capability of simulating NO and N_2O emissions for a wide variety of forest soils across Europe [*Kesik et al.*, 2005]. Recent model applications show that the model can reliably simulate the seasonal and interannual variability of N trace gas fluxes due to changes in environmental conditions [*Stange et al.*, 2000; *Butterbach-Bahl et al.*, 2001; *Kesik et al.*, 2005]. Thus the model can serve as an appropriate tool to evaluate possible feedbacks of forest soil N trace gas emissions to predicted climate changes. In this study we focused on the question of how predicted future changes in climate for Europe will affect the source strength and regional distribution of N_2O and NO emissions from forest soils as compared to present-day conditions.

2. Materials and Methods

2.1. PnET-N-DNDC Model

[5] The biogeochemical model PnET-N-DNDC was used for the calculation of present and future soil N_2O and NO emissions from European forest soils. The model has been applied for regional NO and N_2O emission inventories for European temperate, Mediterranean and boreal forest ecosystems [*Butterbach-Bahl et al.*, 2001, 2004b; *Kesik et al.*, 2005], and recently also for the calculation of a N_2O emission inventory for tropical rain forests in Australia [*Kiese et al.*, 2005]. The PnET-N-DNDC model was developed to predict soil carbon and nitrogen biogeochemistry in temperate forest ecosystems and to simulate the emissions of N_2O and NO from forest soils [*Li et al.*, 2000; *Stange et al.*, 2000]. The model is mainly based on the PnET model (Photosynthesis-Evapotranspiration-Model), the DNDC model (Denitrification-Decomposition-Model), and a nitrification module. For further details on the PnET-N-DNDC model, we refer to *Li et al.* [1992, 1996, 2000], *Li* [2000], *Stange et al.* [2000], *Butterbach-Bahl et al.* [2001, 2004b], *Kiese et al.* [2005], and *Kesik et al.* [2005].

[6] To simulate N trace gas emissions for a specific site in daily resolution the PnET-N-DNDC requires the following input parameters: daily climate data (precipitation, minimum and maximum air temperature, optional: solar radiation), soil properties (texture, clay content, pH, soil organic carbon content, stone content, humus type), and information on forest properties (forest type and age, aboveground and below-ground biomass, plant physiology parameters). The PnET-N-DNDC is currently parameterized for 12 tree species/genera, i.e., pine, spruce, hemlock, fir, hardwoods, oak, birch, beech, slash pine, larch, cypress and evergreen oak. If there are no site-specific forest data available except for the forest type and age, the model will use default values. For each forest type these default values are taken from an internal database, which is based on available literature data on tree physiological (e.g., maximum photosynthesis rate, water use efficiency) or forest stand properties (e.g., forest biomass) [*Li et al.*, 2000]. Furthermore, the model needs information about inorganic N concentrations in rainfall, which are used to calculate throughfall values for N, a surrogate of wet and dry deposition. The amount of throughfall is dependent on forest type and N concentration [*Li et al.*, 2000].

[7] The capability of the PnET-N-DNDC model to simulate N trace gas emissions from forest soils for Europe was tested by comparing model results with results from field measurements at 19 different field sites across Europe and one in the USA [*Kesik et al.*, 2005]. The testing sites were located in different climatic regions, namely boreal, temperate oceanic, temperate continental, Mediterranean, in order to assure a wide applicability of the model. The results of the study by *Kesik et al.* [2005] show that the PnET-N-DNDC model was capable of capturing observed differences between high and low emitting sites, on the basis of general information on soil and vegetation properties and by considering the local climatic conditions. The linear regression between simulated and observed annual

Table 1. Seasonal Variations in N_2O and NO Emissions From Forest Soils, Precipitation, Air Surface Temperature, and Water-Filled Pore Space (WFPS) for Present (1991–2000) and Future (2031–2039) Climate Conditions[a]

		N_2O		NO				
Season	Present/Future	kg N ha^{-1}	kt N	kg N ha^{-1}	kt N	Precipitation, mm	Temperature, deg	WFPS, %
Dec–Feb	Present	0.08 a	10.3 a	0.08 a	9.7 a	246 a	1.1 a	0.61 a
	Future	0.08 a	10.3 a	0.06 a	8.3 a	257 a	2.9 b	0.66 b
March–May	Present	0.17 b	21.4 b	0.09 ab	12.4 ab	181 b	5.0 c	0.56 ac
	Future	0.13 c	17.2 c	0.12 bc	14.8 bc	167 b	7.2 d	0.59 a
June-Aug	Present	0.18 d	23.7 d	0.22 d	28.7 d	110 c	15.8 e	0.42 d
	Future	0.18 bd	23.0 bd	0.26 d	32.8 d	104 c	17.5 f	0.40 d
Sep–Nov	Present	0.10 e	12.8 e	0.13 c	17.1 c	245 a	8.4 g	0.51 ce
	Future	0.11 e	13.7 e	0.14 c	18.4 c	245 a	9.9 h	0.50 e
Year	Present	0.53	68.3	0.52	68.0	782	7.6	0.53
	Future	0.50	64.3	0.58	74.3	773	9.4	0.54

[a]Different letters after values indicate significant seasonal differences for the individual parameters.

mean emission rates was $r^2 = 0.68$ for N_2O and $r^2 = 0.78$ for NO [*Kesik et al.*, 2005]. For both N trace gases the model tended to nonsystematically underestimate emissions at the test sites by approximately 24% for N_2O and by approximately 27% for NO. For further details on the model evaluation and performance, see *Kesik et al.* [2005], and the earlier work by *Stange et al.* [2000] and *Butterbach-Bahl et al.* [2001, 2004b]. Differences in N_2O and NO emissions, precipitation and air surface temperature for present (1991–2000) and future (2031–2039) climate conditions were analyzed using analysis of variance (ANOVA, $\alpha = 0.05$). The LSD test was used for multiple comparisons between means. All statistical analyses were performed with SPSS 8.0 (SPSS Inc., Chicago) and Microcal Origin 4.0 (Microcal Software, Northampton).

2.2. GIS Database Construction

[8] For the regionalization of N trace gas emissions by use of the PnET-N-DNDC model a detailed GIS database covering all EU states plus Romania, Bulgaria, Switzerland and Norway was created. This GIS database contained all relevant initialization and driving parameters and variables. Spatially resolved information included soil, forest and climate properties.

[9] Climate information for the years 1991–2000 and 2031–2039 was obtained from calculations by the coupled climate-chemistry model MCCM (Multiscale Climate Chemistry Model [*Grell et al.*, 2000]) using ECHAM4 simulations for current and future climate as boundary conditions. The ECHAM4 model runs by the Max-Planck Institute for Meteorology in Hamburg, Germany, are based on historic atmospheric CO_2 concentrations for the years 1860–1990 and on the IPCC IS92a scenario [*IPCC*, 1992] for the years 1990–2100. From this simulation the results, representing present (1991–2000) and future climate conditions (2031–2039), have been used for calculating a regional climate simulation for Europe (except the part of Scandinavia, north of 66°N and Iceland, which were out of the domain of the regional climate model) with MCCM. The MCCM calculates simultaneously the meteorology and chemistry for a defined region in high spatial resolution. For the climate simulation the MCCM model has been directly nested into the global ECHAM4 model with a resolution of 60 km × 60 km. By this nesting procedure, the climate information of the global ECHAM4 model with a resolution of only 200–300 km (T42) was regionalized [*Forkel and Knoche*, 2006; *Knoche et al.*, 2003]. The climate data, resulting from the MCCM simulation runs, were used as climate input for the PnET-N-DNDC model, i.e., daily precipitation, daily minimum and maximum air temperature and daily mean solar radiation.

[10] Within the NOFRETETE project (http://195.127.136.75/nofretete/), information on atmospheric N deposition for the year 2000 was provided by the Norwegian Meteorological Institute (DNMI), from the inputs of the EMEP MSC-W photo-oxidant model [*Simpson et al.*, 2003]. In our model runs we assumed that N deposition remains at the year 2000 level, which is in line with conclusions by *Galloway et al.* [2004] that the magnitude of total inorganic nitrogen in western Europe will not significantly increase until 2050. Data on soil properties (e.g., pH, SOC, texture, forest type distribution) were provided by the Joint Research Centre (JRC) in Ispra, Italy. Since data were delivered in different formats and projections, transformations into the ArcGIS by ESRI format with the Lambert-Azimuthal projection on the basis of the EMEP (European Monitoring and Evaluation Program) raster were necessary. The used EMEP raster is a polar stereographic projected grid with a resolution of 50 km × 50 km at 60° North [*Simpson et al.*, 2003] (http://www.emep.int). For more details on forest and soil information, we refer to *Kesik et al.* [2005].

[11] The forest, soil, and climate information was aggregated and linked to the EMEP raster. An individual identification number was assigned to each of the 2386 grid cells of the EMEP raster covering the simulated area of Europe.

3. Results and Discussion

3.1. Simulated Changes in European Climate

[12] The regionalized climate scenarios show that for the period 2031–2039 mean annual surface temperatures in Europe will be approximately 1.8°C higher (from 7.6°C to 9.4°C, Table 1) compared to the period of 1991–2000 (Table 1). The highest average increases in surface temperatures are predicted for the winter and spring season across Europe with 1.8°C and 2.2°C, respectively. The increases in average summer and autumn temperatures across Europe are 1.7°C and 1.5°C, respectively. However, the model runs show a distinct regional pattern of temperature changes in

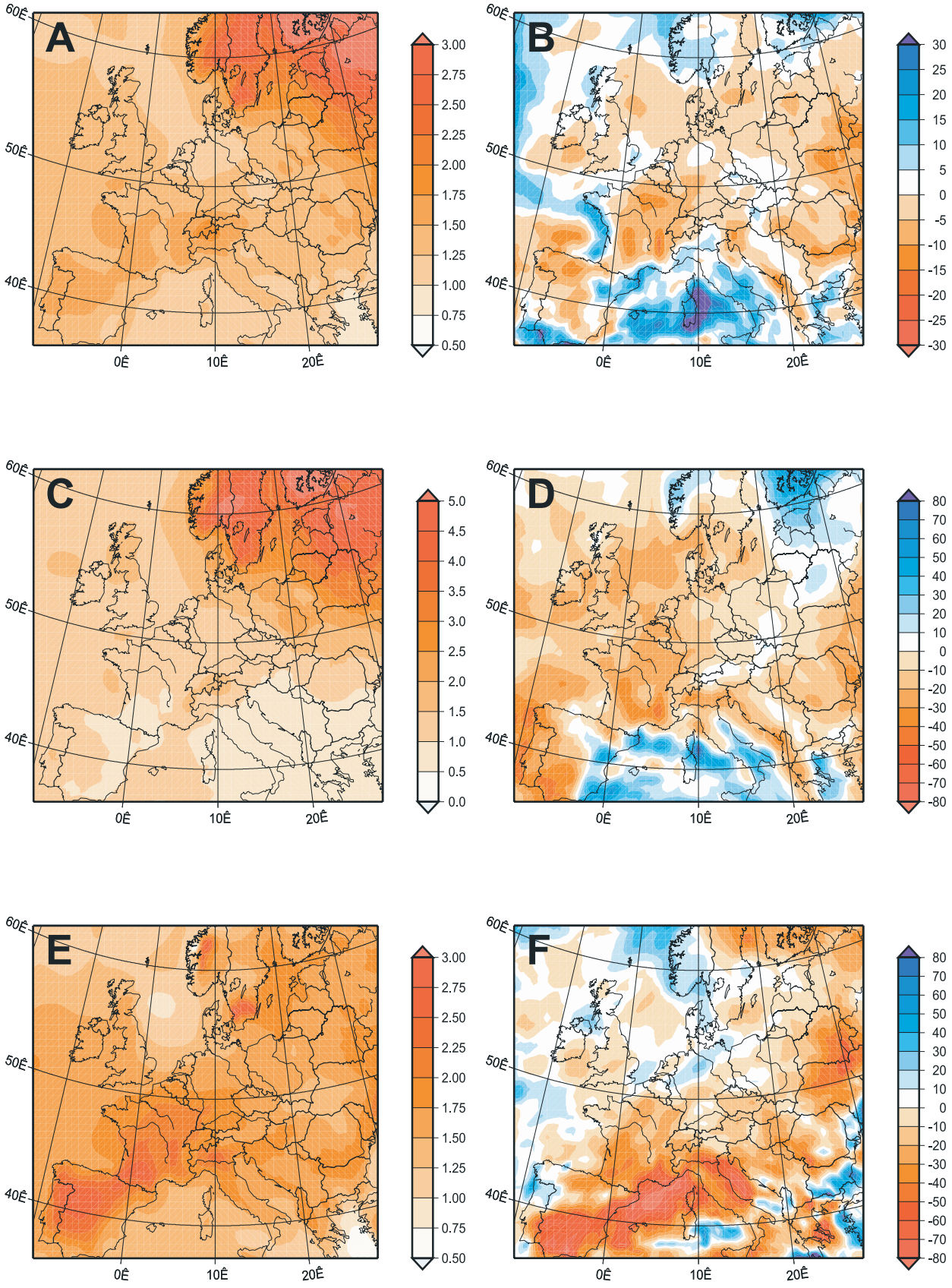

Figure 1. Absolute changes in (a) mean annual temperatures (°C), (c) spring temperatures, and (e) summer temperatures between future (2031–2039) and present (1991–2000) climate conditions. Relative changes in the (b) annual sum of precipitation (%) or (d) summer period precipitation or (f) summer period precipitation between future (2031–2039) and present (1991–2000) climate conditions.

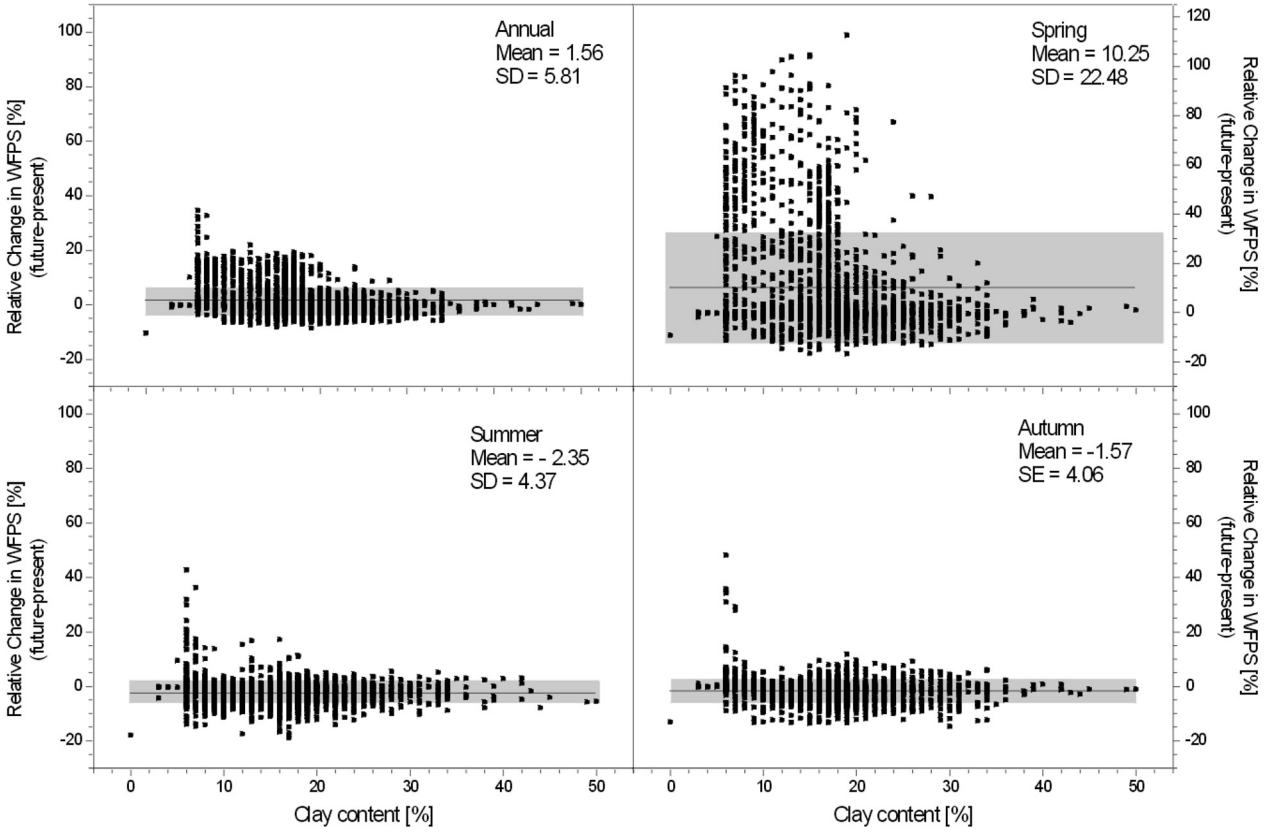

Figure 2. Relative changes in soil moisture (given as percent water filled pore space, WFPS) for European forest soils under future climate conditions as compared to present day as a function of classified percent clay content. Gray bars indicate the range of SD from the mean (straight line).

Europe. Figure 1 shows an increase in the average annual temperature in Scandinavia, the Baltic States, and parts of Ukraine and Russia for the period 2031–2039 of 2°C or more. For other areas such as the western part of the Alps and some maritime areas of Portugal, Spain and France the predicted temperature increase is in the range of 1.5°–2.0°C. For all other parts of Europe, i.e., for most of the Mediterranean area, central Europe, and the UK and Ireland, the predicted mean annual temperature change is less pronounced, and in the range of 0.75°–1.5°C. Both in the Mediterranean region and in Southern Norway and Sweden future summer temperatures may strongly increase by up to 2.5°C. This locally fixed temperature increase in southern Norway and Sweden can be due to an overestimation of the temperature for the simulated future climate (2031–2039), as such a persistent trend of temperature increase for this region can not be found for the simulation years 1991–2000. For the rest of Europe the temperature increase is about 1.5°–2°C.

[13] Total average annual precipitation is predicted to be nearly unchanged across Europe for the period 2031–2039 as compared to the period 1991–2000 (Table 1). However, regional and seasonal changes in precipitation do occur. Figure 1 shows that in some parts of the Mediterranean region and parts of the west coast of France and Scotland annual precipitation is predicted to increase up to 30%. In all other European regions, except for parts of Norway and Finland, annual precipitation is predicted to decrease in the range of 0–20%. Considering the seasonality of rainfall, the MCCM model predicts slightly higher values for winter precipitation, but lower precipitation for spring and summer, in most areas. However, none of the seasonal changes in precipitation between the present and the future climate are statistically significant (Table 1). Especially pronounced are the seasonal changes in precipitation for the Mediterranean area, where summer precipitation is predicted to decrease regionally by up to 80%. Also for other regions such as central Europe (except northern Germany), Sweden and Finland, the east and southeast of Europe, decreasing values of summer precipitation are predicted for the period 2031–2039. However, along the east coast of the North Sea, mainly for Norway, Denmark, and northern Germany, parts of Scotland and Northern Ireland, and northern Portugal, precipitation is predicted to increase up to 30% during the summer months.

[14] Future changes in precipitation and temperature will also feedback on the soil moisture. Figure 2 shows that under future climate conditions mean annual soil moisture across Europe, as calculated by the PnET-N-DNDC model, will not be changed significantly (1.6%). Also no obvious relationship between predicted soil moisture changes and soil texture can be demonstrated (Figure 2). Significant changes in soil moisture could only be found on a seasonal basis (Figure 3), with a marked increase in soil moisture in

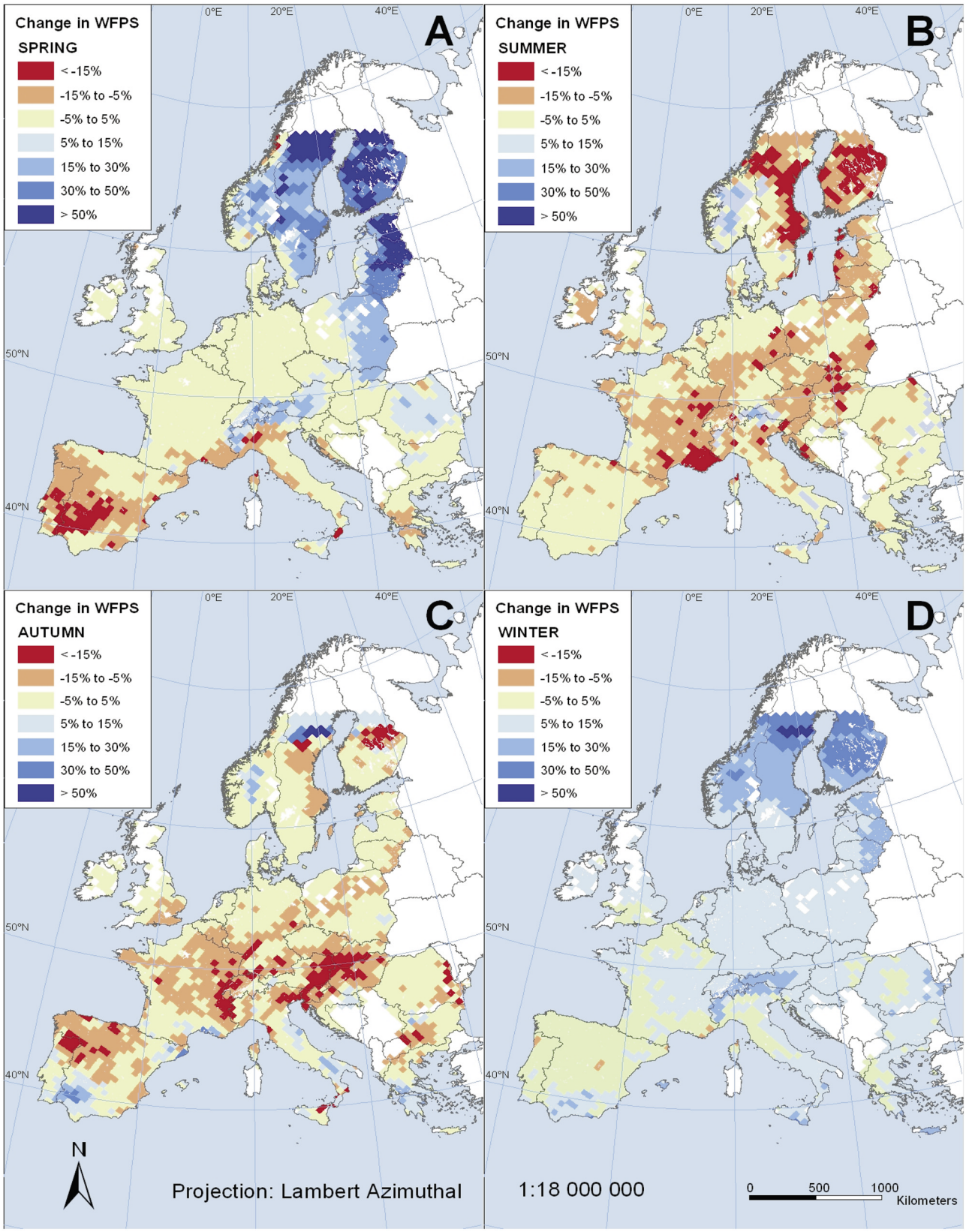

Figure 3. Relative changes in soil moisture (as percent change in WFPS with WFPS: percent water filled pore space) for European forest soils under future climate conditions as compared to present day for winter (DJF) spring (MAM), summer (JJA), and autumn (SON).

Table 2. Interannual Variations in Mean Annual N_2O and NO Emissions From Forest Soils, Air Surface Temperature and Mean Annual Sum of Precipitation for Present (1991–2000) and Future (2031–2039) Climate Conditions[a]

	Temperature, °C	Precipitation, mm	N_2O, kg N ha^{-1}	NO, kg N ha^{-1}
		Present		
1991	7.53	824	0.51	0.49
1992	6.71	751	0.55	0.24
1993	7.40	812	0.53	0.81
1994	6.84	733	0.59	0.45
1995	7.81	730	0.54	0.54
1996	8.00	803	0.53	0.47
1997	8.01	816	0.48	0.51
1998	7.32	711	0.56	0.49
1999	7.65	856	0.55	0.52
2000	8.90	787	0.48	0.55
Mean	7.62	782	0.53	0.51
CV, %	8.25	6.16	6.70	27.29
		Future		
2031	9.05	801	0.52	0.58
2032	9.58	759	0.48	0.59
2033	8.74	753	0.59	0.58
2034	8.82	709	0.52	0.56
2035	10.48	769	0.47	0.62
2036	9.40	809	0.48	0.59
2037	8.59	782	0.52	0.53
2038	9.55	826	0.49	0.59
2039	10.49	749	0.45	0.59
Mean	9.41	773	0.50	0.58
CV, %	7.48	4.62	8.16	4.48

[a]CV represents the coefficient of variation.

spring (+22%) and slight decreases in summer (−2.4%) and autumn (−1.6%). However, on a regional basis these changes were more pronounced and mirrored changes in precipitation (Figure 3).

[15] The calculated changes in future climate as calculated by the MCCM model are supported by another recent study. *Räisänen et al.* [2004] calculated the climate change from 1961–1990 to 2071–2100 with the regional model RCAO driven by the global models HadAM3H and ECHAM4/OPYC3. These authors used the two SRES scenarios A2 and B2. All four simulations by *Räisänen et al.* [2004] indicate for northern Europe a larger warming in winter than in summer. In southern and central Europe a very large increase in summer temperatures was predicted, which was most pronounced for the southwestern parts of Europe and most notably in the ECHAM4/OPYC3-based A2 scenario. For this scenario the warming locally exceeds 10°C (e.g., in France). These results by *Räisänen et al.* [2004] are consistent with results obtained by the MCCM simulation, even though predicted changes in summer temperatures for France by MCCM are less pronounced. Also with regard to precipitation changes the regional climate simulation used in this study is in agreement with results of *Räisänen et al.* [2004]. In the four scenario simulations these authors found a general increase in winter precipitation in northern and central Europe and a decrease in summer precipitation in central and southern Europe. The latter finding was also supported by MCCM regional climate predictions, i.e., a precipitation decrease in the summer months for central and south Europe. The range as well as the regional pattern of predicted changes in precipitation and temperature used in our study are also consistent with a series of recent studies on future climate change in Europe such as *Maracchi et al.* [2005], *Benestad* [2005], *Giorgi et al.* [2004], and *Kjellstrom* [2004].

[16] It needs to be noted that in this study only the output of regionalized ECHAM4 data for the IPCC 92a scenario were used as drivers for the biogeochemical model. Outputs of other global climate models (GCM) for future climate have been shown to be highly variable with regard to regional precipitation patterns [*Dubrovsky et al.*, 2005; *Wang*, 2005; *Hanssen-Bauer et al.*, 2003]. However, for Europe the majority of GCMs is highly consistent in predicting future precipitation responses: a substantial increase in precipitation for December, January and February for middle and high latitudes, but a decrease for the Mediterranean. Also for the summer period June, July and August, increased drought periods are consistently predicted by GCMs for the Mediterranean, but not for northern Europe [*Wang*, 2005]. Predicted changes in soil moisture are even more variable, since the global and regional pattern of the direction of soil moisture changes differs significantly from model to model mostly owing to differences in land surface parameterization [*Wang*, 2005]. However, in our study we calculated soil moisture values with our biogeochemical model based on predicted meteorological data and soil and forest stand properties. The variability in the predictions of future changes in precipitation among different GCMs would directly feedback on the magnitude of N trace gas emissions from forest soils. For entire Europe, *Kesik et al.* [2005] showed that forest soil N_2O and NO emissions can vary under present climate conditions by 15% for different meteorological years. We do need to assume that the use of other GCMs' climate predictions would have resulted at least in a comparable uncertainty range with regard to forest soil N trace gas emissions.

3.2. Future Changes in Regional N_2O Emissions

[17] For exploring possible feedbacks of future climate change on N trace gas emissions from European forest soils the PnET-N-DNDC model was run for the periods 1991–2000 and 2031–2039 with the climate scenarios described above. In our simulations, mean annual N_2O emissions from forest soils across Europe were found to slightly decrease by 4 kt N_2O-N (−6%) for the period 2031–2039 as compared to the period 1991–2000 (68.3 kt N_2O-N) (Tables 1–3). This is mainly due to the significant decrease in emissions during spring from 21.4 kt N_2O-N under present climate conditions to 17.2 kt N_2O-N under future climate conditions (Tables 1 and 2). However, the model runs with PnET-N-DNDC also revealed a pronounced interannual variability in N_2O (but also NO) emissions (Table 2), which are due to changes in the meteorological conditions from year to year. This reflects the sensitivity of the PnET-N-DNDC model toward the meteorological drivers. Furthermore, the model runs also revealed a pronounced regional pattern of future changes in N_2O emissions due to climate change (Table 3 and Figure 4). In Scandinavia, and in some regions of Poland, Estonia, Latvia, Lithuania, Romania, Slovakia, and Bulgaria future N_2O emissions may decrease by up to 33%. Also, for the Alpine region the model predicted a decrease of N_2O emissions from forest soils by up to 30% in

Table 3. Average and Total Simulated N_2O and NO Emissions From Forest Soils for Present and Future Climatic Conditions for Individual European Countries

Country	Forest Area, km^2	N_2O 1991–2000 kg N ha^{-1} yr^{-1}	N_2O 1991–2000 kt N yr^{-1}	N_2O 2031–2039 kg N ha^{-1} yr^{-1}	N_2O 2031–2039 kt N yr^{-1}	Change in N_2O Emission, %	NO 1991–2000 kg N ha^{-1} yr^{-1}	NO 1991–2000 kt N yr^{-1}	NO 2031–2039 kg N ha^{-1} yr^{-1}	NO 2031–2039 kt N yr^{-1}	Change in NO Emission, %
Andorra	232	0.16	3.7×10^{-3}	0.17	3.9×10^{-3}	6	0.21	4.9×10^{-3}	0.12	2.8×10^{-3}	−44
Austria	24,032	0.46	1.11	0.43	1.03	−7	0.44	1.07	0.41	1.00	−6
Belgium	7699	0.77	0.59	0.87	0.67	14	1.53	1.18	1.73	1.33	13
Bulgaria	28,494	0.52	1.50	0.51	1.45	−3	0.32	0.90	0.30	0.86	−4
Croatia	12,574	0.46	0.57	0.49	0.62	8	0.46	0.58	0.46	0.58	1
Czech.	20,406	0.43	0.88	0.44	0.91	3	0.66	1.36	0.68	1.39	2
Republic	18,608	0.60	1.12	0.72	1.34	21	0.89	1.66	1.05	1.95	18
Denmark	18,341	0.60	1.10	0.40	0.73	−33	0.50	0.91	0.61	1.12	23
Estonia	116,126	0.82	9.54	0.62	7.21	−24	0.48	5.59	0.59	6.80	22
Finland	132,395	0.44	5.81	0.48	6.34	9	0.55	7.23	0.55	7.32	1
Germany	117,849	0.56	6.57	0.63	7.43	13	0.95	11.15	1.04	12.24	10
Gibraltar	0.43	0.58	2.5×10^{-5}	0.63	2.7×10^{-5}	9	0.06	2.7×10^{-6}	0.07	2.9×10^{-6}	7
Greece	30,676	0.50	1.54	0.53	1.64	7	0.28	0.87	0.29	0.88	1
Hungary	21,181	0.63	1.32	0.62	1.32	0	0.35	0.73	0.34	0.72	−2
Irish Republic	5523	0.20	0.11	0.24	0.13	20	0.50	0.28	0.49	0.27	−3
Italy	59,834	0.48	2.89	0.49	2.96	3	0.40	2.39	0.40	2.42	1
Latvia	28,229	0.66	1.86	0.46	1.29	−30	0.57	1.60	0.67	1.89	18
Liechtenstein	89	0.56	4.9×10^{-3}	0.36	3.2×10^{-3}	−35	0.42	3.8×10^{-3}	0.30	2.6×10^{-3}	−30
Lithuania	18,843	0.46	0.87	0.36	0.68	−23	0.40	0.76	0.41	0.78	2
Luxembourg	1032	0.45	0.05	0.52	0.05	15	0.81	0.08	0.82	0.08	2
Monaco	0.21	0.19	3.9×10^{-6}	0.21	4.4×10^{-6}	12	0.11	2.4×10^{-6}	0.08	1.7×10^{-6}	−28
Netherlands	8271	1.17	0.97	1.36	1.13	16	2.53	2.09	3.01	2.49	19
Norway	108,987	0.18	1.91	0.13	1.45	−24	0.16	1.74	0.06	0.67	−62
Poland	78,358	0.56	4.26	0.50	3.82	−10	0.76	5.84	0.86	6.58	13
Portugal	32,713	0.41	1.35	0.44	1.44	7	0.14	0.47	0.12	0.40	−15
Romania	41,284	0.69	2.85	0.62	2.56	−10	0.41	1.70	0.42	1.73	2
San Marino	0.35	0.23	8.2×10^{-6}	0.25	8.9×10^{-6}	8	0.24	8.4×10^{-6}	0.20	7.0×10^{-6}	−17
Slovakia	9162	0.68	0.62	0.60	0.55	−12	0.47	0.43	0.48	0.44	2
Slovenia	7881	0.48	0.3	0.49	0.39	2	0.49	0.39	0.45	0.35	−8
Spain	128,484	0.54	7.49	0.58	8.08	8	0.25	3.49	0.24	3.27	−6
Sweden	163,782	0.60	9.91	0.48	7.93	−20	0.71	11.70	0.92	15.12	29
Switzerland	12,407	0.40	0.49	0.35	0.43	−12	0.42	0.53	0.34	0.42	−21
United Kingdom	22,481	0.27	0.62	0.33	0.73	19	0.56	1.27	0.55	1.23	−3
Sum	1,283,978		68.27		64.32			67.96		74.32	
Average		0.53		0.50		−6	0.53		0.58		9

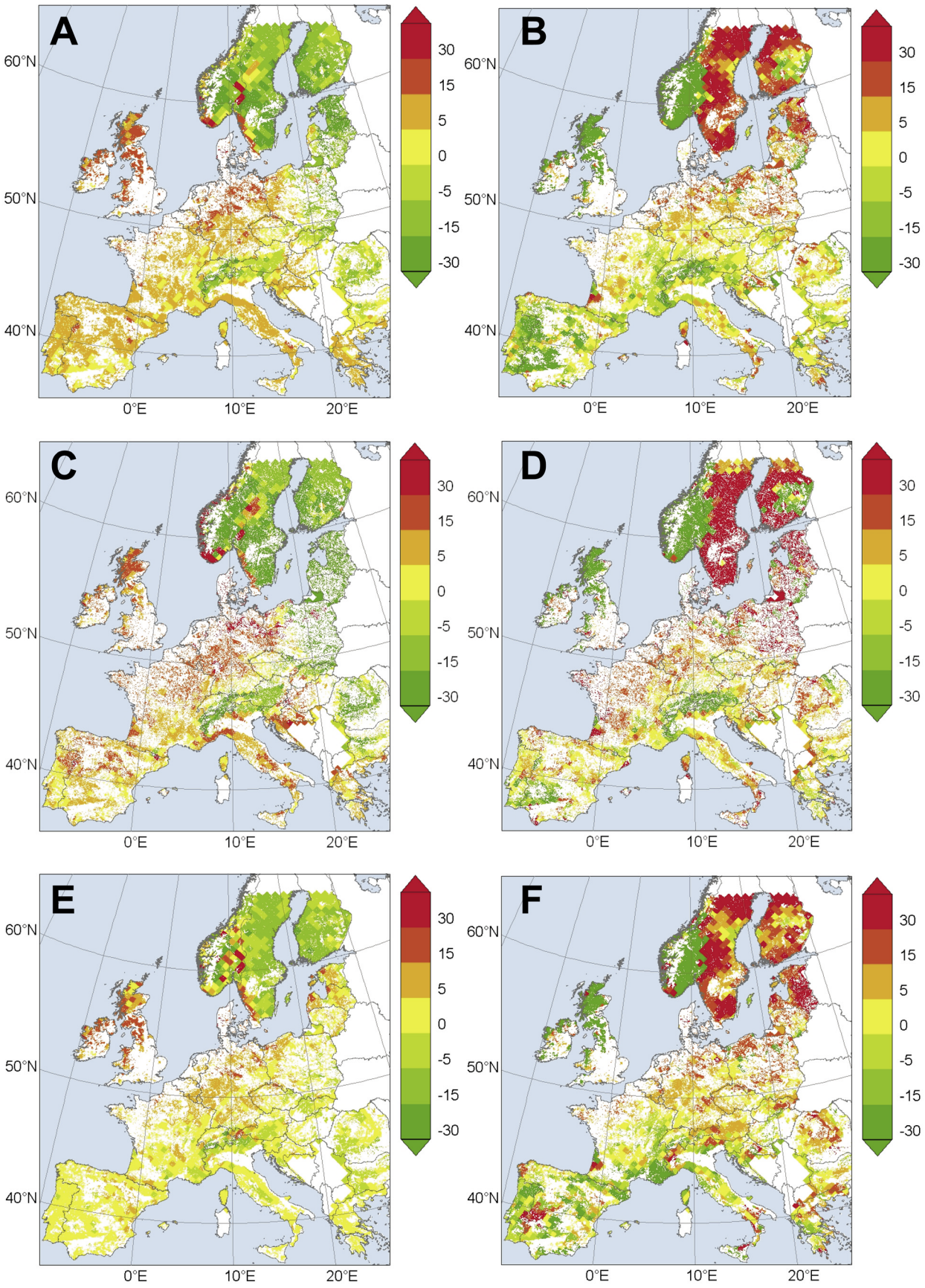

Figure 4

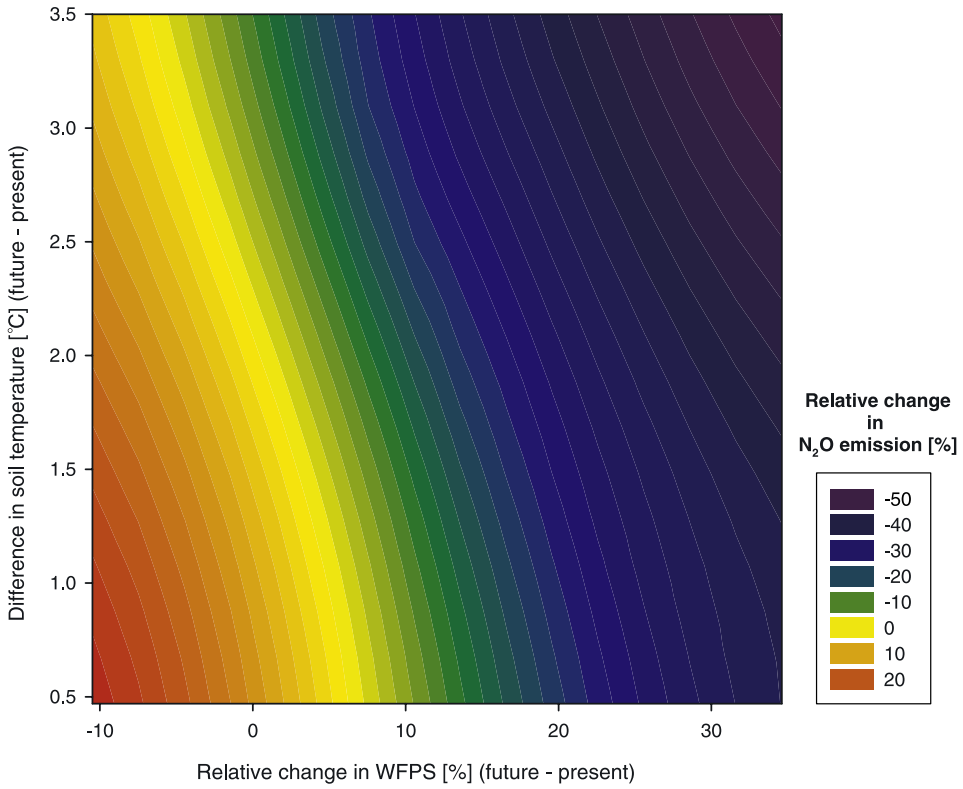

Figure 5. Contour plot showing the effect of average annual relative changes in soil water filled pore space (%) and absolute changes in soil temperature (°C) on relative changes in forest soil N_2O emissions (%). For this analysis, simulation results for present and future climate predictions for all grid cells across Europe were used. Prior to the calculation of contour lines with SigmaPlot2000 (SPSS, Inc.) data were smoothed using a second-order polynom (r^2 of the underlying polynom = 0.68).

the future. In most of these regions light texture soils predominate, i.e., soils with clay contents mostly below 15% (see, e.g., soil texture map of *Kesik et al.* [2005]). For such soils, stable or decreasing precipitation and increasing temperature under future climatic conditions will result in decreased soil moisture values especially for the summer and autumn season (see, e.g., Figures 3b and 3c). Owing to the improved aeration the denitrification activity in such soils, and thus, N_2O production by denitrification, decreases. On the other hand NO production by nitrification increases in these regions during these periods (see also below). For winter and spring seasons a significant increase in soil moisture can be observed for Scandinavia and the Baltic States. This also feedbacks on forest soil N_2O emissions, since under such conditions even in light textured soils oxygen diffusion into the soil profile is strongly reduced. As a consequence, predominantly anaerobic soil conditions are predicted and the end product of denitrification is N_2 rather than N_2O (see also below). However, in central Europe and in the Mediterranean area our model predicted an increase of forest soil N_2O emissions by approximately 15%. In northern Germany, the Benelux states and the UK with Ireland, N_2O emissions may even increase by up to 20%.

[18] The magnitude of forest soil N_2O emissions for present-day conditions in this study is well in agreement with results from previous work by *Kesik et al.* [2005]. On the basis of an extensive model testing for various sites across Europe, *Kesik et al.* [2005] used the GIS coupled PnET-N-DNDC model to estimate present-day N trace gas emissions from forest soils using daily meteorological data for the years 1990, 1995 and 2000 as derived from the EMEP MSC-W model [*Sandnes-Lenschow and Tsyro*, 2000; *Simpson et al.*, 2003]. Mean N_2O emissions in the study by *Kesik et al.* [2005] using EMEP climate data were on average slightly higher (0.58 kg N_2O-N ha^{-1} yr^{-1}) than those found in this study (0.53 kg N_2O-N ha^{-1} yr^{-1}), owing to differences in the simulation area (in the current study we excluded parts of Scandinavia), length of the simulation period (10 years versus 3 years), and differences in the climate data sets (MCCM versus EMEP).

[19] The simulation results show that even in view of a general increase in temperature under future climate conditions, N_2O emissions are projected to slightly decrease.

Figure 4. Relative changes in (a) mean annual N_2O emissions (%), (c) mean spring N_20 emissions, and (e) mean summer N_2O emissions between future (2031–2039) and present (1991–2000) climate conditions. Relative changes in mean (b) annual or (d) spring or (f) summer NO emissions between future (2031–2039) and the present (1991–2000) climate conditions for NO.

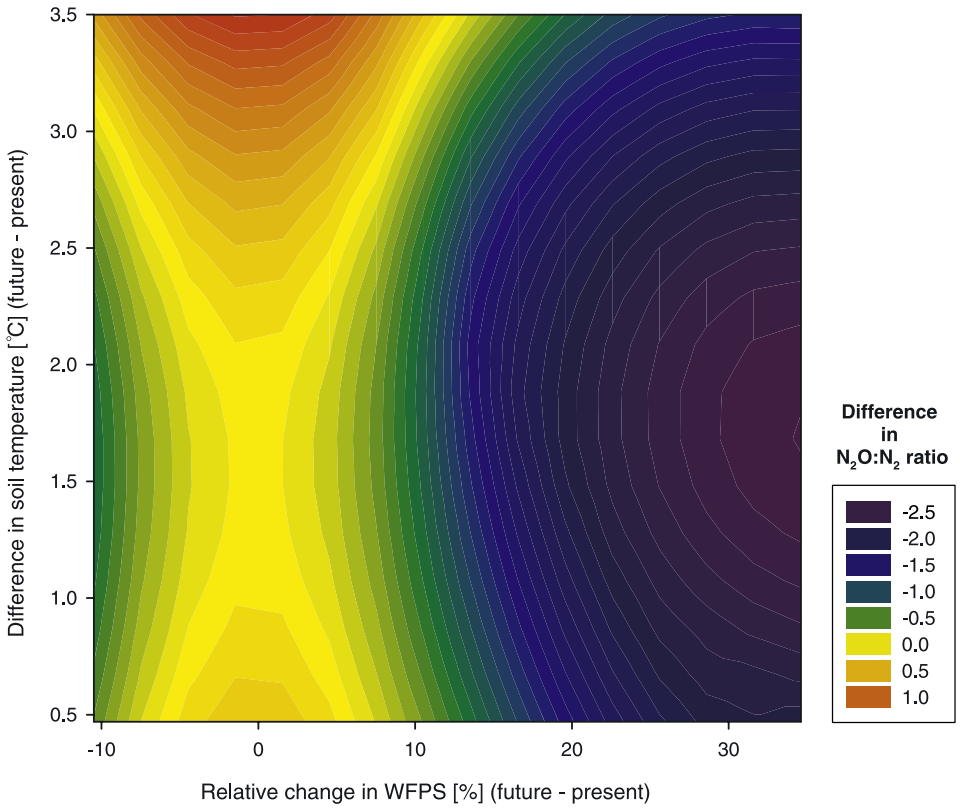

Figure 6. Contour plot showing the differences in the average annual N_2O:N_2 ratio between future and present climate conditions as influenced by relative changes in soil water filled pore space (%) and the difference in soil temperature (°C) between future and present climate conditions. Positive values of the N_2O:N_2 ratio imply an increase in N_2O emissions and negative values imply an increase in N_2 emissions. For this analysis, simulation results for present and future climate predictions for all grid cells across Europe were used. Prior to the calculation of contour lines with SigmaPlot2000 (SPSS, Inc.) data were smoothed using a second-order polynom (r^2 of the underlying polynom = 0.25).

Most field and laboratory studies show that temperature has a stimulating effect on N_2O emissions [e.g., *Granli and Bøckmann*, 1994; *Brumme*, 1995; *Papen and Butterbach-Bahl*, 1999]. Reported Q_{10} values for soil N_2O emissions are in the range of 0.9 to 23 [see, e.g., *Smith*, 1997]. For this reason, one would expect that under future climate conditions N_2O emissions should generally increase with a predicted increase in temperature across Europe. The much more differentiated picture on future changes in forest soil N_2O emissions as obtained in our model study is a result of the complexity of the processes involved in production and consumption of this trace gas. If mean annual soil moisture increases by more than 10% (relative change in water-filled pore space (WFPS); for mean absolute values of WFPS across Europe, see Table 1) and mean annual soil temperature by more than 2.0°C under future climate conditions, simulated N_2O emissions are predicted to decrease by at least 10% (Figure 5). Only under the conditions with average annual soil moisture remaining unchanged or only slightly decreasing in comparison with the decrease in present-day conditions, N_2O emissions are predicted to increase. The main reason for the simulated decrease in N_2O emissions is a shift in the relative proportions of N_2O versus N_2 emitted from the soils under the future climate conditions (Figure 6). In our simulations the emitted N_2O:N_2 ratio is mostly predicted to decrease. This means that under future climate conditions in regions for which higher annual average soil moisture values as well as higher soil temperature are predicted, a tendency can be found that more nitrogen will be emitted as N_2 rather than N_2O. These predictions are in line with laboratory studies, which have shown that the N_2O:N_2 ratio decreases with increasing temperature [*Nommik*, 1956; *Keeney et al.*, 1979]. Moreover, it is well known that if WFPS increases above a certain threshold of approximately 70–80% [*Davidson*, 1991], N_2 rather than N_2O will be the main product of denitrification.

[20] The provided insights in possible consequences of future climate changes on forest soil N trace gas emissions can only be obtained if biogeochemical models such as PnET-N-DNDC are used, which do not only rely on empirical relationships between, for example, temperature, moisture and N trace gas fluxes, but which are based on the underlying main microbial and physico-chemical processes involved in the production, consumption and emission of N trace gases [*Li et al.*, 2000]. For example, denitrification is described in the model as a series of sequential reductions driven by microorganisms using N oxides as electron acceptors under anaerobic conditions [e.g., *Kuenen and Robertson*, 1987]. As intermediates of the processes, NO

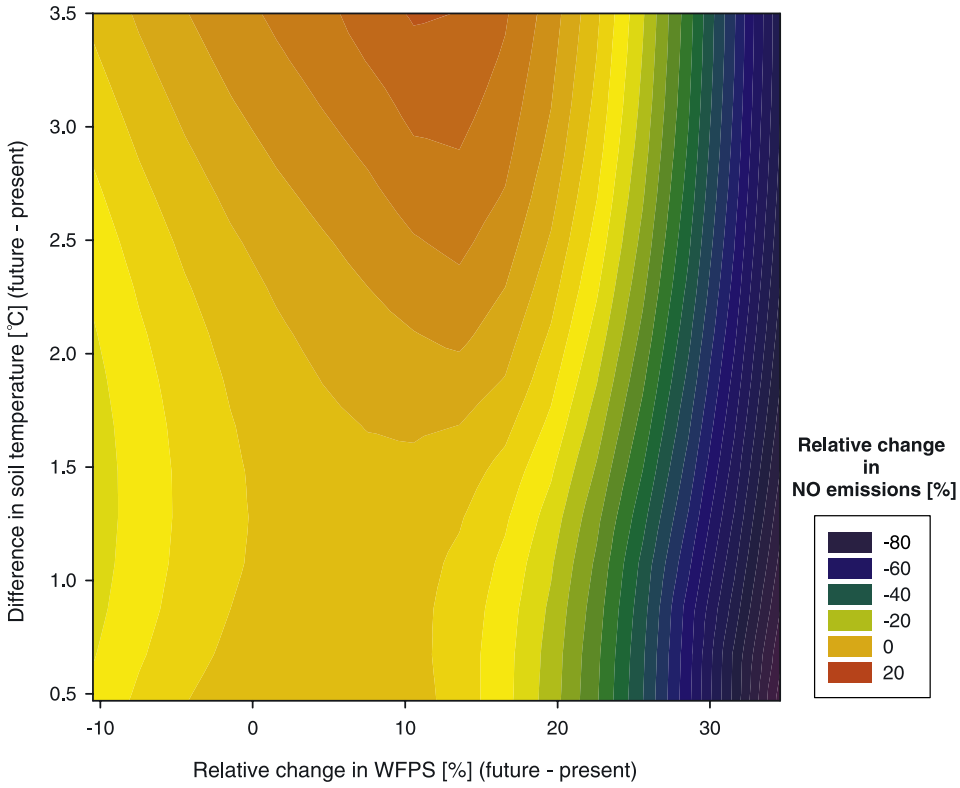

Figure 7. Contour plot showing the effect of relative changes in soil water filled pore space (%) and absolute changes in soil temperature (°C) on relative changes in forest soil NO emissions (%). For this analysis simulation results for present and future climate predictions for all grid cells across Europe were used. Prior to the calculation of contour lines with SigmaPlot2000 (SPSS, Inc.) data were smoothed using a second-order polynom (r^2 of the underlying polynom < 0.1).

and N_2O are tightly controlled by the kinetics of each step in the sequential reactions [*Li et al.*, 2000]. As a soil becomes increasingly anaerobic, for example, owing to high WFPS or to stimulated soil respiration at higher soil temperatures, the model will simulate that more N_2O, either derived from nitrification or denitrification, will be reduced to N_2 as compared to conditions when the soil is well aerated. This is in accordance also with laboratory studies on soil N_2O and N_2 emissions [e.g., *Nommik*, 1956; *Keeney et al.*, 1979].

3.3. Future Changes in Regional NO Emissions

[21] In contrast to the average decrease of forest soil N_2O emissions under predicted future climate changes, forest soil NO emissions are predicted to increase in the future by 9% on average (from 68.0 to 74.3 kt NO-N) (Tables 1–3). The increase in NO emissions is most pronounced in summer with a predicted increase from 28.7 kt NO-N under present-day climate conditions to 32.8 kt NO-N in the future. The model-simulated distinct regional differences in NO emissions in Europe under predicted climate changes. Only for a few regions such as the Alpine region, the UK, Ireland, Norway, Spain, Portugal and some countries in east Europe (Bulgaria, Hungary, Slovenia) a decrease of average annual NO emissions under future climate conditions was predicted (down to 66%). However, in all other regions the model predicted an increase of NO emissions for the period 2031–2039 as compared to the period 1991–2000. Especially for the Baltic Sea region, NO emissions from forest soils may increase by up to 29% (Table 3 and Figure 4). As already outlined above, this region is characterized by prevailing light textured soils. The regional NO emission changes (Figure 4) in summer are not significantly different from that of annual average NO emission changes under future climate conditions. However, for central Europe the increase of forest soil NO emissions are more pronounced in the summer months than throughout the year.

[22] NO emissions from soils are mainly driven by the activity of nitrifying organisms in the soil [e.g., *Conrad*, 1996, 2002]. NO production in soils and NO emissions at the soil-atmosphere interface have been found to be positively correlated with temperature [*Valente and Thornton*, 1993; *Gasche and Papen*, 1999; *Ludwig et al.*, 2001], mostly owing to the stimulating effect of temperature on NO production via nitrification [*Conrad*, 2002]. The optimal soil moisture range for NO emissions is less than for N_2O emissions, since at higher soil moisture values the O_2 availability in the soil profile decreases owing to diffusion restrictions. Besides soil moisture the soil texture has a main influence on O_2 availability in the soil profile. For that reason, regions with predominating light textured soils, which do facilitate O_2 diffusion into the soil profile, as, for example, in the area of the Baltic Sea, tend to have elevated NO emissions. Laboratory and field studies showed that at WFPS values above 60% NO will be further reduced to N_2O or N_2 [e.g., *Davidson*, 1991; *Bollmann and*

Conrad, 1998]. Most of the NO is already consumed in the soil before it will be released to the atmosphere. Comparable consumption and production mechanisms are also implemented in the PnET-N-DNDC model. In the model we use the concept of an anaerobic balloon to describe the prevalence of aerobic or anaerobic zones in dependency of the aeration status of the soil [*Li et al.*, 2000], i.e., on the basis of a gas diffusion model which takes into account soil texture and moisture as well as considering heterotrophic and autotrophic O_2 consumption the availability of O_2 is calculated for the different soil layers. On the basis of the O_2 availability the soil layer is partitioned into anaerobic and aerobic soil zones. If a soil becomes predominantly anaerobic, for example, owing to diffusion restrictions at high WFPS values, NO produced by nitrification (or denitrification) can be taken up and further reduced by denitrifiers (the model does not allow aerobic NO consumption at present). In our simulations, mean annual NO emissions were predominantly stimulated in those regions which showed the highest increase in mean annual temperature and an increase in WFPS of less than 18% (Figure 7). If mean annual WFPS was further increased under future climate conditions NO emissions would strongly be reduced to N_2O or N_2, owing to enhanced denitrification under anaerobic conditions. The decrease in summer NO emissions for some Mediterranean regions in our model simulations were due to the effect of water stress on microbial processes. This prediction is in accordance with results from field and laboratory studies, which reveal a strong decrease in NO emissions if soils experience a longer dry period [e.g., *Davidson*, 1991; *Ludwig et al.*, 2001], even though large pulses of NO emissions may occurring following rewetting [*Davidson et al.*, 1993; *Butterbach-Bahl et al.*, 2004a].

4. Conclusion

[23] In this study we have explored the consequences of predicted future climate changes on forest soil NO and N_2O emissions using a GIS-coupled biogeochemical model. The results show that future changes in N trace gas emissions from forest soils cannot be predicted by changes in one factor (e.g., temperature) alone. In our study, changes in precipitation and thus, in soil moisture, exerted a greater effect on N_2O emissions than changes in temperature. For NO, temperature was the main driving factor. Overall, mean N_2O emissions across Europe were predicted to decrease by 6%, whereas NO emissions were predicted to increase by 9%. The decrease in N_2O emissions was mainly due to the decrease in the N_2O:N_2 ratio, i.e., under future climate conditions the model simulated an increase in N_2 emission by denitrification at the expense of N_2O emission via denitrification. However, our knowledge about the combined effect of changes in moisture and temperature on annual N_2O, NO and N_2 emissions from soils is still rather limited. This is especially true with regard to N_2 emissions due to denitrification in soils. Furthermore, our study shows a complex, regionally differentiated response of N trace gas emissions to future climate change, and underlines that more experimental and modeling studies are required to better understand the consequences of climate changes for biosphere-atmosphere exchange processes. Especially, multifactorial manipulation experiments in which the combined effects of changes in temperature, precipitation and atmospheric CO_2 concentrations on biosphere-atmosphere greenhouse gas exchange are investigated are urgently needed for further model validation.

[24] **Acknowledgments.** The work was funded by the European Commission in the NOFRETETE project (EVK2-CT2001-00106) of the fifth framework program and the NATAIR project (contract 513699) of the sixth framework programme. The work of David Simpson was also supported by the Co-operative Programme for monitoring and Evaluation of the Long-range Transmission of Air Pollutants in Europe (EMEP) under UNECE.

References

Benestad, R. E. (2005), Climate change scenarios for northern Europe from multi-model IPCC AR4 climate simulations, *Geophys. Res. Lett.*, *32*(17), L17704, doi:10.1029/2005GL023401.

Boeckx, P., and O. Van Cleemput (2001), Estimates of N_2O and CH_4 fluxes from agricultural lands in various regions in Europe, *Nutr. Cycl. Agroecosyst.*, *60*, 35–47.

Bollmann, A., and R. Conrad (1998), Influence of O_2 availability on NO and N_2O release by nitrification and denitrification in soils, *Global Change Biol.*, *4*(4), 387–396.

Brumme, R. (1995), Mechanisms of carbon and nutrient release and retention in beech forest gaps: 3. Environmental-regulation of soil respiration and nitrous-oxide emissions along a microclimatic gradient, *Plant Soil*, *169*, 593–600.

Brumme, R., and F. Beese (1992), Effects of liming and nitrogen fertilization on emissions of CO_2 and N_2O from a temperate forest, *J. Geophys. Res.*, *97*, 12,851–12,858.

Butterbach-Bahl, K., R. Gasche, L. Breuer, and H. Papen (1997), Fluxes of NO and N_2O from temperate forest soils: Impact of forest type, N deposition and of liming on the NO and N_2O emission, *Nutr. Cycl. Agroecosyst.*, *48*, 79–90.

Butterbach-Bahl, K., F. Stange, H. Papen, and C. Li (2001), Regional inventory of nitric oxide and nitrous oxide emissions for forest soils of southeast Germany using the biogeochemical model PnET-N-DNDC, *J. Geophys. Res.*, *106*, 34,155–34,166.

Butterbach-Bahl, K., L. Breuer, R. Gasche, G. Willibald, and H. Papen (2002), Exchange of trace gases between soils and the atmosphere in Scots pine forest ecosystems of the North Eastern German Lowlands: 1. Fluxes of N_2O, NO/NO_2 and CH_4 at forest sites with different N-deposition, *For. Ecol. Manage.*, *167*, 123–134.

Butterbach-Bahl, K., M. Kock, G. Willibald, B. Hewett, S. Buhagiar, H. Papen, and R. Kiese (2004a), Temporal variations of fluxes of NO, NO_2, N_2O, CO_2 and CH_4 in a tropical rain forest ecosystem, *Global Biogeochem. Cycles*, *18*, GB3012, doi:10.1029/2004GB002243.

Butterbach-Bahl, K., M. Kesik, P. Miehle, H. Papen, and C. Li (2004b), Quantifying the regional source strength of N-trace gases across agricultural and forest ecosystems with process based models, *Plant Soil*, *260*, 311–329.

Cicerone, R. J. (1987), Changes in stratospheric ozone, *Science*, *237*(4810), 35–42.

Conrad, R. (1996), Soil microorganisms as controllers of atmospheric trace gases (H_2, CO, CH_4, OCS, N_2O and NO), *Microbiol. Rev.*, *60*, 609–640.

Conrad, R. (2002), Microbiological and biochemical background of production and consumption of NO and N_2O in soil, in *Trace Gas Exchange in Forest Ecosystems*, edited by R. Gasche, H. Papen, and H. Rennenberg, pp. 3–33, Springer, New York.

Crutzen, P. J. (1976), The influence of nitrogen oxides on the atmospheric ozone content, *Q. J. R. Meteorol. Soc.*, *96*, 320–325.

Crutzen, P. J. (1995), Ozone in the troposphere, in *Composition, Chemistry, and Climate of the Atmosphere*, edited by H. B. Sing, pp. 349–393, Van Nostrand Reinhold, Hoboken, N. J.

Davidson, E. A. (1991), Fluxes of nitrous oxide and nitric oxide from terrestrial ecosystems, in *Microbial Production and Consumption of Greenhouse Gases: Methane, Nitrogen Oxides and Halomethanes*, edited by J. E. Rogers, and W. B. Whitman, pp. 219–235, Am. Soc. for Microbiol., Washington, D. C.

Davidson, E. A., and W. Kingerlee (1997), A global inventory of nitric oxide emissions from soils, *Nutr. Cycl. Agroecosyst.*, *48*, 37–50.

Davidson, E. A., P. A. Matson, P. M. Vitousek, R. Riley, K. Dinkin, G. Garcia-Méndez, and J. M. Maass (1993), Processes regulating soil emission of NO and N_2O in a seasonally dry tropical forest, *Ecology*, *74*, 130–139.

Davidson, E. A., M. Keller, H. E. Erickson, L. V. Verchot, and E. Veldkamp (2000), Testing a conceptual model of soil emissions of nitrous oxides, *BioScience*, *8*, 667–680.

Dubrovsky, M., I. Nemesova, and J. Kalvova (2005), Uncertainties in climate change scenarios for the Czech Republic, *Clim. Res.*, *29*, 139–156.

Firestone, M. K., and E. A. Davidson (1989), Microbiological basis of NO and N_2O production and consumption in soil, in *Exchange of Trace Gases Between Terrestrial Ecosystems and the Atmosphere*, edited by M. O. Andreae and D. S. Schimel, pp. 7–21, John Wiley, Hoboken, N. J.

Forkel, R., and R. Knoche (2006), Regional climate change and its impacts on photooxidant concentrations in southern Germany: Simulations with a coupled regional climate-chemistry model, *J. Geophys. Res.*, doi:10.1029/2005JD006748, in press.

Galloway, J. N., et al. (2004), Nitrogen cycles: Past, present, and future, *Biogeochemistry*, *70*, 153–226.

Gasche, R., and H. Papen (1999), A 3–year continuous record of nitrogen trace gas fluxes from untreated and limed soil of a N-saturated spruce and beech forest ecosystem in Germany: 2. NO and NO_2 fluxes, *J. Geophys. Res.*, *104*, 18,505–18,520.

Giorgi, F., X. Q. Bi, and J. Pal (2004), Mean, interannual variability and trends in a regional climate change experiment over Europe: II. Climate change scenarios (2071–2100), *Clim. Dyn.*, *23*, 839–858.

Granli, T., and O. C. Bøckmann (Eds.) (1994), *Nitrous Oxide From Agriculture*, *Norw. J. Agric. Sci.*, suppl. 12, 128 pp.

Grell, G. A., S. Emeis, W. R. Stockwell, T. Schoenemayer, R. Forkel, J. Michalakes, R. Knoche, and W. Seidl (2000), Application of a multiscale, coupled MM5/chemistry model to the complex terrain of the VOTALP Valley campaign, *Atmos. Environ.*, *34*, 1435–1453.

Hanssen-Bauer, I., E. J. Forland, E. J. Haugen, and O. E. Tveito (2003), Temperature and precipitation scenarios for Norway: Comparison of results from dynamical and empirical downscaling, *Clim. Res.*, *25*, 15–27.

Intergovernmental Panel on Climate Change (1992), *IPCC, 1992: Climate Change 1992: The Supplementary Report to the IPCC Scientific Assessment*, 198 pp., Cambridge Univ. Press, New York.

Intergovernmental Panel on Climate Change (2001), *IPCC, 2001: Climate Change 2001: The Scientific Basis. Contribution of Working Group I to the Third Assessment Report of the Intergovernmental Panel on Climate Change*, 881 pp., Cambridge Univ. Press, New York.

Keeney, D. R., I. R. Fillery, and G. P. Marx (1979), Effect of temperature on the gaseous nitrogen products of denitrification in a silt loam soil, *Soil Sci. Soc. Am. J.*, *43*, 1124–1128.

Kesik, M., et al. (2005), Inventories of N_2O and NO emissions from European forest soils, *Biogeosciences*, *2*, 353–375.

Khalil, M. A. K., and R. A. Rasmussen (1992), The global sources of nitrous oxide, *J. Geophys. Res.*, *97*, 14,651–14,660.

Kiese, R., C. Li, D. W. Hilbert, H. Papen, and K. Butterbach-Bahl (2005), Regional application of PnET-N-DNDC for estimating the N_2O source strength of tropical rainforests in the wet tropics of Australia, *Global Change Biol.*, *11*(1), 128–144.

Kjellstrom, E. (2004), Recent and future signatures of climate change in Europe, *Ambio*, *33*, 193–198.

Knoche, R., R. Forkel, and H. Kunstmann (2003), Regionale Klimasimulationen für Süddeutschland und den Alpenraum, in *Forum für Hydrologie und Wasserbewirtschaftung*, vol. 1, pp. 11–18, ATV-DVWK, Hennef, Germany.

Kuenen, J. G., and L. A. Robertson (1987), Ecology of nitrification and denitrification, in *The Nitrogen and Sulphur Cycles: Symposia of the Society for General Microbiology*, vol. 42, edited by J. A. Cole and S. J. Ferguson, pp. 161–218, Cambridge Univ. Press, New York.

Li, C. (2000), Modeling trace gas emissions from agricultural ecosystems, *Nutr. Cycl. Agroecosyst.*, *58*, 259–276.

Li, C., S. Frolking, and T. A. Frolking (1992), A model of nitrous oxide evolution from soil driven by rainfall events: 1. Model structure and sensitivity, *J. Geophys. Res.*, *97*, 9759–9776.

Li, C., V. Narayanan, and R. Harris (1996), Model estimates of nitrous oxide emissions from agricultural lands in the United States, *Global Biogeochem. Cycles*, *10*, 297–306.

Li, C., J. Aber, F. Stange, K. Butterbach-Bahl, and H. Papen (2000), A process-oriented model of N_2O and NO emissions from forest soils: 1. Model development, *J. Geophys. Res.*, *105*, 4369–4384.

Ludwig, J., F. X. Meixner, B. Vogel, and J. Foerstner (2001), Soil-air exchange of nitric oxide: An overview of processes, environmental factors, and modelling studies, *Biogeochemistry*, *52*, 225–257.

Maracchi, G., O. Sirotenko, and M. Bindi (2005), Impacts of present and future climate variability on agriculture and forestry in the temperate regions: Europe, *Clim. Change*, *70*, 117–135.

Nommik, H. (1956), Investigations on denitrification in soil, *Acta Agric. Scand.*, *6*, 195–228.

Papen, H., and K. Butterbach-Bahl (1999), A 3–year continuous record of nitrogen trace gas fluxes from untreated and limed soil of a N-saturated spruce and beech forest ecosystem in Germany: 1. N_2O emissions, *J. Geophys. Res.*, *104*, 18,487–18,503.

Pilegaard, K., P. Hummelshøj, and N. O. Jensen (1999), Nitric oxide emission from a Norway spruce forest floor, *J. Geophys. Res.*, *104*, 3433–3445.

Potter, C. S., P. A. Matson, P. M. Vitousek, and E. A. Davidson (1996), Process modelling of controls on nitrogen trace gas emissions from soils worldwide, *J. Geophys. Res.*, *101*, 1361–1377.

Räisänen, J., U. Hansson, A. Ullerstig, R. Döscher, L. P. Graham, C. Jones, H. E. M. Meier, P. Samuelsson, and U. Willén (2004), European climate in the late twenty-first century: Regional simulations with two driving global models and two forcing scenarios, *Clim. Dyn.*, *22*, 13–31.

Sandnes-Lenschow, H., and S. Tsyro (2000), Meteorological input data for EMEP/MSC-W air pollution models, *EMEP MSC-W Note 2/2000*, Norw. Meteorol. Inst., Oslo.

Simpson, D., H. Fagerli, J. E. Jonson, S. Tsyro, P. Wind, and J.-P. Tuovinen (2003), The EMEP Unified Eulerian Model: Model description, *EMEP MSC-W Report 1/2003*, Norw. Meteorol. Inst., Oslo.

Smith, K. A. (1980), A model of the extent of anaerobic zones in aggregated soils, and its potential application to estimates of denitrification, *J. Soil Sci.*, *31*, 263–277.

Smith, K. A. (1997), The potential feedback effects induced by global warming on emissions of nitrous oxide by soils, *Global Change Biol.*, *3*, 327–338.

Stange, F., K. Butterbach-Bahl, and H. Papen (2000), A process-oriented model of N_2O and NO emissions from forest soils: 2. Sensitivity analysis and validation, *J. Geophys. Res.*, *105*, 4385–4398.

Valente, R. J., and F. C. Thornton (1993), Emissions of NO from soil at a rural site in central Tennessee, *J. Geophys. Res.*, *98*, 16,745–16,753.

Van Dijk, S. M., and J. H. Duyzer (1999), Nitric oxide emissions from forest soils, *J. Geophys. Res.*, *104*, 15,955–15,961.

Wang, G. (2005), Agricultural drought in a future climate: Results from 15 global climate models participating in the IPCC 4th assessment, *Clim. Dyn.*, *25*, 739–753.

Zechmeister-Boltenstern, S., M. Hahn, S. Meger, and R. Jandl (2002), Nitrous oxide emissions and nitrate leaching in relation to microbial biomass dynamics in a beech forest soil, *Soil Biol. Biochem.*, *34*, 823–832.

N. Brüggemann, K. Butterbach-Bahl, R. Forkel, M. Kesik, R. Kiese, and R. Knoche, Institute for Meteorology and Climate Research, Atmospheric Environmental Research (IMK-IFU), Karlsruhe Research Center, Kreuzeckbahnstr. 19, DE-82467 Garmisch-Partenkirchen, Germany. (nicolas.brueggemann@imk.fzk.de; klaus.butterbach@imk.fzk.de; renate.forkel@imk.fzk.de; magda.kesik@imk.fzk.de; ralf.kiese@imk.fzk.de; hans-richard.knoche@imk.fzk.de)

C. Li, Complex Systems Research Center, Institute for the Study of Earth, Oceans and Space, University of New Hampshire, Morse Hall, Durham, NH 03824, USA. (changsheng.li@unh.edu)

G. Seufert, Institute for Environment and Sustainability, Joint Research Centre, I-21020, Ispra, Italy. (guenther.seufert@jrc.it)

D. Simpson, Norwegian Meteorology Institute, EMEP MSC-W, P.B. 43 Blindern, Oslo, Norway. (david.simpson@met.no)

Geomicrobiology Journal, 23:165–176, 2006

ISSN: 0149-0451 print / 1521-0529 online
DOI: 10.1080/01490450600599221

Taylor & Francis
Taylor & Francis Group

Production of NO and N_2O by the Heterotrophic Nitrifier *Alcaligenes faecalis parafaecalis* under Varying Conditions of Oxygen Saturation

S. A. Blagodatsky, M. Kesik, H. Papen, and K. Butterbach-Bahl
Institute for Meteorology and Climate Research, Atmospheric Environmental Research, Research Centre Karlsruhe, Garmisch-Partenkirchen, Germany

Production of NO and N_2O by the heterotrophic nitrifier *Alcaligenes faecalis* subsp. *parafaecalis* was studied during growth in batch and continuous culture on peptone-meat extract medium. Depending on oxygen saturation level, medium redox status and amount of substrate supplied, the microorganisms produced 0.002–0.25 mg NO-N h^{-1} (g protein)$^{-1}$ and 0.16–2.4 mg N_2O-N h^{-1} (g protein)$^{-1}$. Maximum rates of nitrogen oxides production were observed during peak events initiated by sudden changes of oxygen supply in the medium and were due to combined nitrification/denitrification taking place simultaneously within the cells. Based on model simulations of enzymatic kinetics of denitrification, possible mechanisms of increased nitrogen oxides production during periods of changes in oxygen supply are suggested.

Keywords aeration, *Alcaligenes faecalis parafaecalis*, heterotrophic nitrification, NO production, N_2O production

INTRODUCTION

Increasing concentrations of primarily and secondarily radiative active trace gases in the atmosphere, such as carbon dioxide (CO_2), methane (CH_4), nitrous oxide (N_2O) and nitric oxide (NO), are responsible for the observed global warming. For all mentioned trace gases the biosphere can function both as a significant sink as well as source. Especially, with regard to NO and N_2O soils have been found to be significant sources within the global atmospheric N-budget. In spite of scientific efforts made in the last decades, the mechanisms controlling the emission of N-trace gases from soils are still not fully understood (Conrad 2002). This is mainly due to the multiple interacting biotic and abiotic factors that affect the emission strength for these gases. The key for predicting N trace gas emissions is a thorough understanding of the particular conditions and mechanisms regulating the chains of enzymatic reactions in microbial cells summarized as nitrification and denitrification.

Nitrification is the oxidation of ammonia to nitrite and further to nitrate. Autotrophic bacteria gain energy from the oxidation of ammonia i.e., *Nitrosomonas sp.* or nitrite i.e., *Nitrobacter sp.* and obtain cell carbon from carbon dioxide fixation (Wood 1986). A wide range of heterotrophic organisms oxidizes ammonia to nitrate (or in some cases to nitrite and other intermediates). We will call this process heterotrophic nitrification (Conrad 2002) having in mind that to our current knowledge organisms do not gain energy for growth from these processes per se and need an organic source of energy for growth.

The role of heterotrophic (bacterial and fungal) and autotrophic nitrification in production and emission of gaseous nitrogen oxides from soils is still under discussion. Different authors have suggested that at least in soils with low pH (as acid forest soils) heterotrophic nitrification could be the dominant source of NO and N_2O production (Anderson et al. 1993; Killham 1990; Papen and Berg 1998), since autotrophic nitrifiers are highly sensitive to low pH values (de Boer and Kowalchuk 2001; Prosser 1989). Common soil bacteria genera such as *Pseudomonas* and *Alcaligenes* were found to show heterotrophic nitrification activity (Daum et al. 1998; Kuenen and Robertson 1994; Papen et al. 1989;) and in view of their high biomass level in many forest soils these microorganisms are most likely significant contributors to NO and N_2O emissions from soils (Papen and Berg 1998). A direct determination of the contribution of heterotrophic nitrifiers to the NO and N_2O emissions cannot be performed at present due to the lack of selective inhibitors (Conrad 2002; Pennington and Ellis 1993). Reliable prediction of emission rates of NO and N_2O from soils

Received 7 July 2005; accepted 14 November 2005.
We thank Dr. Ralf Kiese, Dr. Rainer Gasche and Dr. Markus Teuber for scientific advice and Elisabeth Zumbusch and George Willibald for expert technical assistance. The work was supported by the European Commission in the NOFRETETE project (EVK2-CT2001-00106) of the fifth framework program. We would like to thank two anonymous reviewers for their helpful comments on earlier version of this manuscript.
S. A. Blagodatsky is also affiliated with the Institute of Physicochemical and Biological Problems in Soil Science, Pushchino, Russia.
Address correspondence to S. Blagodatsky, Institute of Physicochemical and Biological Problems in Soil Science Russian Academy of Science, 142290 Pushchino, Russia. E-mail: sblag@itaec.ru

is even more difficult due to a high temporal and spatial variability of these processes. However, comprehensive understanding of mechanism of heterotrophic nitrification based on the detailed physiological studies in batch and continuous cultures is needed.

In the last 15 years, new metabolic pathways were discovered showing a great flexibility of microorganisms to metabolize nitrogen compounds (Jetten et al. 1997). Some microorganisms are capable of performing simultaneous biochemical reactions in oxidative (nitrification) and reductive (denitrification) ways. The so-called aerobic denitrification can be designated as an ability of microorganisms to simultaneously use two different electron acceptors: oxygen and oxidized forms of nitrogen: nitrate, nitrite, NO, N_2O (Kuenen and Robertson 1994). Denitrifiers typically found in soils (Gamble et al. 1977) are also often capable of performing heterotrophic nitrification and completing aerobic denitrification (Patureau et al. 2000), so that in the end the combination of nitrification and denitrification processes leads to the production of NO and N_2O (Kuenen and Robertson 1994; Papen and Berg 1998; Robertson and Kuenen 1990). Furthermore, the common view of denitrification and nitrification as strictly separated processes controlled by the aeration status of the soil, needs to be reconsidered as experimental results provide increasing evidence for a combined process of aerobic denitrification and heterotrophic nitrification for several organisms (Robertson et al. 1989).

In Figure 1 a scheme of possible metabolic pathways leading to the emission of NO and N_2O by nitrifying heterotrophs is given. The most striking point is that during such a hybrid nitrification-denitrification process microorganisms can produce remarkably high quantities of NO and N_2O. This phenomenon was demonstrated for N_2O production by *Alcaligenes faecalis* in transient conditions of a chemostat culture by Otte et al. (1996). However, these authors did not consider NO production. Kester and co-authors (1997) observed transitional increase in NO and N_2O production by the autotrophic nitrifier *Nitrosomonas europaea* and by the denitrifiers *Alcaligenes eutrophus* and *Pseudomonas stutzeri* in chemostat cultures with transient conditions of oxygen saturation. But in this experiment (Kester et al. 1997) heterotrophic microorganisms were supplied with nitrates, so that the produced NO and N_2O originated mainly from denitrification and not from the combined processes of heterotrophic nitrification and aerobic denitrification. Therefore, the mechanisms of NO and N_2O production by heterotrophic nitrifiers deserves further investigations. The available data suggest that—in order to improve our understanding of tightly coupled nitrification-denitrification processes—special emphasis should be given to short-term changes of fluxes of these gases in periods of transitional changes in oxygen supply.

The objective of our study was to investigate the dynamics of NO and N_2O production by *Alcaligenes faecalis* subsp. *parafaecalis* during growth in a peptone meat-extract medium under steady-state conditions at different levels of air saturation and during the transient phase from aerobic to anaerobic conditions and vice versa.

MATERIALS AND METHODS

Organism and Media

The chemoorganotrophic bacterium *A. faecalis* subsp. *parafaecalis* was used in this study. The strain (DSM 13975) was

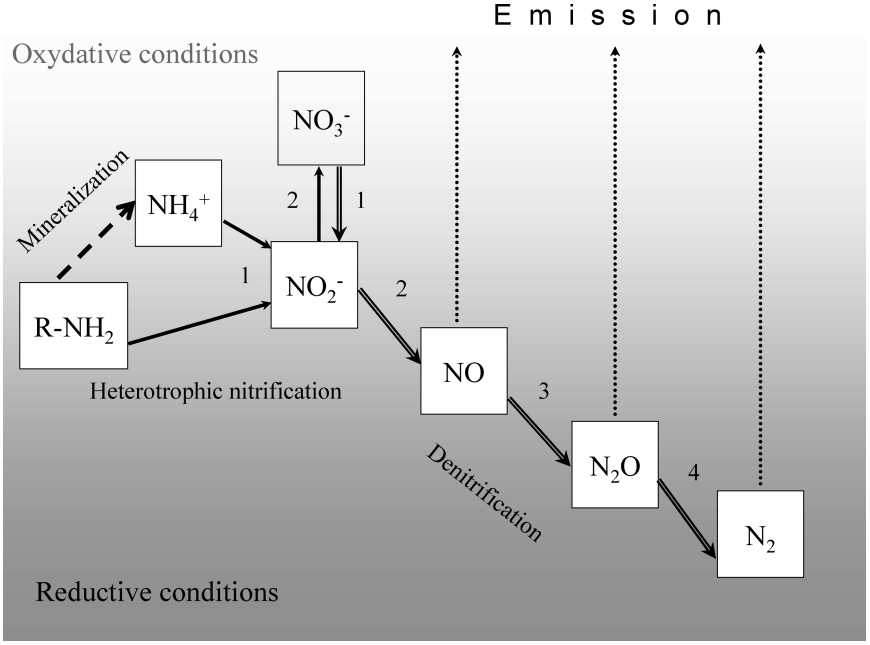

FIG. 1. Summary of processes leading to N oxides production in cultures of *Alcaligenes faecalis parafaecalis*.

provided by the German collection of microorganisms and cell cultures (DSMZ, Braunschweig). Experiments on heterotrophic nitrification and nitrogen oxide production were performed as batch and continuous cultures using peptone meat-extract (PM) media: 5 g of peptone from meat (Merck, Darmstadt, Germany) and 3 g extract of meat (Merck) per liter of aqua bidest. The mean.C:N ratio of the medium was 2.6. PM media diluted by distilled H_2O in ratio 1:2 was used in continuous culture experiments in order to have growth of *A. faecalis* subsp. *parafaecalis* limited by carbon source.

Culture Methods

Prior to further cultivation, samples from stock cultures were cultured on PM-agar medium (as described above but with 1.5% (wt/vol) agar). Precultures (300 ml) were made at 28°C and 150 rpm on a rotary shaker. Mid-log washed cells of *A. faecalis* subsp. *parafaecalis* (10 ml for batch culture and 150 ml for continuous culture) were added to fresh medium (2.5 1) in the BioFlo III batch/continuous chemostat (New Brunswick Scientific, Nürtingen, Germany). Cultures were grown in batch conditions, i.e., without fresh medium supply, during the first 10–l5 hours after addition of microorganisms to the chemostat vessel. Hourly sampling for microbial biomass estimations during initial phase of growth were performed only in two cases (results are shown on Figure 2). During two experiments in which continuous steady-state growth was reached we manipulated the oxygen saturation level. Other experiments with continuous cultivation were used for studying effects of pH and temperature on NO and N_2O emissions (Kesik et al., 2006).

Batch and continuous cultures were incubated at 28°C and continuously sparged (1 1 min^{-1}) with filtered (pore size 0.2 μm) air or with a defined mixture of N_2 and O_2. In addition the medium was stirred at 100 or 300 rpm. Dissolved oxygen concentration (% air saturation), redox potential and pH of the media were monitored automatically by the dissolved oxygen sensor inPro 6800, redox and pH electrodes (all sensors: Mettler Toledo, Switzerland). Data were acquired with the "Advanced Fermentation Software" (New Brunswick Scientific, Nürtingen, Germany), which controlled the BioFlo III chemostat. Experiments in continuous cultures were conducted at a constant pH (7.0) with a medium dilution rate of 0.1 h^{-1} if another value is not stated in the text. In part of the experiments the level of air saturation was kept at a predetermined value by automatic regulation of N_2 and O_2 (or synthetic air) flow rates using the Advanced Fermentation Software and mass-flow controllers (Tylan FC 280 SA, UK).

Culture samples (8 ml) were aseptically taken every hour by using the automated MX3 Biosampler (New Brunswick Scientific, Nürtingen, Germany). After optical density measurements, subsamples of the supernatant (14,000 g) were taken for further analysis of NH_4^+, NO_3^- and NO_2^-, and immediately frozen in liquid nitrogen. Pellets were washed twice with weak phosphate buffer (0.01 M, pH 7.6) and resuspended before freezing. The purity of the culture was routinely checked by microscopy and by plating on PM agar.

Gas concentrations of NO, N_2O and CO_2 were measured in the outflowing air of the chemostat either by direct continuous analysis (NO and CO_2) or by hourly sampling and subsequent analysis.

Analytical Procedures

The optical density of cell suspension was measured spectrophotometrically at 600 nm. Nitrite and nitrate concentrations were determined immediately after thawing of the supernatant samples, which were stored frozen at −20°C. NO_2^- was determined colorimetrically (Griess-Ilosvay reaction) at 546 nm by the method of Snell and Snell (1949). NO_3^- and NH_4^+ were determined colorimetrically with salicylic acid (Cataldo et al. 1975) and by the hypochlorite method (DIN 38406-E5), respectively. After thawing, subsamples of washed cell suspension were taken for protein determination by the modified Lowry method (Herbert et al. 1971) and for C and N determination with a CN analyser (DIMATOC 2000, Dimatec Analysentechnik GmbH, Essen, Germany).

N_2O concentrations in the outflow air were measured by taking air samples with a gas tight syringe and subsequent analysis with a gas chromatograph (GC-14A, Shimadzu, Japan) equipped with a ^{63}Ni electron capture detector and a packed 3 m 1/8″ column filled with Porapak-N. CO_2 concentrations in the outflowing air were measured with an infrared gas analyser (Binos, Leybold-Heraeus, Germany), whereas NO concentrations were measured with a highly sensitive chemoluminescence detector (CLD 770 AL ppt plus photolysis converter PLC 760, Ecophysics AG, Durnten, Switzerland). Data on NO and CO_2 concentration were obtained every 3 minutes and were automatically stored on computer hard disk. Details of calibration procedures and measurement techniques for NO and N_2O are described elsewhere (Butterbach-Bahl et al. 1997; Papen and Butterbach-Bahl 1999).

Analytical measurements were made in duplicate, gas production rates were calculated as mean values for at least 10 readings. Simulation of nitrification, denitrification, associated NO and N_2O production and enzyme activities was done by the use of ModelMaker Software (Cherwell Scientific Publishing).

RESULTS

In batch culture and at constant rate of air supply the transition from aerobic to oxygen limited micro-aerobic growth conditions was due to oxygen consumption of the respiring growing cell population (Figure 2A). Microbial biomass growth in batch culture was preceded by a short lag-phase (Figure 2A). The following exponential increase in microbial biomass C and corresponding increase in CO_2 evolution rate (Figure 2A) were observed from the 4th to the 9th hour of cultivation. During this time span the specific growth rate (μ) of *A. faecalis parafaecalis*

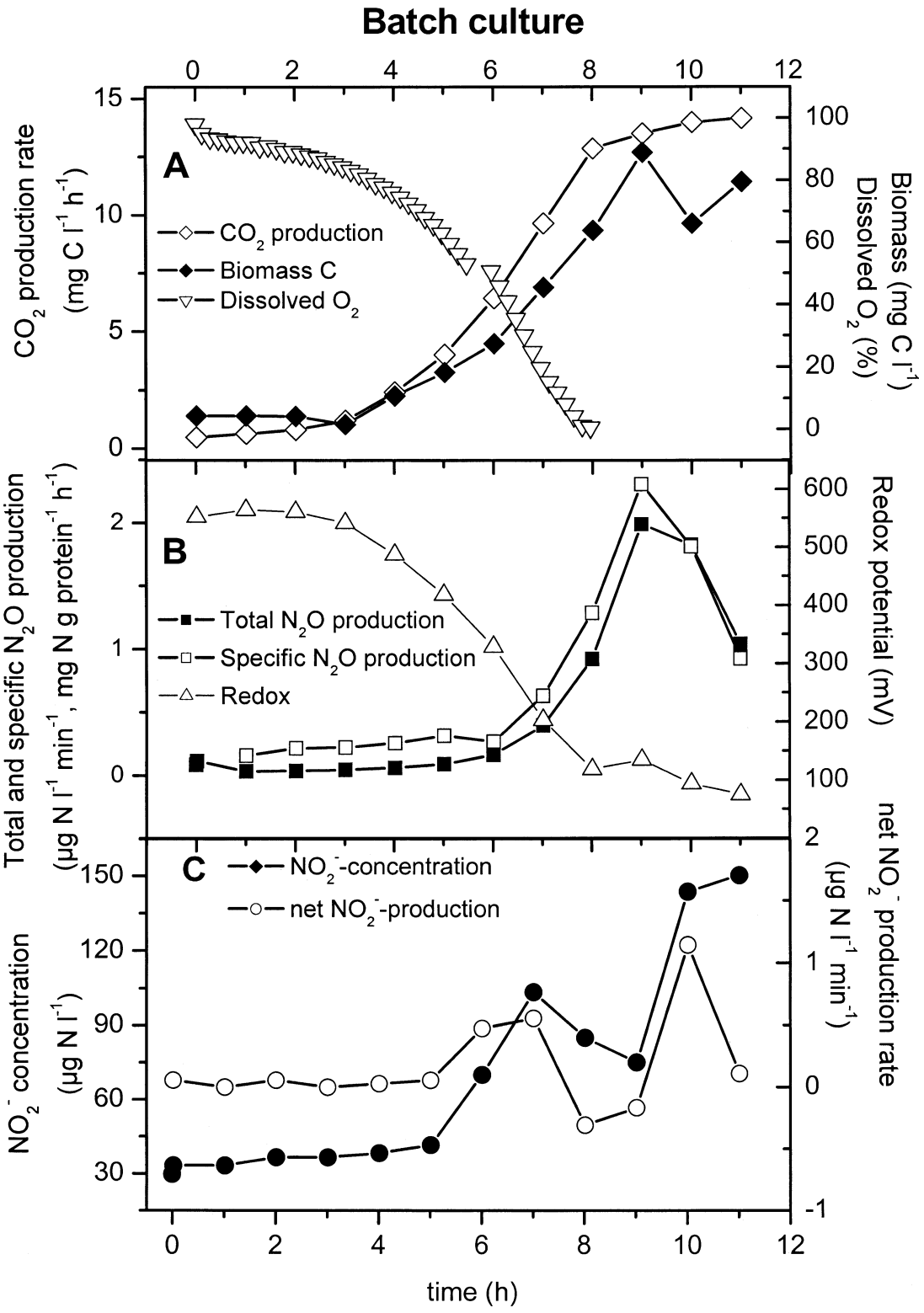

FIG. 2. CO_2 production rate, dissolved oxygen and microbial biomass C (A), redox potential, total and specific N_2O production rate (B), and NO_2^- concentration and net NO_2^- production rate (C) in batch culture *of Alcaligenes faecalis* subsp. *parafaecalis*.

was 0.46 h^{-1}. The decrease in redox potential (Figure 2B) was in accordance with changes in oxygen concentration and biomass growth as shown at Figure 2A. In these batch experiments the substrate pH value was not fixed and increased gradually from 7.0 at the beginning to 7.2 at the end of the experiments.

N_2O production by the bacterial culture increased exponentially with 2 hours delay as compared to the increase in biomass and C_2O production (Figure 2B). The specific rate of N_2O production increased from the 7th to the 9th hour of incubation, meanwhile nitrite concentrations—produced via heterotrophic nitrification activity of the bacteria—in the medium already decreased after having reached a maximum at 7 hours after the start of incubation (Figure 2C). The maximum specific net N_2O production (2.4 mg N_2O-N g protein^{-1} h^{-1}) was observed at a late exponential phase of the batch culture at times with already decreasing nitrite concentrations. This indicates that the denitrification process had already been initialized and that the combined processes of heterotrophic nitrification and denitrification contributed to the N_2O production during this period of time. At the stationary phase (>11 h) the total rate of N_2O production was still high but variable (1–1.4 μg N_2O-N l^{-1} min^{-1}—data not shown), whereas the specific N_2O production rate gradually decreased to values lower than 1 μg N_2O-N mg protein^{-1} h^{-1}. Nitrite concentration during the stationary phase varied in a range of 105–155 μg N l^{-1} with mean value 137 μg N l^{-1}.

Since the addition of nitrite to autoclaved medium, which had not been inoculated with bacteria, did not lead to the production of NO or N_2O at pH level used in our experiment, chemodenitrification can be excluded as a source of NO and N_2O production, i.e., both gases must have been produced by microbiological processes.

Figure 3 gives an example of experiment performed in continuous culture in order to clarify how the release of NO and N_2O was affected by controlled changes in the oxygen supply. In this case, only the O_2 concentration in the medium was changed, whereas other factors such as the dilution rate and nutrients concentration in the medium were kept constant. Steady-state conditions in terms of microbial biomass concentration were established for the first time after approximately 40 hours. The graph indicates that (i) rates of net NO, N_2O and NO_2^- production are depending on the oxygen concentration within the medium, and (ii) highest levels of net NO production (>50 μg NO-N l^{-1} h^{-1}) were observed in a short-term transition phase directly after the O_2 supply had been switched off and the medium was purged with N_2 (air saturation during this time period was approx. 0.l–1.5%, i.e., microaerobic growth conditions). This forced oxygen limitation led to a decrease in microbial biomass from 98 to 32 mg protein l^{-1} and a decrease in CO_2 production rate by microbes (Figure 3, Table 1). A new equilibrium was reached after 30 hours. The results obtained from continuous culture experiments are summarized in Figure 4 and Table 1. Figure 4A shows that net production of nitrite sharply decreased from >5 mg N g^{-1} protein h^{-1} to <4.2 mg N g^{-1} protein h^{-1} when levels of air saturation dropped to values <11%. In contrast, the production of NO and N_2O showed an optimum at approx. 6.5% air saturation (Figure 4A) with values of 0.25 ± 0.02 mg N g^{-1} protein h^{-1} (NO) and 2.0 ± 0.2 mg N g^{-1} protein h^{-1} (N_2O). At higher O_2 supply rates (air saturation >11%) rates of net NO and N_2O production were in a range of 0.002–0.078 mg N g^{-1} protein h^{-1} (NO) and 0.44–1.03 mg N g^{-1} protein h^{-1} (N_2O), whereas at microaerobic conditions (0.1% air saturation) rates of net NO and N_2O production were 0.06 and 0.23 mg N g^{-1} protein h^{-1}, respectively (Figure 4A). The relationship between O_2 concentration and net N_2O production found in the continuous culture experiments was in general agreement with those obtained in the batch culture experiments (see e.g., Figure 4A and Figure 2A, 2B). However, in batch culture experiments highest N_2O production was observed at oxygen concentrations close to zero (<0.5%), whereas in continuous culture experiments maximum rates of N_2O production were observed for an air saturation level of 6%. Ratios of net N_2O to net NO production varied substantially with the availability of O_2 in the medium and were as low as 3.7 at 0.1% air saturation and as high as 181 at 81% air saturation (Figure 4B).

Changes in rates of net NO_2^-, N_2O and NO production at 121 hours of incubation (Figure 3) were caused by the abrupt change of the aeration status of the continuous culture of *A. faecalis parafaecalis*. During the transition period from aerobic to anaerobic growth a huge peak in the net NO production rate (>1 mg N (g protein)$^{-1}$ h^{-1}) was observed (Figure 3), whereas the net N_2O production increased only slightly. According to our calculations, the decrease in NO_2^- concentration during the transition to anaerobic growth can only be explained by simultaneous decrease of nitrite production via heterotrophic nitrification from 7.3 to 1.5 mg (g protein)$^{-1}$ h^{-1} (Figure 3, 12–37 h), and the reductive consumption of NO_2^- to NO by denitrification. Resupplying the micro-aerobically growing culture with O_2 until an air saturation level of approx. 50% was reached, led to a sharp increase in rates of net N_2O and NO_3^- (Table 1) production, a slight increase in net NO production and in a marked decrease in net NO_2^- production (Figure 3, 165 h).

DISCUSSION

Rates of NO and N_2O Production by *A. faecalis* subsp. *parafaecalis*

The specific nitric and nitrous oxide production rates determined in our experiments with *A. faecalis* subsp. *parafaecalis* varied in a range of 0.002–0.253 mg NO-N g^{-1} protein h^{-1} and 0.16–2.4 mg N_2O-N g^{-1} protein h^{-1}. These values are comparable to those reported for *A. faecalis* DSM 30030 by Papen and coauthors (1989) and, as concerned to N_2O production rate, for *A. faecalis* TUD LMD 89.147 (Otte et al. 1996). However, our estimations of N_2O production rates were remarkably higher than values found for another strain of this microorganism (Anderson

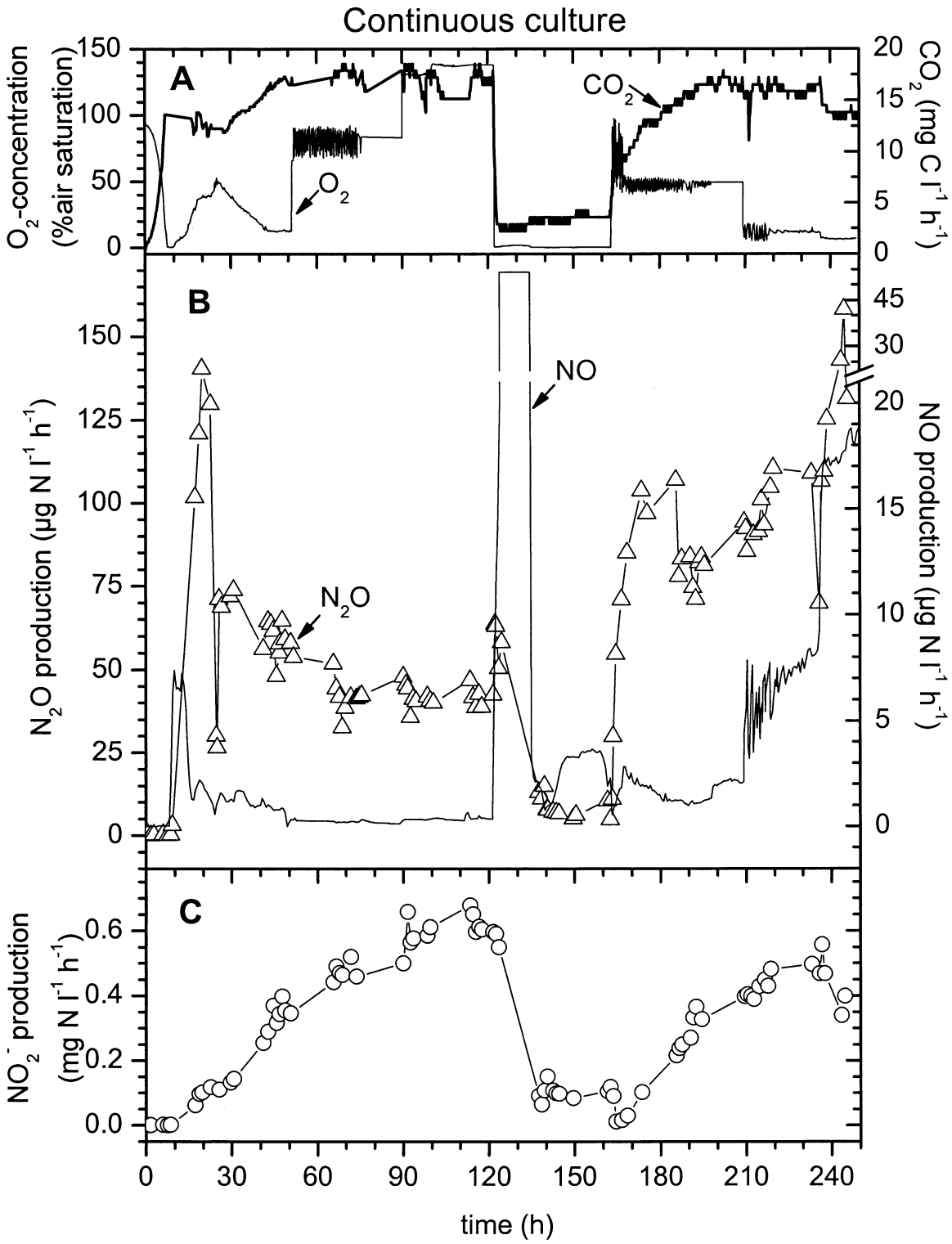

FIG. 3. Effect of different levels of air saturation on CO_2 production rate (A), net rates of N_2O, NO (B) and NO_2^- production (C) in continuous culture of *Alcaligenes faecalis* subsp. *parafaecalis*.

TABLE 1
Effect of dissolved oxygen concentration on N transformation rates in continuous culture of *Alcaligenes faecalis* subsp. *parafaecalis*

	Oxygen concentration in the media (% of air saturation)					
Measured N concentrations, mg l^{-1}	131 ± 1.4	81 ± 7	47.9 ± 2	11.7 ± 0.6	6.5 ± 0.3	0.1 ± 0.02
NH_4^+ in supplied medium	28 ± 3	28 ± 3	28 ± 3	28 ± 3	28 ± 3	28 ± 3
NH_4^+ in cultivation vessel	40.2 ± 3.2	32.9 ± 5.5	27.6 ± 1.3	36.8 ± 1.2	39.9 ± 3.8	20.9 ± 0.2
$\triangle NH_4^+$	12.2	4.75	−0.55	8.65	11.75	−7.25
NO_2^- in supplied medium	0.01 ± 0.002	0.01 ± 0.002	0.01 ± 0.002	0.01 ± 0.002	0.01 ± 0.002	0.01 ± 0.002
NO_2^- in cultivation vessel	6.25 ± 0.23	4.94 ± 0.1	3.4 ± 0.3	5.02 ± 0.21	3.08 ± 0.92	1.17 ± 0.1
$\triangle NO_2^-$	6.24	4.89	3.39	5.01	3.07	1.16
NO_3^- in supplied medium	0.48 ± 0.08	0.48 ± 0.08	0.48 ± 0.08	0.48 ± 0.08	0.48 ± 0.08	0.48 ± 0.08
NO_3^- in cultivation vessel	2.95 ± 0.6	2.9 ± 1.5	3.5 ± 0.3	3.7 ± 0.7	4.3 ± 0.7	0.64 ± 0.05
$\triangle NO_3^-$	2.47	2.42	3.98	2.33	4.27	0.16
N biomass	36 ± 1	30.5 ± 2	21.2 ± 2.7	32.4 ± 2.5	26.0 ± 0.4	10.6 ± 0.6
Protein biomass, mg l^{-1}	97.9 ± 2.1	91 ± 1.2	61.8 ± 6.8	95.8 ± 5.3	72.0 ± 2.4	31.9 ± 4.4
Specific respiration rate, g C-CO_2 g^{-1} protein h^{-1}	0.22 ± 0.06	0.19 ± 0.01	0.26 ± 0.03	0.17 ± 0.01	0.19 ± 0.004	0.11 ± 0.02
Calculated N transformation rates, mg N g^{-1} protein h^{-1}						
NH_4^- production/consumption rate	12.2	5.1	−0.9	8.8	16.0	−22.3
Net NO_2^- production rate	6.2	5.3	5.3	5.1	4.18	3.56
Net NO_3^- production rate	2.5	2.6	4.8	3.3	5.2	0.0
Net NO production rate	0.003	0.002	0.020	0.078	0.253	0.061
Net N_2O production rate	0.44	0.44	1.31	1.03	2.04	0.23

The medium (peptone-meat extract) dilution rate was 0.1 h^{-1}. SD is shown for averaged values (3–8 samples taken during steady-state conditions of continuous culture).

et al. 1993), other heterotrophic nitrifiers and *Nitrosomonas europea* ATCC19718 (Table 2). Rates of NO production measured in our experiments are in a comparable range as reported rates of NO production by *N. europaea* ATCC19718 (Anderson et al. 1993; Kester et al. 1997), Table 2. However, the specific nitrification rates of autotrophic ammonia oxidizers are usually significantly higher than nitrification rates of heterotrophs (Kuenen and Robertson 1994). NO and N_2O production rates for *N. europaea* strain 28 measured by Remde and Conrad (1990) were approximately 10–100 times higher (Table 2) than our values, but also higher than the values obtained for *N. europaea* by Anderson with co-authors (1993) or Kester with co-authors (1997). Remde and Conrad (1990) were able to demonstrate that NO and N_2O were produced by the reduction of nitrite, after nitrite had accumulated in the media. Nevertheless the very high rates of NO and N_2O production are still surprising and may be due to a more active strain used in this experiment as well as due to the fact that Remde and Conrad (1990) investigated NO and N_2O production in washed cell suspension taken from batch culture and not in continuous culture as done by others. The co-culture of *N. europaea* with *Nitrobacter winogradskii,* which is able to transform nitrite to nitrate, shows a negligible production of NO and N_2O (Kester et al. 1997). This means, that the reductive production of NO and N_2O by autotrophic nitrifiers may only start from nitrite.

The span of measured rates of NO and N_2O productions by the culture of *A. faecalis* subsp. *parafaecalis* is rather high. Low and high limits for NO production rate differ by more than 2 orders of magnitude, N_2O production rates differ by more than a factor of 10. With regard to NO production this huge span can be explained by its sensitivity to the concentration of dissolved oxygen in the media and to the redox status. In our experiments highest rates of NO production were recorded at low (6.5% air saturation) but not at the lowest or zero concentrations of dissolved oxygen in medium (Table 1), which is in accordance with the results obtained for *Pseudomonas stutzeri* (Körner and Zumft 1989) and in soil studies (Bollmann and Conrad 1998; McKeeney et al. 2001). Highest rates of N_2O production were observed at the late exponential stage of the batch culture (Figure 2C) and during the transient state in continuous culture. These peak values for NO and N_2O production rates were recorded during short-term periods that were caused by changing the oxygen concentration in media. However, it is important to emphasize that during the change from high to low oxygen saturation levels the peak in NO production was comparable or even more pronounced as for N_2O, whereas during the inverse transition from low to high oxygen saturation levels only the N_2O production increased markedly but not the NO production (Figure 3). We hypothesize that the different behaviour during the transition phase from oxygenated medium to oxygen-free medium and

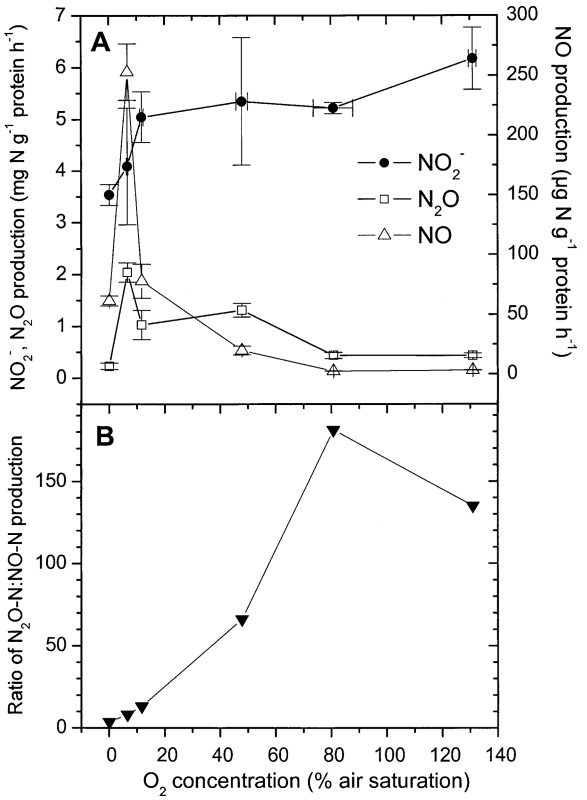

FIG. 4. Specific net NO_2^-, N_2O and NO production rates (A) and ratio of N_2O: NO production (B) in dependence from air saturation in continuous culture of *Alcaligenes faecalis* subsp. *parafaecalis*.

vice versa is due to a higher sensitivity of the N_2O-reductase to oxygen in comparison with the NO-reductase. This means that short-term increases in oxygen concentration of the media affected the activity of the enzymes nitrite reductase and NO-reductase in equal extent. Consequently the production of NO was still counterbalanced by its reductive consumption to N_2O, whereas the reduction of N_2O to N_2 was suppressed by the increase in oxygen concentration. As a result we observed a distinct increase in N_2O production with re-aeration, while such an increase was not observed for NO production. The different sensitivities of the N_2O- or NO-reductase to oxygen can also be used to explain the increase in the N_2O/NO ratio at elevated medium oxygen concnetrations (Figure 4B). Another explanation for this phenomenon would be the chemical or biological (Baumgartner et al. 1996) NO oxidation in medium with higher oxygen saturation levels. However, there is no evidence for such a mechanism.

High production rates of NO and N_2O during the change in aeration status (oxygen availability) is a general phenomenon that has been observed for autotrophic (Kester et al. 1997; Remde and Conrad 1990) as well as for heterotrophic nitrifiers that possess the ability to denitrify (N_2O was measured by Otte et al. 1996, N_2O and NO in this work) and for denitrifying bacteria (Baumann et al.1996; McKenney et al. 1994). It is likely that in all three cases the main source of NO and N_2O production is the reductive production of these gases by denitrification reactions, i.e., that we do have to acknowledge nitrifier denitrification. However, the high rates of N trace gas production during the transition phase can only be explained by the assumption that subsequent reductive denitrification reactions are not balanced, i.e., that the further reduction of N-oxides is inhibited. The reduction rates, in turn, are controlled by activities of respective denitrification enzymes and by the oxygen concentration. In the following we hypothesize a mechanism based on the enzymatic activity and O_2 concentration to explain the observed NO and N_2O production dynamics in our experiments.

Simulation of the NO and N_2O Peak Production in Transient Regime

The observed time course of net NO and N2O production by *A. faecalis* subsp. *parafaecalis* was simulated according to the concept of coupled nitrification-denitrification processes (Figure 1). Our approach is based on existing knowledge connecting the nitrogen oxides reduction rates with availability of substrate and activity of respective enzymes (Betlach and Tiedje 1981; Dendooven et al. 1994; Dendooven and Anderson 1995; Leffelaar and Wessel 1988). Differential equations used for the description of substrate conversion rates and parameter values are given in the Appendix.

In our model we used the following assumptions:

- Rates of NO_3^-, NO_2^-, NO and N_2O transformations depend on concentrations of respective nitrogen compounds and the relative activity of respective denitrification enzymes;
- Microbial biomass concentration and quantity of C and energy sources are assumed to be constant or are assumed to not influencing the rates of N transformations;
- The rate of nitrite production by heterotorophic nitrification depends only on O_2 level. An excess of ammonium was always observed in simulated experiments, that is why we assume that nitirification was not substrate limited.

In the model the medium oxygen concentration was controlled by the partial oxygen pressure in the supplied airflow (Eq. 1). Kinetics of denitrification enzyme induction/repression was described using the "activity" function (Blagodatsky, Richter 1998; Li et al. 2000), which takes values from 0 to 1 (Eq. 2). The activity of denitrification enzymes depended on the anaerobic volume fraction (anvf) of the medium and was calculated separately for each enzyme (Eq. 3). The empirical anvf-function (Li et al. 2000) describes the occurrence of anaerobic zones in dependence of the oxygen partial pressure and O_2 consumption due to microbial metabolism. The values of parameters p_NaR, p_NiR, p_NOR and p_N_2OR determine different sensitivities of corresponding enzymes to the oxygen level. The

TABLE 2
Compilation of reported N oxides production rates and nitrification rates by pure cultures of heterotrophic and autotrophic nitrifiers

Microorganism	Growth conditions	NO production rate, mg N g^{-1} protein h^{-1}	N_2O production rate, mg N g^{-1} protein h^{-1}	NO_2^-/NO_3^- production, mg N g^{-1} protein h^{-1}	Reference
Alcaligenes faecalis DSM 30030	Batch culture[a] peptone-meat medium, aerobic[b]	0.322	0.406	74.76 (NO_2^-) 36.4 (NO_3^-)	Papen et al. (1989)
	Ammonium-citrate medium, aerobic[b]	0.196	8.26	39.06 (NO_2) 15.54 (NO_3^-)	
A. faecalis ATCC 8750	Batch culture,[a] pO_2 = 1.6 kPa, ammonium-citrate medium	0.0106	0.0595	Net consumption of NO_2^- no NO_3^- produced	Anderson et al. (1993)[c]
A. faecalis TUD LMD 89.147	Continuous culture, ammonium-acetate medium	ND[d]	0.7–12.74	0.7–1.82 NO_2^- production	Otte et al. (1996)[c]
A. faecalis subsp. *parafaecalis* DSM 13975	Batch culture,[a] peptone-meat medium	ND	0.16–2.42	From net consumption till 11.14(NO_2^-)	This publication; see details in text
	Continuous culture, peptone-meat medium	0.002–0.25 (>1 at transient conditions)	0.17–2.0 (4.8 at transient conditions)	0.11–6.2 (NO_2^-)	
Paracoccus pantotrophus (*Thiosphaera pantotropha* LMD 92.63)	Continuous culture, ammonium acetate medium	ND	4.06–20.02	16.8–56.7[e]	Arts et al. (1995)
Pseudomonas putida DSMZ-1088-260	Batch culture,[a] mineral medium with amino-N	0.21×10^{-3}–2.1×10^{-3}	No N_2O produced	2.94×10^{-3}–5.6×10^{-3} (NO_2^-) 1.54×10^{-3}–3.5×10^{-3} (NO_3^-)	Daum et al. (1998)
Nitrosomonas europaea ATCC 19718	Batch culture[a] ammonium-carbonate medium	0.013	0.005	0.503 NO_2^- production	Anderson et al. (1993)[c]
N. europaea strain 28	Cell suspension in phosphate buffer + NH_4Cl, aerobic/transient to anaerobic	2.618/8.134	0.001/68.6	187.04/312.9 NO_2^- production	Remde and Conrad (1990)[c]
N. europaea ATCC 19718	Continuous culture, ammonium-organic medium	$(0.966–2.56) \times 10^{-3}$ (35×10^{-3} at transient conditions)	$(0.14–0.84) \times 10^{-3}$ (13.2×10^{-3} at transient conditions)	0.262 (NO_2^-)	Kester et al. (1997)[c]

[a]Phase of exponential growth; [b]11–22%O_2 in headspace of incubation flask; [c]data recalculated to comparable units; [d]not determined; [e]calculated from NH_4^+ consumption.

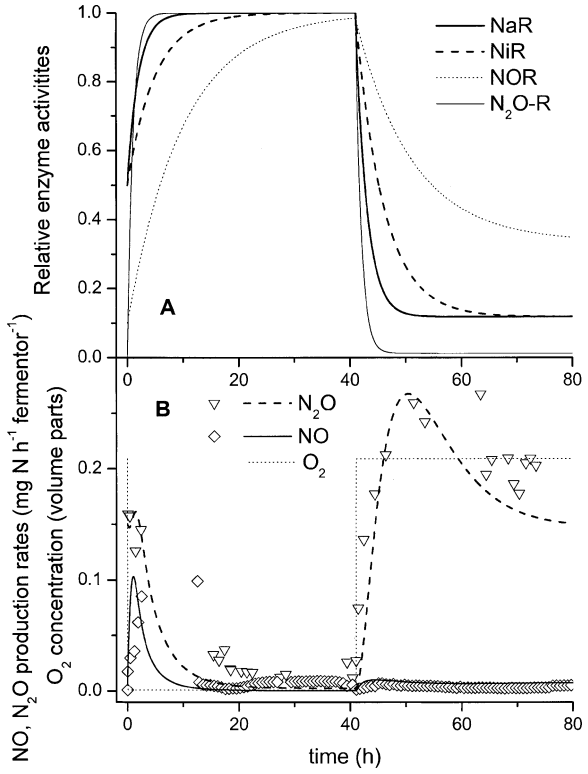

FIG. 5. Simulation of effects of de-oxygenation and re-oxygenation on the kinetic of NO and N_2O production. Equations are shown in the Appendix. (A) dynamical change in relative denitrification enzymes activity; (B) oxygen concentration and net rates of NO and N_2O production, data points for NO and N_2O rates are taken from continuous culture experiment.

example model run (Figure 5) with the parameters as given in the Appendix can be used to simulate the observed dynamic changes in NO and N_2O production during periods of de-oxygenation and re-oxygenation. The transient peaks of net NO and N_2O production were simulated by the sequential induction of the denitrificaion enzymes: nitrite reductase (NiR), NO-reductase (NOR) and N_2O reductase (N_2OR) after switching off the O_2 supply (Figure 5). Our model work demonstrate that the higher sensitivity of the N2OR to oxygen as compared to NOR (Figure 5A) can be used to explain the contrasting behaviour of NO and N_2O production during periods of de- and re-oxygenation. However, at present we cannot fully exclude that (i) oxidative consumption of NO by microbes (Baumgärtner et al. 1996) or (ii) different chemical stability and/or diffusion rates of NO under oxidative versus reductive conditions may partly contribute to the observed pattern. Further investigations—also involving the use of stable isotopes—are necessary to finally clarify this point. Nevertheless, we are convinced that the data obtained in our experiments and the proposed simulation approach are useful to further improve existing denitrification models. The proposed mechanism helps to better understand and describe short-term increases of N oxides emission in conjunction with rain events, since during such events the oxygen status of soils is changing dynamically accompanied with an increase of substrate availability.

Heterotrophic Nitrification—Link Between Aerobic Metabolism and Denitrification

Our experiments clearly show that both nitrification as well as denitrification can take place under conditions of oxygen limitation. As shown in Figure 4A and in Table 1 microbial nitrite production was observed at all levels of air saturation (4.19–6.2 mg N g^{-1} protein h^{-1}). Nitrate was produced in lower quantities (2.5–5.2 mg N g^{-1} protein h^{-1}) except at 0.1% of air saturation where no nitrate production could be detected. The combined supply of ammonium by the medium and the ammonification activity of the bacteria provided sufficient substrate to support nitrification (Table 1). During our experiments the amounts of NO_3^- and NO_2^- in the medium was not sufficient to explain the observed rates of NO and N_2O production solely by denitrification of oxidized nitrogen compounds in the medium (Table 1). The strong dependency of N trace gas production from the oxygen concentration in the medium as well as maximum N trace gas production rates at low O_2 tensions indicates that in our experiments N trace gas production was due to combined nitrification-denitrification processes in which nitrite served as a link between both processes.

As was suggested originally for *Paracoccus pantotrophus* (former *Thiosphaera panthotropha*) (Arts et al. 1995; Robertson and Kuenen 1990), heterotrophic nitrifiers are able to utilize simultaneously two electron acceptors: oxygen and nitrate (nitrite), so that the so-called "aerobic" denitrification can take place. However, one may ask: What is the ecological advantage for microorganisms for "aerobic" denitrification and the coupled nitrification-denitrification processes?

Under oxygen-limited conditions, heterotrophic nitrifiers are able to use the nitrification process as a tool to supply the denitrification process with additional electron acceptors (Arts et al. 1995; Robertson and Kuenen 1990). Even though the heterotrophic nitrifiers may not gain any energy from the nitrification process itself, they will have an advantage in growth rate (not in efficiency) when substrate with low C:N ratio is in excess relatively to electron acceptors in the microbial cells, i.e., that a "bottleneck" exists on the way from NAD(P)H to oxygen (Robertson and Kuenen 1990). It is obvious that the complete anaerobic growth (i.e., classical denitrification) would slow down the efficiency and the rate of growth, but a lack of oxidised nitrogen compounds (NO_3^-, NO_2^-) would also limit denitrification. The fastest-growing bacteria (real r-strategists): (a) produce nitrite from ammonium as an alternative electron acceptor, and (b) are able to denitrify under aerobic conditions using both oxygen and nitrite produced via nitrification as electron acceptors. In other words, these bacteria use simultaneously two metabolic pathways (denitrification and aerobic oxidation) under conditions of electron donor excess (reducing equivalents), resulting in an advantage in growth rate during periods with "unlimited"

substrate availability. Good examples for such behaviours were obtained in our experiments with *A. faecalis* subsp. *parafaecalis* and are presented in Figure 2 (batch culture) and Figures 3 and 5 (transient state in continuous culture). The described features of combined microbial nitrification-denitrification may e.g., occur in upper horizons of forest soils after input of fresh litter and rain events and could explain (at least partially) the observed temporal flushes of gaseous nitrogen oxides from forest soils. (Gasche and Papen 1999; Papen and Butterbach-Bahl 1999).

REFERENCES

Anderson IC, Poth M, Homstead J, Burdige D. 1993. A comparison of NO and N_2O production by the autotrophic nitrifier *Nitrosomonas europaea* and the heterotrophic nitrifier *Alcaligeries faecalis*. Appl Environ Microbiol 11:3525–3533.

Arts PAM, Robertson LA, Kuenen JG. 1995. Nitrification and denitrification by *Thiosphaera pantotropha* in aerobic chemostat cultures. FEMS Microbiol Ecol 18:305–315.

Baumann B, Snozzi M, Zehnder A, Van Der Meer J. 1996. Dynamics of denitrification activity of *Paracoccus denitrificans* in continuous culture during aerobic-anaerobic changes. J Bacteriol l78:4367–4374.

Baumgartner M, Koschorreck M, Conrad R. 1996. Oxidative consumption of nitric oxide by heterotrophic bacteria in soil. FEMS Microbiol Ecol 19:165–170.

Betlach MR, Tiedje JM. 1981. Kinetic explanation for accumulation of nitrite, nitric oxide, and nitrous oxide during bacterial denitrification. Appl Environ Microbiol 42:1074–l084.

Blagodatsky SA, Richter O. 1998. Microbial growth in soil and nitrogen turnover: a theoretical model considering the activity state of microorganisms. Soil Biol Biochem 13:1743–1755.

Bollmann A, Conrad R. 1998. Influence of O_2 availability on NO and N_2O release by nitrification and denitrification in soils. Global Change Biol 4:387–396.

Butterbach-Bahl K, Gasche R, Breuer L, Papen H. 1997. Fluxes of NO and N_2O from temperate forest soils: impact of forest type, N deposition and of liming on the NO and N_2O emissions. Nutr Cycl Agroecosyst 48:79–90.

Cataldo DA, Haroon M, Schrader LE, Youngs VL. 1975. Rapid colorimetic determination of nitrate in plant tissue by nitration of salicylic acid. Commun Soil Sci Plant Anal 6:71–80.

Conrad R. 2002. Microbiological and biochemical background of production and consumption of NO and N_2O in soil. In Gasche R, Papen H, Rennenberg H, editors. Trace Gas Exchange in Forest Ecosystems. Dordrecht: Kluwer Academic Publishers. P 3–33.

Daum M, Zimmer W, Papen H, Kloos K, Nawrath K, Bothe H. 1998. Physiological and molecular biological characterization of ammonia oxidation of the heterotrophic nitrifier *Pseudomonas putida*. Curr Microbiol 37:281–288.

de Boer W, Kowalchuk GA. 2001. Nitrification in acid soils: micro-organisms and mechanisms. Soil Biol Biochem 33:853–866.

Dendooven L, Anderson JM. 1995. Use of a "least square" optimization procedure to estimate enzyme characteristics and substrate affinities in the denitrification reactions in soil. Soil Biol Biochem 27(10):1261–1270.

Dendooven L, Splatt P, Anderson JM, Scholefield D. 1994. Kinetics of the denitrification process in a soil under permanent pasture. Soil Biol Biochem 26(3):361–370.

Deutsche Einheitsverfahren zur Wasser-, Abwasser- und Schlammuntersuchung. Bestimmung des Ammonium-Stickstoffs. DIN 38 406-E5-2, S.1-14.

Gamble TN, Betlach MR, Tiedje JM. 1977. Numerically dominant denitrifying bacteria, from world soils. Appl Environ Microbiol 33:926–939.

Gasche R, Papen H. 1999. A 3-year continuous record of nitrogen trace gas fluxes from untreated and limed soil of a N-saturated spruce and beech forest ecosystem in Germany-2. NO and NO_2 fluxes. J Geophys Res Atmosph 104(D15):18505–18520.

Jetten MSM, Logemann S, Muyzer G, Robertson LA, De Vries S, van Loosdrecht M-CM, Kuenen JG. 1997. Novel principles in the microbial conversion of nitrogen compounds. Antonie van Leeuwenhoek 71:75–93.

Herbert D, Phipps PJ, Strange RE. 1971. Chemical analysis of microbial cells. Methods Microbiol 5B:209–304.

Kesik M, Blagodatsky S, Papen H, Butterbach-Bahl K. 2006. Effect of pH, temperature and substrate on N_2O, NO and CO_2 production by Alcaligenes faecalis p. Appl Microbiol in press.

Kester RA, de Boer W, Laanbroek HJ. 1997. Production of NO and N_2O by pure cultures of nitrifying and denitrifying bacteria during changes in aeration. Appl Environ Microbiol 63:3872–3877.

Killham K. 1990. Nitrification in coniferous forest soils. Plant Soil 128:31–44.

Körner H, Zumft WG. 1989. Expression of denitrification enzymes in response to the dissolved oxygen level and respiratory substrate in continuous culture of *Pseudomonas stutzeri*. Appl Environ Microbiol 55:1670–1676.

Kuenen JG, Robertson LA. 1994. Combined nitrification-denitrification processes. FEMS Microbiol Rev 15:109–117.

Leffelaar PA, Wessel WW. 1988. Denitrification in a homogeneous, closed system: experiment and simulation. Soil Sci 146:335–349.

Li C, Aber JD, Stange F, Butterbach-Bahl K, Papen H. 2000. A process-oriented model of N_2O and NO emissions from forest soils: 1. model development. J Geophys Res 105:4369–4384.

McKenney DJ, Drury CF, Findlay WI, Mutus B, McDonnell T, Gajda C. 1994. Kinetics of denitrification by *Pseudomonas fluorescens*: oxygen effects. Soil Biol Biochem 26:90l–908.

McKenney DJ, Drury CF, Wang SW. 2001. Effects of oxygen on denitrification inhibition, repression, and derepression in soil columns. Soil Sci Soc Am J 65:126–132.

Otte S, Grobben NG, Robertson LA, Jetten MSM, Kuenen JG. 1996. Nitrous oxide production by *Alcaligenes faecalis* under transient and dynamic aerobic and anaerobic conditions. Appl Environ Microbiol 62:2421–2426.

Papen H, Berg R. 1998. A most probable number method (MPN) for the estimation of cell numbers of heterotrophic nitrifying bacteria in soil. Plant Soil 199:123–130.

Papen H, Berg R, Hinkel I, Thoene B, Rennenberg H. 1989. Heterotrophic nitrification by *Alcaligenes faecalis*: NO_2^-, NO_3^-, N_2O, and NO production in exponentially growing cultures. Appl Environ Microbiol 55:2068–2072.

Papen H, Butterbach-Bahl K. 1999. A 3-year continuous record of nitrogen trace gas fluxes from untreated and limed soil of a N-saturated spruce and beech forest ecosystem in Germany-1. N_2O emissions. J Geophys Res-Atmosph 104(D15):18487–18503.

Patureau D, Zumstein E, Delgenes JP, Moletta R. 2000. Aerobic denitrifiers isolated from natural and managed ecosystems. Microb Ecol 39:145–152.

Pennington PI, Ellis RC. 1993. Autotrophic and heterotrophic nitrification in acidic forest and native grassland soils. Soil Biol Biochem 25:1399–1408.

Prosser JI. 1989. Autotrophic nitrification in bacteria. Adv Microb Physiol 30:125–181.

Remde A, Conrad R. 1990. Production of nitric oxide in *Nitrosomonas europea* by reduction of nitrite. Arch Microbiol 154:187–191.

Robertson LA, Cornelisse R, de Vos P, Hadioetomo R, Kuenen R. 1989. Aerobic denitrification in various heterotrophic nitrifiers. Antonie van Leeuwenhoek 56:289–299.

Robertson LA, Kuenen JG. 1990. Combined heterotrophic nitrification and aerobic denitrification in *Thiosphera panthotropha* and other bacteria. Antonie van Leeuwenhoek 57:139–152.

Snell FD, Snell CT. 1949. Colorimetric Methods of Analysis, Vol. 3. New York: Van Noslrand, p 804–805.

Wood P. 1986. Nitrification as a bacterial energy source. In: Prosser JI, editor. Nitrification. Oxford: IRL Press. P 39–62.

APPENDIX

Parameters and functions used in the simulation of N transformations and net production of NO and N_2O by continuous culture of *A faecalis* subsp. *parafaecalis:*

Parameter/variable and unit	Notation	Value
Rate constant for nitrate reduction, h^{-1}	dnf_1	0.1
Rate constant for nitrite reduction, h^{-1}	dnf_2	0.5
Rate constant for NO reduction, h^{-1}	dnf_3	10
Rate constant for N_2O reduction, h^{-1}	dnf_4	1.5
Potential rate of oxidative nitrite formation, g N·h^{-1}	μ_nitrl	0.02
Potential rate of nitrite oxidation to NO_3^-, h^{-1}	μ_nitr2	0.2
Rate constant for NaR induction/repression, nondimensional	μ_NaR	0.5
Rate constant for NiR induction/repression, nondimensional	μ_NiR	0.2
Rate constant for NOR induction/repression, nondimensional	μ_NOR	0.1
Rate constant for N_2OR induction/repression, nondimensional	μ_N_2OR	1
Parameters normalizing reductase sensitivity to O_2, nondimensional		
Na-R	p_NaR	7
Ni-R	p_NiR	7
NO-R	p_NOR	5
N_2O R	p_N_2OR	10
Gas exchange coefficient, l^{-1}	k_d	0.001
Gas exchange rate, l*h^{-1}	k_flow	60
Dilution rate, h^{-1}	D	0.1

Rates of pool change

Oxygen partial pressure in chemostat, undimensional

$$\frac{dO_2}{dt} = k\_flow \cdot O_2\_in - k\_flow \cdot O_2 \quad [1]$$

where O_2_*in*-partial pressure of oxygen of inflow, initial value = 0.209

Relative activity of denitrification enzymes, undimensional

$$\frac{dNxR}{dt} = \mu_{NxR} \cdot (anvf_{NxR} - NxR) \quad [2]$$

where *NxR* stands for NaR—Nitrate reductase, initial value = 0.5; NiR—Nitrite reductase, initial value = 0.5; NOR—NO reductase, initial value = 0.1; N_2OR—N_2O reductase, initial value = 0.00001. and $anvf_{NxR}$—empirical functions for calculation of anaerobic volume fraction (Li et al. 2000) for respective enzyme, for example

$$anvf_{NiR} = e^{-((p\_NiR \cdot O_2)^2)} \quad [3]$$

Rates of all denitrification steps (1–4 as shown on Figure 1) are calculated as:

$$denitrification\_i = dnf\_i \cdot NxR \cdot N_x O_y \quad [4]$$

where $i = 1, 2, 3, 4$, and *NxR*—activity of corresponding reductase and N_xO_y—concentration of corresponding nitrogen oxide.

Nitrate concentration, g per chemostat

$$\frac{dnitrate}{dt} = nitrification\_2 - denitrification\_1 + D \cdot (nitrate\_in - nitrate) \quad [5]$$
$$\text{initial value} = 0.021,$$

where *nitrate_in*—nitrate concentration in inflow medium, rate of nitrite oxidation to NO_3^- is calculated as

$$nitrification\_2 = \mu\_nitr2 \cdot nitrite \cdot O_2 \quad [6]$$

Nitrite concentration, g per chemostat

$$\frac{dnitrite}{dt} = \mu\_nitr1 \cdot O_2 + dentrification\_1 - dentrification\_2 - D \cdot nitrite \quad [7]$$
$$\text{initial value} = 0.016$$

where the first term is the rate of oxidative nitrite formation, which is not limited by N source.

Nitric oxide (NO) concentration, g per chemostat

$$\frac{dNO}{dt} = denitrification\_2 - denitrification\_3 - k\_flow \cdot k\_d \cdot NO - D \cdot NO \quad [8]$$
$$\text{initial value} = 0.0001$$

where the last two terms are losses of NO with gaseous and culture outflow.

Nitrous oxide (N_2O) concentration, g per chemostat

$$\frac{dN_2O}{dt} = denitrification\_3 - denitrification\_4 - k\_flow \cdot k\_d \cdot N_2O - D \cdot N_2O \quad [9]$$
$$\text{initial value} = 0.0025$$

where the last two terms are losses of N_2O with gaseous and culture outflow.

Available online at www.sciencedirect.com
ScienceDirect
Atmospheric Environment 40 (2006) 5712–5726
ATMOSPHERIC ENVIRONMENT
www.elsevier.com/locate/atmosenv

Deposition and emissions of reactive nitrogen over European forests: A modelling study

D. Simpson[a,*], K. Butterbach-Bahl[b], H. Fagerli[a], M. Kesik[b], U. Skiba[c], S. Tang[c]

[a]*Norwegian Meteorological Institute, Oslo, Norway*
[b]*Forschungszentrum Karslruhe, Institute for Meteorology and Climate Research, Atmospheric Environmental Research (IMK-IFU), Garmisch-Partenkirchen, Germany*
[c]*Centre of Ecology and Hydrology (CEH), Bush Estate, Penicuik, Scotland*

Received 19 December 2005; received in revised form 4 April 2006; accepted 13 April 2006

Abstract

The EMEP MSC-W Eulerian chemical transport model is used to investigate a number of features concerning the concentrations and depositions of reactive nitrogen species over Europe, with a focus on forest ecosystems and soil emissions. We illustrate the relative contributions of oxidised versus reduced nitrogen, and of dry versus wet deposition, to nitrogen inputs to forests. A comparison with measurements, including data for the NOFRETETE sites, showed that the EMEP model performs generally well for N-compounds, although with some problems for NH_3 which is difficult to model with a large-scale model.

The model was modified to make use of a new forest-soil–NO inventory (with daily resolution) from the NOFRETETE project and used to calculate the potential effects of these emissions on N-deposition to forests, and on the ozone-indicator AOT40. The contribution of soil–NO to these environmental measures was found to be generally small, but significant in some areas, with changes ranging between 0–20% in Central Europe and even greater in Scandinavia. Given the large uncertainties in soil–NO emission estimates, it is clear that this source is potentially comparable in its importance to many combustion sources in parts of Europe, and deserves more attention.

Keywords: Nitrogen oxides; Deposition; Soil emissions; Modelling; EMEP

1. Introduction

Nitrogen exists in many forms in the atmosphere, most notably as the very stable species molecular N_2. Reactive nitrogen as discussed here consists of gases which are present in very small amounts (typically ppb levels or lower), but which play a large role in tropospheric chemistry. Oxidised nitrogen compounds (hereafter OXN), comprising mainly NO, NO_2, HNO_3, nitrate aerosol (NO_3^-), and some organic species (e.g. peroxy-acetyl-nitrate, PAN) play a key role in the atmosphere, controlling ozone production and levels of key radical species such as OH (e.g. Seinfeld and Pandis, 1998). Reduced nitrogen species (RDN) consist primarily of gaseous ammonia (NH_3) and particulate ammonium (NH_4^+).

*Corresponding author. Also at Department of Radio and Space Science, Chalmers Technical University, Gothenburg, Sweden. Tel.: +46 31 772 1588; fax: +46 31 772 1884.
E-mail address: david.simpson@met.no (D. Simpson).

1352-2310/$ - see front matter © 2006 Elsevier Ltd. All rights reserved.
doi:10.1016/j.atmosenv.2006.04.063

Although deposition of nitrogen compounds is of concern for many ecosystem types, deposition loads to forests are typically greater than to other ecosystems. This is because of the enhanced dry deposition caused by the greater aerodynamic roughness of forests, and their ability to capture fine particles (e.g. Ruijgrok et al., 1997). The deposition of both oxidised and reduced nitrogen to forests is associated with acidification and eutrophication, and changes in species composition and bio-diversity (e.g. Kreutzer and Weiss, 1998; Nilsson and Grennfelt, 1988; Pitcairn et al., 1998; Schulze, 1989).

The major source of OXN to the atmosphere is through the burning of fossil fuels, from the industrialised continents, shipping and aircraft (Lee et al., 1997). Other sources include biomass burning, lightning and production from soil microbes (Lee et al., 1997). In Europe the magnitude of soil NO_x emissions is generally estimated to be small in comparison to combustion-derived NO_x emissions, but there is considerable uncertainty in the estimates (Kesik et al., 2005; Simpson et al., 1999). Further, soil–NO emissions typically occur in low-NO_x regions where ozone formation is most sensitive to NO_x availability (Sillman et al., 1990; Simpson, 1995), and the highest fluxes of NO occur in the warmer months of the year, times when photochemical smog is of concern.

In order to improve the emission inventories available for NO (and N_2O) from forests in Europe, Kesik et al. (2005) further developed the PnET-N-DNDC model, within the EU project NOFRETETE. This model represents the most advanced method to date of dealing with such emissions in Europe. Forest-soil emissions of NO were estimated as 85–100 kt (N) yr^{-1} in Europe, which is less than 1% of the pyrogenic emissions from this area. Although small in comparison to combustion or agricultural sources, these emissions are very uncertain. It is therefore important to quantify their contribution to atmospheric chemistry, in order to assess the order of magnitude of their effects. Further, for forest ecosystems, the re-capture of emitted NO as NO_2 deposited onto the forest foliage may have implications for deposition estimates for this ecosystem and for associated critical levels (Nilsson and Grennfelt, 1988; Johansson et al., 2001).

This paper has three major aims, which are to estimate: (a) the nitrogen deposition loads on European forests through the use of model simulations; (b) the importance of soil–NO emissions for ozone production over Europe; (c) the importance of soil–NO emissions for the deposition load on forests, including an estimate of the relative contribution of the canopy-retention effect (see Section 3.1). We will also present a comparison with observed data from the NOFRETETE forests sites, in order to complement previous model evaluations.

2. Soil–NO emissions

Nitric oxide (as well as N_2 and N_2O) is produced in intermediate steps in microbial nitrification and denitrification processes. As emissions depend on the amounts of nitrogen going through these processes, agricultural soils, subject to direct fertilisation and manure, are responsible for the great majority of emissions, and some ecosystems may have NO_x fluxes approaching those of anthropogenic sources (Williams et al., 1992; Ludwig et al., 2001; Davidson and Kingerlee, 1997; Skiba et al., 1997; Veldkamp and Keller, 1997; Hutchinson et al., 1997). Emissions of nitrogen oxide (NO) from forest soils have long been thought to be negligible compared to corresponding emissions from agricultural landscapes (e.g. Davidson et al., 1998; Simpson et al., 1999). However, various studies have shown that in areas where N-deposition levels are high, emissions of NO from soils are also significant (Butterbach-Bahl et al., 1997; Davidson and Kingerlee, 1997; Van Dijk and Duyzer, 1999; Kesik et al., 2005; Gasche and Papen, 1999; Pilegaard et al., 1999).

A number of methodologies are available for estimating soil NO_x emissions. The most widely used so far by the atmospheric modelling community is that of Novak and Pierce (1993), commonly known as the second version of the Biogenic Emissions Inventory System (BEIS-2). This method, derived from the results of Williams et al. (1992), has been applied previously in Europe by Simpson et al. (1995) and Stohl et al. (1996). A more detailed method has been presented by Yienger and Levy (1995) for global soil–NO_x emissions. In this approach, the variation in soil–NO emissions is associated with biomass burning, rainfall events (pulsing), temperature, soil moisture, vegetation cover type (biome), canopy reductions, and fertilisation rate. This approach also included a canopy-reduction factor (CRF, see below) to allow for the deposition of NO_x within a vegetation canopy.

As noted in the Introduction, Kesik et al. (2005) further developed the PnET-N-DNDC model, in order to improve the emission inventories available for NO (and N_2O) in Europe. This model made use of daily values of N-deposition, daily temperature, precipitation, and photosynthetically active radiation (PAR) from the EMEP model, together with fine-scale landuse and soil maps. The PnET-N-DNDC model was validated with field observations from a number of sites across Europe. This new inventory predicted maximum forest-soil N emissions from The Netherlands and neighbouring areas, with around 7.0 kg (N) ha^{-1} yr^{-1}. For forest soils in most parts of Germany, Belgium, Poland, and the Massif Central in France, emissions were around 1–3 kg (N) ha^{-1} yr^{-1}. Furthermore, elevated NO emissions of around 3.0 kg (N) ha^{-1} yr^{-1} were found in Sweden. As discussed in more detail in Kesik et al. (2005), the high emissions found in Sweden in particular can be attributed to the low-pH levels (<4.0) assigned to this region from the input soil data. Such low-pH levels promote chemo-denitrification and thus NO production. Emissions show a clear maxima in the summer months, especially in central and northern Europe. The best estimate of NO emissions from forest soils in the EU for the years 1990, 1995, and 2000 are predicted to amount to 98, 85, and 99 kt (N) yr^{-1}, respectively. An extensive sensitivity analysis showed a range of between 44 and 254 kt (N) yr^{-1} for the year 2000 emissions.

3. The Eulerian EMEP model

Regional concentrations of ozone and acidifying compounds have been calculated with the EMEP MSC-W Unified Eulerian model, revision rv2_0. This model is a development of earlier EMEP models (Berge and Jakobsen, 1998; Jonson et al., 1998), and is fully documented in Simpson et al. (2003a) and Fagerli et al. (2004). Briefly, the model has 20 vertical layers for use at European scale with a horizontal resolution of ca. $50 \times 50\,km^2$ (at 60°N) on a polar stereographic grid. The chemical scheme uses about 140 reactions between 70 species (Simpson et al., 1993; Simpson, 1995), and makes use of the EQSAM module of Metzger et al. (2002) to describe equilibria between the inorganic aerosol components. Boundary conditions for nitrogen species in the model are prescribed as functions of month, latitude, and elevation in the model, with values based primarily upon observational data (Simpson et al., 2003a). The model uses meteorological data from a dedicated version of the operational HIRLAM model (High Resolution Limited Area Model) maintained and verified at the Norwegian Meteorological Institute. The deposition module makes use of a stomatal conductance algorithm which was originally developed for calculation of ozone fluxes, but which is now applied to all pollutants where stomatal control is important (Emberson et al., 2000; Simpson et al., 2001, 2003c; Tuovinen et al., 2004). Non-stomatal deposition for NH_3 is parameterised as a function of temperature, humidity, and the molar SO_2/NH_3, combining ideas from Smith et al. (2000) and Nemitz et al. (2001). Details of this and the treatment of other gases is given in Simpson et al. (2003a).

The main emission sources to the EMEP model comprise annual data on SO_2, NO_x, NMVOC, CO, NH_3 from fossil fuel and other anthropogenic sources. These data are taken as far as possible from official submissions, otherwise from estimates within EMEP MSC-W (Vestreng et al., 2004), and temporally disaggregated to hourly values using procedures detailed in Simpson et al. (2003a). Additionally, hourly biogenic emissions of NMVOC arising from forests are calculated by the model using the emission algorithms of Guenther et al. (1995), combined with emission factors and forest maps specific to Europe (Simpson et al., 1999, 2003a). For soil–NO emissions, we make use of daily emission fields of NO provided by the Kesik et al. (2005) work discussed above, with data aggregated for the coniferous and deciduous forest areas for each EMEP grid element.

3.1. Interactions with the canopy

Bakwin et al. (1990) pointed out that some of the NO emitted from soils is quickly converted to NO_2. This gas is deposited within a vegetation canopy, thereby reducing the NO_x flux to the atmosphere. Yienger and Levy (1995) proposed a simple methodology of calculating this CRF, based upon leaf-area index and stomatal-area index for different canopy types. They calculated a global emission estimate of 10.2 Tg (N) yr^{-1} without these CRF factors, but only 5.5 Tg (N) yr^{-1} when it was included—or in other words on average 50% of the emitted soil NO was assumed to be retained within the canopy. For forests, emissions are usually both measured and estimated below the foliage

canopy, so CRFs may be important to account for the losses as the NO_x passes through the foliage.

Air masses within a forest canopy are subject to a large number of complex interactions, involving emissions of NO from the forest floor, turbulent exchange with the air above, chemical reactions between NO, NO_2, and O_3, and with VOC associated with aloft air masses or emitted by vegetation (Lenschow and Delany, 1987; Meyers and Baldocchi, 1988; Duyzer et al., 1995; Ganzeveld et al., 2002; Dorsey et al., 2004). In principal, we could have used a canopy model in the present study to try to account for such interactions, but for a number of reasons we have adopted a simpler approach. Firstly, there are well-known problems with the application of multi-layer models, partly associated with the complex 3D and intermittent nature of turbulence within a forest canopy (Raupach, 1979). Secondly, standard chemical approaches such as assuming photo-stationary state (e.g. Seinfeld and Pandis, 1998) may fail, since equilibria may not be established in the dark canopy space. (For example, photo-stationary model approaches would suggest that essentially all NO_x existed as NO_2 in the trunk space, whereas Dorsey et al., 2004 found that 58% of emitted NO survived to the 7 m level within the canopy.) Thirdly, application of multi-layer models is difficult within regional air-pollution models, since the canopy-scale modelling often requires much shorter time-steps, and hence much greater computer time, than are needed for the regional modelling. Finally, much of the data that would be needed to drive canopy models over Europe is lacking. Most importantly, there are no pan-European maps of leaf-area index, and indeed little information in many areas beyond the simple classifications of coniferous, deciduous or mixed forest. In such a data-poor situation we have preferred to make use of a simple but robust approach to account for CRF effects. In this paper we present model results using two canopy assumptions:

(1) CRF0—no retention of emitted soil NO within the canopy.
(2) CRF50—50% retention of emitted soil NO within the canopy.

This approach is believed to cover the likely range of CRFs for European forests, and thus enables us to assess the range of effects of soil–NO emissions without the need for complex and difficult-to-evaluate canopy modelling. Retention of emitted NO is effectively an increased deposition within the forest.

4. Comparison with observations

Evaluations of model performance for many compounds are regularly reported in EMEP reports, e.g. Fagerli (2004), for sulphur and nitrogen and Simpson et al. (2003b) for ozone and AOT40. Here we briefly summarise some relevant results for nitrogen compounds, with a focus on new data for the NOFRETETE sites.

It should be noted that the EMEP model, with its grid size of approx. $50 \times 50\,km^2$ (at 60°N), and surface grid-cell depths of ca. 90 m, cannot be expected to reproduce small-scale variations in deposition regimes, caused by such factors as local emissions (especially important for NH_3 close to agricultural sources, e.g. Sutton et al., 1998), topography (which has strong effects on rainfall amount and deposition, e.g. Dore et al., 1992; Fowler et al., 1988), or where processes not included in the model (e.g. occult deposition) are important. These problems are difficult to address, but by comparison with measurements we can make an assessment of the degree of agreement between the model and observed values.

4.1. EMEP data

The EMEP measurement network (www.emep.int) consists of a wide range of gas, particle and deposition measurements across Europe, all subject to regular quality control (Aas et al., 2004). Table 1 summarises the results for a comparison of EMEP model results and EMEP measurements for 2000. Only a few site report results for the gaseous compounds, 15 for HNO_3 and 11 for NH_3, and of these only two use denuders whilst the others use filter-pack methods. Separation of gas and particulates by filter packs are uncertain (EMEP, 1996), thus these results should be interpreted with caution. Results for the sums ($NH_3 + NH_4^+$, and $HNO_3 + NO_3^-$) are more reliable than for the gas components.

From Table 1 we see that total nitrate and aerosol nitrate in air are systematically overestimated, whilst nitric acid is underestimated by on average 6% (some sites are overestimated and some are underestimated). An inspection of seasonal time-series reveals that winter-time aerosol nitrate is

Table 1
Comparison of annual EMEP model results and EMEP measurements for 2000

Component	Unit	No. sites	Obs.[a]	Bias (%)	r[b]
$NO_3^- + HNO_3$	$\mu g\,(N)\,m^{-3}$	45	0.45	29	0.87
HNO_3	$\mu g\,(N)\,m^{-3}$	15	0.13	−6	0.65
NO_3^- in aerosol	$\mu g\,(N)\,m^{-3}$	26	0.40	23	0.75
$NH_4^+ + NH_3$	$\mu g\,(N)\,m^{-3}$	40	1.29	13	0.71
NH_3	$\mu g\,(N)\,m^{-3}$	11	0.86	−53	0.75
NH_4^+ in aerosol	$\mu g\,(N)\,m^{-3}$	28	0.70	25	0.77
NO_3^- wet dep.	$mg\,(N)\,m^{-2}$	61	284	−25	0.80
NO_3^- conc. in precip.	$mg\,(N)\,l^{-1}$	61	0.39	−29	0.66
NH_4^+ wet dep.	$mg\,(N)\,m^{-2}$	61	315	−14	0.68
NH_4^+ conc. in precip.	$mg\,(N)\,l^{-1}$	61	0.41	−16	0.62

[a]Mean of observed values.
[b]Correlation coefficient.

overestimated, whilst summer-time results show an opposite tendency. However, no systematic bias in winter- or summer-time HNO_3 is noted. The results for $NH_3 + NH_4^+$ in air are also overestimated in winter time, as are aerosol NH_4^+, whilst NH_3 is systematically underestimated. Some of these results could suggest that the overestimation of total nitrate and $NH_3 + NH_4^+$ in air is either caused by a too fast conversion to NH_4NO_3 in cold periods, or too high production of nitric acid or a combination. This is not consistent though with the lack of bias in HNO_3, and the underestimation of NH_3 is expected given the location of many EMEP sites in rural areas, close to sources (see also discussion in Section 4.2). Measurement uncertainties may partly explain some discrepancies, but some problems must also be related to wet scavenging processes, as nitrate and NH_4^+ wet depositions and concentrations in precipitation are underestimated. However, the underestimation in precipitation is not only related to the winter period, but is similar throughout the year.

More good-quality measurements of the gas and particle-phase components of total nitrate and $NH_3 + NH_4^+$ in air, and a better understanding of precipitation scavenging (and possible sub-grid and orographic effects) will clearly be required in order for us to understand the reasons for the overestimation of nitrogen in air, and the underestimation of nitrogen in precipitation, respectively. However, despite these problems, we can note that the EMEP model captures the concentration levels of gaseous N species (except NH_3), and of wet-deposition N components, to within 30%.

4.2. NOFRETETE NO_2 and NH_3

In order to provide some additional information of the contribution of dry deposition of N to the forest soils studied in NOFRETETE, NH_3 and NO_2 passive samplers were installed at nine sites for a one-year period. Atmospheric concentrations of NH_3 and NO_2 were measured by passive diffusion samplers inside the forest canopy (at a height of 1.5 m) and above or outside (at a height of 1.5 m) the forest canopy between May/June 2002 and June/July 2003.

For NO_2 a modification of the GRADKO diffusion tube (Stevenson et al., 2001; Bush et al., 2001) was employed. The modification consists of adding a turbulence damping membrane across the inlet, and has been rigorously tested against measurements by continuous chemiluminescence analysers (McGowan et al., 2002; Cape et al., 2004). The CEH adapted low-cost passive high absorption (ALPHA) sampler was developed with an optimised sampling rate for long-term ambient monitoring of atmospheric NH_3 (one or two monthly periods, $LOD = 0.02\,\mu g\,(N)\,m^{-3}$, Tang et al., 2001). The ALPHA sampler has been tested at several UK and European sites, and against a reference system (Sutton et al., 2001a,b, 1999). Further details of these measurements, including analysis of the differences between in-canopy and above-canopy or open-field data are given in Skiba et al. (2005). As the EMEP model is not designed to calculate in-canopy concentrations, here we present a comparison of the model against the data which are most comparable, open sites when available, otherwise above-canopy data.

Table 2 summarises the results of this comparison, and Figs. 1 and 2 illustrate results for selected sites. For NO_2, the annual mean concentrations are reproduced rather well by the model at most sites. Exceptions occur mainly for the Austrian and Italian sites. For the Austrian sites Schottenwald and Klausen-L., the problem may well lie in the coarse grid resolution of the EMEP model, and the fact that these sites are located rather close to Vienna, a large source of NO_x. Regional models such as EMEP are not able to resolve the very different NO_x concentrations in the vicinity of such sources. For the Italian site the model underpredicts by a factor of 2 throughout the year, also an indication of local NO_x sources which are not resolved by the model. For all other sites though, the EMEP model captures both the levels and

Table 2
Modelled and observed concentrations of NO_2 and NH_3 at NOFRETETE sites ($\mu g\,m^{-3}$)

Site		NO_2 (obs)	NO_2 (mod)	NH_3 (obs)	NH_3 (mod)
Finland	Hyytiälä	1.7	2.1	0.10	0.12
Scotland	Glencorse	6.5	8.5	0.57	1.1
Denmark	Sorø	7.5	9.1	1.7	1.6
The Netherlands	Speulderbos	15.4	16.1	4.9	7.1
Germany	Höglwald	10.8	10.6	1.7	4.4
Austria 1	Schottenwald	8.3	4.8	1.4	1.0
Austria 2	Klausen-L.	4.5	8.6	0.34	1.1
Austria 3	Achenkirk	6.4	5.0	0.63	0.94
Italy	San Rossore	11.5	4.9	0.46	0.92

For further site details, see Skiba et al. (2005) and Schindlbacher et al. (2004).

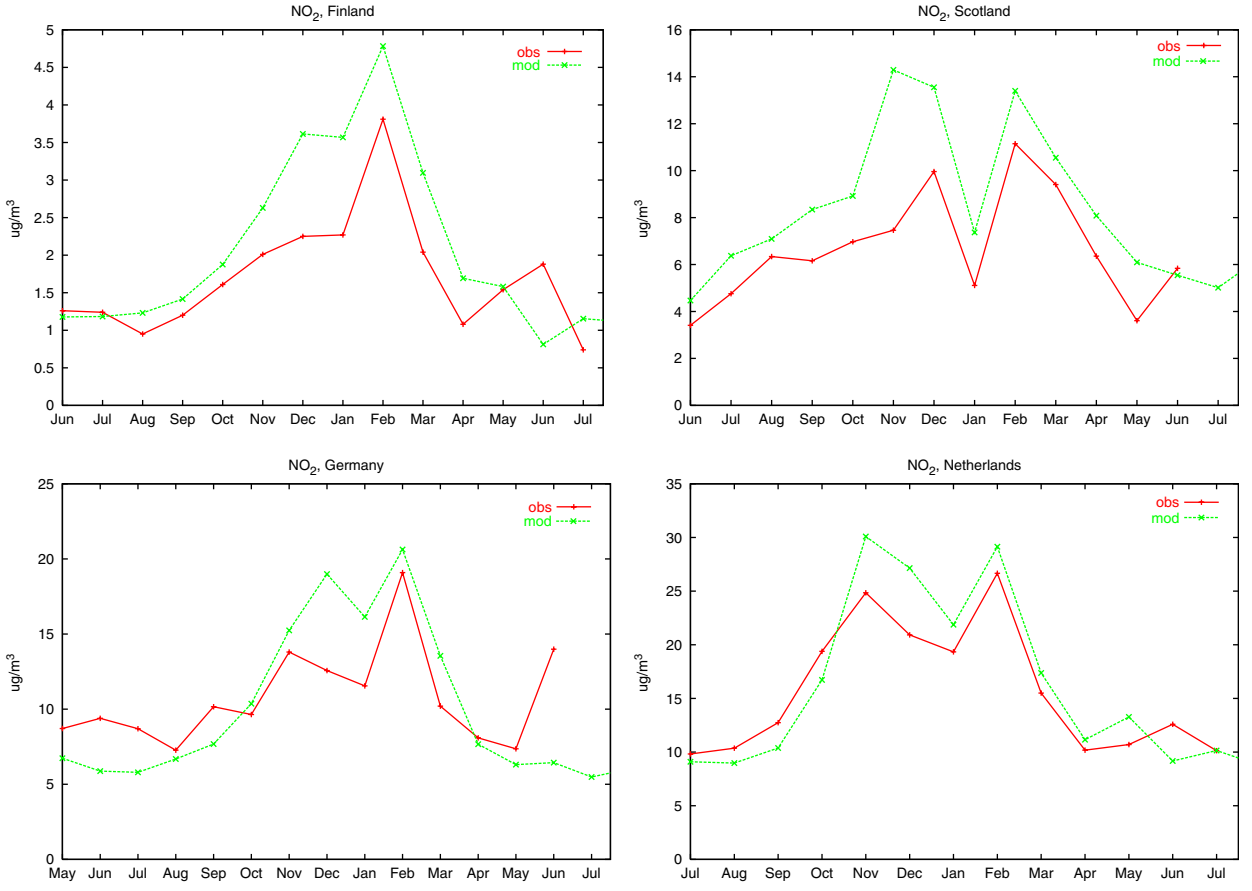

Fig. 1. Comparison of modelled versus observed monthly average NO_2 at NOFRETETE sites.

seasonal variation of NO_2, ranging from the very clean environment of Finland (ca. $2\,\mu g\,m^{-3}$) to the most highly polluted Netherlands site (ca. $15\,\mu g\,m^{-3}$).

For NH_3, results are more mixed (Table 2, Fig. 2). The range of NH_3 is captured fairly well though, from $0.1\,\mu g\,m^{-3}$ in Finland to ca. $5\,\mu g\,m^{-3}$ in The Netherlands, but discrepancies are larger than for NO_2. A noticeable feature of Fig. 2 is that where discrepancies are large, NH_3 is overestimated, whereas in comparisons at standard EMEP sites the model tends to underestimate NH_3 by about 50% (cf. Table 1). A likely reason for this difference is that forests are among the landuse classes with lowest NH_3 emissions, so that when we model the grid average we overestimate for forests, and

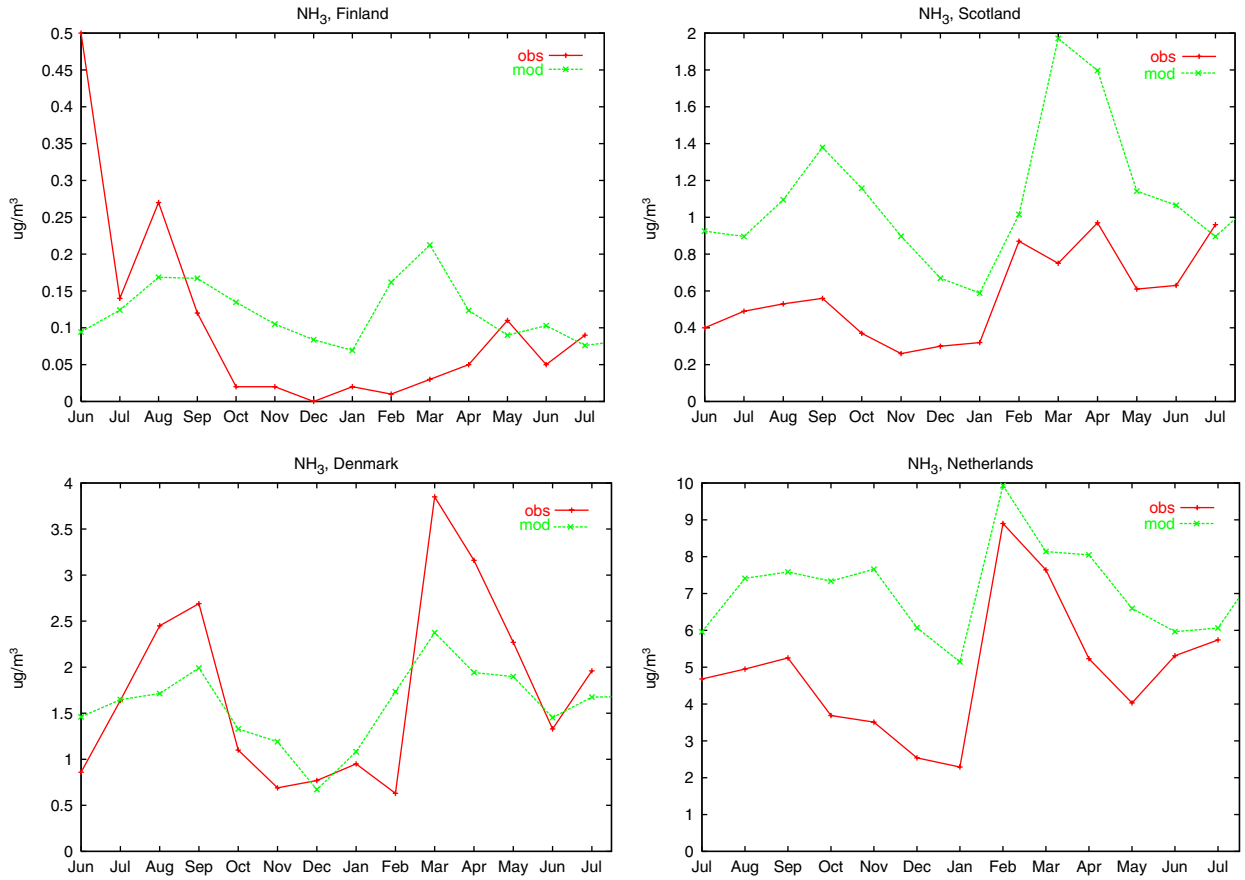

Fig. 2. Comparison of modelled versus observed monthly average NH_3 at NOFRETETE sites.

underestimate for agricultural landscapes and grasslands where both emissions and vertical gradients are strongest. Site characteristics and local (subgrid) emissions also play a strong role. For example, the German site Höglwald is surrounded by agricultural areas (Huber and Kreutzer, 2002).

On the whole, these comparisons indicate that the EMEP model captures rather well both the concentration gradients and seasonal variation in NO_2 and at least the concentration gradients in NH_3 for these sites. This result is very encouraging, given that these sites cover extremes of both high (Speulderbos) and low (Hyytiälä) N-deposition regimes in Europe.

4.3. Deposition budget

Although wet deposition represents an important fraction of N-deposition over Europe, dry deposition is also important (Fig. 4). Unfortunately, the EMEP network has no specific measurements of dry deposition. However, dry deposition monitoring has been performed over many years at Speulderbos in The Netherlands (e.g. Erisman et al., 1997, 2001), and indeed this was the NOFRETETE site with by far the highest deposition loads.

Erisman et al. (2001) presented estimates of wet and dry deposition of oxidised and reduced nitrogen for Speulderbos, over the period 1995–1998. Data are not available for the year 2000, so we present here a comparison with EMEP model results for the year 1995. The modelled total deposition for the Speulderbos grid square in 1995 is 5200 mg (N) m^{-2}, within 10% of that found in the measurements (4798 mg (N) m^{-2}). Table 3 illustrates the percentage breakdowns of this total deposition between wet/dry/OXN/RDN components. These relative contributions are remarkably similar, with reduced nitrogen accounting for about $\frac{2}{3}$ of total deposition, and dry deposition dominating both the OXN and RDN contributions. The closeness of this agreement is certainly partly fortuitous, given that we are

comparing just one site, and that deposition estimates from observations also have uncertainties. Still, this limited comparison suggests that the EMEP model is capturing the main deposition processes in a reasonable way in that part of Europe where N-deposition is predicted to be greatest.

5. Results from base-model

This section presents results from the base-version of the EMEP model (without soil–NO emissions), along with some model evaluation. The focus is on nitrogen compounds, we will also illustrate results for the ozone-indicator AOT40, since changes in ozone are of environmental concern. All calculations are for the year 2000.

Fig. 3(a) shows the calculated deposition of nitrogen to coniferous forest, per unit area of forest. This figure clearly illustrates the large gradients of N-deposition across Europe, and that areas around The Netherlands receive the highest loadings of N-deposition. Fig. 4 illustrates the calculated relative contributions of dry and wet deposition, for oxidised and reduced nitrogen, to the total reactive nitrogen deposition over coniferous forests in Europe. The relative contributions vary markedly across Europe. In the Nordic countries, dry and wet deposition of oxidised nitrogen dominate, although wet deposition of reduced nitrogen accounts for around 20–30% of the total. Dry deposition of RDN is, however, the most significant contributor in many areas of central Europe, including parts of France, the UK, Ireland, and The Netherlands. Over southern Europe dry deposition tends to dominate over wet, as should be expected given the lower precipitation rates.

In order to map potential risk to forest ecosystems in Europe brought about by ozone, the AOT40 index has been developed. AOT40 (accumulated ozone over threshold 40 ppb) is the sum of all daytime hourly ozone concentrations in excess of 40 ppb, taken over an assumed growing season for forests of April–September (Fuhrer et al., 1997; Mills, 2004). The units used is ppb × h, or ppb h. AOT40 is also a useful integrated measure of ozone over the summer season. Fig. 3(b) shows AOT40 calculated over Europe with the base-case simulations. Levels are highest in southern Europe

Table 3
Comparison of observed and modelled contributions (%) of dry and wet deposition of oxidised (OXN) and reduced nitrogen (RDN) to total N-deposition (OXN + RDN) at Speulderbos forest, The Netherlands, 1995

	Observed			Modelled		
	Dry	Wet	Dry + wet	Dry	Wet	Dry + wet
OXN	18	11	29	22	9	31
RDN	47	24	71	54	15	69

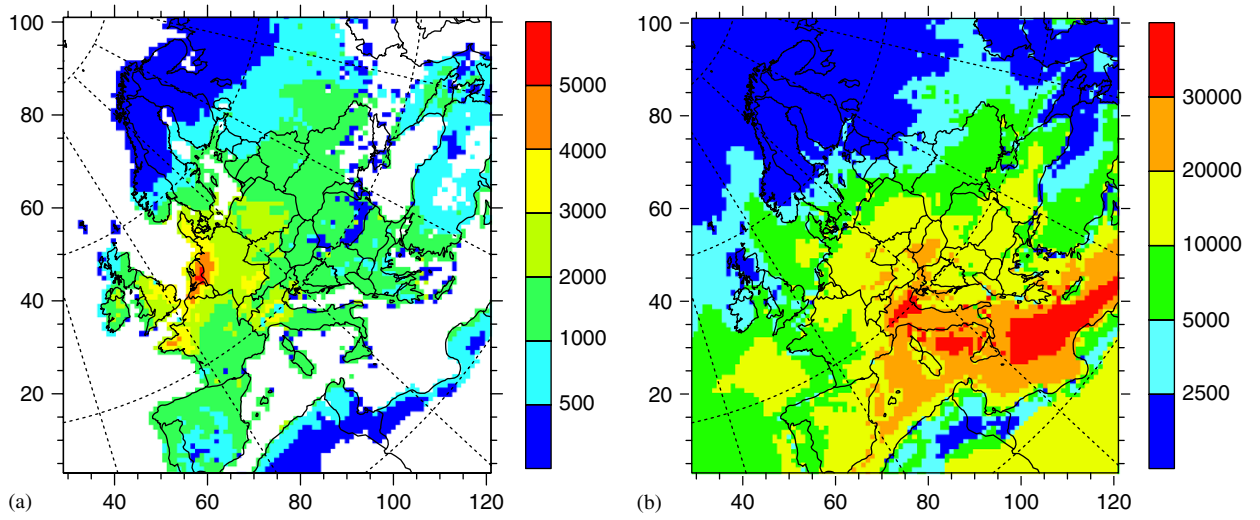

Fig. 3. Base-case calculations for year 2000. (a) Deposition of nitrogen to coniferous forest, per unit forest area (mg (N) m^{-2}) and (b) AOT40 for forests (ppb h).

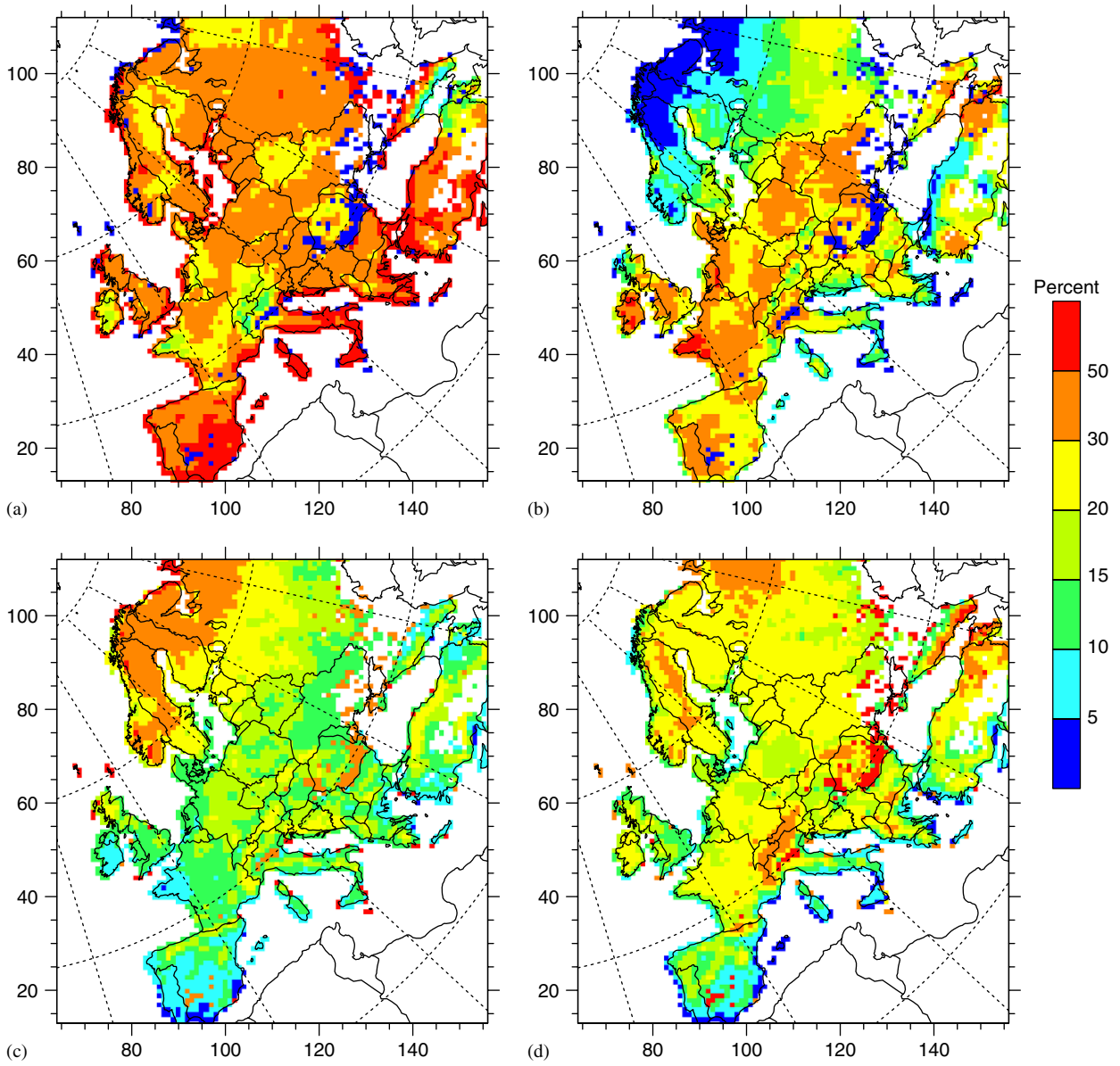

Fig. 4. Calculated percentage contributions to total nitrogen deposition to coniferous forest (year 2000): (a) dry deposition of oxidised N, (b) dry deposition of reduced N, (c) wet deposition of oxidised N, and (d) wet deposition of reduced N.

(>30 000 ppb h), and very low (<2500 ppb h) in Northern Scandinavia.

6. Contributions from soil NO

As described in Section 3.1, two different assumptions are explored with regard to canopy-retention factors (CRFs) in this work, CRF0 (zero canopy retention), and CRF50 (50% retention).

Fig. 5 illustrates the changes in N-deposition to coniferous forests, for the CRF0 scenario. Increases in N-deposition are seen to be modest (<5%) over most of Europe with this scenario, except in Sweden and Finland. The large percentage increases in these areas reflect both the small base-case depositions and the relatively larger soil NO_x from these areas.

Fig. 6 illustrates the changes in N-deposition to coniferous forests, for the CRF50 scenario, in which 50% of emitted soil N is assumed to be re-deposited within the canopy. Increases in N-deposition are now much greater, with changes over Sweden >50% and between 5% and 20% over many other

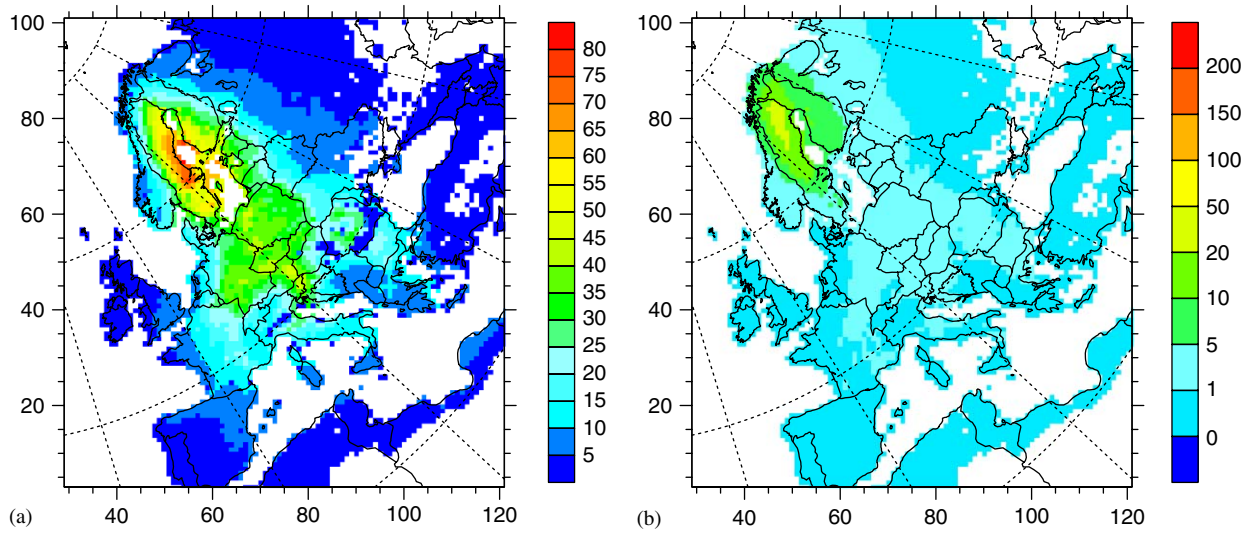

Fig. 5. Calculated change in N-deposition to coniferous forests brought about by soil–NO emissions, expressed as (a) absolute difference (mg (N) m^{-2}, forest area) and (b) % difference from base-case. Scenario CRF0, year 2000.

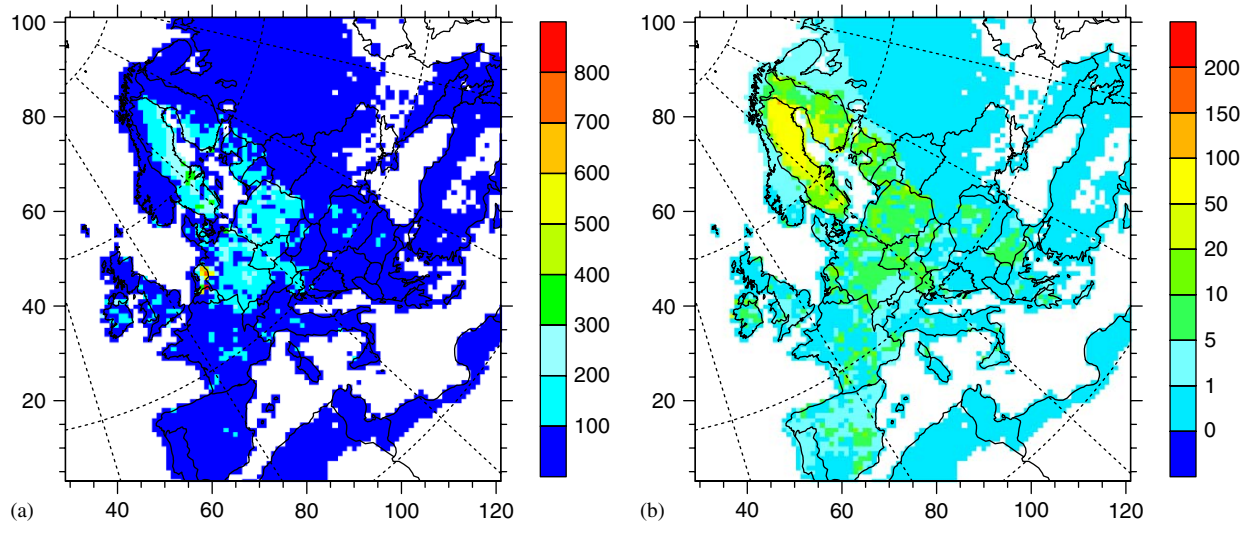

Fig. 6. Calculated change in N-deposition to coniferous forests brought about by soil–NO emissions, expressed as (a) absolute difference (mg (N) m^{-2}, forest area) and (b) % difference from base-case. Scenario CRF50, year 2000.

parts of Europe. Absolute changes lie around 100–200 mg (N) m^{-2} in many parts of Germany, Poland for example, with a maximum increase of around 800 mg (N) m^{-2} in the Benelux area.

Fig. 7 illustrates the changes in AOT40 occurring with the CRF0 model runs—those releasing most NO_x to the free atmosphere. AOT40 increases over much of central Europe by ca. 200–1000 ppb h, with much smaller absolute changes in, for example, the UK, Scandinavia, the Iberian peninsula, and Russia. Percentage changes (Fig. 7(b)) are greatest in Sweden and Finland (a consequence of the small base-case AOT40 values), but are still significant (>5–10%) in large areas where the base-case AOT40 levels exceeded the critical threshold value of 5000 ppb h (Mills, 2004). Results for the CRF50 scenario (not shown) are very similar to those shown for the CRF0 scenario, but with changes in AOT40 approximately a factor 2 lower. This behaviour fits well with the expected linearity

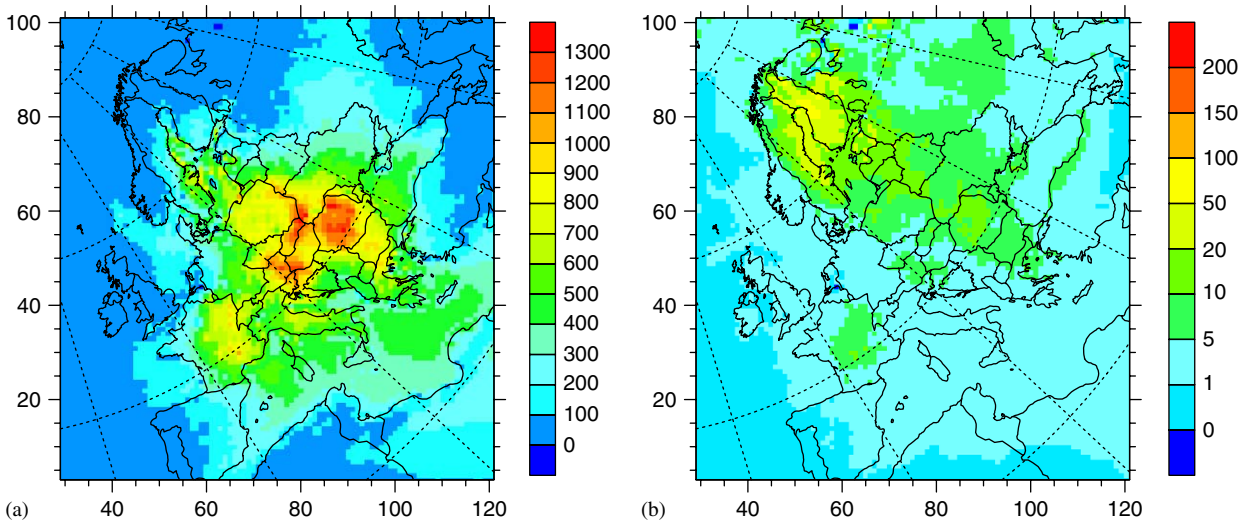

Fig. 7. Calculated change in AOT40 brought about by soil–NO emissions, expressed as (a) absolute difference (ppb h) and (b) % difference from base-case. Calculations for year 2000.

between NO_x emissions and resulting O_3 concentrations expected over most of Europe (Simpson, 1995).

6.1. Discussion of soil NO contribution

The model results presented above suggest that compared to total N-deposition and AOT40 levels, NO emissions from forest soils have a generally small, but not insignificant contribution to both N-deposition and AOT40. As noted above, the large changes over Sweden may stem from problems in the soil pH databases available for the PnET-N-DNDC model (Kesik et al., 2005). However, over areas such as Germany and Poland, soil NO was estimated to contribute around 50–300 mg (N) m^{-2} (1–20%) to OXN-deposition over forest areas (with CRF50), or around 100–800 ppb h (also 1–20%) of AOT40.

We can compare these contributions to deposition and ozone levels with the changes expected from anthropogenic combustion sources. Jonson and Benedictow (2003) presented changes in sulphur and nitrogen deposition, and in various ozone indicators, in response to changes in emissions from man-made sources. These calculations were made by running the EMEP model for each emitter country in turn, building up a set of 'source–receptor' relationships. In order to save computer time, changes in SO_x and NO_x emissions were made simultaneously, but for N-deposition and ozone we may assume that it was the changes in NO_x emissions which are important. Reducing German NO_x emissions by 25% resulted in changes in OXN-deposition over Germany of around 50 mg (N) m^{-2}, and changes in AOT40 ranging from reductions of 900 ppb h to increases (over NW Germany) of 900 ppb h. Reducing Polish NO_x emissions resulted in changes in OXN-deposition over Poland of around 20–60 mg (N) m^{-2}, and decreases in AOT40 of between 300 and 900 ppb h. Thus, the changes in OXN-deposition or AOT40 associated with the soil–NO emissions are of the same order of magnitude as those associated with quite significant changes in the combustion-source emissions.

At first sight, this comparability seems somewhat surprising. Soil–NO emissions represent only ~3% of combustion-source emissions for our two example countries. However, as seen in Section 6, the major contribution to N-deposition from forest soils is predicted to be associated with the CRF. With the CRF50 model, 50% of the emissions are directly deposited onto the forest canopy, and not dispersed over non-forest regions or throughout the model domain. With the combustion-source emissions on the other hand, deposition occurs over all types of land and sea surface, and the areas with highest NO_x emissions are frequently areas with low forest density. Thus, only a small fraction of these emissions ends up depositing onto forest canopies.

For ozone, other factors play a role. Combustion emissions of NO_x are greatest in winter time and

thus contribute relatively less to ozone formation and AOT40 (which is calculated between April–September). Conversely, forest-soil emissions are greatest in the summer months. Further, as noted above, forest soil–NO emissions typically occur in more rural areas, and in such low-NO_x areas ozone formation is most sensitive to NO_x availability (Sillman et al., 1990; Simpson, 1995).

7. Conclusions

In this study we have made use of the EMEP MSC-W Eulerian chemical transport model to quantify some features of biosphere–atmosphere exchange for reactive nitrogen species over Europe, with a focus on forest ecosystems and making use of a new forest-soil–NO inventory (with daily resolution) from the NOFRETETE project (Kesik et al., 2005).

This paper has had three major aims, which are to estimate (a) the nitrogen deposition loads on European forests through the use of model simulations; (b) the importance of soil–NO emissions for ozone production over Europe; and (c) the importance of soil–NO emissions for the deposition load on forests, including an estimate of the relative contribution of the canopy-retention effect. In addition, we have compared modelled and observed concentration and deposition data, with a focus on the NOFRETETE forest sites, in order to complement previous model evaluations.

The model estimates show that the relative contributions of oxidised, reduced, wet and dry deposition of nitrogen vary markedly across Europe. In the Nordic countries, dry and wet deposition of oxidised nitrogen dominate, although wet deposition of reduced nitrogen (RDN) accounts for around 20–30% of the total. Dry deposition of RDN is, however, the most significant contributor in many areas of central Europe, including parts of France, the UK, Ireland, and The Netherlands. Over southern Europe dry deposition tends to dominate over wet, as should be expected given the lower precipitation rates of that region.

The model was also used to calculate the potential effects of forest-soil–NO emissions on N-deposition to forests, and on the ozone-indicator AOT40. The contribution of soil NO to these environmental measures was found to be generally small, as would be expected from the low emissions, but not insignificant, with changes ranging between 0% and 20% in most areas. The most significant percentage changes were seen in Northern Europe, especially for Sweden in terms of N-deposition and Finland for AOT40. The large changes over Sweden (ca. 50% increases) stem from the relatively large NO emissions predicted in the inventory. If these emissions are realistic, then the changes in N-deposition predicted here are important and deserve further investigation.

Of course, given the very large uncertainties in soil–NO emissions, the contributions calculated in this study may represent significant over or underestimates of the true contribution of soil emissions. Apart from uncertainties in the soil–NO emissions themselves, the assumptions regarding the CRF are here seen to play a very large role in determining the amount of nitrogen deposited to the canopy. It seems clear that soil–NO emissions deserve more attention, as their effects are potentially comparable to the man-made combustion sources which are the focus of emission reduction strategies.

Finally, we can note that there are unfortunately very few data with which to make a good evaluation of such model results. We have shown in previous studies that the EMEP model generally does a good job in reproducing air concentrations and depositions at EMEP stations, and this was confirmed also with the forest site measurements of NO_2 and NH_3 presented here. Still, we are not able to verify the predicted relative contributions of oxidised versus reduced, or wet versus dry deposition illustrated in this work, except at the one site presented here. Extending this verification awaits better and more comprehensive measurement data, comprising both concentrations and depositions.

Acknowledgements

This work was supported by the EU-funded NOFRETETE Project (contract No. EVK2-CT2001-00106), as well by the Co-operative Programme for Monitoring and Evaluation of the Long-Range Transmission of Air pollutants in Europe (EMEP) under UNECE. Thank are due to Netty van Dijk of CEH for the analysis of NO_2 and NH_3, and to Jan Willem Erisman for providing data for Speulderbos forest.

References

Aas, W., Hjellbrekke, A.-G., Manø, S., Uggerud, H., 2004. Data quality 2002, quality assurance, and field comparisons. EMEP

Report 4/2004, The Norwegian Institute for Air Research (NILU), Kjeller, Norway.

Bakwin, P., Wofsy, S., Fan, S.-M., Keller, M., Trumbore, S., Da Costa, J., 1990. Emissions of nitric oxide (NO) from tropical forest soils and exchange of NO between the forest canopy and the atmospheric boundary layers. Journal of Geophysical Research 95 (D10), 16755–16764.

Berge, E., Jakobsen, H.A., 1998. A regional scale multi-layer model for the calculation of long-term transport and deposition of air pollution in Europe. Tellus 50, 205–223.

Bush, T., Smith, S., Stevenson, K., Moorcroft, S., 2001. Validation of nitrogen dioxide diffusion tube methodology in the UK. Atmospheric Environment 35, 289–296.

Butterbach-Bahl, K., Gasche, R., Breuer, L., Papen, H., 1997. Fluxes of NO emissions and N_2O from temperate forest soils: impact of forest type, N deposition and of liming on the NO and N_2O. Nutrient Cycling in Agroecosystems 48, 79–90.

Cape, J., Tang, Y., van Dijk, N., Love, L., Sutton, M., Palmer, S., 2004. Concentrations of ammonia and nitrogen dioxide at roadside verges and their contribution to nitrogen deposition. Environmental Pollution 132, 469–478.

Davidson, E., Potter, C., Schlesinger, P., Klooster, S., 1998. Model estimates of regional nitric oxide emissions from soils of the southeastern United States. Ecological Applications 8 (3), 748–759.

Davidson, E.A., Kingerlee, W., 1997. A global inventory of nitric oxide emissions from soils. Nutrient Cycling in Agroecosystems 48, 91–104.

Dore, A., Choularton, T., Fowler, D., 1992. An improved wet deposition map of the United Kingdom incorporating the seeder–feeder effect over mountaneous terrain. Atmospheric Environment 26A, 1375–1381.

Dorsey, J., Duyzer, J., Gallagher, M., Coe, H., Pilegaard, K., Westrate, J., Jensen, N., Walton, S., 2004. Oxidised nitrogen and ozone interaction with forests. I: experimental observations and analysis of exchange with Douglas fir. The Quarterly Journal of the Royal Meteorological Society 130, 1941–1955.

Duyzer, J., Deinum, G., Baak, J., 1995. The interpretation of measurements of surface exchange of nitrogen oxides: corrections for chemical reactions. Philosophical Transactions of the Royal Society of London A 351, 231–248.

Emberson, L., Simpson, D., Tuovinen, J.-P., Ashmore, M., Cambridge, H., 2000. Towards a model of ozone deposition and stomatal uptake over Europe. EMEP MSC-W Note 6/2000. The Norwegian Meteorological Institute, Oslo, Norway.

EMEP, 1996. EMEP Manual for sampling and chemical analysis. EMEP/CCC-Report 1995, Norwegian Institute for Air Research, Kjeller (last revision in 2001), ⟨http://www.nilu.no/projects/ccc/manual/index.html⟩.

Erisman, J., Draaijers, G., Duyzer, J., Hofschreuder, P., van Leeuwen, N., Römer, F., Ruijgrok, W., Wyers, P., Gallagher, M., 1997. Particle deposition to forests—summary of results and application. Atmospheric Environment 31 (3), 321–322.

Erisman, J.W., Hensen, A., Fowler, D., Flechard, C.R., Grüner, A., Spindler, G., Duyzer, J.H., Weststrate, H., Römer, F., Vonk, A.W., Jaarsveld, H.V., 2001. Dry deposition monitoring in Europe. Water, Air and Soil Pollution: Focus 1, 17–27.

Fagerli, H., 2004. Air concentrations and depositions of acidifying and eutrophying components, status 2002. In: Transboundary Acidification, Eutrophication and Ground Level Ozone in Europe. EMEP Status Report 1/2004. The Norwegian Meteorological Institute, Oslo, Norway, pp. 77–107.

Fagerli, H., Simpson, D., Tsyro, S., 2004. Unified EMEP model: updates. In: Transboundary Acidification, Eutrophication and Ground Level Ozone in Europe. EMEP Status Report 1/2004. The Norwegian Meteorological Institute, Oslo, Norway, pp. 11–18.

Fowler, D., Cape, J., Leith, I., Choularton, T., Gay, M., Jones, A., 1988. The influence of altitude on rainfall composition at Great Dun Fell. Atmospheric Environment 22, 1355–1362.

Fuhrer, J., Skärby, L., Ashmore, M., 1997. Critical levels for ozone effects on vegetation in Europe. Environmental Pollution, 91–106.

Ganzeveld, L., Lelieveld, J., Dentener, F., Krol, M., Roelofs, G.-J., 2002. Atmosphere–biosphere trace gas exchanges simulated with a single-column model. Journal of Geophysical Research 107 (D16), 4297.

Gasche, R., Papen, H., 1999. A 3-year continuous record of nitrogen trace gas fluxes from untreated and limed soil of a N-saturated spruce and beech forest ecosystem in Germany 2 NO and NO_2 fluxes. Journal of Geophysical Research 104, 18505–18520.

Guenther, A., Hewitt, C., Erickson, D., Fall, R., Geron, C., Graedel, T., Harley, P., Klinger, L., Lerdau, M., McKay, W., Pierce, T., Scholes, R., Steinbrecher, R., Tallamraju, R., Taylor, J., Zimmerman, P., 1995. A global model of natural volatile organic compound emissions. Journal of Geophysical Research 100 (D5), 8873–8892.

Huber, C., Kreutzer, K., 2002. Three years of continuous measurements of atmospheric ammonia concentrations over a forest stand at the Höglwald site in southern Bavaria. Plant and Soil 240, 13–22.

Hutchinson, G., Vigil, M.F., Doran, J.W., Kessavalou, A., 1997. Coarse-scale soil–atmosphere NO_x exchange modelling: status and limitations. Nutrient Cycling in Agroecosystems 48, 25–35.

Johansson, M., Suutari, R., Bak, J., Lövblad, G., Posch, M., Simpson, D., Tuovinen, J.-P., Tørseth, K., 2001. The importance of nitrogen oxides for the exceedance of critical thresholds in the Nordic countries. Water, Air and Soil Pollution 130, 1739–1744.

Jonson, J., Benedictow, A., 2003. Appendix B. 2000 source–receptor relationships: overview by country. In: Tarrasón, L. (Ed.), Transboundary Acidification, Eutrophication and Ground Level Ozone in Europe. EMEP Status Report 1/2003, Part III Source–Receptor Relationships. The Norwegian Meteorological Institute, Oslo, Norway, pp. B:1–B:194

Jonson, J., Bartnicki, J., Olendrzynski, K., Jokobsen, H., Berge, E., 1998. EMEP Eulerian model for atmospheric transport and deposition of nitrogen species over Europe. Environmental Pollution 102, 289–298.

Kesik, M., Ambus, P., Baritz, R., Brüggemann, N., Butterbach-Bahl, K., Damm, M., Duyzer, J., Horváth, L., Kiese, R., Kitlzer, B., Leip, A., Li, C., Pihlatie, M., Pilegaard, K., Seufert, G., Simpson, D., Skiba, U., Smiatek, G., Vesala, T., Zechmeister-Boltenstern, S., 2005. Inventory of N_2O and NO emissions from European forest soils. Biogeosciences 2, 353–375.

Kreutzer, K., Weiss, T., 1998. The Höglwald field experiments—aims, concepts and basic data. Plant and Soil 199, 1–10.

Lee, D.S., Köhler, I., Grobler, E., Rohrer, F., Sausen, R., Gallardo-Klenner, L., Olivier, J.G.J., Dentener, F.J., Bouwman, A.F., 1997. Estimates of global NO_x emissions and their uncertainties. Atmospheric Environment 31, 1735–1749.

Lenschow, D., Delany, A., 1987. An analytic formulation for NO and NO_2 flux profiles in the atmospheric surface layer. Journal of Atmospheric Chemistry 5, 301–309.

Ludwig, J., Meixner, F., Vogel, B., Förstner, J., 2001. Soil–air exchange of nitric oxide: an overview of processes, environmental factors, and modeling studies. Biogeochemistry 52, 225–257.

McGowan, G., Palmer, S., Tang, Y., van Dijk, N., Cape, J., Sutton, M., 2002. Biodiversity in roadside verges. 1. Extensive botanical survey; 2. Test and validation of passive diffusion sampling methods for long-term ambient monitoring of NO_2 and NH_3 concentrations. Report to Scottish Executive (SEERAD), Centre for Ecology and Hydrology (CEH), Scotland.

Metzger, S.M., Dentener, F.J., Lelieveld, J., Pandis, S.N., 2002. Gas/aerosol partitioning 1. A computationally efficient model. Joural of Geophysical Research 107 (D16), ACH 16.

Meyers, T., Baldocchi, D., 1988. A comparison of models for deriving dry deposition fluxes of O_3 and SO_2 to a forest canopy. Tellus 40B, 270–284.

Mills, G., 2004. Mapping critical levels for vegetation. In: UBA (Ed.), UNECE Convention on Long-Range Transboundary Air Pollution. Manual on Methodologies and Criteria for Mapping Critical Loads and Levels and Air Pollution Effects, Risks and Trends. Updated versions available at: ⟨http://www.oekodata.com/icpmapping/⟩.

Nemitz, E., Milford, C., Sutton, M.A., 2001. A two-level canopy compensation point model for describing bi-directional biosphere–atmosphere exchange of ammonia. The Quarterly Journal of the Royal Meteorological Society 127, 815–833.

Nilsson, J., Grennfelt, P. (Eds.), 1988. Critical Loads for Sulphur and Nitrogen, vol. 97. Nordic Council of Ministers, Copenhagen, Denmark, Nord, 418pp.

Novak, J., Pierce, T., 1993. Natural emissions of oxidant precursors. Water, Air and Soil Pollution 67, 57–77.

Pilegaard, K., Hummelshøj, P., Jensen, N., 1999. Nitric oxide emission from a Norway spruce forest floor. Journal of Geophysical Research 104, 3433–3445.

Pitcairn, C., Leith, I., Sheppard, L., Sutton, M., Fowler, D., Munro, R., Tang, S., Wilson, D., 1998. The relationship between nitrogen deposition species composition and foliar nitrogen concentrations in woodland flora. Environmental Pollution 102 (S1), 41–48.

Raupach, M.R., 1979. Anomalies in flux gradient relationships over forest. Boundary Layer Meteorology 16, 467–486.

Ruijgrok, W., Tieben, H., Eisinga, P., 1997. The dry deposition of particles to forest canopy: a comparison of model and experimental results. Atmospheric Environment 31, 399–415.

Schindlbacher, A., Zechmeister-Boltenstern, S., Butterbach-Bahl, K., 2004. Effects of soil moisture and temperature on NO, NO_2, and N_2O emissions from European forest soils. Journal of Geophysical Research 109, D17302.

Schulze, E.D., 1989. Air pollution and forest decline in spruce Picea abies forest. Science 244, 776–783.

Seinfeld, J., Pandis, S., 1998. Atmospheric Chemistry and Physics. From Air Pollution to Climate Change. Wiley, New York.

Sillman, S., Logan, J., Wofsy, S., 1990. The sensitivity of ozone to nitrogen oxides and hydrocarbons in regional ozone episodes. Journal of Geophysical Research 95 (D2), 1837–1851.

Simpson, D., 1995. Biogenic emissions in Europe 2: implications for ozone control strategies. Journal of Geophysical Research 100 (D11), 22891–22906.

Simpson, D., Andersson-Sköld, Y., Jenkin, M.E., 1993. Updating the chemical scheme for the EMEP MSC-W oxidant model: current status. EMEP MSC-W Note 2/93, The Norwegian Meteorological Institute, Oslo, Norway.

Simpson, D., Guenther, A., Hewitt, C., Steinbrecher, R., 1995. Biogenic emissions in Europe 1. Estimates and uncertainties. Journal of Geophysical Research 100 (D11), 22875–22890.

Simpson, D., Winiwarter, W., Börjesson, G., Cinderby, S., Ferreiro, A., Guenther, A., Hewitt, C.N., Janson, R., Khalil, M.A.K., Owen, S., Pierce, T.E., Puxbaum, H., Shearer, M., Skiba, U., Steinbrecher, R., Tarrasón, L., Öquist, M.G., 1999. Inventorying emissions from nature in Europe. Journal of Geophysical Research 104 (D7), 8113–8152.

Simpson, D., Tuovinen, J.-P., Emberson, L., Ashmore, M., 2001. Characteristics of an ozone deposition module. Water, Air and Soil Pollution: Focus 1, 253–262.

Simpson, D., Fagerli, H., Jonson, J., Tsyro, S., Wind, P., Tuovinen, J.-P., 2003a. The EMEP unified Eulerian model. Model description. EMEP MSC-W Report 1/2003, The Norwegian Meteorological Institute, Oslo, Norway.

Simpson, D., Fagerli, H., Solberg, S., Ås, W., 2003b. Photooxidants. In: EMEP Report 1/2003, Transboundary Acidification, Eutrophication and Ground Level Ozone in Europe. The Norwegian Meteorological Institute, Oslo, Norway, pp. 67–102.

Simpson, D., Tuovinen, J.-P., Emberson, L., Ashmore, M., 2003c. Characteristics of an ozone deposition module II: sensitivity analysis. Water, Air and Soil Pollution 143, 123–137.

Skiba, U., Fowler, D., Smith, K., 1997. Nitric oxide emissions from agricultural soils in temperate and tropical climates: sources, controls and mitigation options. Nutrient Cycling in Agroecosystems 48, 139–153.

Skiba, U., Dick, J., Storeton-West, R., Fernades-Lopez, S., Wood, C., Tang, S., 2005. Effect of forest type and N-deposition on N-trace gas fluxes. In: Butterbach-Bahl, K. (Ed.), Nitrogen Oxides Emissions from European Forest Ecosystems (NOFRETETE). Final Report, NOFRETETE Project. Institute for Meteorology and Climate Research, IMK-IFU, Karlsruhe Research Centre (FZK), Garmisch-Partnkirchen, pp. 26–41.

Smith, R., Fowler, D., Sutton, M.A., Flechard, C., Coyle, M., 2000. Regional estimation of pollutant gas dry deposition in the UK: model description, sensitivity analyses and outputs. Atmospheric Environment 34, 3757–3777.

Stevenson, K., Bush, T., Mooney, D., 2001. Five years of nitrogen dioxide measurement with diffusion tube samplers at over 1000 sites in the UK. Atmospheric Environment 35, 281–287.

Stohl, A., Williams, E., Wotawa, G., Kromp-Kolb, H., 1996. A European inventory of soil nitric oxide emissions and the effect of these emissions on the photochemical formation of ozone in Europe. Atmospheric Environment 30, 3741–3755.

Sutton, M., Tang, Y., Milford, C., Haria, M., Rosset, F., Fillat, G., Wohlfarht, E., Tasser, E., Bitterlich, W., Bayfield, N., 1999. Assessment of ammonia fluxes for European mountain

ecosystems: application of a bidirectional inferential model for the ECOMONT transect. ECOMONT Final Report.

Sutton, M., Tang, Y., Dragosits, U., Fournier, N., Dore, A., Smith, R., Weston, K., Fowler, D., 2001a. A spatial analysis of atmospheric ammonia and ammonium in the UK. The Scientific World 1 (S2), 275–286.

Sutton, M., Tang, Y., Miners, B., Fowler, D., 2001b. A new diffusion denuder system for long-term regional monitoring of atmospheric ammonia and ammonium. Water, Air and Soil Pollution: Focus 1 (Part 5/6), 145–156.

Sutton, M.A., Milford, C., Dragosits, U., Place, C.J., Singles, R.J., Smith, R.I., Pitcairn, C.E.R., Fowler, D., Hill, J., ApSimon, H.M., 1998. Dispersion, deposition and impacts of atmospheric ammonia: quantifying local budgets and spatial variability. Environmental Pollution 102 (1), 349–361.

Tang, Y., Cape, J., Sutton, M., 2001. Development and types of passive samplers for monitoring atmospheric NO_2 and NH_3 concentrations. The Scientific World 1, 513–529.

Tuovinen, J.-P., Ashmore, M., Emberson, L., Simpson, D., 2004. Testing and improving the EMEP ozone deposition module. Atmospheric Environment 38, 2373–2385.

Van Dijk, S., Duyzer, J., 1999. Nitric oxide emissions from forest soils. Journal of Geophysical Research 104, 15955–15961.

Veldkamp, E., Keller, M., 1997. Fertilizer-induced nitric oxide emissions from agricultural soils. Nutrient Cycling in Agroecosystems 48, 69–77.

Vestreng, V., Adams, M., Goodwin, J., 2004. Inventory Review 2004. Emission data reported to CLRTAP and under the NEC directive. EMEP/EEA Joint Review Report. EMEP-MSCW Report 1/2004, The Norwegian Meteorological Institute, Oslo, Norway.

Williams, E., Guenther, A., Fehsenfeld, F., 1992. An inventory of nitric oxide emissions from soils in the United States. Journal of Geophysical Research 97, 7511–7519.

Yienger, J., Levy, H., 1995. Empirical model of global soil-biogenic NO_x emissions. Journal of Geophysical Research 100, 11447–11464.